Alginate-Encapsulated Human Hepatocytes for Transplantation

Jitraruch, Suttiruk

Awarding institution:
King's College London

Alginate-Encapsulated Human Hepatocytes for Transplantation

Suttiruk Jitraruch

A thesis submitted to University of London
in fulfilment of the conditions governing
candidates for the degree of PhD

June 2014

Institute of Liver Studies,
King's College London School of Medicine
at King's College Hospital,
London

ACKNOWLEDGEMENTS

First, I would like to thank my principal supervisor, Dr Ragai R. Mitry, for his continuous support and encouragement during my PhD study and for allowing me to grow as a research scientist. I am also grateful to my supervisors Professor Anil Dhawan and Dr. Robin D. Hughes for their invaluable advice and guidance throughout my PhD.

My sincere thanks also go to my colleagues in the Hepatocyte Transplantation Team: Miss Sharon Lehec, Dr Emer Fitzpatrick, Dr Sanjay Bansal, Dr Harry Qin, Dr Juliana Puppi and especially Dr Celine Filippi for their contribution and friendship. I would also like to thanks many people within the Institute of Liver Studies: Dr Maria Serena Longhi, Dr John Cardone, Dr Beth Holder, and Dr Vish Patel for their support.

I am grateful to Professor Nigel Heaton, Professor Mohamed Rela, Mr Hector Vilca-Melendez and all the Liver Transplantation team at King's College Hospital and also Dr Alberto Quaglia, Dr Alex Knisely and Dr Yoh Zen for providing the liver tissues for my research.

I would like to thank Dr Daniel Soong for his help with confocal microscopy, Dr Gema Vizcay for her help with electron microscopy, Dr Kelvin Mills and Dr Wendy Heywood for the help with proteomics, Professor Roy Sherwood for performing the biochemical assays and Dr Salma Ayis for her help and advice with statistics.

I would also like to thank all of my friends who supported me during these years of study.

Finally, a special thanks to my family, words cannot express how grateful I am to my parents, brothers and nephews for their unconditional support and encouragement for me to pursue my dreams.

ABSTRACT

Intraperitoneal transplantation of alginate-microencapsulated human hepatocytes is an attractive option for the management of acute liver failure by providing short-term support to bridge patients to liver transplantation or allow native liver regeneration. Its success depends on mechanical stability, optimal permeability, and biocompatibility of the encapsulated cells to provide good viability and function. The main aims of this study were to optimise protocols for production and cryopreservation of human hepatocyte microbeads (HMBs) for future clinical use.

HMBs were prepared using sterile ultrapure materials. Physical integrity of HMBs was evaluated using an osmotic stress test. A polymerisation of 15min provided mechanical stability with well-maintained cell viability and function. Cell content in HMBs was optimised and a density of $3.5x10^6$cells/ml alginate provided the highest cell viability with hepatocytes evenly distributed within microbeads. Permeability of optimised HMBs was measured and the largest protein which could diffuse out of microbeads had a molecular weight of 164kDa. Immune activation of human peripheral blood mononuclear cells was assessed by flow cytometry after co-culture with empty microbeads and HMBs. No evidence of cellular immune activation was observed. Optimisation of hepatocyte microbead cryopreservation was performed using rat and human hepatocytes. Improved outcome of cryopreservation was found when hepatocyte microbeads were cryopreserved in UW solution containing 10% DMSO, 5% glucose and 60μM benzyloxycarbonyl-Val-Ala-DL-Asp-fluoromethylketone (ZVAD).

Safety, therapeutic effects, and immunogenicity of hepatocyte microbeads produced were confirmed in immunocompetent rats with and without acute liver failure. HMBs showed functionality with no inflammatory response in rats over 7 days. Transplantation of rat hepatocyte microbeads was safe and able to support the failing liver. Cryopreserved microbeads showed an encouraging outcome, but may require greater cell numbers compared to fresh microbead.

In conclusion, optimised protocols for production and cryopreservation of GMP grade alginate-encapsulated hepatocytes were established. These high quality microbeads are suitable for clinical transplantation.

TABLE OF CONTENTS

ABBREVIATIONS

7-ER	7-ethoxyresorufin	**EDTA**	Ethylene diamine tetra Acetate
ALF	Acute liver failure	**EGTA**	Ethylene glycol tetraacetic Acid
ALT	Alanine aminotransferase	**ELIS**	Enzyme-linked immunosorbent assay
ANOVA	Analysis of variance	**EMEM**	Eagle's minimal essential medium
APA	Alginate-poly-L-lysine-Alginate	**EROD**	Ethoxyresorufin O-deethylation
APC	Allophycocyanin	**ESC**	Embryonic stem cells
AST	Aspartate aminotransferase	**FCS**	Fetal calf serum
ATP	Adenosine triphosphate	**FDA**	Fluorescence diacetate
BMSC	Bone marrow mesenchymal stem cells	**FITC**	Fluorescein isothiocyanate
BSA	Bovine serum albumin	**GMP**	Good manufacturing practice
CMRL	Connaught Medical Research Laboratories	**HBSS**	Hank's balanced salt solution
CRF	Controlled -rate freezer	**HC**	Hepatocyte
CYP	Cytochrome	**H&E**	Haematoxylin and eosin
DFO	Desferoxamine	**HEPES**	4-(2-hydroxyethyl)-1-piperazin-1-yl] ethanesulfonic acid
D-GalN	D-galactosamine	**HRP**	Hoarse raddish peroxidase
dH_2O	Distilled water	**HSA**	Human serum albumin
DMEM	Dulbecco's modified Eagle's Medium	**HTK**	Histidine-tryptophan-ketoglutarate
DMSO	Dimethyl sulphoxide	**HTS**	HypoThermosol
DPBS	Dulbecco's Phosphate-Buffered Saline	**HUVEC**	Human umbilical cord vein endothelial cells
ECM	Extracellular matrixs	**Hz**	Hertz
IFN-γ	Interferon gamma	**PE**	Phycoerythrin

Ig	Immunoglobulin	**PerCP**	Peridinin chlorophyll Protein
IL	Interleukin	**PI**	Propidium iodide
INR	International normalised Ratio	**PLL**	Poly-L-lysine
iPS	Induced pluripotent stem cell	**PT**	Prothrombin time
ISEC	Inverse-size exclusion Chromatography	**ROS**	Reactive oxygen species
kDa	Kilo Dalton	**RPMI**	Roswell Park Memorial Institute
kV	Kilo voltage	**RT**	Room temperature
mOsm	milliosmole	**SEM**	Scanning electron Microscopy
MSC	Mesenchymal stem cell	**SRB**	Sulphorhodamine B
MTT	3-(4,5-dimethylthiazol-2-yl)-5-biphenyl tetrazolium bromide	**TBS**	Tris-buffered saline
MW	Molecular weight	**TMB**	3,3′,5,5′-tetramethylbenzidine
MWCO	Molecular weight cut off	**UBC**	Umbilical cord blood
OD	Optical density	**UW**	University of Wisconsin
OLT	Orthotopic liver Transplantation	**WEM**	Williams' E medium
PBMC	Peripheral blood mononuclear cell	**ZVAD**	Benzyloxycarbonyl-Val-Ala-DL-Asp-fluoromethylketone
PBS	Phosphate-buffered saline		

LIST OF FIGURES

LIST OF TABLES

CHAPTER 1

1. Introduction

Acute liver failure is (ALF) is a devastating and complex condition which causes an abrupt loss of hepatic function in a person with previously normal liver function leading to encephalopathy, coagulopathy and progressive multiple organ failure within a short period of time. ALF represents a syndrome of heterogeneous conditions rather than a specific disease in which the underlying etiology, age of the patients and the time course are involved in the outcome (Bernal et al. 2010; O'Grady 2005). In adults, O'Grady et al (1993) classified ALF into 3 categories regarding the progression of hepatic encephalopathy from the initial liver injury these are hyperacute (≤7 days), acute (8-28 days) and subacute (>28 days). This definition provides clues to the underlying cause and prognostic outcome with medical supportive care. In patients with rapid evolution, hyperacute, the most likely causes are acetaminophen toxicity or hepatitis A and E and have a better chance of recovery compared to subacute patients. In children, the signs of hepatic encephalopathy are difficult to identify as it can be subtle or late presentation during the course of illness. Therefore, for children modifications of ALF criteria are used based mainly on coagulopathy, an International normalized ratio (INR) >1.5 with encephalopathy or INR>2.0 without any encephalopathy (Squires et al. 2006).

The most common etiology of ALF in adults are viruses and drugs however, there are geographic variations where acetaminophen and other drug induced liver injury are the common causes in a developed country (Bernal and Wendon 2013). The causes of ALF in children differ from adults because these also vary by age. Viral hepatitis is the most common in south East Asia and Latin America, whereas in Northern America and Europe, the most common etiology remains indeterminate. However, acetaminophen overdose and Wilson disease have become more frequent in the older children with ages 3 to 18 years (Squires et al. 2006; Dhawan 2012).

According to the unpredictable natural history of ALF the mortality rate of ALF is variable depending on the etiology ranging from 10% to 90% without liver transplantation. In the pre-liver transplantation era, the mortality rate was 80% or higher (Hoofnagle et al. 1995). However, the development of multidisciplinary critical care protocols and the use of emergency liver transplantation have considerably improved survival rates in recent years with overall mortality rate about 30% (Lee et al. 2008). Orthotopic liver transplantation (OLT) is currently the only effective approach for treatment. However, the limitations of this therapeutic approach are well

known, namely scarcity of organ donors, surgical risk, and requirement for life-long immunosuppressive drugs. Furthermore, the decision to proceed to transplantation is not always straightforward, because some of these patients might have a chance of spontaneous liver recovery. To date, various prognostic evaluation systems have been used to select the ALF patient for OLT but none of them provide accurate prediction (Mochida et al. 2008; Bernuau et al. 1986; O'Grady et al. 1993).

More recently, auxiliary orthotopic transplantation has become an exciting concept to bridge ALF patients to survival without the need for life-long immunosuppression. The right lobe of the native liver is usually resected and replaced with the donor graft while the native left lobe remains in situ. The donor graft provides supportive function while the native liver regenerates. Within 1-3 years, the immunosuppression is carefully withdrawn resulting in atrophy of the allograft. The success of this technique supports the concept of spontaneous recovery of liver cell mass. In our experience 20 children underwent auxiliary liver transplantation and 17 survived. Of these 11 children (65% of the survivors) showed complete native liver recovery and subsequent withdrawal of immunosuppression (Faraj et al. 2010). Currently, the alternative concepts of liver transplantation to provide adjunctive and temporary liver support for patients with ALF the other potential are being investigated including liver support systems and hepatocyte or stem cells transplantation

1.1 Extracorporeal Liver Support Systems

Extracorporeal liver support consists of artificial and bioartificial liver supports systems. The concept of temporary extracorporeal liver support is a life support system comparable to kidney dialysis machines, but specifically for liver failure patients. These systems have been extensively investigated for over three decades; however, the clinical outcomes have not shown significant benefit in improving transplant free survival (Liu et al. 2004; Stutchfield et al. 2011; Struecker et al. 2013). Artificial liver support systems are non biological devices incorporating hemodialysis, hemofiltration and/or plasma exchange units based on albumin dialysis to clear toxins that accumulate in patients. There are two artificial liver support devices have been extensively evaluated in the clinical setting, the Molecular Absorbent Recirculating System (MARS®; Gambro, Stockholm, Sweden) and the fractionated plasma separation and absorption system (Prometheus®, Fresenius Medical Care, Bad Homburg, Germany), (Khuroo et al. 2004; Oppert et al. 2009; Schaefer and Schmitt 2013). Bioartificial systems consist of either porcine hepatocytes or hepatoblastoma cells in bioreactors that aim to perform both detoxification and synthetic functions. To maintain these complex tasks, liver cells are cultured in a 3D manner

within a network of hollow fibers or a porous barrier to isolate cells from immunoglobulins and leukocytes in patient's blood or plasma. HepatAssist® system (Alliqua Inc. Langhorne, PA, USA) which is based on cryopreserved porcine hepatocytes and the Extracorporeal Liver Assist Device (ELAD®; Vital Therapies Inc., San Diego, CA, USA) uses a hepatoblastoma cell line are the most common two systems which have been studied (Millis et al. 2002; Demetriou et al. 2004). The limitations of artificial support systems are due to detoxification being more complex than just removal of albumin-bound toxins. In addition, the charcoal and resin might absorb growth factors and cytokines that might effect on liver regeneration. The clinical proof of efficacy of bioartificial systems is limited by the risk of tumorgenic products, immunogenicity (anti-pig IgG and IgM) and xenozoonoses (Struecker et al. 2013).

1.2 Hepatocyte Transplantation

Hepatocyte transplantation has been shown to be of benefit as a bridge to transplantation for patients with ALF (Fisher and Strom 2006). Hepatocytes provide the essential functions that the native liver has lost. The use of hepatocyte infusion into the portovenous system has some advantages compared to whole organ or auxiliary liver transplantation. Cell therapy is far less invasive than organ transplantation and can be repeated several times if required during the clinical course. Hepatocytes are isolated from liver donors that are unsuitable for OLT. Cells isolated from one donor can be transplanted into several patients and also can be cryopreserved and stored for the scheduled or emergency use. Importantly, the native liver remains in place, allowing for the possibility of regeneration and spontaneous recovery (Hughes et al. 2012; Dhawan et al. 2010). In addition, in ALF high levels of growth factors may stimulate the transplanted hepatocytes to proliferate in the host liver which may result in their beneficial effect (Meyburg et al. 2009). Transplantation of hepatocytes has been investigated in various ALF animal models. Animals were transplanted with 1-2% of the liver mass via splenic, portal or peritoneal transplantation and this led to improvement of the survival rate compared to the control groups (Demetriou et al. 1988; Sommer et al. 1979; Sutherland et al. 1977). However, in clinical setting to provide efficient function the number of hepatocytes needed maybe higher than that for metabolic disorders (5-10% liver mass) and require repeated infusion. The results of hepatocyte transplantation in 37 patients with ALF were reviewed by Fischer et al. (2006) in which most cases received repeated administration of allogeneic adult human hepatocytes. The doses of cells were extremely varied between patients ranging from less than 0.01% up to approximately 5% of liver mass in some cases. After transplantation, seven cases fully recovered without OLT and half of the patients showed improvement in hepatic encephalopathy and a reduction in blood ammonia (Fisher and Strom 2006). Although, the results were

promising, all studies to date have been uncontrolled and the sample sizes are too small to draw any conclusions. The overall data of hepatocyte transplantation for ALF in both children and adult are summarised in Table 1.1.

Nevertheless, the main obstacles of intrahepatic hepatocyte transplantation in coagulopathic patients are the potential risk of bleeding as a result of invasive catheter placement, critical shortage of hepatocytes and immunologic reaction necessitating immunosuppression (Soltys et al. 2010). To circumvent these limitations, intraperitoneal transplantation as a minimal invasive route of cell delivery with cells protected from host immune reaction may be of interest. Intraperitoneal transplantation of microencapsulated hepatocytes (hepatocyte microbeads) could be an attractive option (Umehara et al. 2001; Aoki et al. 2000). Furthermore the limited supply of human liver to isolate primary hepatocytes could be addressed by establishing a good quality hepatocyte bank and the uses of alternative cell sources of hepatocyte-like cells such as liver stem and /or progenitor, fetal liver and embryonic stem cells (Herrera et al. 2013; Najimi et al. 2007).

1.3 Alternative Cell Sources

The limited availability of primary hepatocytes has encouraged researchers to investigate new sustainable sources of cells. Stem cells from both fetal and adult donors are good candidates due to their self-renewal and ability to differentiate into hepatocyte-like cells under specific conditions (Ishikawa et al. 2012). Hepatocyte-like cells derived from embryonic stem cells (ESC) and induced pluripotent stem cells (iPS) which involves reprogramming of the development process have shown some benefits in ALF animal models. Machimoto et al. (2007) showed that transplantation of hepatic progenitor cells isolated from fetal liver improved the survival rate of mice with liver injury. However, the disadvantages of these cells are the complexity of the differentiation protocol, ethical issues and more importantly the safety concerns of tumourgenicity and immunogenicity which have withheld them so far from clinical use. Mesenchymal stem cells (MSC) either from bone marrow, adipose tissue or umbilical cord have been intensively studied, given their promise of clinical application. Recently, Li et al. (2012) demonstrated that intraportally transplanted human bone marrow MSCs rescued pigs with ALF perhaps by promoting liver regeneration and hepatic transdifferentiation. Of note, comparison of the therapeutic effects of adult, fetal and embryonic stem cell-derived hepatocytes in ALF mice indicated that adult hepatocytes were the most effective cells (Kamimura et al. 2012).

Table 1.1 Clinical experiences of hepatocyte transplantation for patients with ALF

Etiology	Study	Pts	Infusion	Cell dose	Route	Outcome
Drug						
	Soriano et al. (1997)	16 yr	1	$4.x10^7$	PV	Died day 2
		12 yr	3	$1x10^8$	PV	Died day 7
		10 yr	3	$2.8x10^9$	PV	Died day 7
	Bilir et al.(2000)	32 yr	1	$1.3x10^9$	IS	Died day 14
		35 yr	1	$1x10^9$	IS	Died day 20
		55 yr	1	$3.9x10^9$	IS	Died 6 hrs
	Strom et al.(1999)	13 yr	1	$1x10^9$	PV	Died day 4
		43 yr	NA	NA	NA	Died day 35
	Fisher et al. (2000)	14 yr	1	$2.5x10^9$	PV	OLT day 1
	Fisher and Strom (2006)	27 yr	1	$2.8x10^7$	IS	OLT day 10
		26 yr	1	$1.2x10^9$	IS	OLT day 2
		21 yr	3	$9x10^8$(2), $2.5x10^7$	IS	Died day 1
		35 yr	1	$5.4x10^9$	PV	Died day 18
		35 yr	1	$3.7x10^9$	PV	Full recovery
		51 yr	1	$3.9x10^9$	PV	Died day 3
	Habibullah et al.(1994)[a]	32 yr	1	$6x10^7$/kg	IP	Died 30 hrs
		29 yr	1	$6x10^7$/kg	IP	Died 37 hrs
		20 yr	1	$6x10^7$/kg	IP	Died 48 hrs
		20 yr	1	$6x10^7$/kg	IP	Full recovery
		24 yr	1	$6x10^7$/kg	IP	Full recovery
Viral						
	Fisher and Strom (2006)	4 yr	2	$1.7x10^9$	PV	Died day 2
		54 yr	1	$6.6x10^9$	PV	Died day 7
	Bilir et al. (2000)	29 yr	1	$1x10^{10}$	PV,IS	Died 18 hrs
		65 yr	1	$3x10^{10}$	PV,IS	Died d52
	Strom et al. (1999)	28 yr	1	$1.69x10^8$	IS	OLT day 3
		37 yr	1	$1.2x10^8$	IS	Died day 5
		43 yr	3	$2.43x10^8$	PV	OLT day 1
	Fisher et al. (2000)	37 yr	1	$8.8x10^8$	IS	Full recovery
	Habibullah et al. (1994)[a]	40 yr	1	$6x10^7$/kg	IP	Died 13 hrs
Idiopathic						
	Soriano et al. (1997)	3 yr	9	$4x10^9$	PV	Full recovery
		5 yr	7	$2x10^9$	PV	OLT day 4
	Fisher et al.(2000)	3.5 mo	1	$1.8x10^8$	PV	OLT day 1
		23 yr	2	$2.86x10^8$, $1.52x10^8$	IS	OLT day5, died day 13
		48yr	1	$7.5x10^8$	PV	Died day 1
	Habibullah et al. (1994)[a]	8yr	1	6x107/kg	IP	Full recovery
Others (Mushroom poisoning, post-surgical, acute fatty liver of pregnancy)						
	Schneider et al. (2006)	64 yr	1	$4.9x10^{91}$	PV	Full recovery
	Strom et al.(1999)	69 yr	2	$3.6x10^8$, $1.7x10^8$	IS	Died day 2
	Khan et al.(2004)[a]	26 yr	1		IP	Full recovery

[a]Fetal hepatocytes. Abbreviation: IP, intraperitoneal; IS, intrasplenic; NA, not available; OLT, orthotopic liver transplantation; and PV, portal vein.

1.4 Decellularised-recellularised Liver Matrix

Tissue engineering has recently developed a novel technique to generate transplantable liver grafts with a decellularised liver matrix. This decellularisation process involves removing cells and other antigenic material from the liver, but preserves the structural and functional characteristics of the native microvascular network and this serves as an ideal biomatrix for cellular repopulation. This is followed by recellularisation with cells such as adult hepatocytes, stem cells, and stellate cells. The liver matrix is matured in a bio-reactor and then a functional liver organoid is produced and implanted in a patient with ALF or it can be incorporated in an extracorporeal liver support system. Uygun et al (2010) recellularised the median lobe of rat liver with adult hepatocytes and demonstrated comparable viability and function of hepatocytes in the neo-liver to that in normal culture conditions. The liver graft was perfused with minimal ischemic damage after transplantation into rats (Uygun et al. 2010). Bao et al (2011) recellularised rat hepatocyte spheroids into a decellularised liver lobe and implanted this into the portal system of rats that had undergone 90% hepatectomy. The transplanted rats showed improvement of their liver function and prolonged survival. Although, the results of experimental studies are encouraging, the translation of whole organ engineering into the clinic is still distant. Summary of liver support principles based on cell therapy is shown in Figure 1.1

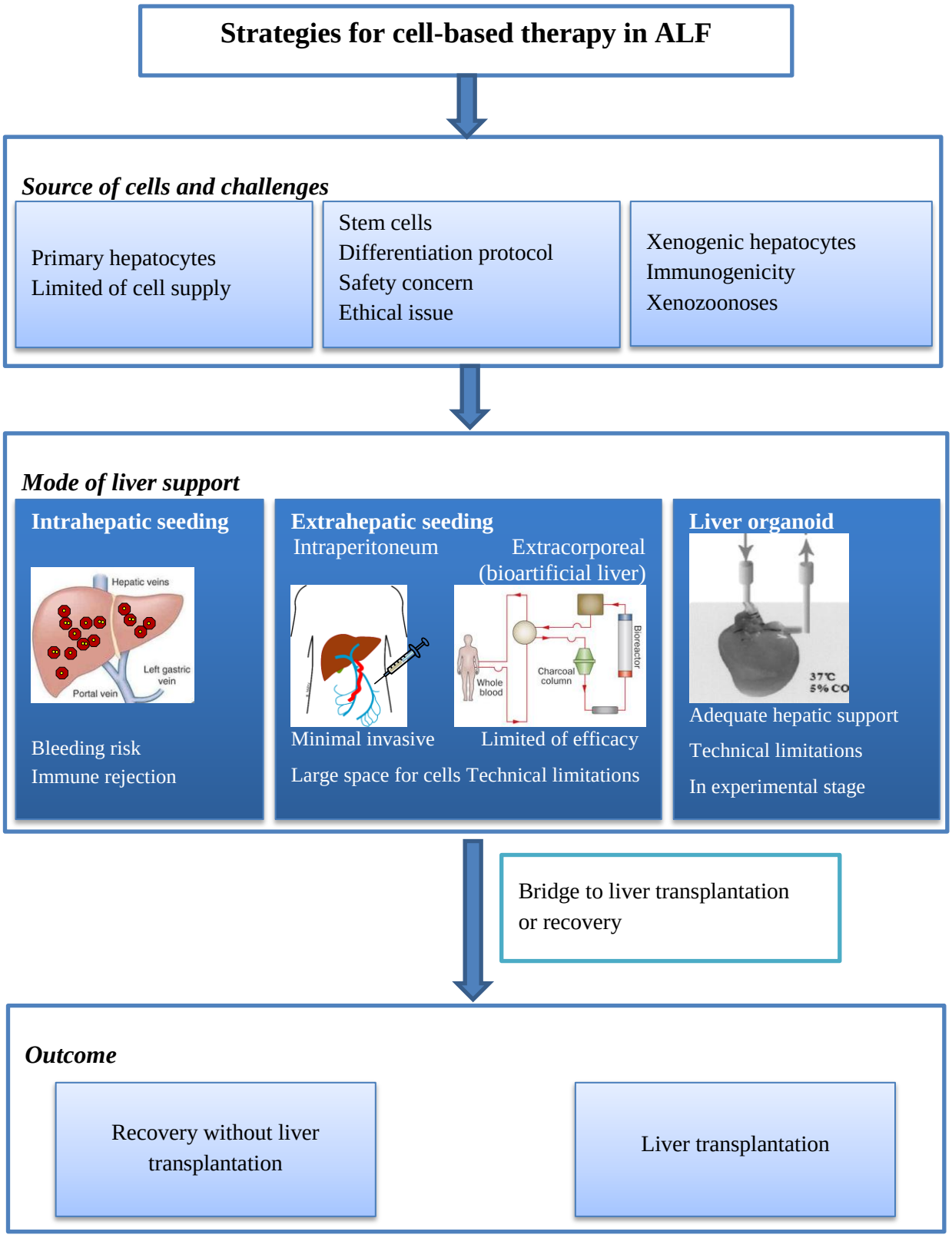

Figure 1.1: Schematic presentation of the strategies of cell therapy in patients with ALF.

1.5 Cell Microencapsulation

Cell encapsulation technology is based on immobilization of transplanted cells in an artificial, semipermeable membrane structure which aims to protect cells from both mechanical stress and the host's immune response, while allowing bi-directional diffusion of nutrient, oxygen and metabolic products which is essential for cell survival and does not interfere with cell function (Figure 1.2). As a result, the encapsulated cells can be transplanted without the need for immunosuppression. (Hernandez et al. 2010; Uludag et al. 2000; Zimmermann et al. 2007). Moreover, this three-dimensional (3-D) scaffold system provides the possibility of transplantation of non-human cells (xenotransplantation) which might be considered as an alternative source of cells. Microencapsulation provides a number of advantages over other cell therapy systems or devices, including greater surface to volume ratio, ease of implantation and retrievability by lavage and needle aspiration (Lanza et al. 1996). Encapsulation has been explored and continues to develop over the past three decades due to the promising outcomes. The pioneering study carried out by Chang using ultrathin polymer membrane microcapsules introduced the term of "artificial cells" (Chang 1964). Later in 1980 Lim and Sun. performed the first successful transplantation of xenograft islet microcapsules in rats. Since then, there have been tremendous efforts towards developing and understanding the technological and biological requirements for transplantation of microencapsulated cells in small and large animal models. Pre-clinical in vivo studies were shown to be successful in diabetes (Lim and Sun 1980), haemophilia (Hortelano et al. 1996), cancer (Cirone et al. 2002), renal failure (Prakash and Chang 1996), and Huntington's disease (Emerich et al. 2006). The encouraging results of animal studies have provided a scientific basis for microencapsulated cell transplantation in several clinical trials (Calafiore et al. 2006; Lohr et al. 2001; Soon-Shiong et al. 1994). However, the progress in this field of research relatively lags behind the expectation. As a consequence, in the past few years, a number of studies focused on a stepwise analysis on the essential obstacles and limitations of the microencapsulation technique and microcapsule properties to gear up this method closer to a realistic proposal for clinical application (Orive et al. 2003; Murua et al. 2008; Orive et al. 2004).

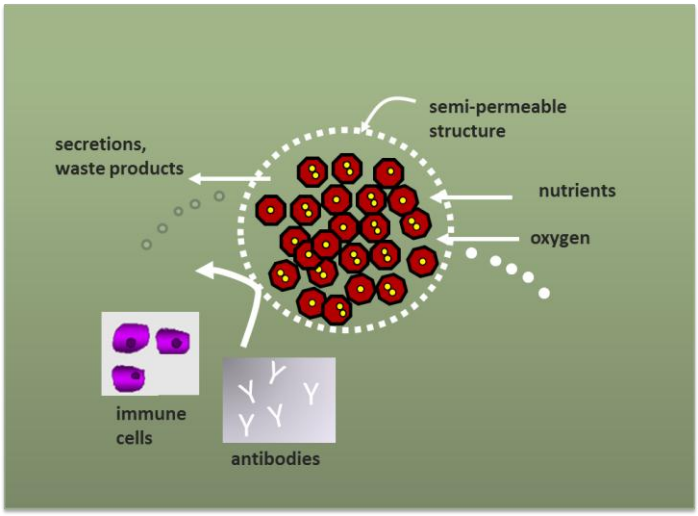

Figure 1.2: Schematic diagram of cell encapsulation illustrates the semi-permeable structure allowing bi-directional diffusion of oxygen, nutrients therapeutic and waste products while protecting cells from immune cells and antibodies.

1.6 Microencapsulation Methods

Microcapsules can be classified into five categories based on their structure as demonstrated in Figure 1.3 (Whelehan and Marison 2011). Type A, liquid-core microcapsules or simple/single core microcapsule; type B, double/multi-shells; type C, polynuclear (multi-core); type D, microbeads/microspheres, and type E, irregular or non-spherical shape. Microcapsules are typically spherical in shape with a well-defined shell and core (type A-C). The multiple shells (layers) are added to modify stability and permeability of microcapsules. However, microbeads (type D) in which cells are entrapped within a solid matrix without a coating membrane is the most common use in biomedical field. Microbeads can be converted to type A microcapsule by adding outer layer followed by depolymerisation of the centre of microbeads. Lim and Sun (1980) developed the classical technique of coating poly-L-lysine (PLL) on the surface of the alginate microcapsules which has been widely used. However, liquefaction or depolymerisation of inner core in the original protocol reduces the structural stability of microcapsules.

Generally, all methods for microencapsulation are based on simple dropping of polymer into a crosslinking solution bath to form solid beads. With the traditional simple dropping technique, through a needle, is difficult to the control size of microbeads and there is a low production rate. Currently, the prevalent technique is a controlled-size droplet extrusion through a nozzle using different mechanical forces to increase the rate of production. The main commonly used are coaxial air flow, electrostatic extrusion, vibrating nozzle and jet-cutting (Figure 1.4). The

coaxial air-flow and the electrostatic generate droplets at the nozzle tip with additional air-flow or electric field surrounding an outer nozzle to enhance dropping (Lewińska et al. 2004; Prüsse et al. 2008). The vibrating-jet (nozzle) technique is one of the most widely used methods based on the principle of laminar jet-break by vibration frequency with defined amplitude to the extruded jet (Senuma et al. 2000; Whelehan and Marison 2011). JetCutter is a new technology for high-throughput encapsulation based on a mechanical impact of the rotating cutting wire on the liquid jet (Schwinger et al. 2002). Prüsse et al (2008) compared these microencapsulation technologies using different viscosities of sodium alginate performed by seven laboratories in Europe. They demonstrated that microbeads prepared with alginate contents of 0.5-2.0% were uniform in their spherical size all 4 technologies, but only electrostatic and JetCutter produced uniform microbeads with high viscosity alginate (3-4%). The production rate of the vibrating technique is 20-40 times higher than those of the coaxial air-flow and electrostatic technologies, but about 10 times lower than the JetCutter. The JetCutter seems to be an efficient technology ranging from lab-scale to industrial production; however, application for the clinical purposes has not as yet been established.

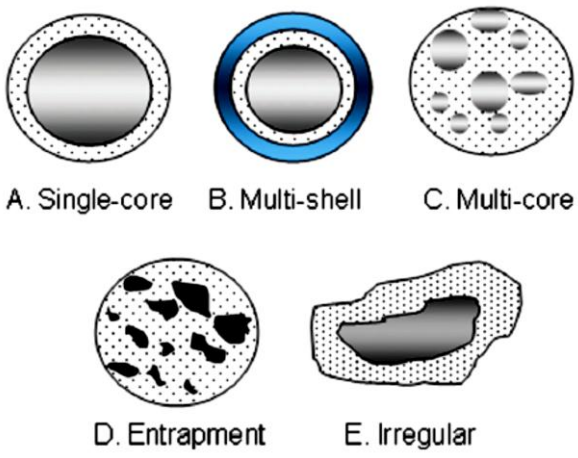

Figure 1.3: The microcapsules structural classification.(A) single-core or liquid-core microcapsule; (B) double/multi-shells microcapsules; (C) polynuclear (multi-core); (D) microbeads/microspheres and (E) irregular or non-spherical shape. [Adapted from Whelehan and Marison (2011)].

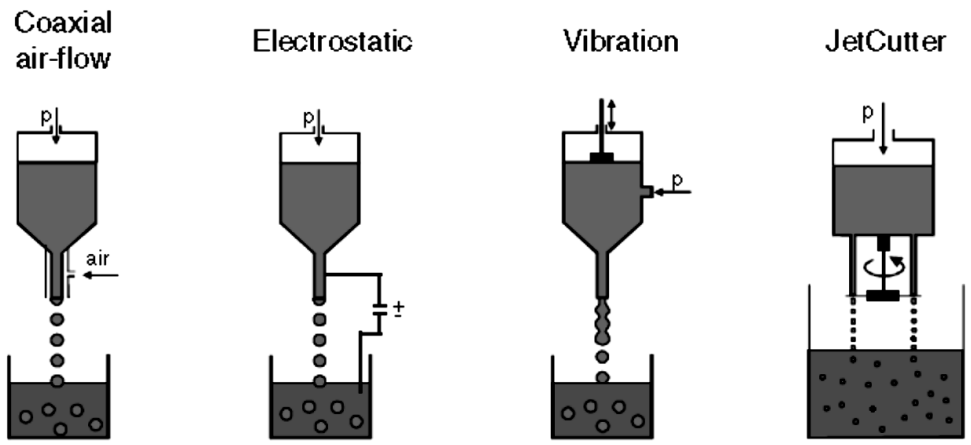

Figure 1.4: Schematic representative of microbeads' production technologies. [Adapted from Prüsse et al. (2008)].

1.7 Alginates for Cell Encapsulation

Suitable biomaterials are important in development of encapsulation technologies. Many different materials are employed to encapsulate cells such as alginate, chitosan, and agarose. Among them, alginate is the most extensively studied and used nowadays due to its excellent ionotropic properties, low toxicity and biocompatibility. Alginates are natural polymers found in brown seaweeds and in bacterial species. They are composed of linear copolymers of 1-4 linked ß-D-mannuronic acid (M) and α-L-glucoronic acid (G) residues. The blocks contain of consecutive G residue and consecutive M and alternating M and G residues (Figure 1.5A). They are negatively charged and gelation of alginates take place when multi-valent cations such as calcium (Ca^{2+}), barium (Ba^{2+}), and aluminium (Al^{3+}) or polyelectrolytes crosslink with the carboxyl group blocks of glucoronic residues, between two different chains resulting in a three-dimensional network (Figure 1.5B). These structural patterns are similar to extracellular matrixes (ECM) of living tissue, therefore are benefit for delivery of bioactive agents (small chemical drugs and proteins) and cell transplantation. The mechanical strength, elasticity, and swelling characteristics are dependent on the nature of the cross-linking cations, the M:G ratio, the percentage of the block structures and the length of polymeric chains (Zimmermann et al. 2001). Stiffness of cross-linked alginate increases: MG < MM < GG blocks, while the flexibility increases: GG < MM < MG blocks. Alginates tend to be contaminated with endotoxins and proteins due to their natural origin and are difficult to purify using an in house protocol (Zimmermann et al. 2007). However, commercial ultrapure alginate is now available.

Modification of alginate is becoming interesting approach to improve the quality of microencapsulation by creating polymers that mimic the ECM. A variety of ECM molecules (collagen and fibronectin) or synthetic peptides like arginine-glycine-aspartic acid (RGD) were studied by mixing together with alginate. Nevertheless, although these modified materials have been developed, the *in vivo* data and the biocompatibility data have not been well-studied. Therefore, to date alginate is the most suitable biomaterial for cell encapsulation (Murua et al. 2008).

Glicklis and colleagues examined the behavior of rat hepatocytes seeded within a three 3D scaffold based on alginate with diameters of 100-150µm, seeding hepatocytes onto the alginate sponges was efficient. Total cell number within the sponges did not change over 2 weeks demonstrated by DNA measurements indicating that hepatocytes do not proliferate under these culture conditions. Most of the seeded cells were viable and provided function including albumin production and fibronectin synthesis. They concluded that 3D arrangement of hepatocytes within alginate provides a useful environment to facilitate the performance of hepatocytes (Glicklis et al. 2000).

The key elements for alginate microencapsulation for clinical transplantation are biocompatibility, stability, permeability and size of microbeads. These parameters need to be fine-tuned since enhancing one parameter might cause negative effects on other parameters. Moreover, reproducible methods using precise parameters to obtain the optimal quality of microcapsules are important, moreover the technique should not affect cell viability and integrity both during the encapsulation steps, and after transplantation. Indeed, the success for alginate microbeads is maintenance of free exchange of nutrients and oxygen, while waste products are freely secreted simultaneously to avoid swelling and subsequent rupture of microbeads. Capsule breakage would result in functional loss of cells with graft failure and immune rejection (Hernandez et al. 2010; Zimmermann et al. 2005).

A.

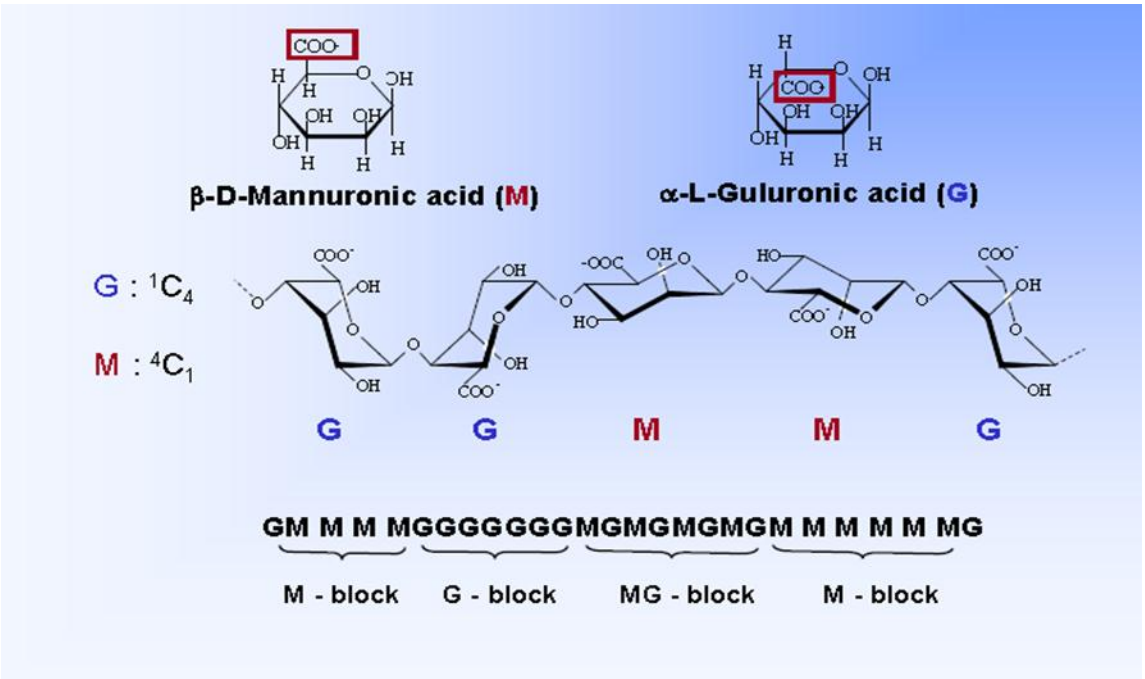

B.

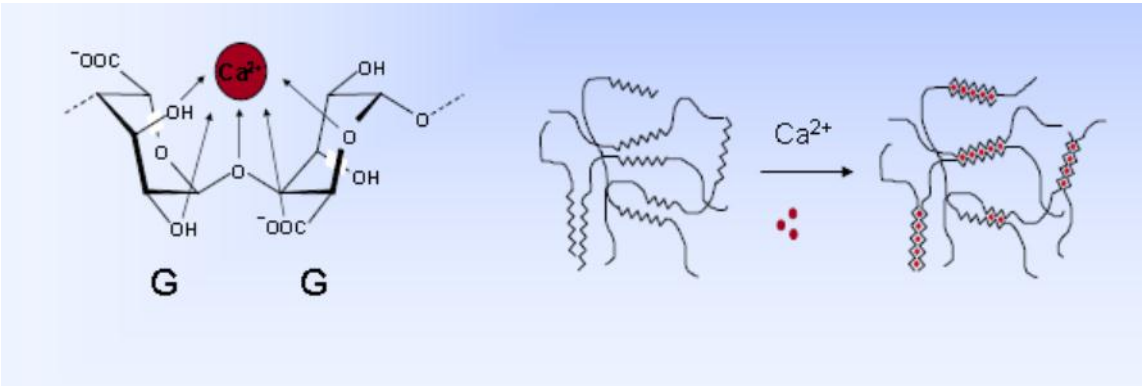

Figure 1.5: (A) The alginate chemical structure, and (B) glucoronate blocks bind the divalent ion, "egg box model". [Adapted from NorvaMatrix].

1.7.1 Biocompatibility

Biocompatibility of alginate microbeads is a critical issue for long-term efficacy following transplantation so that alginate microbeads can function without eliciting any undesirable local or systemic host responses. Numerous studies have explored three main factors which determine the biocompatibility of alginate. Firstly, the degree of alginate purity was shown to be of great importance in determining biocompatibility in both *in vitro* and *in vivo* studies (De Vos et al. 1997; Orive et al. 2002). As alginate is a natural polymer, it is important to minimise endotoxin and protein content which can affect biocompatibility. According to the Food and Drug Administration clinical-grade alginate must have total content of endotoxin < 350EU per

patient. Currently, purified GMP alginates have endotoxin content < 100EU/g. Secondly, the composition of alginate has been an area of controversy as several studies proposed that alginate with high-M content provokes inflammatory responses by stimulating monocytes to produced cytokines e.g. interleukins (IL-1, IL-6), and tumor necrosis factor-α (TNF-α), (Espevik et al. 1993; Otterlei et al. 1991). On the other hand, some studies reported more severe cellular overgrowth in high-G alginate capsules (Clayton et al. 1991; De Vos et al. 1997). Finally, the positive charge of some polycations used such as poly-L-lysine (PLL) on alginate microbeads is shown to be immunogenic. Orive G et al. (2006) found that alginate-PLL-alginate (APA) microbeads activated complement and IL-1 and TNF-α production by macrophages (Orive et al. 2006). Tam et al. (2011) reported that alginate coating was unable to "neutralize" the positive charge of PLL on the membrane, hence did not improve the biocompatibility of alginate-polycation microbeads. Additionally, it has been recognised recently that the implantation procedure of microencapsulated cells itself initiated a host response caused by disruption of host vasculature associated with the release of bioactive proteins such as fibrinogen, thrombin, histamine, and fibronectin. These factors may adhere the microcapsule surface and have a chemotactic effect on inflammatory cells during the first days after implantation. Neutrophils, basophils, lymphocytes are primarily involve in a transient non-specific reaction which gradually disappears from the graft site. Whereas macrophages and some fibroblasts remain attached and lead to pericapsular fibrosis at later stages that interfere with diffusion of nutrients and oxygen supply. Some small cytokines released during a chronic inflammation process might directly damage encapsulated cells leading to cell death and graft failure (De Vos et al. 2006; Orive et al. 2006), (Figure 1.6). The degree of biocompatibility of microbeads can be assessed by evaluation of pericapsular cell overgrowth, viability of encapsulated cells, and recovery rate (retrieval) of microbeads (de Vos et al. 2009) *in vivo*.

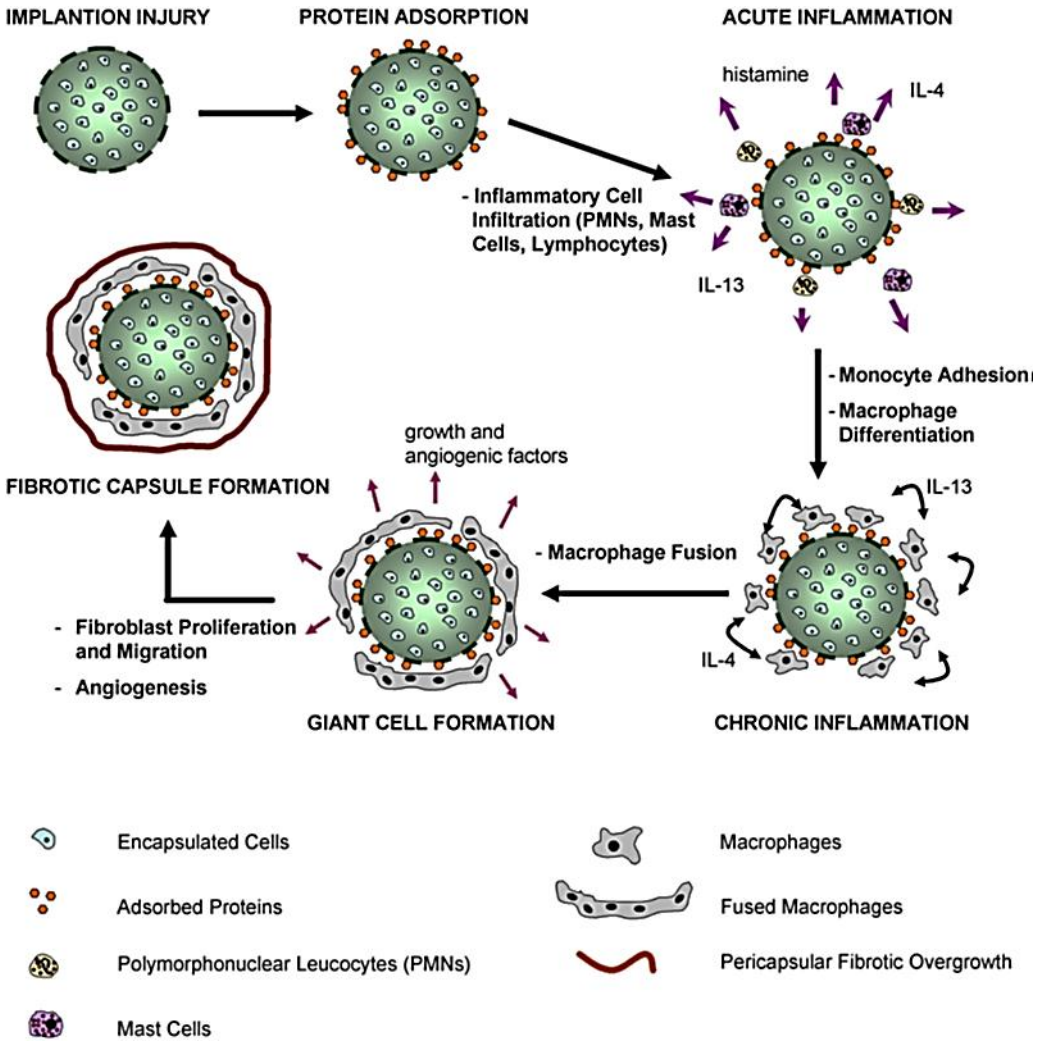

Figure 1.6: A simplified diagram showing the process of acute and chronic inflammatory responses against implanted biomaterial. [Adapted from Hernandez et al. (2010)].

1.7.2 Mechanical Stability of Microbeads

The mechanical properties of microbeads are one of the important factors to ensure the persistent therapeutic efficacy of encapsulated cells. Microbeads applied for transplantation must be durable to maintain their physical integrity for a period as long as the cells function. The mechanical stability of microbeads needed includes stiffness (resistance to deformation) and toughness (resistance to fracture) to structurally protect transplanted cells. Nevertheless, microbeads may lose their mechanical integrity during the transplantation procedure (mechanical stress) or over time post transplantation due to exposure to the hostile environment and immune system in a specific transplantation site (Schmidt et al. 2008; Thanos et al. 2007), (Figure 1.7). Disintegration of microbeads means impaired immunoprotection from the host

response resulting in graft failure. The stability of microbeads mainly depends on the ionic linkage between alginate backbone and the gelling cations; divalent (usually calcium) or polycations. Under physiological conditions, the microbeads show a tendency to disintegrate due to osmotic swelling and calcium ions are constantly exchanged with monovalent ions. In fact, increasing the strength of microbeads has to be carefully adjusted owing to the influence on other parameters such as permeability and intracellular microenvironment (Chang 2005). Up to now, various techniques to improve the mechanical properties and stabilities of have been studied. One strategy to enhance the durability of microbeads is using cations with higher affinity (Mørch et al. 2006). Among divalent cations, Ba^{2+} provides higher mechanical strength of microcapsule than Ca^{2+} and is commonly used to encapsulate pancreatic islets due to long-term durability (Duvivier-Kali et al. 2001; Li et al. 2006). Zimmermann et al. (2005) produced Ba^{2+}-gelled microbeads of ultrahigh viscosity of alginate (35%M and 65%G) using a crystal gun method strengthening the integrity without impeding flux across the membrane. Although Ba^{2+} offered high affinity, its toxicity is a concern for clinical used. Covalent stabilisation of alginate microbeads has been recently achieved using Staudinger ligation, which is chemoselective ligation of azide and phosphine groups. Gattas-Asfura and Stabler (2009) demonstrated that covalent binding with phosphine-terminated poly (ethylene glycol) conjugated with azide-functionalized alginate provide high resistance against osmotic swelling. Addition of an alginate-tyramine conjugates which could form both ionic crosslinks with Ca^{2+} and covalent links through enzymatic reaction (Sakai and Kawakami 2008). Photoinitaited polymerisation is also popular due to the formation of covalent crosslinks, however, photoinitiator solutions and the free radical generation following initiation of bond formation can lead to cell toxicity (Williams et al. 2005). Coating with polycations such as PLL and poly-L-ornithine (Thanos et al. 2007) on surface of the alginate microbeads have been attempted to improve the stability. The addition of this polymer layer also effect on permeability within microbeads. Therefore, increasing mechanical stability might limit mass transport properties. Moreover, the serious drawback of polycations coating is the poor biocompatibility (Anderson et al. 2008; Orive et al. 2006).

Microbeads mechanical stability can be assessed by many techniques including subjecting microbeads to osmotic shock (osmotic pressure test), applying compressive force, and high speed shaking. None of these techniques is well established. Example: osmotic pressure test in which microbeads are exposed to deleterious solutions causing swelling of capsules is one of the most commonly used assays due to its simplicity (Van Raamsdonk and Chang 2001; Yin et al. 2003).

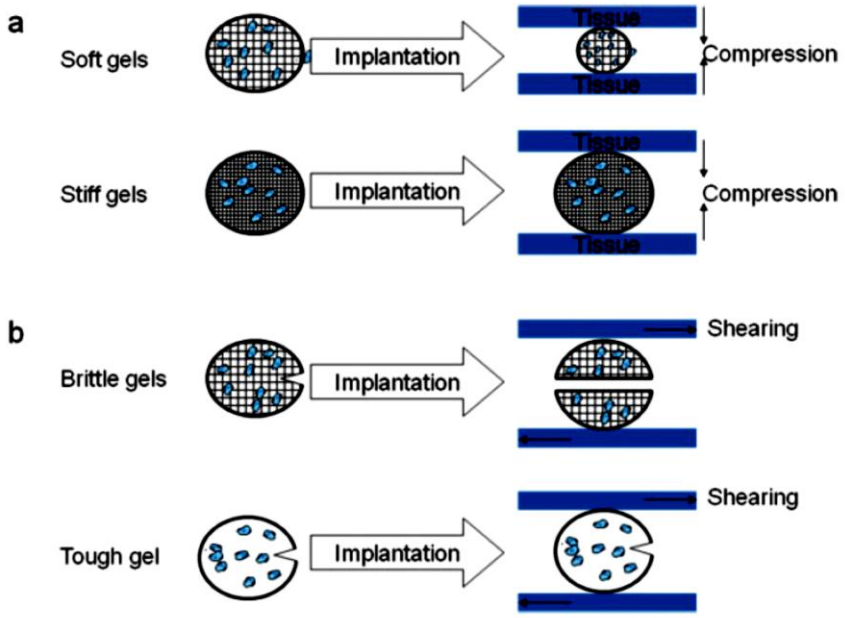

Figure 1.7: The impact of external forces on the structural stability of microbeads. (a) Stiff microbeads maintain their integrity under stress, while (b) brittle and tough microbeads are damaged and fail to protect the cells. [Adapted from Schmidt et al. (2008)].

1.7.3 Permeability of Microbeads

The permeability is a fundamental factor for microbeads as a semi-permeable structure which aims to protect the enclosed cells from host immune response but permits nutrients, oxygen and metabolites to diffuse across microbeads is needed. Metabolic function and viability of cells especially hepatocytes are primarily controlled by transport of oxygen, therefore maintenance of sufficient oxygen levels within microbeads is desirable to avoid local necrotic and/or hypometabolic cells. Even though this basic principle of permeability has been studied for many years, the standard requirement to meet these aims still has not been described. The permeability of microbeads is influenced by several factors including the concentration and composition of alginate electric charge on microbead surface, and actual size of the microbead. Stabler et al (2001) showed that microbeads produced with high molecular weight and concentration of high guluronic acid prolonged diffusion of metabolic molecules and interfered with cell growth. The effect of residue charges, presence of counter ions, polar and hydrophobic interactions on the diffusion of solute have been demonstrated in several studies. The surface charges can be measured by the zeta potential and hydrophilicity. A hydrophilic surface is favored for microbeads because of its high wettability and low water contact angle, whereas hydrophobic surfaces possess a potential for protein adsorption and denaturation leading to immune cells adherence to the surface. Tam et al (2011) showed that a polycation coating on alginate

microbeads increases the hydrophobicity. A negative surface-charge comparable to the encapsulated cell membrane is desirable for microbeads. Similar to hydrophobic surfaces, positive charge stimulate adsorption of protein.

To determine the permeability of microbeads, two main factors are of interest a) the rate of solute diffusion which correlates with mass transfer and diffusion coefficient, and b) the pore size represents the exclusion limit or molecular weight cut-off (MWCO). MCWO defined as a minimum molecular weight of a solute that is entirely rejected by microcapsule membranes (De Vos et al. 2009). Most of the studies only focus on MWCO to measure the permeability. Rokstad et al. (2011) suggested uncoated Ca^{2+}-alginate microbeads are permeable to a molecular weight (MW) up to 350kDa, whilst with coated ones the MWCO is much smaller, 120 kDa (Dixit et al. 1990). Moreover, coated Ba^{2+}-microbeads offer smaller pore size with a MWCO of 70 kDa (Chang and Prakash 1998). However, MWCO is not enough to predict the diffusion properties due to the fact that immersion of microbeads in different solutes results in variation of the alginate/solute interaction. Moreover, non-uniform pore size and their distribution across membranes may play an important role in microbead permeability. Generally, measurement of microbeads permeability is more accurate when using two complementary methods namely size exclusion chromatography with dextran molecular weight standards and a series of biologically relevant proteins using encapsulated protein A–sepharose (Brissova et al. 1998). Recently, a new technique known as the inverse-size exclusion chromatography (ISEC) has been used and this is more reliable since this method provides information on both MWCO and on the pore size distribution (De Vos et al. 2009). Vaithilingam et al determined the permeability of Ba^{2+} microbeads using ISEC and found MWCO of a 250 kDa which is permeable to immunoglobulin G (IgG), (Vaithilingam et al. 2011). Ideally, immunoglobulins should be completely excluded, however several studies shown that even IgG permeate into microbeads the encapsulated cells still survive and function (Kobayashi et al. 2003; Lanza et al. 1995). The molecular weight of substances of interest is shown in Table 1.2.

1.7.4 Microbead Size and Morphology

The spherical shape and suitable size of microbeads is another important factor to take into consideration for optimal permeability, mechanical stability and immunocompatibility. Conventionally, the diameter of microbeads is between 200µm to 3.0mm (Chang 1995). The large size of microbeads may limit an adequate mass transfer properties leading to cellular necrosis as the reduction of surface area-to-volume ratio. Stabler et al (2001) observed cells death in the centre of microbeads with diameter of 0.9-1mm. Canaple et al (2002) reported that

smaller microbeads size (400µm) enhances cell functions by minimising the mass transfer time compared to larger microbeads (1mm). In addition, smaller size microbeads are more biocompatible than the larger microbeads (Sakai et al. 2006). However, reduction in size (<350µm) may lead to decrease in the microbead structural stability (De Vos et al. 1996). Zimmermann et al. (2007) reported that the diameter of microbeads needs to be approximately 600µm for Ba^{2+}-gelled microbeads to achieve maximum stability and permeability.

Physical irregularities of microbeads such as tails, craters and protruding cells may elicit immunological response after transplantation. The studies conducted by De Vos et al have shown cellular overgrowth infiltrating around a defective site of microbeads (De Vos et al. 1996; De Vos et al. 2002).

Table 1.2: Molecular weight of various proteins, antibodies, complements and common metabolites.

Substances	Molecular weight (kDa)	Substances	Molecular weight (kDa)
Immunoglobulin M	950	**Prothrombin**	72
Fibrinogen	340	**Albumin**	66.25
Factor V	330	**Hemoglobin**	64
Complement C4	210	**Tumor necrosis factor**	51
Complement C5	195	**Factor VII**	50
Immunoglobulin E	190	**Nerve growth factor**	13
Complement C3	185	**Insulin**	9
Immunoglobulin A	170	**Complement C3a**	5.73
Complement C2	170	**Complement C5a**	4
Complement C8	163	**Glucose**	0.20
Immunoglobulin D	160	**Tyrosine**	0.16
Immunoglobulin G	150	**Phenylalanine**	0.15
Complement C6	110	**Glutamine**	0.13
Complement C7	100	**Asparagine**	0.11
Complement C9	79	**Oxygen (O_2)**	0.03

1.8 Microencapsulated Hepatocytes

Microencapsulated hepatocytes (hepatocyte microbeads) were initially developed as a means to improve bioartificial liver support system studies in pre-clinical ALF animal models. The microbead structure protects cells from mechanical forces such as shear force, and also from the direct effect of toxic substances in liver failure plasma (Nagaki et al. 2005). Transplanting hepatocyte microbeads can functionally replace the missing metabolic and synthetic function of damaged hepatocytes either for a short period bridging an ALF patient to OLT or to allow liver regeneration potential recovery without the need for OLT. Intraperitoneal transplantation offers considerable advantages in treatment of patients with ALF, without the requirement for immunosuppression.

1.8.1 Microencapsulated Cells for Bioartificial Liver

Fundamentally, a bioartificial liver system should consist of a large amount of functional hepatocytes able to support or stabilise the critical condition of ALF. Hepatocyte cell lines such as HepG2, C3A and hepatocytes are the most investigated alternative source of cells instead of primary human hepatocytes. Originally, these cells were placed in a bioreactor with direct contact of patient blood and/or plasma flow, without secure barriers. Therefore, researchers developed systems to address this problem by placing hepatocytes as spheroids in hollow-fibers, or microcarriers coated with various biological matrices (Lazar et al. 1995; Nyberg et al. 1993; Rozga et al. 1993). However, these systems could not provide an adequate immunoprotective barrier. Hence, microencapsulated cells became the method of interest to overcome this challenge. Joly et al. (1997) showed that microencapsulated porcine hepatocytes provided function and protected cells from large molecular weight molecules, such as immunoglobulins suitable for the design of an extracorporeal bioartificial liver (Joly et al. 1997). Several studies have shown that alginate encapsulation of hepatocyte-derived cell lines enhances proliferation with the expression of differentiated hepatocyte function compared with conventional monolayer culture (Kinasiewicz et al. 2008; Rahman et al. 2004; Selden et al. 1999). Khalil et al (2001) encapsulated HepG2 and cultured them for 8-9 days to let cells proliferate and then form multiple colonies inside. The synthetic and detoxificatory liver functions of HepG2 were significantly increased with encapsulated liver cell spheroids (ELS). Moreover, these ELS showed the ability to maintain their function in human liver failure plasma due to a protective effect by alginate encapsulation (Coward et al. 2009). Another potential advantage of microbeads is cryopreservability with recovery of function on thawing in a highly-convenient physical form, so as to be ready for charging an extracorporeal device when needed. Currently,

the studies in the field of bioartificial liver are continuing with the aim to address the challenge of design and production of the devices (Table 1.3) and scale-up from bench to bedside with microbeads. The preclinical studies using microbeads in a bioartificial liver device are shown in Table 1.4.

Table 1.3: The main design constraints for bioartificial livers (Chan et al. 2004).

Parameter/component	Desired value and property
Minimum functional capacity	1%-10% of liver
Maximum promising volume	1L
Maximum distance between cells and nutrient supply	1mm
Maximum size of cell aggregates	100μm
Scaffold material	Biocompatible and supports hepatocytes differentiated function

Table 1.4: Published preclinical data of bioartificial livers using microencapsulated cells for ALF

Cells	ALF animal model	Outcome	Study
HepG2			
	Rabbit; acetaminophen	Improved systemic parameter of liver failure	Rahman et al.(2004)
	Pig; hepatic artery ligation	Improved biochemical parameters of liver failure	Selden et al. (2013)
Porcine hepatocytes			
	Rat; hepatectomy (95%)	Increased survival rate	Sarkis et al. (2000)[a]
	Pig; D-galactosamine (iv)	Prolonged survival time and improved biochemical parameters	Lv et al. (2011)[b]
	Pig; portahepatis ligation	Improved encephalopathy	Desille et al. (2002)
	Dog; portacaval shunt and CBD ligation	Improved survival rate and biochemical parameters	Chen et al. (2003)

[a]Internal bioartificial liver device, [b]alginate/chitosan microbeads. Abbreviation: CBD, common bile duct; and iv, intravenous.

1.8.2 Microencapsulated Cells for Transplantation

The concept of hepatocyte microencapsulation for treatment of liver diseases such as ALF and metabolic liver disease has been investigated for over two decades. Since 1986, Wong and Chang showed encouraging results of microencapsulated hepatocytes for treatment of ALF in a rat model. One year later Sun et al. (1987) successfully encapsulated rat hepatocytes using a modified alginate-polylysine membrane and demonstrated superior viability and function *in vitro* and after transplantation in the peritoneal cavity of rats for 35 days. The work from the same group highlighted that microencapsulated hepatocytes continued to function *in vitro* up to 5 weeks. The encapsulated cells produced urea, prothrombin and cholinesterase activity into the medium.

Transplantation of microencapsulated hepatocytes as both allo-and xenograft has been extensively studied in animal models without the use of immunosuppression. Intraperitoneal transplantation is the most common site used for microbeads in all studies reported except one that carried out intrasplenic administration (Aoki et al. 2005). Most of the studies have been done using small animals. Only a few studies have been conducted in larger animals for example Khan and co-workers (1995) studied ureagenesis of retrieved microcapsulated rat hepatocytes in normal rabbits. Rodents were the main animal models used including the Gunn rat (Crigler-Najjar type I), Wistar rat, Lewis rat and C57BL/6 mice. The outcome of transplantation of microencapsulated hepatocytes in Gunn rats showed a significant reduction of hyperbilirubinemia (Dixit et al. 1990; Bruni and Chang 1991), and repeated (monthly) transplantation provided long-term correction of hyperbilirubin without any complications (Dixit et al. 1992). Dixit et al. (1993) investigated morphology and function of hepatocyte microbeads after transplantation in Gunn rats with congenital hyperbilirubinemia for 6 months. The hepatocytes in the microbeads remained functioning for 4-6 weeks while viability decreased to 50% by the 4th week and almost all cells were dead by the 8th week. In terms of morphology, the number of broken or damaged microbeads was higher than intact ones after 2 months of transplantation and started to further disintegrate. At six months no intact microbeads could be recovered from the peritoneal cavity. In addition, numerous microbeads were attached throughout the omentum with neo-vascularisation at one month post-transplantation. In contrast, all empty microcapsules appeared intact and dispersed throughout the peritoneal cavity until 6 months.

In the preclinical setting, a number of approaches such as surgical models and the use of hepatotoxic drugs have been developed to induce ALF in a wide variety of animals. Ideally, the model should provide a similar pattern to humans with well-defined clinical and biochemical

criteria (Newsome et al. 2000). Terblanche and Hickman (1991) established the main criteria for an ALF animal model which are widely accepted in research. The model should be reversible, suitable for treatment to improve survival, and reproducible giving the recognised clinical course (biochemical, histological and clinical changes) and interval of death from ALF. The animal size should large enough to permit sufficient blood and tissue samples for analysis. Finally, any method used must represent the minimal risk for researchers. The different approaches to induce ALF possess individual advantage and disadvantages. Surgical models by partial/total hepatectomy lack the effect of inflammatory mediators produced by damaged/necrotic hepatocytes and may lack the possibility for reversibility. These limitations are overcome in a hepatic ischemic model, however the complexity of the surgical procedure require high surgical skills. Whereas chemical models including drugs and toxins are less complex and commonly used, the difficulties of reproducibility which may be due to animal-to-animal variability and/or extrahepatic toxicity are the main concerns. Nevertheless, until now, none of the models is considered to reflect human ALF (Newsome et al. 2000; Tuñón et al. 2009).

Studies of microencapsulated hepatocytes have been performed in ALF animal models and most of them showed promising outcome of both freshly prepared or cryopreserved microencapsulated cells by improving survival rate and biochemical parameters of liver failure (Table 1.5). The total cell number transplanted as microcapsules required to support the ALF condition varies greatly between studies. Some studies suggested that transplantation of microencapsulated hepatocytes constituting less than 5% of the total liver mass was sufficient for supporting the failing liver and prolonging survival rate of the animals (Umehara et al. 2001; Aoki et al. 2005). However, the optimal cell number required in ALF models remains controversial. Although the results of microencapsulated cells for treating ALF are promising in preclinical studies, nearly all studies were done in rodents. The effect of treatment probably should be evaluated in large animal models prior to translation to clinical use. Recently, Machaidze et al. (2011) demonstrated that porcine hepatocyte microbeads improved metabolic function and survival in baboons with ALF [poster presentation at Cell Transplantation Society meeting, Miami 23-26 October, 2011].

Over the past few years, several groups have studied methods to improve hepatocyte specific function and prolong their viability. Co-culturing hepatocytes with different cell types including epithelial-like cells, fibroblast like cells and mesenchymal stem cells are some of these approaches. Liu Z et al. (2000) demonstrated the beneficial effect of allogenic bone marrow cells on hepatocytes when co-cultured or co-encapsulated compared to hepatocytes alone by providing longer viability. Shi and co-workers (2009) obtained similar results for co-

encapsulated hepatocytes with bone marrow mesenchymal stem cells (MSCs). They observed improvement of liver function and survival rate of rats with ALF after transplantation of co-encapsulated cells. In addition, some MSCs transdifferentiated into hepatocyte-like cells after transplantation which expressed albumin and other hepatocyte specific markers. Co-encapsulated hepatocytes with others cells have been shown to have greater function *in vitro* and improve survival rate of animals with ALF as shown in Table 1.6. The mechanisms which underlie the cooperative effect of co-encapsulation with other cell types have not been clearly elucidated. Presumptive mechanisms responsible may be from direct cell-cell and cell-matrix contact or paracrine effects on hepatocytes (Liu and Chang 2002; Shi et al. 2009). Nevertheless, the therapeutic use of stem cells or transgenic cells is not ready for clinical use because it would expose patients to the risk of cancer.

Table 1.5: Summarised data of microencapsulated hepatocyte transplantation in preclinical studies

Study	Donors/ Recipients	ALF model	Type of microcapsule	Cell number/ animal	Outcome	Reference
1	Rats/Rats	D-galactosamine	APA-liquid core	NA	Improved survival rate	Wong and Chang (1986)
2	Rats/Rats	D-galactosamine	APA-liquid core	NA	Improved survival rate Viable cells in recovered microcapsules	Sun et al. (1987)
3	Rats/Rats	D-galactosamine	APA-liquid core	NA	Improved survival rate	Cai et al. (1988)
4	Rats/Mice	D-galactosamine	APA-liquid core	NA	Viability of recovered microcapsules was increased	Wong and Chang (1988)
5	Rats/Gunn Rats[a]	NA	APA-solid core	$1x10^7$	Reduced serum bilirubin	Dixit et al. (1990)
6	Pigs/Rats	D-galactosamine	APA-solid core	$5x10^7$	Improved survival rate	Rivas-Vetencourt et al. (1997)
7	Rats/Rats	3-stage total hepatectomy	APA-solid core	$4x10^7$	Improved survival rate Decreased ammonia	Umehara et al. (2001)
8	Rats/Rats	90% hepatectomy	APA-solid core (IS)	$2x10^7$	Improved survival rate Enable liver regeneration Viable cells in recovered microcapsules	Aoki et al. (2005)

Table 1.5: (Continued)

Study	Donors/ Recipients	ALF model	Type of microcapsule	Cell number/ animal	Outcome	Reference
9	Mice, rats, IHH/ mice	Acetaminophen & 30% hepatectomy	APA-liquid core	$5x10^7$	Improved survival rate	Mai et al. (2005)[b]
10	Pigs/Mice	Acetaminophen & 30% hepatectomy	APA-liquid core	$5x10^7$	Improved survival rate	Mei et al. (2009)[b]
11	Rats, IHH/Mice	Acetaminophen & 30% hepatectomy	APA-liquid core	$4x10^7$	Improved survival rate without modifying liver regeneration	Sgroi et al. (2011)
12	Pigs/Baboons	75% hepatectomy & warm ischemia	APA-liquid core	NA	Improved survival rate and metabolic function	Machaidze et al (2011)[c]
13	Human (UBC)[d]/ Rats	D-galactosamine	APA- sold core	$2x10^6$	Improved survival rate and metabolic function	Zhang et al. (2011)

[a] Gunn rat is a model for congenital unconjugated hyperbilirubinemia; [b] also used cryopreserved microencapsulated hepatocytes for transplantation; [c]poster presentation at Cell Transplantation Society meeting, Miami 23-26 October, 2011; [d] hepatic like-cells from human umbilical cord blood. Abbreviation: APA, alginate-poly-L-lysine-alginate; IHH, immortalised human hepatocytes; IS, Intrasplenic transplantation; and NA, not available.

Table 1.6: Summary of co-encapsulated hepatocytes with other cells transplantation in preclinical studies

Study	Encapsulated cells	Animal model	Type of microcapsule	Cell number/ animal	Outcome	Reference
1	Rat HC+BMSC	Normal rats	APA-liquid core	HC $2x10^7$ BMSC $1x10^7$	Improved viability of microcapsule up to 4 months post transplantation[(a)]	Liu and Chang (2002)
2	Rat HC+BMSC	Rat with D-galactosamine	APA-liquid core	HC $3.3x10^7$ BMSC $1.7x10^7$	Improved survival rate and metabolic function [(a)]	Shi et al. (2009)
3	Rat HC+hFLSC or hFLSC/bFGF	Mice with 70% hepatectomy	APA-solid core	HC $1.25x10^6$ hFLSC or hFLSC/ bFGF $0.18x10^7$	Improved survival rate, metabolic function and liver regeneration[(b)]	Teng et al. (2010)
4	Rat HC+HUVECs	Rat with D-galactosamine	APA-liquid core	HC $5x10^6$ HUVEC $5x10^6$	Improved survival rate and metabolic function[(a)]	Qiu et al. (2012)

[(a)] Statistically significant when compared to microencapsulated hepatocytes and empty capsules and [(b)] statistically significant when compared to microencapsulated hepatocytes and co-microencapsulated hepatocytes with hFLSCs. Abbreviation: APA, alginate-poly-L-lysine-alginate; bFGF, basic fibroblast growth factor; BMSCs, bone marrow mesenchymal stem cells; HC, hepatocytes; hFLSC, human fetal liver stromal cells; and HUVECs, human umbilical vein endothelial cells.

1.9 Cryopreservation

Cryopreservation of hepatocytes for long-term storage and availability in an emergency with high quality of cells is key issue in cell therapy for both direct transplantation and bioartificial liver support. The fundamental of cryopreservation is to preserve the cells by rapid cooling down until freezing and then storing at low temperature over a period of time. The challenge of this method is how to freeze the cells without damaging the cellular structure or metabolism and maintain high viability after recovering the cells (Fuller 2004).

The difficulty of developing a good cryopreservation procedure is due to the cells being subjected to hostile conditions during both freezing and thawing steps. When the temperature drops from 37°C to <–140°C (Karlsson and Toner 1996), biophysical changes occur and water will transfer to a crystalline state resulting in ice crystal formation which is the key basis of cell damage. Once ice formation has started, the electrolyte concentration surrounding the cells is greatly increased, and then intracellular water will diffuse outward by osmosis causing cell shrinkage. The extent of cell dehydration depends on the rate of cooling. Cells may acquire equilibrium with external solution when reaching sufficiently low temperature (<–80°C), osmotic shrinking gives adequate highly viscosity of the intracellular compartment so that the cells eventually vitrify which is relatively stable for preservation (Fuller 2004). However, if the cooling is slower than the optimum rate, cells encounter extreme osmotic loss of water and cells will collapse on themselves (plasmolysis). Cell death due to prolong exposure to hypertonic conditions may occur since the stress of dehydration damages the ultrastructure of cell membranes (destabilisation of lipid bilayer and solubilisation of membrane protein), and denatures proteins. On the other hand, rapid freezing does not allow sufficient time for water to diffuse and equilibrate between intra-and extracellular components. Consequently, the intracellular water rapidly freezes and forms intracellular ice crystals which can disrupt intracellular structures and the plasma membrane (Mazur 1970). Thawing is another critical step that might cause detrimental effects on cells with the influences of temperature and osmotic changes. If the thawing rate is too slow then the intracellular ice will reform and coalesce into larger crystals and damage cell membranes. Furthermore, rapidly dilution of cryoprotectant by ice-cold medium may generate concentration gradients leading to osmotic shock due to inflow of water into the cells. Therefore, optimisation of freezing and thawing is important to prevent mechanical damage from excess intracellular water loss and ice formation (Loretz et al. 1989; Pegg 2002). Another mechanism involved in cell death during cryopreservation is apoptosis. Apoptosis of cells, such as hepatocytes, has been initiated during isolation due to the separation

of anchorage-dependent cells from ECM, known as anoikis (Cardone et al. 1997; Frisch and Francis 1994). Nevertheless, the specific mechanism of cryopreservation-induced apoptosis remains unclear. Yaki and colleagues (2001) suggested that the possible underlying mechanisms are continued anoikis which activates pro-apoptotic cascade including caspases or from the release of cytochrome c from damaged mitochondria to stimulate caspase activation. Hepatocytes are very sensitive to cryoinjury, therefore the need of optimisation of cryopreservation technique is essential. Numerous studies have investigated a wide range of modifications in each step including pretreatment of cells prior freezing, rate of freezing, cryoprotectant, basal freezing medium and thawing cells.

1.9.1 Pretreatment of Cell Prior Freezing

The quality of cells before freezing is one of the important factors to achieve high yield and viable cells after thawing. Percoll® purification has been used to remove dead cells from the cell suspension to improve viability, however, a great amount of cell loss was observed. In addition Percoll is not suitable in clinical use. Pretreatment of hepatocytes by incubating with cryoprotective substances that enhance cellular adenosine triphosphate (ATP) or antioxidants such as fructose and/or alpha-lipoic acid and glucose and insulin showed improvement of viability and attachment of recovered cells (Loven et al. 2005; Terry et al. 2005).

1.9.2 Cryoprotectants

Cryoprotectant is an additive compound that provides protective effect for cells throughout the cryopreservation process (Karlsson and Toner 1996; Fuller 2004). Cryoprotectants are classified into two types based on their ability to pass through cell membranes. First are permeating cryoprotectants such as DMSO, glycerol and 1,2-propanediol. The second group is non-permeating including sugars, polyvinyl pyrrolidone, and hydroxyethyl starch. Up to date, DMSO is the most commonly used. DMSO rapidly permeates into cells to bind to water which then decreases ice crystal formation. It interacts electrostatically with phospholipid bilayers and preserves membrane integrity during freeze-thaw. In addition, DMSO is an oxygen free radical scavenger which is an enhancing factor for cryoprotectants (Fuller 2004). However, DMSO has unfavorable effects at high concentration and high temperature and is potentially toxic to the cells. Different concentrations of DMSO used for cryopreservation have been studied and 10% is the most effective and commonly used (Terry et al. 2006). The addition of DMSO is usually carried out at 4°C. More recently, studies have shown that trehalose provide protective effect on cellular membrane during different stress condition (Katenz et al. 2007).

1.9.3 Basal Freezing Solution

Many different freezing solutions have been used for hepatocyte cryopreservation. Some studies use culture medium (WEM or DMEM) with or without FCS and simply add cryoprotectants before freezing. However, use of FCS is limited to research use due to the possible of adverse reactions and zoonosis. Arikura and co-workers demonstrated that University of Wisconsin (UW) solution which was originally developed for hypothermic preservation of organs provided cytoprotective effect during cryopreservation of rat hepatocytes (Arikura et al. 2002). UW is an intracellular-based solution containing several useful components including lactobionate which prevents cell edema and acidosis, hydroxyethyl starch and raffinose increase the intracellular osmotic pressure and support the cell membrane. In addition, UW also consists of glutathione adenosine (suppress oxidative stress) and allopurinol (stimulates ATP synthesis). HypoThermosol (HTS), another hypothermic preservation solution was studied by Sosef et al. (2005). They reported that using HTS for cryopreservation reduced the level of cell death and provided high viability and hepatocyte function of rat hepatocytes.

1.9.4 Freezing Protocols and Storage

Currently, most of the freezing protocols are based on Diener et al (1993) using multi-step slow cooling protocols in a controlled rate freezer (CRF). They introduce the key steps of the rapid cooling at the point when crystallisation is expected to occur to prevent the heat latent fusion and control ice nucleation, and a "hold" step to achieve enough cellular dehydration, and consequently diminish the risk of intracellular ice formation. The slow-controlled rate freezing protocol is generally accepted as the best strategy for cryopreservation of hepatocytes. A more simple technique and still use in laboratories is using isopropanol progressive freezing container, "Mr. Frosty", to freeze the cells at a constant rate of -1°C/min by placing them in -80°C freezers (Alexandre et al. 2002). However, the rate of freezing might not be constant and thus cause damage to the cells. Other method is direct freezing in freezers (-20°C and -80°C) for a period of time and then plunged into liquid nitrogen (Chesné and Guillouzo 1988; Swales et al. 1996).

The storage after freezing should be keep at temperature less than -130°C at which no chemical reactions occur. Therefore, cells can be stored and the recovery with viable function can be maintained for years (Mazur 1984; Chesné et al. 1993).

1.9.5 Thawing

Rapid thawing at 37°C with slow dilution of cryoprotectants with ice cold medium is the well-known optimal protocol used. This method prevents cell damage from ice crystal reformation, osmotic shock and toxicity of cryoprotectants. Some studies added substances to the thawing solution to minimise osmotic shock after thawing (Chesné and Guillouzo 1988; Swales et al. 1996; Baust et al. 2002). Human serum albumin was also added in thawing medium for clinical use (Mitry et al. 2010).

Cryopreservation of hepatocytes has been extensively investigated and developed since 1980s (Fuller et al. 1980; Chesné and Guillouzo 1988; Loretz et al. 1989). Many groups have attempted to develop new cryopreservation protocols to adequately protect hepatocytes (Adams et al. 1995; Hengstler et al. 2000; Ostrowska et al. 2000; Katenz et al. 2007; Terry et al. 2010); nevertheless, optimum results without cell damage have not been obtained so far (Stéphenne et al. 2010).

1.10 Cryopreservation of Hepatocyte Microbeads

With hepatocytes in conventional storage conditions (cell suspension) the cell membrane is no longer supported by extracellular matrix which may lead to vulnerability of the outer cytoskeletal structure (Koebe et al. 1999). Microencapsulation is an attractive technique for protecting hepatocytes against freezing injury. In 1993, Dixit et al cryopreserved microencapsulated rat hepatocytes in a freezing solution consisting of 10% DMSO, 20% FCS and 70% RPMI kept at -70°C for 24h and then stored in liquid nitrogen. They reported that cryopreserved encapsulated hepatocytes provided comparable function to cells in culture and in Gunn rats. These findings highlighted the possible protective effects of microencapsulation for cryopreservation processes. More recently, Aoki and his team studied hepatic function, viability and morphology of cryopreserved microencapsulated rat and human hepatocytes *in vitro* and after transplantation into rat spleen. They found that these cryopreserved microbeads retained hepatocyte function with high viability after thawing and transplantation (Aoki et al. 2005). The mechanisms of protection started to be elucidated by Mahler et al (2003). They described that the alginate gel keeps hepatocytes separate from each other avoiding mechanical stress from compaction when extracellular fluid decreases and may help support hepatocyte plasma membranes. In addition, alginate also prevented cold-induced apoptosis in hepatocytes indicated by low level of caspase 3 activity in encapsulated cells. Kusano et al. (2008) studied alginate microbeads in depth using cryomicroscopy during the freezing and thawing processes and

compared the ultrastructure of encapsulated and nonencapsulated cells to examine the extent of injury. The findings showed that alginate gel protects hepatocytes from physical damage caused by ice crystal formation (Kusano et al. 2008). However, alginate gel used in encapsulation is water rich, which might complicate cryopreservation and therefore optimisation of cryopreservation procedures is needed.

1.11 Alginate Encapsulated Hepatocyte Transplantation in ALF-A Pilot Study

In humans, there are no previous published studies using hepatocytes microbeads for treatment of liver diseases. However, therapeutic application of microencapsulated islets has been reported in type 1 diabetic patients with promising outcome (Soon-Shiong et al. 1994; Calafiore et al. 2006; Basta et al. 2011). An open-label study of neonatal porcine islets encapsulated in alginate microcapsule (Diabecell®) in patients with type 1 diabetes is currently recruiting patients. To date, King's College Hospital is the only centre that has started a pilot study of treatment of children with ALF by intraperitoneal transplantation of human hepatocyte microbeads. The study is in progress, and the results are encouraging.

However, due to shortage of donor organs and lack of availability of freshly isolated hepatocytes, cryopreserved cells were used for the preparation of the microbeads transplanted in these patients. Although the outcome was promising, the disadvantage of using cryopreserved cells is their lower viability compared to fresh cells. Therefore, establishment of an optimised protocol for cryopreservation of encapsulated hepatocytes that could to lead to preservation of cell viability, synthetic and metabolic activities on thawing is needed. The main advantages of this process are to have readily available "high" quality hepatocyte microbeads for clinical transplantation, and also save time spent on thawing cryopreserved cells followed by encapsulation

1.12 Hypothesis and Aims

1.12.1 Hypothesis

Optimisation of protocols for production and cryopreservation of GMP grade alginate microencapsulated human hepatocytes (microbeads) would lead to enhanced cell function and activity, and could be used for clinical transplantation. If cryopreservation of clinical grader microbeads is successful, it would be advantageous as they will be available for immediate use in emergency case.

1.12.2 Aims

- To optimise methods for alginate human hepatocyte microbeads production using GMP grade materials
- To investigate the alloimmune response towards clinical grade human hepatocyte microbeads
- To carry out investigation aiming at establishing an optimised cryopreservation protocol for human and rat hepatocyte microbeads
- To investigate the efficacy and safety of fresh and cryopreserved hepatocyte microbeads in an animal model of acute liver failure

CHAPTER 2

2. General Material and Methods

2.1 Materials

All chemicals and buffer solutions were purchased from Sigma-Aldrich Ltd. (Gillimgham, UK), unless otherwise stated.

2.1.1 Equipment

Encapsulator (Model: IE-50R; Inotech Encapsulation AG, Dottikon, Switzerland), Dynex MRX plate reader (Dynex Technologies Ltd., West Sussex, UK), TecanGeNios Pro plate reader (Tecan Group Ltd., Männedrof, Switzerland), and fluorescent microscope (Leica microsystems Ltd., Milton Keynes, UK).

2.1.2 Hepatocytes Isolation Buffer Solutions and Chemicals

Hank's balanced salt solution (HBSS) without calcium or magnesium, Eagle's Minimum Essential Medium (EMEM) without phenol red and with calcium and magnesium, and 1M 4-(2-hydroxyethyl)-1-piperazine-ethanesulfonic acid (HEPES; Lonza Vervieres, S.p.r.l Vervieres, Belgium), ethylene glycol tetraacetic acid (EGTA; Sigma-Aldrich Company Ltd., Dorset, UK). Collagenase P (Roche, East Sussex, UK), Earle's Balanced Salt Solution (EBSS; Life Technologies, Paisley, UK), isoflurane (Abbott Laboratories, Queenborough, UK), Heparin 1,000 IU/ml (CP Pharmaceuticals Ltd., Wrexham, UK), intravascular catheters (Jelco®; Smiths Medical International Ltd., Lancashire, UK), 2-0 Vicryl® sutures (Ethicon Inc. Livingston, Scotland), 4-0 silk suture (Harvard Apparatus Ltd., Kent, UK), silicon-rubber tubing (Masterflex®; Cole Palmer, Hanwell, UK), sterile non-woven swabs (10cm x 10cm; Shermond, Brighton, UK), two hundred micrometer nylon Cell MicroSieves™ (BioDesign Inc. of New York, NY, USA).

2.1.3 Cell and Microbeads Culture

Phenol red-free William's E medium (WEM), heat-inactivated foetal calf serum (FCS), 2mM L-glutamine, dexamethasone (100x), insulin (bovine pancreas, 100x), penicillin/streptomycin

(Sigma-Aldrich Company Ltd., Gillingham, UK.), CMRL medium (Mediatech, Inc., Vancouver, Canada), 6-well, 12-well, 24-well and 96-well plates (Nunc Nalgene, Hereford, UK).

2.1.4 Encapsulation

Highly purified sodium alginate; low viscosity and high glucoronic acid (PRONOVA™ SLG20; NovaMatrix, Sandvika, Norway). 0.9% Sodium chloride (0.9% NaCl; Baxter Healthcare Ltd., Norfolk, UK.), calcium chloride (Arum Pharmaceuticals Ltd., Romford, UK).

2.1.5 Cryopreservation and Thawing

University of Wisconsin (UW) solution (Bristol-Myers Squibb AB, Hounslow, UK), DMSO (WAK-Chemie Medical GmbH, Steinbac, Germany), controlled-rate freezer (Planer, Model: Kryo10 CRF; Planer plc, Middlesex, UK), 50% glucose (Hamlin, Pharmaceuticals Ltd., Gloucester, UK.), Cryovial® (2.0ml and 5.0ml; Elkay Laboratories products UK Ltd., Hampshire, UK), human serum albumin (20%; Baxter Medical AB, Berkshire, UK).

2.1.6 Chemicals and Solutions

Dulbecco's Phosphate-Buffered Saline (DPBS; Gibco, Paisley, UK), VECTASHIELD Mounting media (Vector laboratories Ltd., Peterborough, UK), phosphate-buffered saline (PBS; Life Technologies, Paisley, UK), and ß -glucuronidase/arylsulfatase (Roche, East Sussex, UK).

2.2 Methods

2.2.1 Human Hepatocyte Isolation

Human hepatocytes were isolated from donor liver tissue (rejected or unused for transplantation) or the non-tumoural margin of liver resections from metastatic cancer cases. All tissues were consented for research in accordance with the Research Ethics Committee of King's College Hospital. The donor tissues were maintained in UW solution, while liver tissues from surgical resection were flushed with ice-cold HBSS to remove blood before isolation. The hepatocyte isolation was carried out using a modified collagenase perfusion method based on a published protocol (Mitry 2009). This technique involves the uses of three buffer solutions. The

first solution consists of EGTA (a calcium chelating agent) which breaks the desmosomal junctions of adjacent hepatocytes. The second is plain HBSS to wash out the EGTA and the last solution contains the tissue digestion enzyme collagenase. Briefly, major blood vessels on tissue cut surface were cannulated and the cannulae secured in place by suturing. Smaller blood vessels were sealed to prevent leakage of perfusion solutions. The three buffer solutions were prepared under sterile conditions in a laminar flow cabinet, and maintained at 37°C with oxygenation throughout the perfusion. The tissue was perfused with the first solution [calcium-free HBSS+1M HEPES+0.5mM EGTA]. The liver tissue was then perfused with plain calcium-free HBSS, followed by EMEM containing 0.05% collagenase P. The volume of perfusion solution used varied according to the size of liver tissue. In addition, re-circulation of collagenase solution was carried out until the tissue was well digested. The cannulae and sutures were removed, and the digested tissue was minced in ice-cold EMEM using a pair of sterile scissors. The released cell suspension was passed through two layers of sterile swabs (gauze). Hepatocytes were purified by washing three times with ice-cold EMEM and centrifugation at 50xg, 4°C for 4min. The total number of hepatocytes and viability were estimated using the standard trypan blue exclusion test. All hepatocytes prepared in this study are summarised in Appendix I and II.

2.2.2 Rat Hepatocyte Isolation

Rat liver was obtained from 200-400g, 8-12 wks old, male Sprague Dawley rats (Harlan Olec, Bicester, UK). Animals were housed and received care according to the UK Animal (Scientific) Procedures Act of 1986 and the ethical review process of King's College London. Animals were housed under a 12-hour light-dark cycle in a room with temperature 21±2°C and humidity 55±10%, and allowed to acclimatise to these conditions for at least 7 days before use. Hepatocyte isolation was performed using *in situ* collagenase perfusion technique of the liver as previously published (Wu and Gupta 2009); (Neufeld 1997) with some modifications. Three perfusion buffer solutions were buffer 1 (EBSS 1M HEPES+0.5mM EGTA), buffer 2 (plain EBSS) and buffer 3 (2mM $CaCl_2$+0.025% collagenase P). All solutions were adjusted to pH 7.4 and kept at 37°C in water bath and delivered with a peristaltic pump (Waterson-Marlow 313, Watson-Marlow Limited, Falmouth, UK). The animals were anesthetised with isoflurane inhalation for the procedure. The rats were secured by taping down the extremities, and then the abdominal area was shaved and disinfected with 70% ethanol. A mid-line laparotomy incision was performed followed by injection of 100IU of heparin into the inferior vena cava. A 20-guage intravascular catheter (Jelco®) was inserted in the portal vein, placed and secured just before the bifurcation with 2-0 silk suture. Liver perfusion with buffer 1 was immediately

started at the rate of 20ml/min for 5min. To drain the solution, the abdominal aorta was cut after initiating the perfusion. The chest cavity was then opened to insert another cannula, 14-guage, into the right atrium via the superior vena cava. The outflow end of the pumping system was then transferred from the cannula in the portal vein to the cannula in the heart. The tissue was then perfused with buffer 2 for 5min, followed by buffer 3 which contained collagenase for 10min or until the liver was completely digested. The digested liver was immediately removed into a sterile plastic bowl containing 50ml ice-cold EMEM, and the tissue gently minced to release the cells. Cell suspension was filtered through swabs and 200µm nylon mesh. Isolated hepatocytes were purified by 3x low speed centrifugation (50xg, 4°C for 5min) and washed with ice-cold EMEM. The total number of hepatocytes and viability were determined using the standard trypan blue exclusion test.

2.2.3 Cell Viability and Yield -Trypan Blue Exclusion Test

Equal volumes of 0.4% trypan blue and cell suspension were gently mixed and left for 1min at room temperature. The two chambers of a neubauer haemocytometer were each filled with 10µl of cell/trypan blue suspension and total cell number and cell viability (clear cells that excluded the dye) were estimated using a light microscope and mean % viability was calculated.

2.2.4 Percoll® Centrifugation

In order to separate the viable hepatocytes and improve the overall percentage of viability, different concentrations of Percoll® and centrifugation settings were tested. Percoll® (1.13g/ml) was mixed with 10x HBSS at 9:1 (v:v). Diluted Percoll® was added to the cell suspension to obtain a final concentration of Percoll® to 15-35% and cell density of less than 1x 10^6cells/ml. The mixture was then centrifuged at 2 different speeds (250xg or 100xg), at 4°C for 10min to separate viable from dead cells. The viable hepatocytes were purified by washing with ice-cold EMEM and centrifuged at 50xg, 4°C for 4min. Total cell number and viability were determined. The optimal setting for human hepatocytes was 25% Percoll® and centrifugation at 200xg, while for rat hepatocytes was 35% Percoll® and centrifugation at 250xg. These settings were used throughout the study.

2.2.5 Culture of Human and Rat Hepatocytes

Isolated human and rat hepatocytes were resuspended in standard hepatocyte culture medium which consisted of WEM supplemented with 10% FCS, 10mM HEPES, 2mM L-glutamine,

0.1μM dexamethasone, 0.1μM insulin, penicillin (50U/ml) and streptomycin (50μg/ml). Hepatocytes were plated in collagen type-I coated 24-, 12- or 6-well plates (Nunc A/S, Roskilde, Denmark) as required, at a density of $1.6x10^5$viable cells/cm^2, and incubated in a humidified incubator at 37°C, 5% CO_2. Serum-free culture medium was also used in some experiments to avoid any effects of FCS on assay measurements.

2.2.5.1 Hepatocyte Protein Content

Hepatocytes seeded onto 24-well plates ($3.0x10^5$viable cells/well) were incubated for 24h. After incubation, total cell lysate was performed based on Mitry et al. (1997). The protein content of each cell lysate sample was determined using the modified Lowry technique (Schacterle and Pollack 1973; Lowry et al. 1951). Briefly, 50μl of alkaline copper reagent was added to the samples and incubated at room temperature (RT) for 10min. The diluted Folin-Ciocalteu's reagent (200μl) was then added, and left for 15min. The duplicates of bovine serum albumin standards (0-1mg) and samples were measured at a 650nm wavelength using Dynex MRX plate reader.

2.2.6 Empty and Human Hepatocyte Microbeads

Empty and human hepatocyte microbeads (EMBs and HMBs) were produced using the IE-50R encapsulator (Inotech Encapsulation AG) using clinical grade and GMP materials. PRONOVA™ SLG20 sodium alginate (low viscosity and high glucoronic acid; NovaMatrix) was dissolved in 0.9% NaCl to give a final concentration of 1.5% alginate solution (w/v), with mixing overnight using a magnetic stirrer. The calcium ion-polymerisation solution consisted of 1.2 % $CaCl_2$ diluted in 0.9% NaCl. The human hepatocyte pellet was gently mixed with alginate solution. The sodium alginate (without or with hepatocytes) was drawn into a 50ml syringe, which was then attached to the encapsulator. EMBs and HMBs were produced using a 250μm nozzle, and polymerised in 1.2% $CaCl_2$ solution for 15min. The microbeads were washed twice (7min each) with 0.9% NaCl to remove excess $CaCl_2$, and finally collected in a sterile flask.

2.2.7 Hepatocyte Microbeads Culture

HMBs were resuspended in culture medium consisting of CMRL medium supplemented with 10% FCS, 2mM L-glutamine, 0.1μM dexamethasone, 0.1μM insulin, penicillin (50U/ml) and streptomycin (50μg/ml). HMBs were cultured in the medium at a ratio of 1:4 (v:v) and

maintained in a humidified incubator at 37°C, 5% CO_2 for 24h up to 7 days. Supernatants were removed and media changed every alternate day.

2.2.7.1 Depolymerisation of Microbeads to Recover Hepatocytes

Six alginate depolymerisation protocols based on previous studies (Ringel et al. 2005; Serra et al. 2011; Hang et al. 2010; Massie et al. 2011) with some modifications were tested. Briefly, 250µl microbeads were placed in a 1.5ml microfuge tube and washed with PBS. Hepatocytes were released from microbeads by mixing with 500µl of depolymerisation solution containing calcium chelators (sodium citrate, EDTA or EGTA) and incubation at either RT or 37°C. The released cells were collected by centrifugation at 100xg for 5min. The yield and viability of the released cells were estimated. The protocol containing 100mM sodium citrate, 10mM HEPES, 150mM NaCl and 0.1% glucose (37°C, 10min) was less detrimental to viability of the released cells with less cell loss compared to pre-encapsulation. This optimised protocol was used throughout the study.

2.2.7.2 Hepatocyte Protein Content in Microbead

After depolymerisation and recovery of the hepatocytes from microbeads, cells were lysed and the measurement of protein concentration was performed using the modified Lowry technique (Section 2.2.5.1).

2.2.8 Cryopreservation Hepatocytes, and Microbeads

The cryopreservation protocol used throughout the study was based on the protocol for cryopreservation of clinical grade human hepatocytes at the Institute of Liver Studies, King's College Hospital, and various cryoprotectants were tested. Table 2.1 shows the standard freezing protocol used at Institute of Liver Studies, King's College Hospital.

2.2.8.1 Cryopreservation of Hepatocytes

Cryopreservation solution consisted of UW solution containing 10% DMSO (v/v) and 5% glucose (v/v) was prepared and maintained on ice. Hepatocytes were pelleted and then resuspended in cryopreservation solutions at the density of $1.0x10^7$cells/ml followed by adding the hepatocytes suspension into cryovials. The cell suspension was then maintained on ice before the freezing process started (Terry et al. 2010).

2.2.8.2 Cryopreservation of Hepatocyte Microbeads

Microbeads (1ml) were slowly mixed with cryopreservation solution (4ml; UW/10% DMSO/ 5% glucose) in 5ml cryovials. The microbeads suspensions were then maintained on ice before transfer to the controlled-rate freezer (CRF). Table 2.1 shows the standard freezing protocol used at the Institute of Liver Studies King's College Hospital.

Table 2.1: Standard CRF protocol for human hepatocytes

Step	Start Temperature	Rate	Time	End Temperature
1	8°C	-1°C/min	8min	0°C
2	0°C	Hold	8min	0°C
3	0°C	-2°C/min	4min	-8°C
4	-8°C	-35°C/min	33sec	-28°C
5	-28°C	-2.5°C/min	2min	-33°C
6	-33°C	+2°C/min	2min	-28°C
7	-28°C	-1°C/min	32min	-60°C
8	-60°C	-10°C/min	4min	-100°C
9	-100°C	-20°C/min	2min	-140°C

When the CRF had reached the start temperature, the cryovials were placed into the tube rack inside the chamber, and the set freezing program was run. After the freezing process was completed, the tubes were immediately transferred to a -140°C freezer and stored for 2 weeks.

2.2.8.3 Thawing Cryopreserved Cells and Microbeads

The thawing protocol was based on published protocols (Terry et al. 2010; Steinberg et al. 1999). Briefly, frozen cell suspension was quickly thawed using a 37°C water bath with gentle shaking until ice crystals just disappeared, while the tubes were still cold. Ice-cold EMEM was slowly added (drop wise) with gentle shaking to dilute the cryopreservation solution, until a total volume of 10x thawed cell suspension volume was reached. Hepatocytes were pelleted at 50xg, 4°C for 5min. The supernatant was removed and the cells were washed 2x with ice-cold

EMEM and centrifugation at 50xg, 4°C for 5min. The pellet was resuspended in a known volume of WEM. The cell number and viability was determined using the trypan blue exclusion test (Section 2.2.3). The cells were then placed into culture medium at specific culture conditions according to the experimental setup.

Similarly cryopreserved HMBs were thawed and diluted as above, without the need for centrifugation as the microbeads easily settle. Note: the thawing solution included adding 2% (v/v) HSA to ice-cold EMEM.

2.2.9 Cell Attachment and Viability

For these assays, cells were cultured in collagen-coated 96-well plates ($5.0x10^4$cells/well). The measurements were perform in duplicate and repeated at least 3 times.

2.2.9.1 Sulphorhodamine (SRB) – Cell Attachment

Hepatocyte attachment was assessed using the Sulphorhodamine B (SRB) assay (Mitry et al. 2000). Culture medium was removed from each well of the 96-well plate and cells were fixed using 50% trichloroacetic acid (TCA; Sigma-Aldrich). Plates were incubated for 60 min at 4°C. Wells were rinsed 5 times with tap-water. Fixed cells were stained with 0.4% SRB (Sigma-Aldrich) solution for at least 60 min at room temperature. Wells were rinsed 5 times with 1% acetic acid to remove unbound dye, and then left to air dry. Cell membrane bound SRB dye was then solubilised in 10mmol/l unbuffered TRIZMA-base (Sigma-Aldrich) solution on a plate shaker for 1h at RT. Plates were read at OD 564nm using the Dynex MRX microplate reader.

2.2.9.2 MTT Assay - Overall Metabolic Activity

The mitochondrial dehydrogenase activity of the plated hepatocytes was assessed using the MTT (3-[4, 5-dimethylthiazol-2-y1]-2,5-diphenyl tetrazolium bromide) assay (Mitry et al. 2009). Briefly, culture medium was removed and wells were washed with fresh medium, 200µl of medium containing MTT (0.5mg/ml) was placed in each well, and plates were incubated at 37^0C for 4 h. The supernatant was removed and the formazan produced was dissolved in DMSO (200µl/well) on a plate shaker for 20min at RT. Plates were read at OD 550nm using the Dynex MRX plate reader.

2.2.10 Hepatocyte - Specific Functional Assays

The assays described below were performed on cells cultured in collagen-coated 24-well plates ($3.0x10^5$cells/well) and the measurements were done in duplicate. The data obtained were normalised based on the protein content of each well.

2.2.10.1 Albumin Production

Albumin production by hepatocytes was quantified in culture (supernatant) medium after 24h of incubation using, human or rat albumin ELISA quantitation kits (Bethyl Laboratories, Montgomery, USA). All steps were performed at RT. Briefly, 96-well plates (Nunc-immuno plates C96 Maxirorp; Nunc A/S, Roskilde, Denmark) were coated with goat affinity anti-albumin antibody for 1h, washed with wash solution (0.05% Tween 20/Tris-buffered saline) and then blocked with 1% BSA/Tris-buffered saline for 30min. Duplicates of albumin standards (6.25-400ng/ml) and samples were placed in wells and incubated for 1h, followed by 5x washes. Diluted HRP detection antibody was then placed in all wells and incubated for 1h followed by 5x washes with wash solution. Finally, TMB substrate solution (KPL, Gaithersburg, USA) was added the plate was kept in the dark for 15min followed addition of with stop solution to stop reaction. The absorbance at 450nm was measured using the Dynex MRX plate reader.

2.2.10.2 Urea Synthesis

Urea synthesis was analysed in supernatant collected at same time for albumin assay. Medium was replaced by serum free culture medium containing ammonium chloride (NH_4Cl; 5mM) and plates were re-incubated for 6h. The supernatants were collected and analysed using QuantiChrom^{TM} Urea Assay Kit (BioAssay Systems, Hayward CA, USA) to determine the amount of urea secreted into the medium. The optical density at 470-550nm (peak absorbance at 520nm) was measured using the Dynex MRX plate reader.

2.2.11 Viability of Hepatocyte Microbeads

2.2.11.1 Cell Membrane Integrity Assay

Qualitative assessment of cell viability was performed using cell membrane integrity assay. 100µl HMBs were washed and resuspended in 1ml Dulbecco's Phosphate-Buffered Saline (DPBS) followed by incubation with 10µl/ml fluorescence diacetate (FDA: Sigma-Aldrich,

Gilingham, UK) and 20µl/ml propidium iodide (PI; Sigma-Aldrich, Gilingham, UK), in the dark for 90 sec at RT. Microbeads were washed 3x with DPBS followed by adding VECTASHIELD® Mounting Media and then visualised under fluorescent microscopy (Leica Microsystems Ltd.). These fluorescent dyes penetrate the structure of the microbeads and live cells cytoplasm appeared bright green (FDA), while dead cells had bright red stained nuclei (PI). The samples were examined under the fluorescence microscope and photographs of representative fields were taken.

2.2.11.2 HMBs - Overall Metabolic Activity-MTT Assay

Viability of encapsulated hepatocytes was evaluated using the MTT assay (Section 2.2.9.2) with some modifications. A known weight of HMBs was placed in a microfuge tube and gently washed with PBS. MTT solution (5mg/ml MTT in PBS) was diluted in plain medium (1:10). HMBs were incubated in 500µl diluted MTT at 37°C for 4h, and then washed twice with PBS. Formazan formed by cells was dissolved using 500µl DMSO and vigorous shaking for 20min followed by a brief high speed centrifugation for 2min. The optical density of supernatant was read (550 nm) in 200µl duplicates in 96-well plate using the plate reader. The data values are presented as OD reading/100mg HMBs.

2.2.12 Hepatocyte - Specific Functions of Hepatocyte Microbeads

2.2.12.1 Albumin Production

The amount of albumin secreted by encapsulated hepatocytes over 24h was quantified in culture medium using the human or rat albumin ELISA kit (Section 2.2.10.1).

2.2.12.2 Urea Synthesis

To quantify urea synthesis, 500µl HMBs with 1ml serum free medium containing 5mM NH_4Cl and placed in each well of 12-well-plate. After incubation for 6h incubation, at 37°C supernatants was collected and analysed using the urea kit (Section 2.2.10.2).

2.2.12.3 Cytochrome P450 (CYP1A1/2) Activity

Cytochrome P450 (CYP1A1/2) activity was assessed using the ethoxyresorufin O-dethylase (EROD) method (Donato et al. 1993) with some modifications. Microbeads (500µl) were incubated in 1mL serum free medium containing 8µM of 7- ethoxyresorufin and 10µM of dicumarol for 1h. 500µl of supernatant was collected and placed in 1.5ml microfuge tube followed by adding of ß-glucuronidase/arylsulfatase (Roche, East Sussex, UK) and incubated for 2h at 37°C when the reaction was stopped by addition of ethanol. The fluorescence was measured at 530nm excitation, 590nm emission using a TecanGeNios Pro plate reader (Tecan Group Ltd., Männedrof, Switzerland). The total amount of resorufin produced was calculated using a resorufin standard curve (0-800pmol), and data were expressed as pmol/mg protein/min).

2.2.13 Statistical Analysis

Data were analysed using GraphPad Prism® 6 software (GraphPad, San Diego, CA) and SPSS 20 software (Ver.20; IBM, Hampshire, UK). All data are presented as the mean±standard error of the mean (mean±SEM) from at least 4 independent experiments unless otherwise stated. Student *t*-test was applied to compare two independent groups. Comparison between three or more groups with one independent variable was performed using one-way analysis (ANOVA) and multiple comparisons were adjusted by using either Turkey or Bonferroni test. A two-way repeated measurement ANOVA and Turkey's multiple comparisons test were used to compare groups exposed to different conditions. A p-value of ≤0.05 was considered statistically significant.

CHAPTER 3

3. The Encapsulation and Settings Optimisation

3.1 Introduction

The successful application of hepatocyte microbeads for clinical transplantation requires optimised methods for producing a homogeneous uniform size and spherical shape, which can achieve mechanical stability without compromising permeability and biocompatibility. The techniques should be simple and provide high production yield and importantly can be performed under sterile conditions. Currently, most of hepatocyte microencapsulation methods are based on liquid extrusion through a nozzle (orifice) and incorporate mechanical forces such as vibration or cutting forces to generate droplets follow by gelation in a solution bath. These methods give size-controlled microbeads and minimize production time compared to conventional methods. The vibrating–jet (nozzle) technique is widely used on a laboratory scale and can be applied for clinical grade production due to its enclose system design with autoclavable production vessel (Figure 3.1 A). The controlled break up of a laminar jet to obtain uniform size of microbeads can be achieved with optimum parameters including frequency, amplitude, and liquid flow rate to create a permanent sinusoidal force (Serp et al. 2000). The encapsulator IE-50 R used in this study uses this principle. The diagram of the device is shown in Figure 3.1B. Previous studies have suggested that the favorable size of microbeads that offers mechanical strength and effective mass transfer is in the range from 400µm to 600µm (De Vos et al. 1996; Canaple et al. 2002; Zimmermann et al. 2007). For future clinical application, the Encapsulator IE-50 R with 250µm nozzle was used in this study. The aim of this study was investigated the optimal and reproducible encapsulator setting that produce the controllable size and uniformity of microbeads.

A.

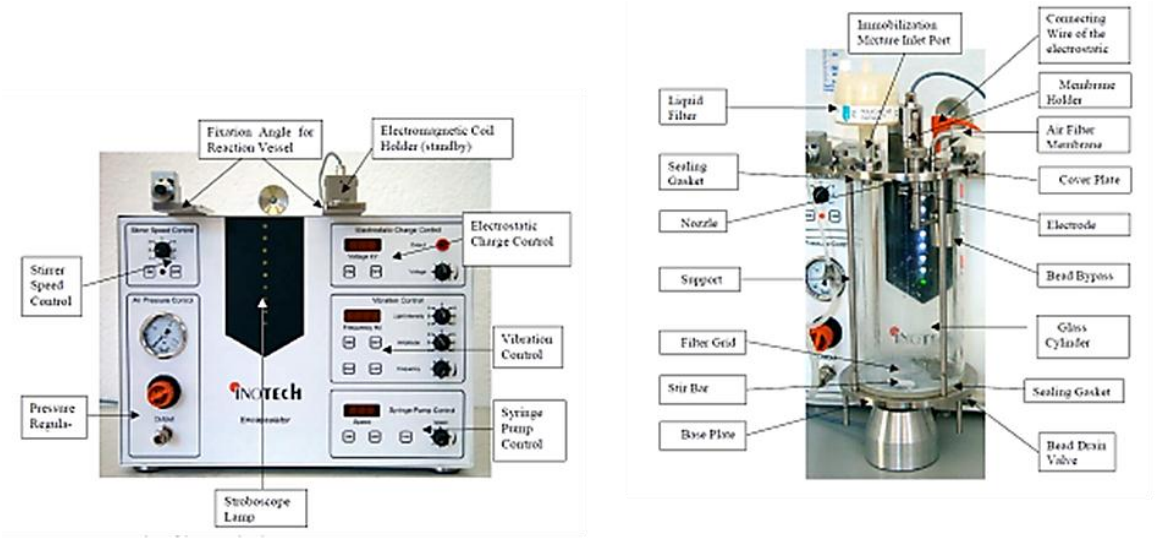

B.

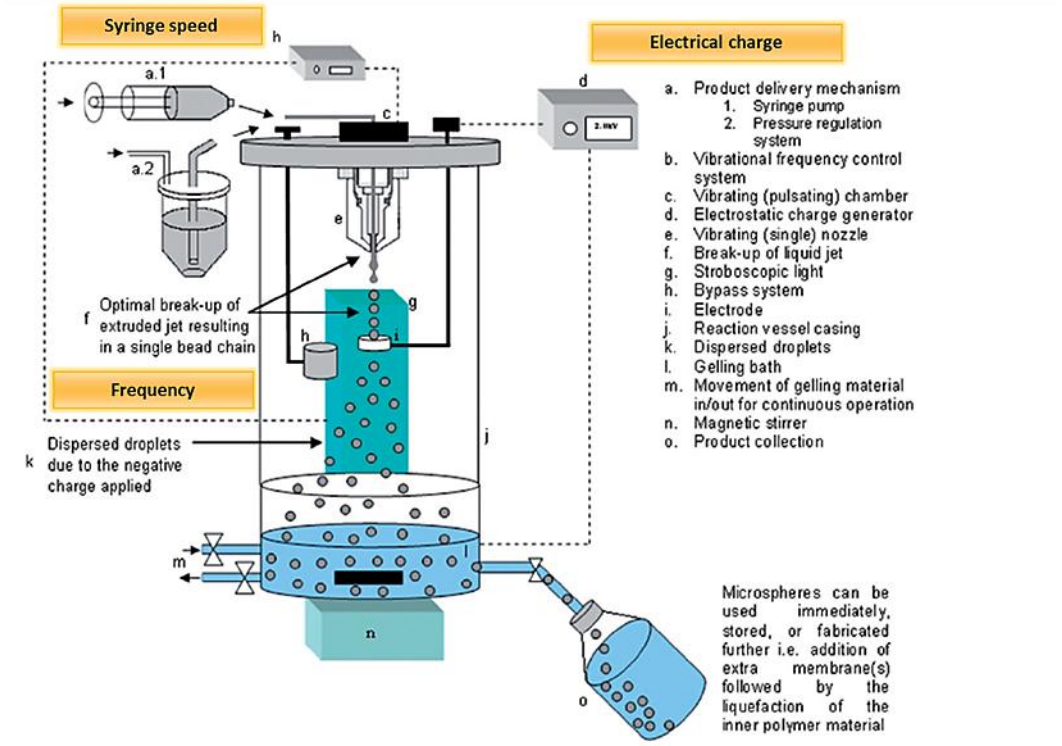

Figure 3.1: Encapsulator device based on vibrating jet nozzle technique (A) The encapsulator main control unit (left), and reaction vessel (right), and (B) the schematic representation of the Encapsulator IE-50 R. [Adapted from Inotech Encapsulator operation Manual, and Whelehan and Marison (2011)].

3.2 Materials and Methods

3.2.1 Materials

Highly purified sodium alginate; low viscosity and high glucoronic acid (PRONOVA™ SLG20; NovaMatrix, Sandvika, Norway). 0.9% Sodium chloride (0.9% NaCl; Baxter Healthcare Ltd., Norfolk, UK.), calcium chloride (Arum Pharmarmaceuticals Ltd., Romford, UK). Encapsulator (Model: IE-50R; Inotech Encapsulation AG, Dottikon, Switzerland), Light microscope (Leica, GmbH, Wetzlar, Germany), and Image J software ver. 1.44p (National Institutes of Health, USA).

3.2.2 Methods

3.2.2.1 Optimisation of Encapsulator Settings

Encapsulation runs were performed to determine the optimal encapsulator settings [vibration frequency (Hz), amplitude voltage (kV), syringe speed, and amplitude] that result in obtaining the highest quality microbeads. A total of 10 runs were performed without cells (empty microbeads; EMBs), and then an additional 6 runs were performed with human hepatocytes (hepatocyte microbeads; HMBs). The optimal settings were then used in the other experiments. [Inotech Encapsulator IE-50R Manual was used as reference, Figure 3.2]

A

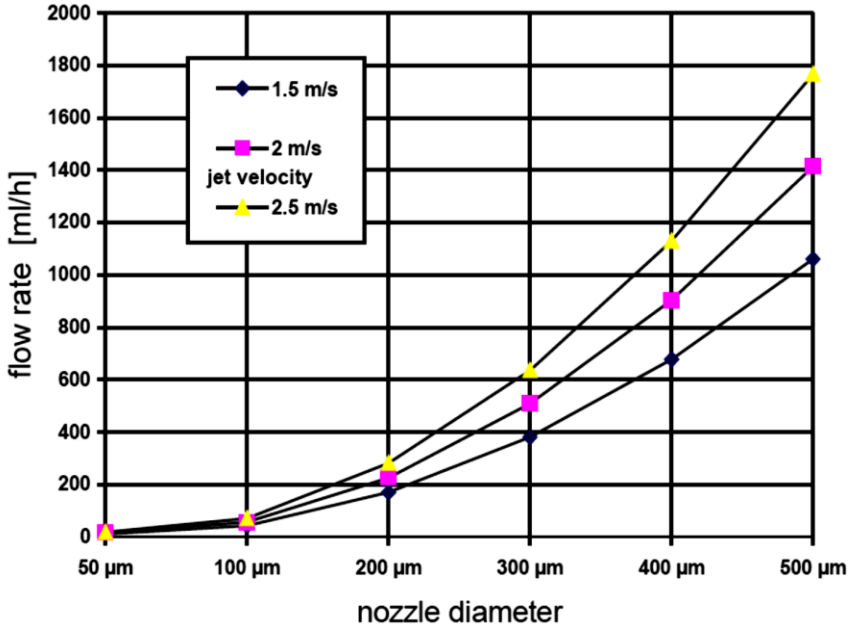

B

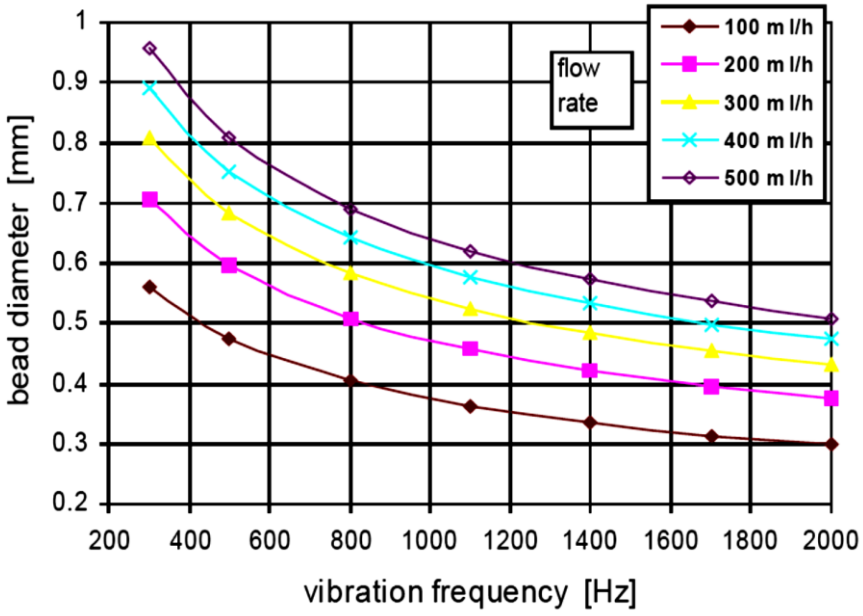

Figure 3.2: Charts from Inotech Encapsulator IE-50R manual. (A) Influence of the liquid jet velocity and the nozzle diameter on the flow rate and (B) influence of the vibration frequency and the flow rate on the microbead diameter.

3.3 Results

3.3.1 Setting Up the Encapsulator

A total of 16 runs were performed in this set of experiments, consisting of 10 runs to produce EMBs, and 6 runs to produce HMBs. Details of parameters in each run used in each experiment for microbeads are shown in Table 3.1 and Table 3.2 respectively. The optimal settings were then used in other experiments.

Table 3.1: Encapsulator settings for optimisation of EMBs size and shape

Run	Frequency (Hz)	Amplitude	Voltage (kV)	Syringe Speed	Comment
1	1880	4	0.00	292	Too large
2	1676	4	0.00	290	Varying in sizes
3	1386	4	0.00	350	Majority joined/fused
4	1079	4	0.00	401	Varying sizes; tailed Microbeads
5	2055	4	0.47	450	Varying in sizes; tailed and joined/fused microbeads
6	1150	4	0.51	339	Varying sizes; large and/or joined/fused microbeads
7	1784	3	0.55	360	Improvement on 6, however still too large
8	1353	3	0.00	387	Microbeads generally small and uniform
9	1206	4	0.63	326	Very large, mainly round but with some few odd shaped microbeads
10	1185	4	0.49	385	Best; all microbeads, round and uniform

Table 3.2: Encapsulator settings for optimisation of microbead size and shape using alginate/hepatocytes suspension

Run	Frequency (Hz)	Amplitude	Voltage (kV)	Syringe Speed	Comment
1	1312	4	0.5	340	Microbeads round, but large
2	1296	3	0.72	310	Good size microbeads, but not uniform
3	1295	4	0.72	281	Good shape microbeads, but a "little" large
4	1295	4	0.73	316	Ideal size and shape microbeads
5	1302	4	0.71	433	Microbeads small, but a few different shapes
6	1303	4	0.71	236	Best microbeads size and shape

Best quality EMBs were obtained when the encapsulator settings were set to frequency=1185Hz, amplitude=4, voltage=0.49kV, and syringe speed=385. The microbeads were round with smooth regular surface, and a mean size was 500±30μm. For hepatocyte microbeads, they were: frequency=1303Hz, amplitude=4, voltage=0.71kV and syringe speed=236. Similar to the blank microbeads they were also uniform with smooth regular surface, and a mean size of 500±50μm. These settings were used throughout the reported experiments. Figure 3.3 demonstrates a representative of microbeads obtained from difference settings.

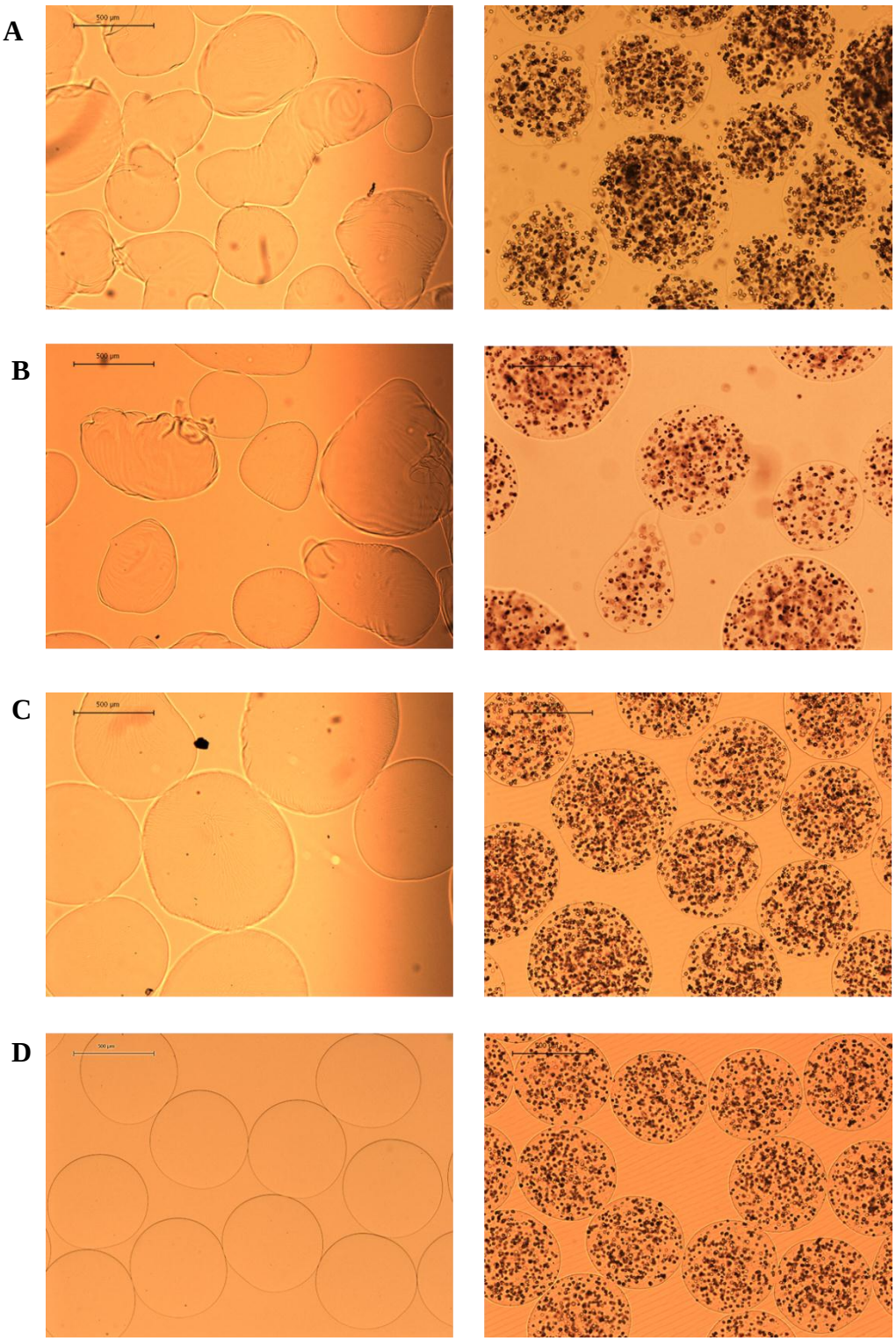

Figure 3.3: Representative images of microbeads produced using different encapsulator settings. Microbeads examined under light microscopy; right panel shows EMBs morphology and left panel shows HMBs morphology. (A)-(C) Imperfect or non-uniform microbeads and, (D) uniform microbeads obtained with optimal setting.

3.4 Discussion

The main principle to obtain uniform microbeads according to the vibrating-jet (nozzle), technique is optimal range of vibration frequency and jet velocity (Heinzen et al., 2004). Microbead size can be adjusted by other parameters including nozzle diameter and viscosity of alginate. The general rule of Inotech encapsulator (IE-50R) for producing microbeads using sodium alginate at concentration 1.5%-2.0% is that the size of microbeads is approximately twice the nozzle diameter. The increasing frequency of the setting, the microbeads produced are smaller for a given nozzle size, while higher speed of the setting provided high production capacity with larger size microbeads. Surface tension of calcium chloride might cause deformity of microbeads (tail) if the setting is not appropriate.

In this study, the optimal settings for EMBs and HMBs were achieved. Certain settings gave standing chain of drops which were clearly seen through the Stroboscope light. Microbeads productions run with these setting were of uniform spherical shape and size of 500µm (with the range of ±20%). And also reproducible outcomes were obtained with these settings. For consistency and better reproducibility, all materials involving in the process of encapsulation should stay with the same quality/brands.

In conclusion, the encapsulator used in this study was easy to set-up and use. Also, high quality alginate microbeads were produced under sterile conditions, which high reproducibility.

CHAPTER 4

4. Optimisation of Microbeads Production

4.1 Introduction

The clinical application of microbeads is critically dependent on the ability of microbeads to protect the encapsulated cells from immune system. As a result, the mechanical stability of microbeads is a crucial factor for clinical transplantation. Microbeads need to maintain their integrity during transplantation and in the implant site, as their breakage would result in functional loss of cells and immune rejection. In addition, microbeads need to be strong enough to resist stress during cryopreservation and thawing. The mechanical stability can be optimised by using different types and concentration of cation, fine-tuning the duration time of cross-linking (polymerisation), and adjusting the spatial distribution of cells. Although, cations with high affinity such as $Ba^{2+}$and Sr^{2+}provide high stability, Ca^{2+} was used in this study for safety reasons. The polymerisation (gelling) process involves interaction of alginate polymers (negative charge) with cations and time required for crosslinking. Theoretically, a longer duration of polymerisation allows more time to form cross-links to give better durability of microbeads and also smaller pore size of the microbeads membrane. However, increasing the gelling time may have detrimental effects on cell viability by prolonging exposure to chemicals and also reduces of oxygen and nutrient permeability.

The number of cells per microbead is one of parameters that have to be considered to obtain sufficient function. As a consequence of increasing the number of cells, the demand of oxygen and nutrient would increase while the compactness of cells within the microbeads might impede mass transport. The nutrient and oxygen transport-limitation across microbead could lead to cells death especially in the centre of microbeads (Huang et al. 2012). In addition, incorporation with various numbers of hepatocytes in alginate would have effects on the structure and the stability of the microbeads produced.

The aims of this study were to determining the effects of polymerisation on the mechanical stability of microbeads and encapsulated hepatocyte viability and function and also studying the influence of cell density on cell viability related to the pattern of cell distribution within microbeads and the effect on physical integrity to determine the ratio of cell mass per volume of alginate which should be used. The permeability of optimised microbeads was also evaluated.

4.2 Materials and Methods

4.2.1 Materials

All chemicals used in this study were from Sigma-Aldrich (Gillingham, UK), unless otherwise stated. Light microscope (Leica, GmbH, Wetzlar, Germany), Image J software ver. 1.44p (National Institutes of Health, USA), Leica SP5 confocal microscope (Leica Microsystems Ltd, Milton Keynes, UK), Volocity software (Perkin Elmer, Cambridge, UK), Mathematica ver. 8.0 (Wolfram Inc., Oxfordsire, UK), microcon® centrifugal filter device (Merck, Darmstadt, Germany), and Mini-Protean tetra cell system and Precision Plus Protein™ standard (Bio-Rad Laboratories Ltd, Hertfordshire, UK).

4.2.2 Methods

4.2.2.1 Assessment of Physical Integrity of Microbeads using Osmotic Pressure Test

EMBs and HMBs were produced without and with human hepatocytes ($2.5x10^6$ cells/ml alginate), respectively (Section 2.2.6). Microbeads were made using 3 different polymerisation times (10, 15, and 20min). Physical stability of microbeads was determined using an osmotic stress test (Van Raamsdonk and Chang 2001). Briefly, after production, 250µl of EMBs were equilibrated in serum-free medium, then incubated for 3h in four hypotonic solutions (culture medium diluted with water) and one isotonic solution [either William E medium (WEM) or CMRL], to establish the stability of microbeads. The hypotonic solution was made by diluting serum free medium with distilled water. Solutions of 0%, 0.78%, 3.25%, 6.25% and 100% serum free medium were 0, 2.3, 9.2, 18.4 and 295mOsm, respectively. The stability of microbeads was assessed after 3h of incubation by measuring the microbead diameter of 100 microbeads per sample under light microscope, and using Image J software. Microbeads immediately after production were used as controls. Based on EMBs findings, physical stability of HMBs was determined in transplant medium (CMRL; isotonic solution) and water (hypotonic solution).

4.2.2.2 Assessment of the Effect of Polymerisation Time on Cell Viability and Functional in HMBs

To study the effect of polymerisation time in $CaCl_2$ on hepatocyte viability and function, three polymerisation times (10, 15, and 20min) were used in the production of HMBs and the products were divided into two sets. First set: HMBs were exposed to osmotic stress test (Section 3.2.2.2) followed by MTT assay to assess encapsulated cell viability (Section 2.2.11.2). Second set: HMBs were maintained in supplemented CMRL medium for 24h before being assessed. Viability and hepatocyte-specific functions of encapsulated cells including albumin (Section 2.2.12.1) and urea production (Section 2.2.12.2) were evaluated after maintenance in culture for a further 24h.

4.2.2.3 Effects of Cell Density on Microbead Morphology, Cell Viability and Function

HMBs were produced using four cell densities: 2.0, 2.5, 3.0 and 3.5 million cells/ml alginate using the same batch of cryopreserved human hepatocytes for each experiment. A higher cell density at $4.0x10^6$cells/ml alginate was also studied in preliminary experiments, however, it was observed that most of the HMBs obtained varied in size (range: 400-1200μm), and some with a distorted shape. Therefore, $3.5x10^6$cells/ml alginate was the maximum cell density studied. HMBs were maintained in culture for 3 days. Microbead morphology was examined immediately after production (control). Cell viability was assessed at day 1 by two techniques including cell membrane integrity and MTT assays (Section 2.2.11). It was assumed that an increase in cell number per microbead, might affect the distribution and viability of the cells, hence confocal microscopy with three dimensional (3D) reconstruction images of the microbeads were used to determine the cell viability in relation to cell distribution across the microbead (outer and inner halves), and in estimating the average number of cells per microbead. Hepatocyte-specific functions (Section 2.2.12) were evaluated on days 1 and 3.

4.2.2.4 Confocal Microscopy to Assess Cell Distribution and Viability Across Microbeads

250μL microliter HMBs were stained with FDA/PI in DPBS for 90sec at RT. VECTASHIELD® Mounting Medium was added to prevent photo bleaching. HMBs were loaded onto a glass slide with a well followed by addition of a drop of glycerol to minimise microbead movement during imaging. Using a Leica SP5 confocal microscope (Leica Microsystems Ltd, Milton Keynes,

UK), microbeads were imaged at 700Hz using a 10x dry objective. The number of slices acquired as dictated by Nyquist oversampling of the optical slice volume resulting from a pinhole size of 1 Airy Unit at a wavelength of 595nm for the entire volume of the microbead. Image stacks were imported into Volocity software and both green and red objects were detected using a custom protocol defined therein based on size, standard deviation intensity, and local contrast adjustment. The centre point of each microbead was defined by bisecting lines through the diagonals of the microbead volume. The x-y-z centroid coordinate of each cell was exported, along with the x-y-z coordinate of the microbead's centre, and then imported into Mathematica 8.0 (Wolfram Inc., Oxfordsire, UK). Viability was calculated as the ratio of green cells/total number of cells (green + red). For each microbead, the viability and cell count for inner and outer bead halves was calculated as a function of distance from the microbead centre coordinate and the outer most point on the edge of the microbead.

4.2.2.5 Permeability Measurement

Cryopreserved hepatocytes (n=2) were used in this set of experiments. Cell viability after thawing was 60% and 70%. HMBs were produced using optimised polymerisation time and cell density and cultured in CMRL medium supplemented with 2mM L-glutamine, 0.1µM dexamethasone, 0.1µM insulin, penicillin (50U/ml) and streptomycin (50µg/ml) at 37°C for 24h. Supernatants of HMBs cultures were collected and store at -80°C until required for analysis. To assess the permeability of microbeads, the detection of proteins that diffused across microbead relative to the molecular size (molecular mass) was performed using 2D electrophoresis and proteomics analysis.

4.2.2.5.1 Sodium Dodecyl Sulfate Polyacrylamide Gel Electrophoresis (SDS-PAGE) of Proteins

The supernatants of microbead culture samples were thawed then transferred into microcon® centrifugal filter device and centrifuged at 14,000xg for 12min at RT to concentrate the proteins. Protein concentration was measured using modified Lowry technique (Section 2.2.5.1). To precipitate the proteins, the concentrated samples (100µl) were mixed with acetone (400µl) and incubated at -20°C for 1h followed by centrifugation at 14,000xg, at RT, for 10min. Supernatants were gently removed and protein pellets were air-dried to eliminate any residual acetone residue. The pellets were resuspended in 2x Laemmli sample buffer containing β-mercaptoethanol and heated at 95°C for 5min to denature the proteins. After cooling, 10µl per sample, and protein standard marker (Precision Plus Protein™ Standard; MW 10-250kD) were

loaded onto a 12% polyacrylamide gel. Electrophoresis was performed using Mini-Protean® Tetra cell system (Bio-Rad Laboratories Ltd, Hertfordshire, UK) operated at 100 volts for 1h. After the run, the gel was removed from its cassette, washed three times with water and stained with Coomassie brilliant blue for 2h then washed again with water for at least 30min to remove unbound background dye from the gel, leaving stained proteins visible as blue bands on a clear background. The image of protein bands on gel was capture using GeneGenius image system (Syngene, Cambridge, UK).

4.2.2.5.2 Proteomics Analysis

The proteomics analysis was performed at the Centre for Translational Omics, Institute of Child Health & Great Ormond Street Hospital for Sick Children, University College London. Briefly, supernatant samples were freeze-dried and their proteins precipitated using acetone. Each protein pellet was resuspended in 20µl of 100mM Tris, pH 7.8, containing 6M urea, and left shaking at RT for 1h. Disulfide bridges were reduced and free thiol groups were carboamidomethylated. The reaction mixture was then diluted with 155µl H_2O and vortexed, before the addition of 2µg sequence-grade trypsin and digestion overnight at 37 °C in a water bath. A standard yeast enolase digest was used as an internal standard for the quantification of each protein. All analyses were performed using a nanoAcquity UPLC and QTOF Premier mass spectrometer (Waters Corporation, Manchester, U.K.). ProteinLynx GlobalServer version 2.4 (Waters, U.K.) was used to process all data acquired. Protein identifications were obtained by searching a human proteome UniProt database to which the sequence of P00924 yeast enolase was added manually. Protein identification from the low/high collision spectra for each sample was processed using a hierarchical approach where more than three fragment ions per peptide, seven fragment ions per protein, and more than two peptides per protein had to be matched. Since single peptide protein identifications are more likely to represent false-positive data points, all proteins with greater than two peptides identified with high confidence were considered for protein quantification. Carboamidomethylation was set as a fixed modification, and oxidation was set as variable modification. The average intensity value of the top three ionizing peptides to yeast enolase was used to convert the average intensity of the top three ionising peptides for proteins to the corresponding absolute quantity of protein loaded on column. The lowest detectable concentration was 0.1 fmol (Manwaring et al. 2013).

4.3 Results

4.3.1 Effect of Optimal Polymerisation Time on Physical Integrity

4.3.1.1 Physical Integrity of EMBs

EMBs obtained were of uniform shape and size. The mean diameter of microbeads in the 10min and 15min polymerisation groups were similar (599.2±1.4µm vs 599.2±1.8µm); whereas, microbeads in the 20min polymerisation group (605.7±1.2µm) were of larger size than the other two groups. With all hypotonic solutions tested, the size of EMBs samples were significantly larger compared to control ($p<0.001$). It was also observed that in water (most stressful osmotic condition), EMBS showed marked changes in diameter, but none of the microbeads ruptured (Figure 4.1). EMBs maintained their size when incubated for 3h in isotonic CMRL medium, but not in WEM (Table 4.1).

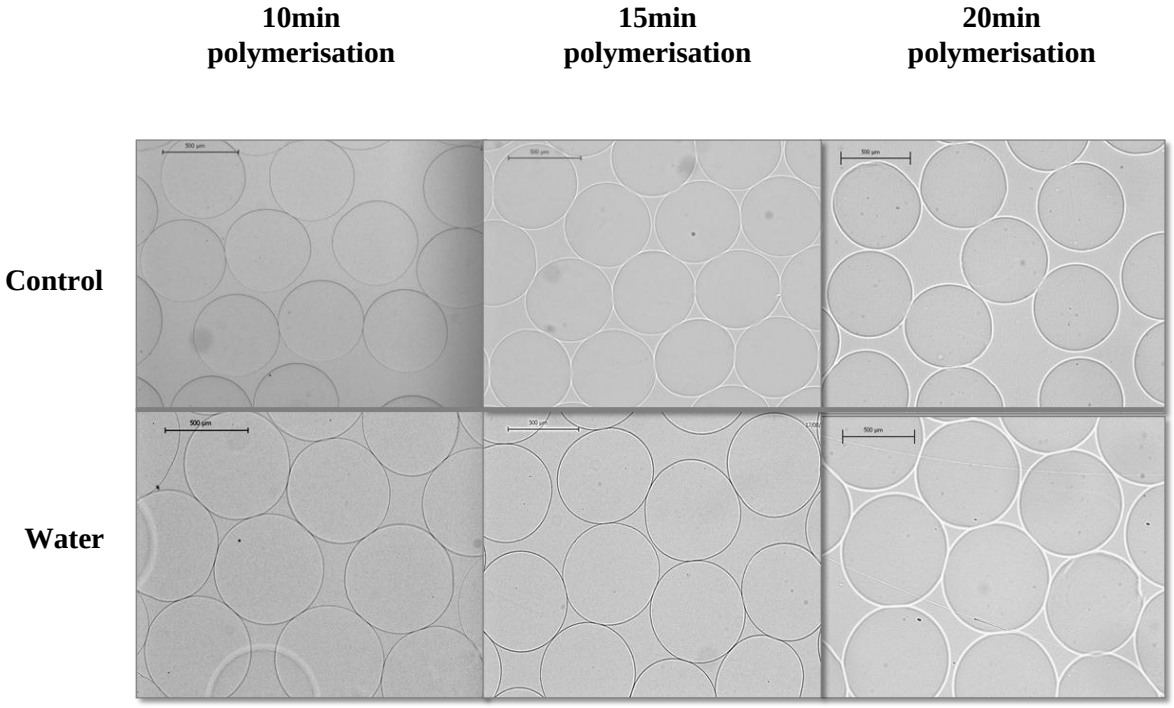

Figure 4.1: Representative examples of mean diameter of EMBs after exposure to osmotic stress. Control (top row); and after exposure to water for 3h (below) showing an increase in microbead size compared to control. Scale bar = 500µm (magnification 5x).

Table 4.1: The size of microbeads produced using 3 different polymerisation times, immediately after production and after exposure to isotonic and hypotonic solutions for 3h

Experimental group	Polymerisation time (min)					
	10		15		20	
	Microbead Size (µm)	p-value	Microbead Size (µm)	p-value	Microbead Size (µm)	p-value
EMBs in WEM						
Control	567.0 ± 1.2		577.5 ± 1.2		587.9 ± 1.9	
0 mOsm	696.3 ± 5.1	< 0.001	629.9 ± 1.3	<0.001	673.0 ± 2.9	< 0.001
2.3 mOsm	676.2 ± 3.8	< 0.001	660.3 ± 1.7	< 0.001	659.8 ± 2.8	< 0.001
9.2 mOsm	673.6 ± 3.1	< 0.001	654.3 ± 1.5	< 0.001	645.5 ± 3.1	< 0.001
18.4 mOsm	659.4 ± 3.0	< 0.001	642.2 ± 1.2	< 0.001	633.3 ± 2.6	< 0.001
295mOsm	561.3 ± 0.9	0.001	559.5 ± 1.2	< 0.001	582.0 ± 1.9	NS
EMBs in CMRL						
Control	599.2± 1.4		599.2± 1.8		605.7 ± 1.2	
0 mOsm	700.0 ± 2.2	< 0.001	680.6 ± 1.8	< 0.001	724.5 ± 1.5	< 0.001
2.3 mOsm	697.2 ± 2.4	< 0.001	673.7 ± 2.5	< 0.001	705.2 ± 1.9	< 0.001
9.2 mOsm	671.1 ± 1.7	< 0.001	679.7 ± 1.7	< 0.001	697.5 ± 1.4	< 0.001
18.4 mOsm	667.9 ± 2.0	< 0.001	666.9 ± 2.2	< 0.001	691.1 ± 1.5	< 0.001
295mOsm	597.0 ± 1.4	NS	595.3 ± 1.7	NS	606.4 ± 1.2	NS

Data presented as mean± SEM; p-value <0.01 was considered statistically significant; NS, not significant.

Comparing three different polymerisation times, EMBs in the 15min polymerisation group tended to resist osmotic shock better than those in the 10min and 20min polymerisation groups by showing a significantly lower mean difference in diameter after exposure to almost all hypotonic solutions ($p<0.01$).

4.3.1.2 Physical Stability of HMBs

HMBs in all three control groups were uniform with a mean diameter of 584±0.9µm (10min), 582.2±1.2µm (15min), and 584.4±1.2µm (20min), with no statistical difference between the 3 polymerisation groups. After incubation for 3h in CMRL and water, HMBs showed a similar trend as is observed in EMBs with no broken microbeads in all conditions (Figure 4.2). There was a significant increase in mean microbeads `diameter in all samples incubated in hypotonic solution compared to both control and CMRL groups ($p<0.001$), but this was not different when comparing control to CMRL (3h). The 15min polymerisation HMBs group had a significantly better mechanical stability compared to the other two groups ($p<0.001$) with a mean microbead diameter difference of 7.1µm (10min vs 15min), and 23.5µm (20min vs 15min) after exposure to water (Figure. 4.3)

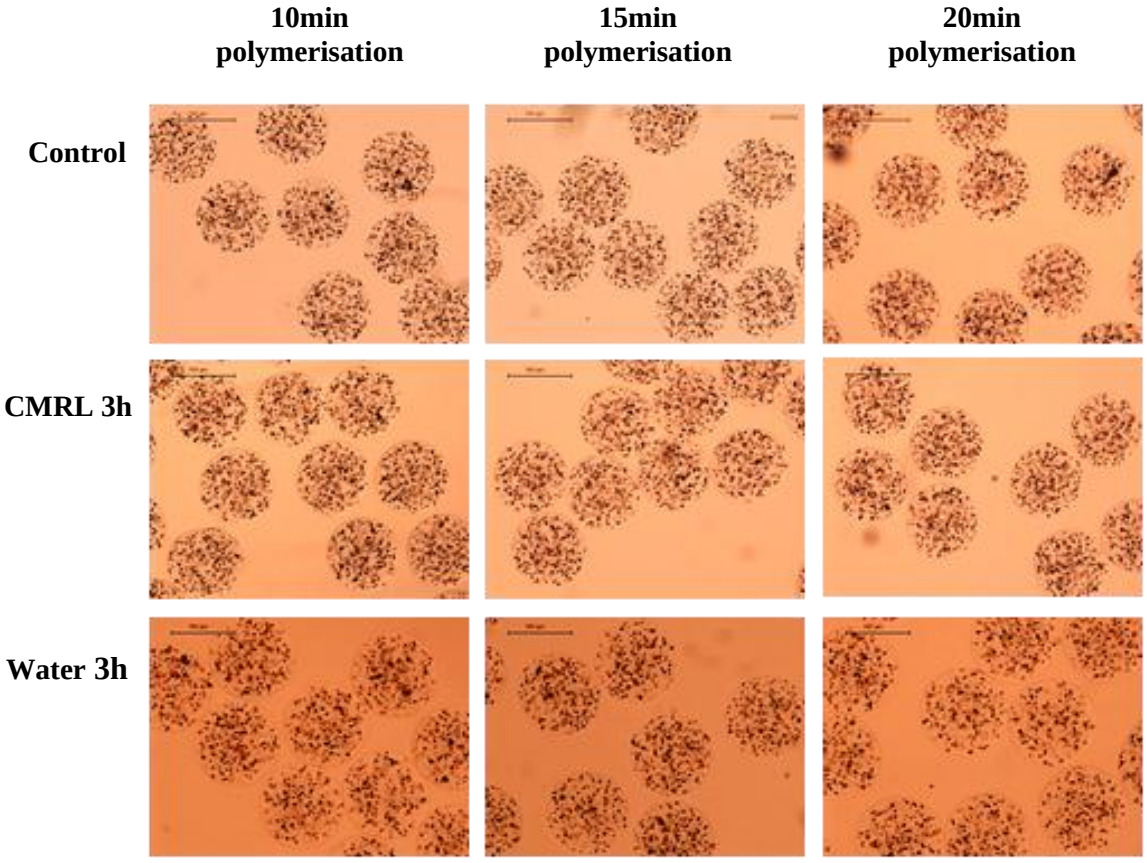

Figure 4.2: Representative examples of mean diameter of HMBs after exposure to osmotic stress. Scale bar = 500µm (magnification 5x).

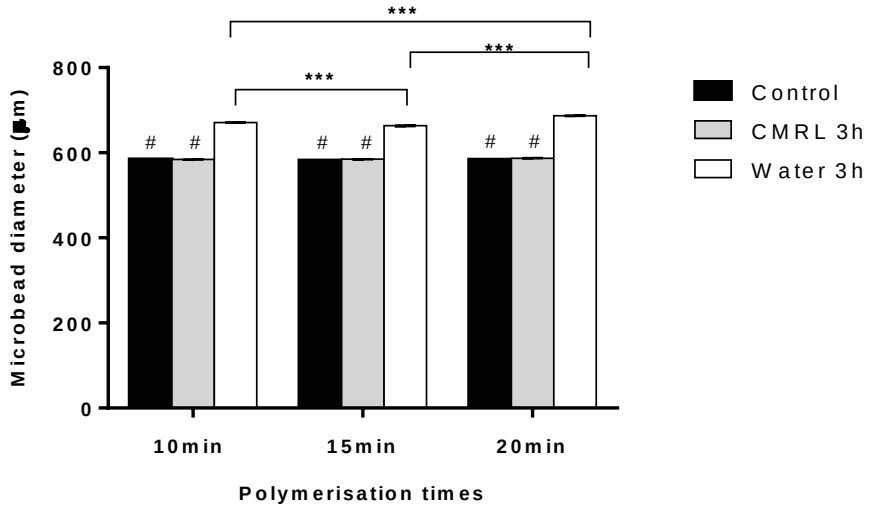

Figure 4.3: Effects of osmotic shock on HMBs diameter. HMBs diameter were significantly increased in all groups after incubated in water (hypotonic solution) compared to control and CMRL ($^{\#}p<0.001$). HMB with 15min polymerisation provided statistically significant stable in diameter size compare to those of 10 and 20min, and also there was a significant difference between HMBs with 10min and 20min after exposure to water (***$p< 0.001$).

4.3.2 Effects of Polymerisation Time on Hepatocyte Viability and Functions of HMBs

There was no statistically significant difference in cell viability determined by MTT activity between the 3 polymerisation times for HMBs under the same conditions. Noticeably, MTT activity was maintained after 3h incubation in CMRL compared to control, however, in all groups there was a substantial decrease in cell activity in microbeads incubated in water ($p<0.02$). HMBs from 3 polymerisation groups provided similar metabolic functions after being maintained in culture for 24h. The amount of albumin production for 10min, 15min and 20min group were 569.0±112.2, 606.3±97.0, and 581.2±103.3 ng/mg protein and urea production were 6.1±1.1, 6.1±1.2, and 6.4±1.2 μg/mg protein, respectively.

4.3.3 Effects of Cell Density on Microbead Morphology

The morphology of HMBs produced using different cell densities ($2.0x10^6$ to $3.5x\ 10^6$cells/ml alginate) showed uniformity and smooth outside surface with no significant differences between the groups (Figure 4.4)

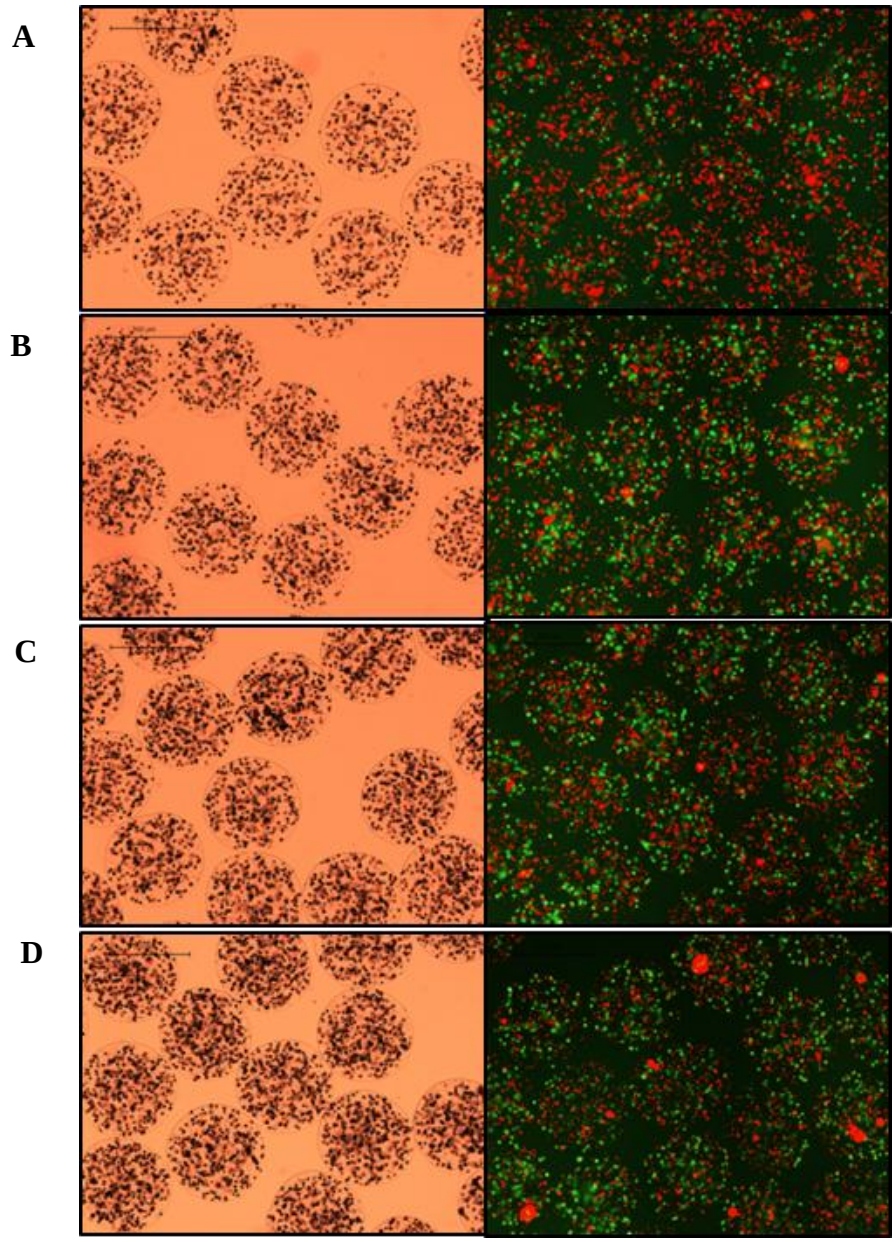

Figure 4.4: Representative images of hepatocytes microbeads produced with different cell densities; (A) $2.0x10^6$cells/ml alginate, (B) $2.5x10^6$cells/ml alginate (C) $3.0x10^6$cells/ml alginate and (D) $3.5x10^6$cells/ml alginate. On the left panel demonstrates microbeads under light microscopy which showed that microbeads at all densities were uniform and intact. On the right panel shows viability of hepatocytes microbeads using FDA/PI staining under fluorescence microscopy (green is viable and red is dead cells) in which $3.5x10^6$cells/ml alginate provided highest viability. Scale bar = 500µm (magnification 5x).

4.3.4 Effects of Cell Density on Hepatocyte Viability and Function of HMBs

The viability of hepatocytes before encapsulation was 61.5±1.1 %. After encapsulation, HMBs were maintained in culture overnight to allow the encapsulated hepatocytes to recover. Cell viability (FDA/PI staining) showed on the following day that the density of $3.5x10^6$ cells/ml provided the highest viability compared to other three groups (Figure. 4.4). The 3D reconstructed images showed that cells were evenly distributed inside the microbead (Figure 4.5) and the average cell number per microbead for each cell density ranged from 201 ($2.0x10^6$ cells/ml alginate) up to 447 ($3.5x10^6$ cells/ml alginate), (Table 4.2).

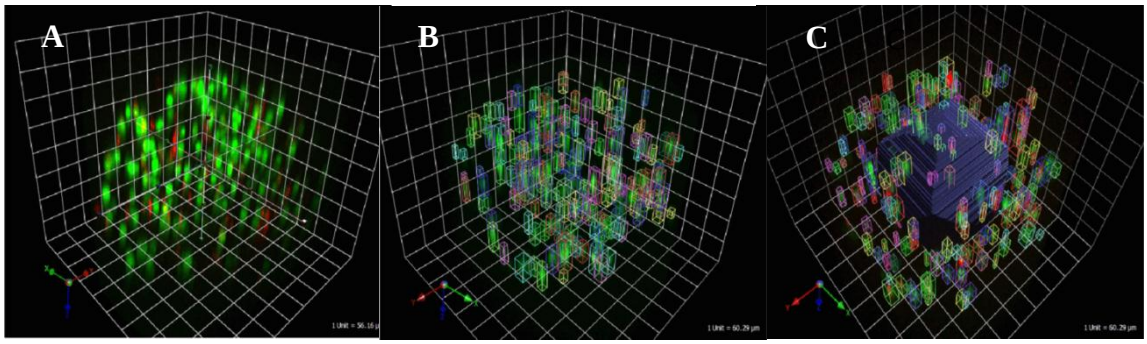

Figure 4.5: Representative confocal microscopy images used in 3D reconstruction to demonstrate (A & B) cell distribution and viability across the microbead, and (C) viability of cells within outer half vs inner half of same microbead.

Table 4.2: Number of cells per microbead and cell densities used alginate

Cell density/ml alginate	Number of cells/microbead
$2.0x10^6$	211±10
$2.5x10^6$	275±4
$3.0x10^6$	320±4
$3.5x10^6$	439±8

Surprisingly, with increasing cell density there was no significant difference in cell viability between outer and inner halves in all groups (Figure 4.6A). Analysis of the outer halves only showed that there was a statistically significant increase in cell viability which correlated with the cell density and number ($3.5x10^6$ vs $2.0x10^6$cells/ml, $p<0.0001$; $3.5x10^6$ vs $2.5x10^6$cells/ml, $p=0.001$). While inner half of $2.0x10^6$cells/ml showed the lowest viability compared to the others ($p<0.05$). The overall viability in the $3.5x10^6$ cells/ml group was significantly higher than $2.0x10^6$ cells/ml (46.1±3.3% vs 31.7±3.3%, $p=0.01$) and also tended to be higher than $2.5x10^6$ cells/ml (37.42 ± 5.17%) but this was not significant ($p=0.06$). Furthermore, MTT assay on day 1 showed a similar trend where the $3.5x10^6$ cells/ml group had a higher activity than other groups. However, on day 3 there was a significant decrease in overall activity in $3.0x10^6$ and $3.5x10^6$cells/ml ($p<0.05$; Figure 4.6B).

Urea and albumin assays showed no significant differences between the 4 groups on either day1 or day3 (Figures. 4.7A and B). However, albumin synthesis showed a similar pattern to cell viability where the higher cell number gave higher production. By contrast, the CYP1A1/2 activity on day 3 of the $2.0x10^6$cells/ml group was significantly higher than 3.0 and 3.5 $x10^6$cells/ml ($p<0.05$; Figure. 4.7C).

A.

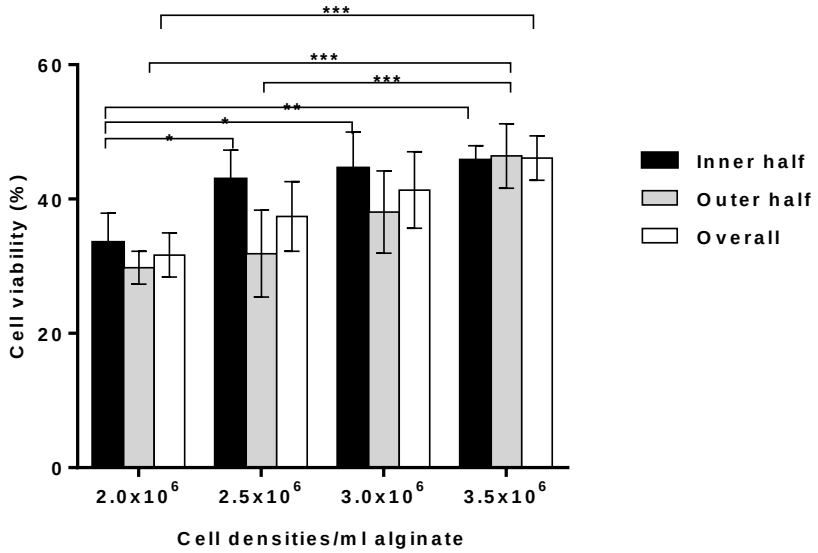

B.

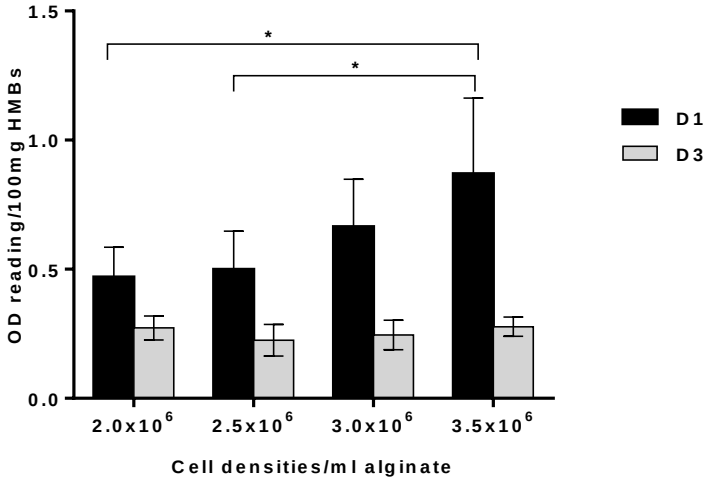

Figure 4.6: Effects of different cell densities on encapsulated hepatocyte viability. (A) viability of encapsulated hepatocytes across microbead using confocal microscopy and 3D reconstruction; and (B) MTT activity of hepatocyte microbeads on day 1 and day 3 of culture; *p<0.05, **p<0.01, ***p<0.001.

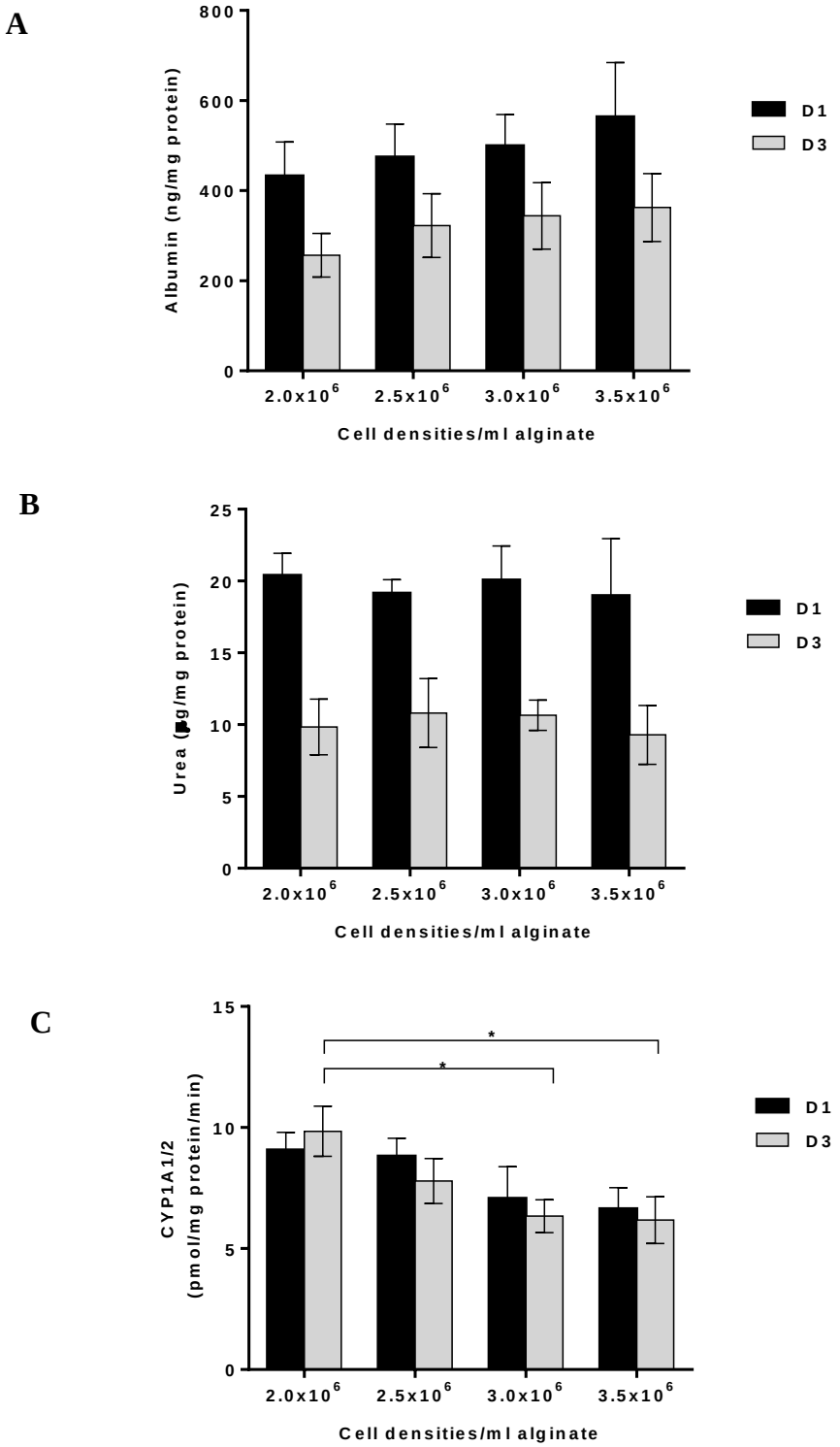

Figure 4.7: Hepatocyte-specific functions of HMBs produced with different cell densities; (A) albumin production, (B) urea production, and (C) cytochrome CYP1A1/2 activity, on day 1 and day 3 maintained in culture medium, *$p<0.05$.

4.3.5 Permeability of Optimised Microbeads

The proteins present in the supernatants of HMBs after culture were separated on polyacrylamide gels (Figure 4.8). The two samples were obtained from HMBs with hepatocyte viability of 60% (sample 1) and 70% (sample 2) before encapsulation. The intensity of some protein bands in sample 2 was higher than those in sample 1 which means higher amounts of those proteins. The thick bands represent the more abundant proteins in both samples within the MW range of 50 to 75kDa when compared to standard protein marker. The largest size of the protein showed in sample 1 was between 150-250kDa. The upper band in sample 2 was not fully separated and gave rise to a streaking of the final bands.

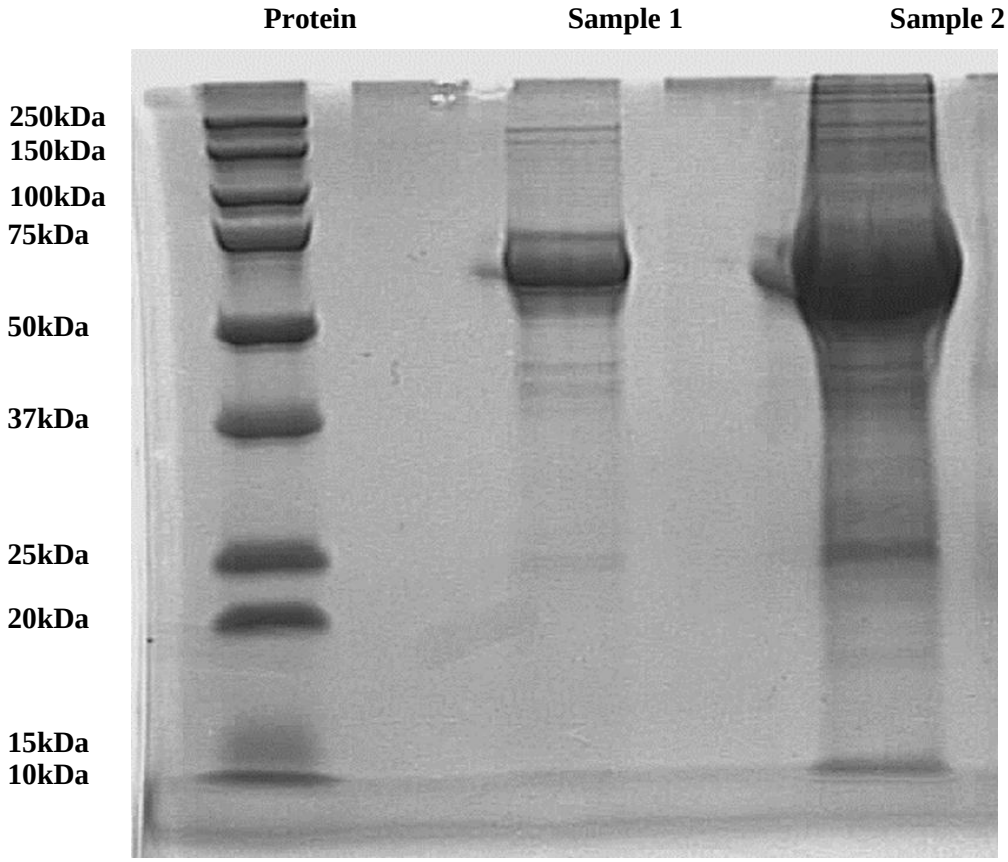

Figure 4.8: Representative example of 2D SDS-PAGE of proteins contained in supernatants of HMBs cultures. Standard protein markers range: 10-250kD.

As the results obtained from 2D protein electrophoresis could not indicate the precise maximum size of proteins that diffused across microbeads, a further study was performed using proteomics analysis. The proteomics profile detected a total 55 proteins (Appendix III). The most abundant protein observed was human serum albumin (MW 69kDa) which constituted approximately 20% of total protein detected. The largest protein that detected was carbamoyl phosphate synthase ammonia (MW 164kDa) which is a ligase enzyme located in the mitochondria involved in the production of urea. These results were corresponded to SD-PAGE data as described above.

4.4 Discussion

4.4.1 Polymerisation Time

In this study, we observed that the size of EMBs immediately after production in the 20min polymerisation group had a significantly larger size compared to 10min or 15min groups, while this pattern was not observed in HMBs. This finding suggests that incorporation of cells may have influenced microbead formation. After exposure to osmotic stress, both EMBs and HMBs demonstrated that a polymerisation time of 15min produced the most physically stable microbeads compared to the other two groups. The likely reason for this finding is that 10min polymerisation is too short for effective cross-linking and equilibration of external $Ca^{2}+$ between the core of alginate and the external medium (Zimmermann et al. 2005), whereas an increase in polymerisation time to 20min made microbeads become too crosslinked and brittle (Thu et al. 2000; Vaithilingam et al. 2011). Therefore an optimised polymerisation time is required to enhance microbead integrity. Our results showed that a prolonged polymerisation time did not have a negative effect on encapsulated cell viability and function supporting previous studies (Haque et al. 2005; Vaithilingam et al. 2011). Additionally, the microbead size and cell viability did not change after incubation in plain CMRL medium for 3h at room temperature, suggesting that the microbeads could be stable in CMRL transplant medium for a minimum of 3h before transplantation.

4.4.2 Effects of Cell Density on HMBs

The current study investigated the influence of cell density on physical integrity, cell viability and function in order to establish the optimal ratio of cell mass per microbead to allow oxygen, nutrients, and metabolite diffusion. Hepatocyte densities of $2.0x10^{6}$, $2.5x10^{6}$, $3.0x10^{6}$, and

$3.5x10^6$cells/ml alginate were studied. The results showed that microbeads produced using these densities had a stable physical integrity with smooth surface but when the cell density exceeded $3.5x10^6$cells/ml alginate, surface irregularities and microbead deformity were observed. These findings are different from a previously published study by Durkurt and colleagues (2013) who suggested that for rat hepatocytes the optimal density is $1.0x10^6$ cells/ml alginate. An increase in cell density will lead to an increase in microbead cell content leading to a considerable change in the microenvironment inside the microbeads with the possibility of apoptotic and hypoxic cell death particularly towards the microbead centre. It is difficult to assess the cells while they are entrapped in the three-dimensional structure. Live-Dead-Assay using fluorescent microscopy has generally been accepted as a method, however, it is inaccurate due to an over-estimation of viability caused by false-positive signals (double marked cells), (Leal-Egaña et al. 2010). Therefore, we determined the cell number, distribution, and viability across microbeads using both fluorescent (2D) and confocal (3D) microscopy. It has been reported that encapsulated hepatocytes lose approximately 20-30% viability after encapsulation (Wang et al. 2000). In this study, cell viability in HMBs was assessed after maintenance in culture for 1 day instead of immediately after preparation to allow stabilisation of cells to the microenvironment. We found that $3.5x10^6$cells/ml alginate HMBs provided the highest cell viability with an overall viability loss after encapsulation of 24%. It must be noted that, the cell viability loss could be attributed to quality of the available hepatocytes used, due to steatosis and cryopreservation injury. The 3D confocal microscopy data showed that cell viability in the centre of microbead did not decrease as the cell number per microbead was increased. The gel network of Ca-alginate is an inhomogeneous structure in which the alginate and calcium concentrations are lower in the core than the outer part of the microbead (Quong et al. 1998; Thu et al. 2000), thus allowing oxygen, nutrients, and metabolites to go across the microbead. Albumin and urea production tended to be better in the higher cell density groups but did not reach statistical significance. CYP1A1/2 activity was, however, lower in the high cell density than the low cell density groups.

4.4.3 Permeability of Optimised Microbeads

The permeability of optimised HMBs, produced with ultrapure alginate at a cell density of $3.5x10^6$cell/ml alginate and polymerisation at 15min, was evaluated with SDS-PAGE gel electrophoresis of protein and proteomic analysis. The new development of proteomic analysis technique provides detailed analysis of protein components released by HMBs and their diffusion into the culture medium. The results showed that albumin was the most abundant protein that HMBs produced and diffused into supernatant. The other proteins such as factor VII

(50kDa), prothrombin were not identified in current study. This could be possibly due to their low concentration or the low molecular mass being masked by the presence of albumin. The maximum protein size that diffused out from HMBs had a MW of 164kDa. Therefore, immunoglobulin G (IgG) which has a MW of 150kDa might permeate into the microbeads. Certainly, the main mechanism involved in destruction of encapsulated cells is direct contact between encapsulated cells and the immune effectors cells, hence, preventing cell contact is important. However, the immunoglobulins alone do not have the ability to destroy the encapsulated cells, as direct cell lysis requires the assembly of immunoglobulins and complements factors which involve the large glycoprotein C1q (410kDa), C3 (185kDa), C4 (210kDa), C5 (190kDa), C8 (170kDa) and the smaller ones; C2, C6, C7, and C9 (MW range of 79-128kDa). Some studies have shown that the permeability of alginate microbead to IgG may not be a major issue (Lanza et al. 1995; Duvivier-Kali et al. 2004; Schneider et al. 2005). Further study regarding immune reaction toward this optimised HMBs is required before translation to clinical use (details in Chapter 5). Proteomics analysis should be carried out on more supernatant samples of HMBs cultures using a technique that can overcome the possible masking effect of abundant proteins without losing important information.

In this study, the cryopreserved hepatocytes were used in some experiments. It is clear that cryopreservation has the negative effect on hepatocyte viability and function, therefore it would be ideal to use freshly isolated hepatocytes in all sets of experiments. The scarcity of the human liver tissue is an important issue and cryopreservation seems prudent for cell therapy. Encapsulation of fresh hepatocytes using the optimised protocol and followed by cryopreservation to establish a good quality of HMBs would be of great benefit in the future.

In conclusion, optimal settings of the encapsulator were established. Optimisation of the polymerisation time and cell density has contributed to the improvement in the efficiency of the microencapsulation hepatocytes. This optimised protocol for production of human hepatocyte microbeads using GMP grade materials provided good cell viability, function, and physical integrity and possibly can be used for preparation of microbeads for clinical transplantation.

CHAPTER 5

5. *In Vitro* Immunogenicity of Alginate Microencapsulated Human Hepatocytes

5.1 Introduction

The biocompatibility of the alginate microbeads is an important issue for efficacy following transplantation into the peritoneum. The strategy for functional grafting of transplanted encapsulated cells is based on the fact that the microbeads should provoke none or, at most, minimal host immune reaction to avoid cellular overgrowth. The formation of a pericapsular fibrotic overgrowth will interfere with oxygen and nutrient diffusion, as well as exchange of essential metabolites that subsequently leads to cell death (Vaithilingam et al. 2011; De Groot et al. 2004). The biomaterial of microbeads, or antigens/chemokines released by encapsulated cells through microbeads pores, may initiate a host immune response and inflammatory reaction leading to cellular overgrowth. The intrinsic characteristics of microbeads or microcapsules involving the compositions (M and G content), electrical charge on the surface, permeability, and types of microbeads/microcapsules (e.g. PLL-coated alginate microbead) are the factors determining the host responses as previously discussed in Section 1.7.1 and Section 1.7.3.

The important issue that should be taken into consideration after transplanting microbeads into the peritoneal cavity is the physiochemical changes of microbeads' surface due to protein adsorption, such as fibrinogen. Protein adsorption is a complex phenomenon which can have a significant impact on the biocompatibility of microbeads. Several studies demonstrated that adsorption of fibrinogen and other proteins onto the microbead surface lead to the activation of host effectors mechanisms including complement, immunoglobulins, and inflammatory cells (Tang and Eaton 1993; Vos et al. 2002; Engberg et al. 2011). It has been shown that alginate microbeads possess high hydrophilicity on the surface, which limits low adsorption of proteins and a gives low degree of denaturation. On the other hand, the alginate-PLL-alginate (APA) has a hydrophobic surface which enhances protein adhesion and conformational changes. The conformational changes of the proteins that adhere onto microbead's surface may lead to a reduction in hydrophilicity (Vogler 2012; De Vos et al. 2006).

The aim of the current study was to investigate the alloimmune response towards optimised clinical grade human hepatocyte microbeads (established in Chapter 4) *in vitro* by assessing the inflammatory responses of peripheral blood mononuclear cells (PBMCs) co-cultured with them.

Studies of host immune response also performed on hepatocytes microbeads after exposure to human ascitic fluid to mimic the environments following intraperitoneal transplantation in clinical settings.

5.2 Materials and Methods

5.2.1 Materials

Ficoll-Hypaque density gradient solution (Amersham Pharmacia, Biotech UK, Little Chalfont, UK), and cell stimulation cocktail plus protein transport inhibitors (e-Bioscience Ltd, Hatfield, UK). All monoclonal antibodies, Cytofix/Cytoperm, and Perm/Wash solution (BD Pharmingen, Oxford, UK).

5.2.2 Methods

5.2.2.1 Encapsulation of Hepatocytes

Hepatocyte isolation was performed as described in Section 2.2.1. HMBs and EMBs were produced using the optimised protocol described in Chapter 4.

5.2.2.2 PBMCs Isolation

PBMCs were obtained from either normal healthy donors (n=6) or patients with acute-on-chronic liver disease (n=2). PBMCs were isolated with a standard Ficoll-Hypaque density centrifugation method (Longhi et al. 2005). Briefly, 20ml of peripheral blood were obtained and mixed with preservative free heparin (10 U/ml). Blood was slowly layered onto an equal volume of Ficoll-Hypaque density gradient solution and centrifuged at 2100 RPM, 21°C for 21min. The mononuclear cells (buffy coat) were collected and washed twice with 40ml PBS at 1900 RPM, 21°C for 5min. Total lymphocyte number and cell viability was assessed by Trypan blue exclusion viability exceeded 98%.

5.2.2.3 Assessment of Immunogenicity of Hepatocytes Microbeads

5.2.2.3.1 Establishing Optimum Ratio of Hepatocytes and PBMCs

To establish the optimum ratio of human hepatocytes to PBMCs that enables the maximum interaction between the two cell populations, PBMCs from healthy donors were co-cultured with human hepatocytes monolayers (n=5). The PBMCs were co-cultured with plated human hepatocytes at PBMCs:hepatocytes 1:5, 1:10 and 1:20 ratios. The cells were cultured in WEM supplemented with 10% heat-inactivated FCS, 2mM L-glutamine, 0.1µM insulin, penicillin (50U/ml) and streptomycin (50µg/ml) and maintained in a humidified incubator at 37°C for 24h. After co-culture, PBMCs were harvested and subsequently stained. The proportion of activated PBMCs following co-culture with hepatocytes was assessed using flow cytometry (FACS), (Section 5.2.2.5).

5.2.2.3.2 HMBs Co-culture with PBMCs

PBMCs isolated from four healthy donors, were either cultured alone (monocultures) or co-cultured with EMBs or HMBs ($3.5x10^6$cells/ml alginate; n=4) in culture medium for 24h under the same conditions. The ratio of PBMCs to encapsulated hepatocytes co-culture was based on the experiment of direct co-culture of PBMCs and plated hepatocytes as described above (Section 5.2.2.3.1).. Microbeads were examined under a light microscope before and after co-culture with PBMCs to evaluate the extent of cell adhesion to their surface. Proportions of activated PBMCs following co-culture with either EMBs or HMBs were assessed by FACS analysis, (Section 5.2.2.5).

5.2.2.4 Evaluation of Immunogenicity of HMBs after Exposure to Ascitic fluid

Human ascitic fluid was obtained from patients with acute-on-chronic liver disease (n=2). 2.4ml HMBs or EMBs were incubated in 6ml ascitic fluid in warm water at 37°C with gentle agitation for 1h. The ascitic fluid was then removed and HMBs and EMBs were washed five times with WEM. PBMCs were isolated from the same patients from whom ascitic fluid was obtained. Five experimental sets were tested; PBMCs alone, EMBs + PBMCs, EMBs (ascitic-treated) + PBMCs, HMBs + PBMCs, and HMBs (ascitic-treated) + PBMCs groups. 1.2ml HMBs and EMBs with or without exposure to ascitic fluid were co-cultured in 6-well plate with $1.6x10^6$ PBMCs in supplemented WEM and incubated at 37°C for 24h (Section 5.2.2.3.1). The day after co-culture, PBMCs were collected, resuspended in 1ml medium and seeded in 12-well plates. In order to analyse the PBMCs activation and the intracellular cytokine production, 2µl of the cell

stimulation cocktail (plus protein transport inhibitors) was added and incubated with PBMCs for 4h at 37°C. Cell stimulation cocktail is a cocktail of phorbol 12-myristate 13-acetate (PMA), ionomycin, brefeldin A and monensin which is used for induction and subsequent intracellular detection of cytokines and other secreted proteins in both *in vitro*-cultured and *ex vivo* cells. PBMCs were then washed with PBS, stained and then analysed by FACS (Section 5.2.2.5). PBMCs monocultures were used as control in all experimental sets.

5.2.2.5 Flow Cytometry Analysis

Twenty four hours after culture, three-color FACS analysis was performed. PBMCs were stained for cell surface markers using the following antibodies: allophycocyanin (APC)-conjugated, or phycoerythrin (PE) conjugated anti-CD3 (T cells), APC-cychrome (CY)-7-conjugated CD4 (T cells), FITC-conjugated, or PE-CY-5-conjugated anti-CD8 (T cells), PE-CY-7-conjugated anti-CD25 (T cells), peridinin chlorophyll protein (PerCP)-conjugated anti-CD14 (monocytes), PE-conjugated anti-CD40L (co-stimulation molecule), FITC-conjugated anti-CD38 (all white blood cells), PE-CY-5-conjugated anti-CD56 (natural killer cell), FITC-conjugated anti-CD19 (B cell), and PE-conjugated anti-CD54 (intercellular adhesion molecule-1). Cells were incubated at 4°C for 30min in the dark, then washed with PBS/1%FCS and re-suspended in 400µL PBS/1% FCS and stored at 4°C until the analysis. Intracellular staining was performed using following antibodies: PE-anti-IFNγ, APC-anti-IL-2, PE-CY-7-anti-IL-17, APC-anti-IL-10, PE-anti-IL-4, FITC-anti-TNFα and PE-anti-IL-6. The cells were permeabilised with 250µl cytofix/cytoperm and incubated for 20 min at 4°C. Cell were then washed with Perm/Wash solution twice and then stained for intracellular cytokines were stained and resuspended in 80µl Perm/Wash solution and incubated at 4°C for 30min in the dark. The cells were then washed twice with Perm/Wash solution and resuspended in 400µl PBS/1%FCS prior to analysis. The stained cells were then analysed using the combinations of surface and intracellular antibody shows in Table 5.1.

FACS analysis was performed on a Becton Dickinson fluorescence activated cell sorter (FACS Canto II, Becton-Dickinson, Immunocytochemistry Systems, CA, USA), and FACS Diva software (ver.6.3.1, Biosciences, CA, USA) was used for data analysis. A minimum of 20,000 lymphocyte-gated events were acquired per sample.

Table 5.1: The combinations of surface and intracellular marker

Type of cell/cytokine	Activation markers
T cell	$CD3^+CD25^+$, $CD4^+CD25^+$, $CD8^+CD25^+$, $CD3^+CD54^+$, $CD4^+CD54^+$, $CD8^+CD54^+$, $CD3^+CD38^+$, $CD4^+CD38^+$, $CD8^+CD38^+$
Monocyte	$CD14^+CD25^+$, $CD14^+CD40L^+$
B cell	$CD19^+CD25^+$, $CD19^+CD54^+$
NK cell	$CD3^+CD56^+$
IFNγ	$CD4^+IFN\gamma^+$, $CD8^+IFN\gamma^+$, $CD56^+IFN\gamma^+$
TNFα	$CD14^+TNF\alpha$
IL-2	$CD4^+IL\text{-}2^+$, $CD8^+IL\text{-}2^+$
IL-4	$CD4^+IL\text{-}4^+$
IL-6	$CD14^+IL\text{-}6^+$
IL-10	$CD4^+IL\text{-}10^+$
IL-17	$CD4^+IL\text{-}17^+$

5.2.2.6 Microbeads Morphology

HMBs and EMBs morphology were examined under light microscopy immediately after production and after 24h co-culture with PBMCs. The degree of inflammatory cell adhesion on the surface of microbeads was determined according to Tam et al (2011).

5.3 Results

5.3.1 Frequency of Activated PBMCs Following Co-culture with EMBs and HMBs

Frequency of activated PBMCs activation after co-culture with hepatocytes at various PBMCs:hepatocytes ratios (1:5, 1:10, and 1:20) are shown in Table 5.2. The percentage of lymphocytes positive for surface activation markers was not significantly different in the three groups compared to control, with the exception of $CD14^+CD25^+$ and $CD14^+CD40L^+$ activated monocytes. $CD14^+CD25^+$ cells were significantly decreased within PBMCs co-cultured with hepatocytes at all ratios ($p<0.001$). The percentage of $CD14^+CD40L^+$was similar in the 1:5 group and control, but it was significantly lower in the 1:10 and 1:20 groups compared to control ($p<0.001$). Therefore, the ratio of 1:5 was chosen for studying the interaction between HMBs and EMBs with PBMCs.

After co-culturing microbeads with PBMCs for 24h, both EMBs and HMBs were still intact and maintained their uniform shape without any apparent PBMCs adherent to their surface (Figure 5.1). The percentage of cells positive for activation markers within PBMCs is shown in Table 5.3. There were no significant differences in the proportions of cells positive for CD38 (i.e.$CD3^+CD38^+$, $CD4^+CD38^+$, $CD8^+CD38^+$) within PBMCs co-cultured with EMBs or HMBs compared to control. In addition, the percentage of $CD4^+CD25^+$, $CD3^+CD25^+$, $CD8^+CD25^+$ T cells did not differ between the PBMCs co-cultured with microbeads (EMBs or HMBs) and control. The frequency of $CD3^+C56^+$ NK cells, $CD19^+CD25^+$and $CD19^+CD54^+$ B cells was also comparable between the three groups. The frequency of $CD14^+CD25^+$ activated monocytes in PBMCs co-cultured with HMBs was significantly lower compared to those co-cultured with EMBs, and PBMCs monocultures (2.66±0.8 vs 22.8±7.7 and 45.7±11.0, respectively; $p< 0.0001$), (Figure 5.2).

Table 5.2: Frequency of activated PBMCs after co-culture with hepatocytes at different ratios

Activation Marker	PBMCs alone (control)	PBMCs:Hepatocytes		
		1:5	1:10	1:20
$CD3^+$ $CD25^+$	4.4±0.60	5.64±0.17	6.66±1.08	6.34±0.59
$CD4^+$ $CD25^+$	3.78±0.28	4.9±0.12	6±0.97	5.68±0.58
$CD8^+$ $CD25^+$	6.52±3.39	7.04±3.47	2.02±0.46	2.6±0.75
$CD14^+$ $CD25^+$	65.02±8.07	42.88±7.41*	31.3±6.01*	31.68±4.42*
CD14 $^+$$CD40L^+$	28.58±17.15	16.88±7.18	6.64±2.26*	5.4±2.26*
$CD3^+$ $CD54^+$	23.98±11.77	22.62±9.76	23.28±9.42	26.58±11.09
$CD4^+$ $CD54^+$	20.02±10.07	18.84±9.15	18.3±8.47	20.74±9.79
$CD3^+$ $CD56^+$	27.04±5.65	26.1±3.82	26.5±3.70	26.78±4.45
$CD8^+$ $CD54^+$	12.3±3.65	11.66±2.77	12.38±2.98	13.28±2.87
$CD3^+$ $CD38^+$	3.08±1.11	3.64±1.07	4.08±2.02	3.64±1.62
$CD4^+$ $CD38^+$	1.26±0.16	1.86±0.89	1.2±0.29	1.46±0.32
$CD8^+$ $CD38^+$	22.94±12.66	27±14.02	17.8±6.06	17.72±6.02
$CD19^+$ $CD25^+$	0.78±0.17	1.22±0.37	2.1±0.99	2.1±0.82
$CD19^+$ $CD54^+$	1.06±0.34	1.82±0.62	2.32±0.98	2.64±0.92

Statistical significant *$p<0.001$ compared to control.

Before co-culture with PBMCs

EMBs **HMBs**

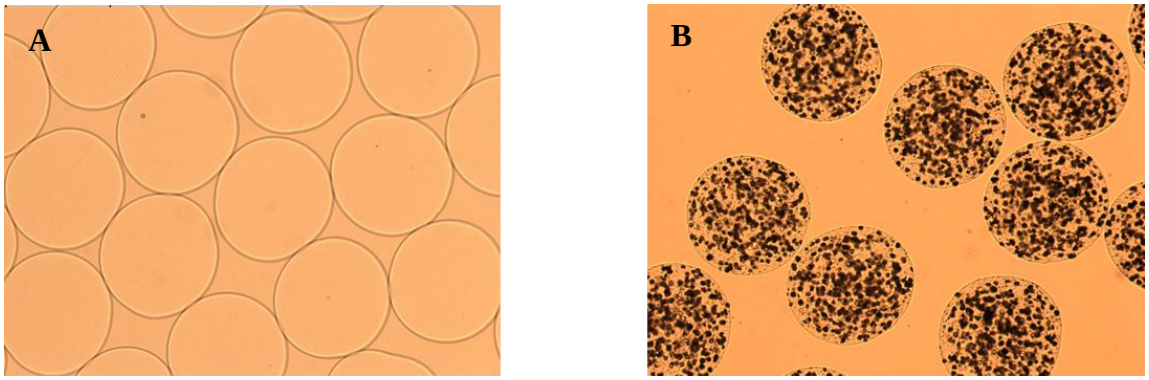

After co-culture with PBMCs

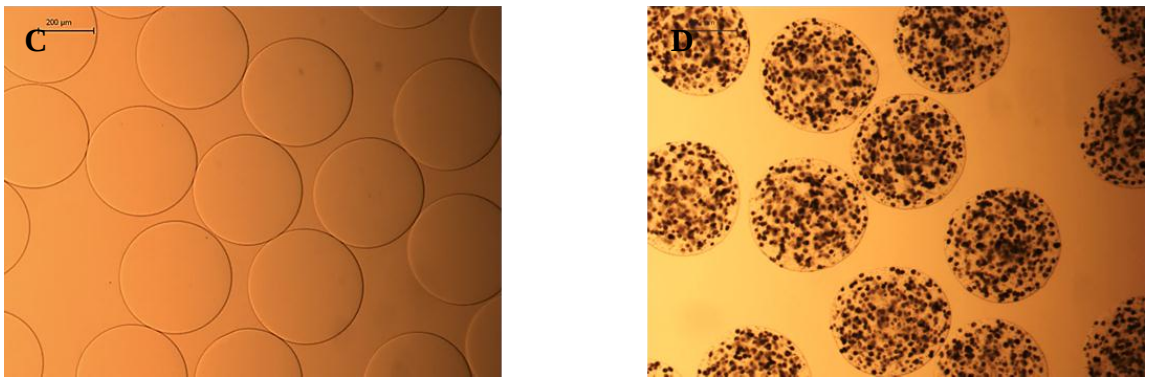

Figure 5.1: Representative images of EMBs and HMBs morphology; (A and B) immediately after production before co-culture with PBMCs, and (C and D) after co-culture with PBMCs for 24h**.**

Table 5.3: Frequency of activated PBMCs after co-cultured with EMBs and HMBs compared to control.

Activation marker	PBMCs Alone	PBMCs after co-culture with EMBs	PBMCs after co-culture with HMBs
$CD3^+CD25^+$	9.70±2.07	10.30±2.55	9.19±1.70
$CD4^+CD25^+$	3.74±0.69	4.32±0.94	4.83±1.07
$CD8^+$ $CD25^+$	2.36± 0.62	1.85±0.51	1.65±0.32
$CD14^+CD25^+$	45.65±10.98	22.76±7.96	2.66±0.80*
$CD14^+CD40L^+$	6.39±1.34	5.32±1.95	6.36±2.32
$CD3^+CD54^+$	14.28±2.98	13.38±1.04	11.36±2.11
$CD4^+CD54^+$	2.53±0.73	4.17±1.17	1.90±0.69
$CD3^+CD56^+$	12.75±3.17	12.10±1.32	9.40±1.48
$CD8^+CD54^+$	13.54±3.52	12.26±1.31	12.64±2.04
$CD3^+CD38^+$	6.11±1.14	6.78±0.68	6.75±0.89
$CD4^+CD38^+$	2.72±0.16	3.22±0.55	2.12±0.34
$CD8^+CD38^+$	10.03±4.99	11.77±5.63	9.90±4.23
$CD19^+CD25^+$	0.61±0.24	1.07±0.29	2.55±1.04
$CD19^+CD54^+$	1.10±0.28	2.30±0.50	5.54±2.14

Statistical significance *p< 0.001 compared to control

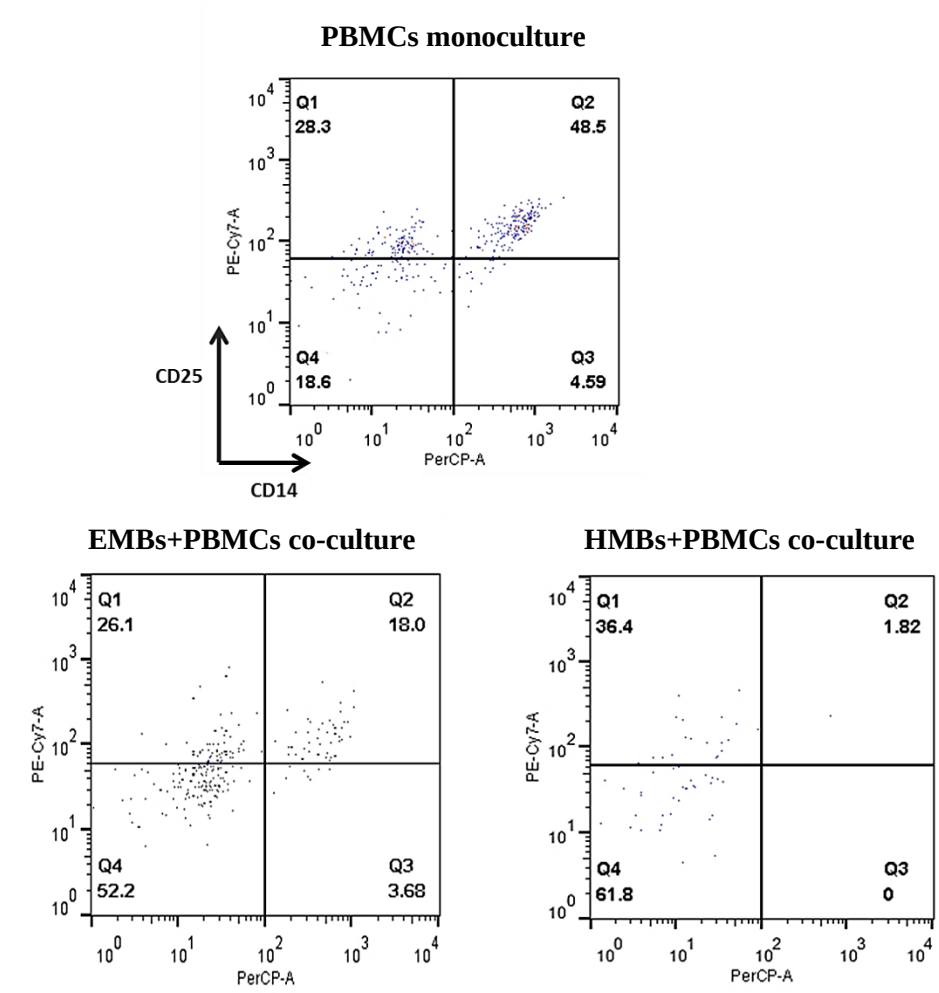

Figure 5.2: Representative of flow cytometry plots demonstrates the decreased expression of $CD14^{+}CD25^{+}$on PMBCs (Q2 quadrant) after co-culture with HMBs for 24h.

5.3.2 Immunogenicity of HMBs after Exposure to Ascitic fluid

There was no difference in microbeads morphology (EMBs and HMBs) between those exposed to ascitic fluid before co-culture with PBMCs compared to the non-exposure groups, where the microbead surface was smooth and clear without any cell adhesion. The percentage of $CD14^{+}CD25^{+}$ cells seemed to be lower in PBMCs co-cultured with both groups of HMBs (either exposed or non-exposed to ascitic fluid) than in those co-cultured with EMBs and control (Table 5.4). The proportion of cells positive for other surface markers was similar in all groups. Additionally, there was no difference in the frequency of cell producing cytokine (IL-2, IL-4, IL-6, IL-10, IL-17, IFN-γ, and TNFα) after PBMCs stimulation in all five groups.

Table 5.4: Frequency of cells positive for activation markers or producing cytokines after co-culture with EMBs and HMBs

	PBMCs alone	EMBs+ PBMCs	EMBs (ascitic) +PMBCs	HMBs+ PBMCs	HMBs (ascitic) +PBMCs
$CD14^+CD25^+$	19.75±1.73	13.8±1.78	12.85±0.84	9.75±0.25	9.1±0.38
$CD14^+CD40L^+$	8.5±2.47	9.15±5.09	10.6±4.55	6.8±2.77	10.7±0.69
$CD4^+CD38^+$	7.9±3.96	9.05±1.93	9.35±1.83	13.8±3.86	6.85±1.83
$CD4^+CD25^+$	14.95±7.86	18.5±8.51	20.95±12.91	17.6±12.26	12.7±6.82
$CD8^+CD25^+$	1.35±0.05	2.35±0.54	0.85±0.15	1.15±0.15	0.85±0.15
$CD4^+CD69^+$	4.25±1.04	5.05±0.15	6.55±1.34	6.7±1.98	3.35±1.73
$CD19^+CD25^+$	4.55±0.15	4.25±0.64	4.5±0.99	4.2±0.5	3.7±1.19
$CD19^+CD54^+$	10.35±3.61	10.65±2.92	9.2±1.98	10.9±3.41	10.1±2.77
$CD3^+CD54^+$	37.3±4.85	35.5±2.62	34.05±2.03	24.9±3.26	28.8±4.65
$CD3^+CD25^+$	10.85±2.82	13.3±0.34	11.35±2.72	9.5±3.36	10.3±3.36
$CD4^+CD54^+$	37.2±2.37	37.75±3.61	34.8±8.07	25.3±6.23	28.4±2.27
Intracellular markers					
$CD4^+IFN\gamma^+$	16.3±3.16	15.55±0.54	13.95±0.15	12.9±4.05	11.85±1.73
$CD4^+IL\text{-}2^+$	22.1±10.33	19.75±8.55	25.1±9.46	16.9±8.6	19.5±11.27
$CD4^+IL\text{-}17^+$	26.95±2.03	30.15±0.84	40.85±7.07	25.4±0.59	32.9±12.96
$CD8^+IFN\gamma^+$	21.1±3.76	19.35±9.84	20.3±13.25	18.55±6.18	13.05±6.77
$CD8^+IL\text{-}2^+$	3.8±1.29	3.25±1.24	4.05±1.83	3.8±1.78	3.4±2.18
$CD56^+IFN\gamma^+$	3.85±2.52	4.7±3.26	3.85±2.72	4.6±0.49	2.85±1.93
$CD4^+IL\text{-}10^+$	0.4±0.1	0.85±0.25	0.85±0.25	2±1.29	1.95±1.34
$CD4^+IL\text{-}4^+$	10±2.67	10.3±3.07	9.25±1.73	7.5±0.49	9.8±1.19
$CD14^+TNF\alpha^+$	0.5±0.2	0.55±0.25	0.6±0.2	0.6±0.1	0.55±0.15
$CD14^+IL\text{-}6^+$	0.35±0.05	0.55±0.25	0.45±0.25	0.5±0.1	0.4±0.1

5.4 Discussion

In the current study, the immunogenicity of optimised GMP grade HMBs was investigated as biocompatibility is one of the key factors for the success of transplantation. No studies published so far have investigated the alloimmune reaction against human hepatocyte microbeads. The appropriate ratio between human hepatocytes and PBMCs was established. With the exception of monocytes, no significant differences were noted in the proportion of T, B or NK cells positive for activation markers following co-culture with human hepatocytes at 1:5, 1:10, and 1:20 ratios. The proportion of $CD14^{+}CD25^{+}$ and $CD14^{+}CD40L^{+}$ cells was significantly lower than in the control group (PBMCs alone) when the 1:10 and 1:20 ratios were tested. Only the proportion of $CD14^{+}CD25^{+}$ cells was lower than in the control at the 1:5 ratio. These findings show that human hepatocytes have low immunogenicity and might even have inhibitory effects on monocyte reactivation. Sana et al. (2013) showed that human hepatocytes present a low immunogenic phenotype, and promote the cell contact-dependent production of IL-10 by myeloid dendritic cells after co-culture with PBMCs. IL-10 is a potent inhibitor of monocyte/macrophage activation which is secreted by a number of cells of the immune system, including monocytes and T cells (Parry et al. 1997). Therefore, the possible explanation for the results in present study might be that human hepatocyte induced IL-10 production by immune cells and subsequently suppressed the monocyte activation

The results presented in this chapter obtained demonstrated that both HMBs and EMBs did not elicit immune activation *in vitro*. This may be due to the use of ultrapure sodium alginate; these findings also support and supporting previous studies which showing that inflammation and immune reaction are related to the purity of alginate (Orive et al. 2002; Kim et al. 2013) and to the uncoated microbeads used in present study (Orive et al. 2006; Tam et al. 2011). Interestingly, a significant decrease in the frequency of activated monocytes was observed in PBMCs/HMBs co-cultures. These findings reflected those obtained following direct hepatocyte/PBMCs co-culture. In addition, an unexpected decrease in the frequency of activated monocytes was seen in PBMCs/EMBs co-cultures. The reason for these findings is unclear; however, release of anti-inflammatory cytokines or chemokines might have played a role in the regulation of monocyte activation including IL-10 production as discussed above. Therefore, analysis of cytokines production was carried out in the next stage of this study.

Host immune response to the transplanted alginate microbeads involves not only the biomaterial of microbeads or encapsulated cells but also the environment in which the transplantation occurs, i.e. the peritoneal cavity. In order to reproduce the '*in vivo*' environment, microbeads were incubated with ascitic fluid in a transudate of plasma consisting of a variety of proteins

including immunoglobulins and complement. The initial results showed that the morphology of HMBs and EMBs after co-culture with PBMCs was intact and clean without any immune cells adherent on microbeads surface regardless of exposure to ascitic fluid or not. There was no difference in the percentage of PBMCs expressing activation markers or producing cytokines in the absence or presence of ascitic fluid. This may indicate that the protein adsorption on both EMBs and HMBs was minimal and did not change the physiochemical properties of microbeads' surface. As a result, the host effector mechanisms involving reactive protein cascades, such as complement, immunoglobulins, and immune cells were not activated. These results also suggest that EMBs and HMBs were biocompatible with the immune and complement system. The findings of this study are in agreement with previous work by, Tam et al. (2009) who detected presence of immunoglobulins (IgG, IgM and IgA) adsorbed to APA microcapsules, but not on alginate microbeads after exposure to human serum and peritoneal fluid, suggesting that the positive charge at the APA capsule surface is responsible for immunoglobulin binding. Another study demonstrated that alginate microbeads are complement-compatible as they did not activate complement after incubation in human whole blood, whereas APA microcapsules activated accumulation of soluble terminal solution complex, C3a, C5a and surface activated leukocyte adhesion (Rokstad et al. 2011). In contrast, Haan et al. (2011) reported a large increase in TNF-α production by PBMCs when exposed to alginate microbeads with human peritoneal (ascitic) fluid, but not by PBMCs exposed to APA microcapsules. However, the peritoneal (ascitic) fluid and PBMCs used in the study by Haan and colleagues were not from the same donors, possibly accounting for immune over-reactivity. The slight decrease in the frequency of activated monocyte was detected in co-culture with both HMBs groups. However, the inhibitory effect was not as strong as in the experiments discussed above. This might be explained by the fact that PBMCs used in the first set of experiments were obtained from healthy donors whereas the later sets were obtained from patients ALF and underlying chronic liver disease. These preliminary experiments highlighted the biocompatibility of HMBs in ascitic fluid. This section of work was, however, limited by the small number of patient's samples available hence more experiments are needed. The study of the immunogenicity of microbeads *in vivo* is important and will be discussed in Chapter 7.

In conclusion, the present study has demonstrated that the optimised EMBs and HMBs produced using ultrapure alginate without PLL coating, 15min of polymerisation time and a cell density of $3.5x10^6$cell/ml alginate were biocompatible with the human PBMCs *in vitro*. The microbeads showed minimal protein adsorption after exposure to ascitic fluid and did not stimulate immune reaction and cytokine production. This supports the clinical application of hepatocyte microbeads transplantation without the need for immunosuppression.

CHAPTER 6

6. Cryopreservation of Hepatocyte Microbeads for Clinical Transplantation

6.1 Introduction

Establishing banked cryopreserved hepatocyte microbeads for long-term storage would be of great benefit for emergency cases such as ALF. Previously published studies have shown protective effects of alginate microencapsulation on hepatocytes during the cryopreservation process (Mahler et al. 2003; Aoki et al. 2005; Kusano et al. 2008; Hang et al. 2010). Alginate microbeads have a high water content (>90%) together with the relatively large size of microbeads compared to single cells make microbeads susceptible to cryodamage by ice-crystal formation (Chin et al. 2004). Studies on cryopreservation of microencapsulated cells have been reported with variable effectiveness due to differences in cryopreservation methods. These differences include cell density, cryopreservation media, cryoprotectants, cooling rate and storage temperature (Lee et al. 2004; Heng et al. 2004; Murua et al. 2009; Massie et al. 2011). Most of the previous studies of a cryopreservation of microencapsulated hepatocytes used cryopreservation medium consisting of culture medium, 10% FCS, and 10% DMSO placed into cryovials and stored in liquid nitrogen (Dixit et al. 1993; Aoki et al. 2005; Kusano et al. 2008; Hang et al. 2010). Even though these protocols gave relatively good viability and function after thawing, they were not acceptable for clinical transplantation.

Pre-treatment or preincubation of cells with various compounds at 37°C before cryopreservation has shown beneficial effects on cryopreserved hepatocytes as these methods allow hepatocytes to recover from the dissociation stress (Silva et al. 1999; Terry et al. 2005). However, no study has shown the benefit of preincubation of microbeads before cryopreservation.

The cryoprotectant is an important element for cryopreservation. 10% DMSO is the choice of cryoprotectant that has been used for clinical cryopreservation of hepatocytes (Terry et al. 2010). The DMSO concentration that has been used for cryopreservation of microencapsulated cells varied from 10% up to 20%. Chin et al (2004) showed that with a microencapsulated kidney cell line cryopreservation with 20% DMSO and 0.25M sucrose improved cell viability without damaging the microcapsules. Murua and co-workers (2009) compared the efficacy of different concentrations of DMSO (1%, 5%, 10%, 20% and 30%) for cryopreservation of

microencapsulated myoblasts and found that 10% was the optimal concentration. Recently, carboxylated poly-L-lysine (COOH-PLL) was studied for cryopreservation of encapsulated vascular smooth muscle cells by Vrana et al. (2011). They showed that this cryoprotectant improved cell viability in encapsulated cells. They suggested that COOH-PLL has the antifreeze protein-like properties which could protect cell membranes (Vrana et al. 2012).

The basal freezing solution is another challenging choice for cryopreservation of microencapsulated cells. Currently, a number of organ preservation solutions are available which can be used as cryopreservation solutions. These solutions include UW solution (ViaSpan), (Lee et al. 2004), Celsior (Massie et al. 2011), and HTS (Sosef et al. 2005). In addition, CryoStor is a family of cryopreservation solutions developed from HTS which have been demonstrated to yield improved cryopreservation of multiple cellular systems (Baust et al. 2000; Stylianou et al. 2006). Malpique et al. (2010) showed that using CryoStor as cryopreservation medium significantly improved post thawing recovery for both nonencapsulated and encapsulated neurospheres compared to standard culture medium (Malpique et al. 2010).

Some investigators have included other compounds in the freezing medium together with the cryoprotectant, such as anti-oxidant or anti-apoptosis agents with the aim of further protection from cryoinjury. These compounds are known as cytoprotective agents as they protect the cells by specific mechanisms during the cryopreservation process but do not inhibit intracellular ice formation. FCS is a common additive agent used in the freezing medium for the maintenance of encapsulated cells and microcapsules but cannot be used clinically as it is of animal origin. The caspase inhibitor benzyloxycarbonyl-Val-Ala-DL-Asp-fluoromethylketone, ZVAD is an anti-apoptosis agent. Adding ZVAD improved the cell viability and function under stressful conditions prone to apoptosis such as isolation and cryopreservation of encapsulated hepatocytes (Nyberg et al. 2000; Mahler et al. 2003). Moreover, ice nucleating agents such as crystalline cholesterol can be added into freezing medium to reduce supercooling and intracellular ice formation (Massie et al. 2011).

The freezing protocol using for cryopreservation of encapsulated cells varies including simple technique (Dixit et al. 1993), multi-step cooling with CRF or cryogen-free cooler (Massie et al. 2011) and vitrification (Lawson et al. 2011). However, for clinical purposes with regard to sterility, toxicity and amount of production, the multi-step slow cooling protocol using CRF is seemed to be an appropriate choice.

The hypothesis of this study was that the cryopreservation of hepatocyte microbeads could be improved by supplementation of the cryopreservation solution with appropriate cytoprotectant agents such as an iron chelator (desferoxamine; DFO), anti-apoptosis drug (ZVAD), and human serum albumin (HSA) targeting protection of hepatocytes from oxidative stress and apoptosis (Yagi et al. 2001; Kerkweg et al. 2002; Fujita et al. 2005) and maintaining microbeads integrity (Schneider et al. 2003). The aim of this study was to develop an optimised protocol for cryopreservation of hepatocyte microbeads for clinical transplantation. Different types of cryopreservation solutions and cytoprotectants which potentially can be used for clinical application were investigated.

6.2 Materials and Methods

6.2.1 Materials

Bambanker (Nippon Genetics, Tokyo, Japan), CryoStor CS10™ (Sigma-Aldrich, Dorset, UK), Histidine-tryptophan-ketoglutarate (HTK: Custodiol™; DR. Franz Kohler Chemie GMB, Alsbach-Hähnlein, Germany), desferoxamine (Sigma-Aldrich, Dorset, UK), ZVAD (R&D system, Abington, UK), and propidium iodide (BD Pharmingen, Oxford, UK).

6.2.2 Methods

Experimental Design

At first, the effects of 4 different freezing solutions were evaluated on non-encapsulated human and rat hepatocytes. The best two freezing solutions that resulted in high cell viability and function after thawing were then selected for study of HMBs and rat hepatocyte microbeads (RMBs) cryopreservation. Then, cytoprotective agents were examined in order to improve the microbeads cryopreservation protocol.

Hepatocytes were isolated from the same donor tissues for each set of experiments. Non-cryopreserved (fresh) hepatocytes and hepatocyte microbeads were prepared identically and maintained in cultures as cryopreserved samples. All assays for cryopreserved samples were performed and compared to fresh samples at similar time points.

6.2.2.1 Hepatocyte Isolation

Human and rat hepatocyte isolations were performed according to the methods described in Section 2.2.1 and 2.2.2, respectively.

6.2.2.2 Encapsulation of Hepatocytes

Human and rat hepatocytes were encapsulated using the optimised technique in Chapter 4 where the microbeads were produced at cell density of $3.5x10^6$ cell/ml alginate and polymerised for 15min. See Section 2.2.6 for the encapsulation processes.

6.2.2.3 Cryopreservation of Hepatocytes in Different Freezing Solutions

Human and rat hepatocytes were used to evaluate four different cryopreservation media. They consisted of two types of hypothermic organ preservation solutions (UW and HTK) and two commercial cryopreservation solutions (CryoStor CS10 and Bambanker). All cryopreservation solutions contained 10% DMSO as cryoprotectant. Based on published and standard protocols used for cryopreservation of human hepatocytes at King's College Hospital, 5% glucose (300mM) was added to UW and HTK (Table 6.1). Briefly, isolated hepatocytes were split into four groups. In each group, hepatocytes were resuspended in ice-cold freezing medium at a density of $1x10^7$ hepatocyte per ml. Hepatocyte suspension was then transferred into 2ml cryovials. Cryopreservation was performed using the standard freezing protocol on the CRF (Section 2.2.8.1). The cryopreserved cells were stored at −140°C for two weeks.

Table 6.1: Freezing solution mixtures

Main solution	**UW (ViaSpan®)**	**HTK (Custodiol™)**	**Bambanker[a]**	**CryoStor CS10[a]**
Application	Organ preservation solution	Organ preservation solution	Cell freezing media	Cell freezing media
Detail of components	K^{+}-lactobionate (100mM) KH_2PO_4 (25mM) Na^{+} (30mM) Raffinose (30mM) Adenosine (5mM) Glutathione (3mM) Allopurinol (1mM) Hydroxyethyl starch (50g/l) Dexamethasone (8mg/l) Penicillin (200,000U/l) Insulin (40U/l) Osmolarity 320mOsM pH 7.4	Na^{+} (15mM) K^{+} (10mM) Mg^{2+} (4mM) Ca^{2+} (0.015) Cl^{-} (50mM) L-Histidine (198mM) Ketoglutarate (1mM) Tryptophan (2mM) Mannitol (30mM) Osmolarity 310mOsM pH 7.2	Ready to use Serum free DMSO -based (10%)	Ready to use Serum free DMSO –based (10%) Modified from HTS Composition of HTS Na^{+} (100mM) K^{+} (42.5mM) Mg^{2+} (5mM) Ca^{2+} (0.05mM) Cl^{-} (17.1mM) $H_2PO_4^{-}$ (10mM) HCO_3^{-}(5mM) HEPES (25mM) Lactobionate (100mM) Sucrose (20mM) Mannitol (20mM) Glucose (5mM) Dextran-40 (6%) Adenosine (2mM) Glutathione (3mM) Osmolarity 360mOsM pH 7.6
DMSO	10%	10%	-	-
Glucose	5%	5%	-	-

[a]The actual composition of Bambanker and CryoStor CS10 are undisclosed.

6.2.2.4 Cryopreservation of Hepatocyte Microbeads using Different Freezing Solutions

HMBs and RMBs were used to further investigate two of the four freezing solutions for cryopreservation of hepatocyte microbeads. Each ice-cold freezing medium was slowly added to the microbeads (1ml microbeads+4ml freezing solution in a 5ml cryovial). The microbead suspensions were then maintained on ice for 15-30min before transfer to the CRF.

The freezing protocol was chosen based on results of a preliminary study. The published protocols by Terry et al. (2010) for cryopreservation of human hepatocytes and for freezing alginate-encapsulated liver cell (HepG2) spheroids by Massie et al. (2011) were compared. These two protocols are multi-step slow cooling which contain an important holding step to allow samples to reach equilibrium and a shock cooling step (from −8°C to−28°C) to control nucleation of ice. They are different in terms of starting temperature (8°C vs 0°C) and total duration of cryopreservation (62min vs 39min, Table 6.2). The findings from a pilot study showed that HMBs cryopreserved according to the Massie et al. protocol provided intact microbeads and higher MTT activity and albumin production at day 1 and 3 post thawing than those cryopreserved with the standard protocol for hepatocytes by Terry et al. Therefore, the freezing protocol by Massie et al. was applied in all following experiments of microbeads cryopreservation (Figure 6.1). After cryopreservation microbeads were stored at −140°C for two weeks.

Table 6.2: Multi-step slow cooling cryopreservation protocols using CRF

Protocol for human hepatocytes (Terry et al. 2010)				
Step	**Start Temperature**	**Rate**	**Time**	**End Temperature**
1	8°C	-1ºC/min	8 min	0°C
2	0°C	Hold	8 min	0°C
3	0°C	-2ºC/min	4 min	-8°C
4	-8°C	-35ºC/min	33 sec	-28°C
5	-28°C	-2.5 ºC/min	2 min	-33°C
6	-33°C	+2.5ºC/min	2 min	-28°C
7	-28°C	-1 ºC/min	32 min	-60°C
8	-60°C	-10 ºC/min	4 min	-100°C
9	-100°C	-20 ºC/min	2 min	-140°C
Protocol for encapsulated liver spheroids (Massie et al. 2011)				
Step	**Start Temperature**	**Rate**	**Time**	**End Temperature**
1	0°C	Hold	8 min	0°C
2	0°C	-2ºC/min	4 min	-8°C
3	-8°C	-35ºC/min	6sec	-28°C
4	-28°C	-2.5 ºC/min	2 min	-33°C
5	-33°C	+2.5ºC/min	2 min	-28°C
6	-28°C	-2ºC/min	16min	-60°C
7	-60°C	-10 ºC/min	4 min	-100°C
8	-100°C	-20 ºC/min	3min	-160°C

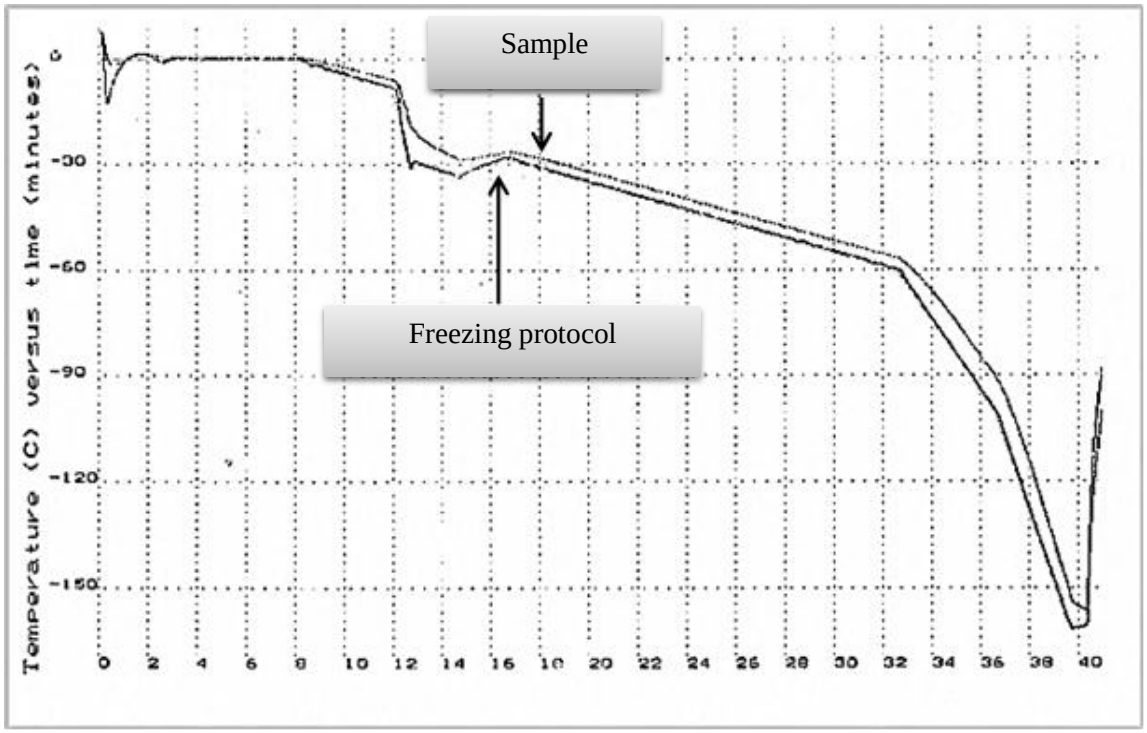

Figure 6.1: Controlled-rate freezer trace of the programmed freezing protocol (below line) and actual temperature of samples (above line).

6.2.2.5 Effect of Cytoprotectant on Hepatocyte Microbeads

The cytoprotectant compounds were chosen based on published data which demonstrated beneficial effects during culture, cold storage or cryopreservation of cells or microencapsulated cells. Compounds which have different mechanisms to protect cells include caspase inhibitor (ZVAD), iron chelator (DFO) and human serum albumin were evaluated. The concentrations used in current study were adjusted according to previously published data. The details of selected cytoprotectants are shown in Table 6.3.

The effects of the compounds were tested on RMBs by adding them to the most effective freezing medium from the prior experiments. RMBs were produced from the same donors. Four experimental groups were performed: a) freezing media without cytoprotectant, b) freezing media with HAS, c) freezing media with DFO, and d) freezing media with ZVAD. The freezing solution for each group was added to 1ml RMBs up to a final volume of 5ml in a cryovial. Cryovials were kept on ice for 15-30min prior to starting freezing using CRF. Cryopreserved RMBs were stored at −140°C for two weeks.

Table 6.3: Cytoprotective compounds used in this study

Compounds	Concentration	Possible mechanism of action	Beneficial effect	Reference
ZVAD	60µM	Inhibit caspase -1,-4, -3 and -7	Prevent apoptosis	Mahler et al. (2003) Nyberg et al. (2000)
Desferoxamine (DFO)	1mM	Inhibit loss of MMP Prevent ROS formation Reduce oxidative stress	Prevent apoptosis and necrotic cell death	Kerkweg et al. (2002) Niu et al. (2010) Terry et al. (unpublished data)
Human serum albumin (HSA)	2%	Mechanical protection Buffering capacity (reduce DMSO toxicity)	Prevent apoptosis Enhance integrity of microbeads	Schneider et al. (2003) De Castro et al. (2006)

MMP, mitochondrial membrane potential; and ROS, Reactive Oxygen Species.

6.2.2.6 Thawing and Culturing Cryopreserved Cells and Microbeads

Hepatocytes and microbeads stocks were rapidly thawed using a 37°C water bath (Section 2.2.8.3). Thawed hepatocytes were then plated and maintained in a humidified incubator at 37°C, 5% CO_2 for 7 days (Section 2.2.5). Similarly, thawed microbeads were resuspended in culture medium and incubated for 7 days (Section 2.2.7).

6.2.2.7 Plated Hepatocyte Viability and Function

Cell viability was determined immediately after thawing using the Trypan blue exclusion test (Section 2.2.3). MTT assay, SRB assay (cell attachment) and hepatocyte specific function were evaluated after maintenance in culture for 24h (Section 2.2.9 and 2.2.10).

6.2.2.8 Hepatocyte Microbeads Viability and Function

Viability of hepatocyte microbeads was evaluated using FDA/PI and MTT assay (Section 2.2.11) immediately post-thaw, day 1, day 3 and day 7. Hepatocyte specific functions of microbeads were studied in supernatants on day 1, day 3 and day 7 cultures (Section 2.2.12).

6.2.2.9 Morphological Examination Using Light Microscopy

The morphology of hepatocytes from each group was examined after thawing and plating on collagen-coated plates for 24h. Microbeads morphology was evaluated immediately post thawing.

6.2.2.10 Hepatocyte Microbeads Ultrastructure Examination Using Electron Microscopy

The exterior and interior ultrastructural morphology of hepatocyte microbeads were studied using scanning electron microscopy (SEM) and transmission electron microscopy (TEM). Microbeads were processed at the Centre for Ultrastructural Imaging, King's College London.

Briefly, samples were fixed overnight with 2.5% glutaraldehyde in 0.15M cacodylate buffer (pH 7.3) at 4°C. For SEM, after the initial fixation, samples were rinsed several times in cacodylate buffer and post fixed with 1% osmium tetroxide in 0.15 M cacodylate buffer (pH 7.3) for 1h. Samples were then washed, dehydrated in a graded series of ethanol and dried by hexamethyldislazane. Dried samples were mounted on stubs (Hitachi) with adhesive carbon tab (TAAB) and sputter coated with gold (Emitech K550X) before examination under a scanning electron microscope. Images recorded using a FEI Quanta 200F field emission scanning electron microscope operated at 5kV in high vacuum mode.

For TEM, after the initial fixation, samples were rinsed several times in cacodylate buffer and post fixed with 1% osmium tetroxide in 0.15M cacodylate buffer (pH 7.3) for 1.5h. Samples were then washed, dehydrated in a graded series of ethanol and equilibrated with propylene oxide before infiltration with SPURR resin (TAAB). Samples were embedded and polymerised at 70°C for 24 hours. Ultrathin Sections (70-90 nm) were prepared using a Reichert-Jung Ultracut E ultramicrotome, mounted on 150 mesh copper grids, contrasted using uranyl acetate and lead citrate and examined on a FEI Tecnai 12 transmission microscope operated at 120 kV. Images were acquired with an AMT 16000M digital camera.

6.2.2.11 Detection of Apoptotic Cells using FACS Analysis

The four groups of cryopreserved hepatocyte microbeads from the cytoprotectant study (Section 6.2.2.5), 1ml per group, were thawed and cultured in 6 well-plates. Additional sample of hepatocyte microbeads which had been cryopreserved in freezing solution without any cryoprotectant were thawed and then incubated with ZVAD (60µM) for 30min prior to culture. After 24h in culture, hepatocytes were released from the microbeads according to the depolymerisation protocol (Section 2.2.7.1). Cells were then washed twice with PBS/1% FCS followed by PI staining. Stained cells were incubated at 4°C for 30 min in the dark, then washed with PBS/1% FCS and re-suspended in 400µL PBS/1% FCS. An equivalent number of cells from each sample were acquired for FACS analysis. FACS was set to detect PI fluorescence at 620±10nm.

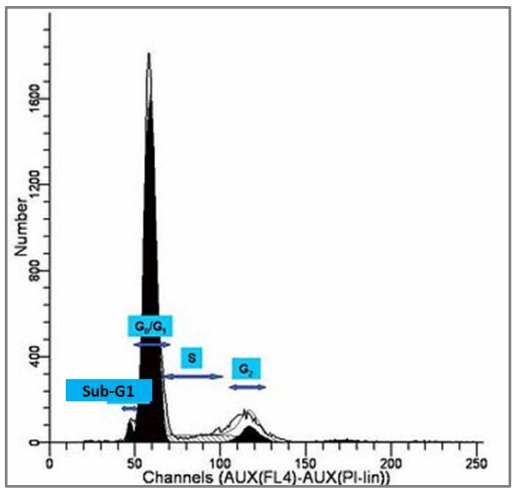

Figure 6.2: A typical flow cytometry histogram for estimation of the percentage of apoptotic nuclei (sub-G1).

6.3 Results

6.3.1 Effect of Freezing Solutions on Hepatocytes

Cell viability of fresh human hepatocytes, immediately after isolation assessed by trypan blue and after plating assessed by overall mitochondrial activity (MTT activity) were 77.0±1.3% and 1.13±0.29 OD reading units, respectively. After cryopreservation with 4 different freezing media and subsequent thawing, there was a significant decrease in cell viability evaluated immediately after thawing and after plating with all freezing media compared to fresh cells (trypan blue: $p<0.05$ and MTT assay: $p<0.001$). There was a no significant difference in post thawing viability between cells cryopreserved with the 4 different solutions (CryoStor CS10: 57.3±5.8%, Bambanker: 54.7±4.3%, UW/DMSO/glucose: 50.4±4.5% and HTK/DMSO/glucose: 44.5±5.3%). Cell attachment (SRB assay) onto collagen-coated plates data showed similar results as cell viability. However, when comparing between cryopreserved cells group, UW/DMSO/glucose group had highest attachment efficacy (0.35±0.09 OD reading units) but this did not reach statistically significance (Figure 6.3).

The morphology of cryopreserved hepatocytes after attachment to the collagen-coated plates was examined under light microscopy and compared with freshly isolated hepatocytes. The appearance of the typical hexagonal shape of hepatocytes was observed in cryopreserved cells. There was no obvious difference in morphological appearance between cryopreserved groups, except in the Bambanker group which showed some “damaged” hepatocytes and irregular cell shape (Figure 6.4).

Comparing albumin synthesis between fresh (167.0±28.3 ng/mg protein) and cryopreserved groups showed a minimal decrease with no statistically significant difference. Nevertheless, cells cryopreserved with HTK/DMSO/glucose produced the lowest amount of albumin (135.5±36.5 ng/mg protein) compared to the other groups. Furthermore, urea synthesis was significantly reduced in HTK/DMSO/glucose cryopreserved cells compared to fresh cells ($p=0.04$), (Figure 6.5).

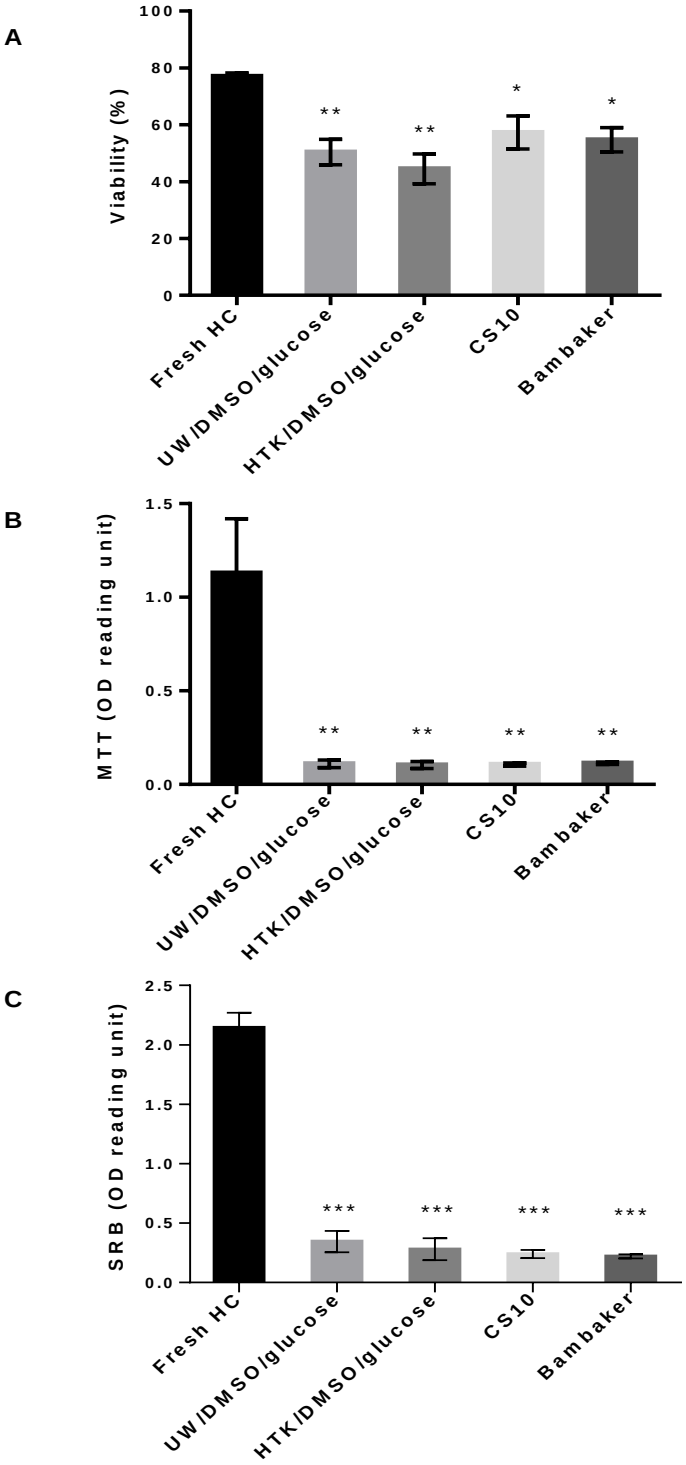

Figure 6.3: Effects of cryopreservation using the four different freezing solutions on human hepatocytes viability and cell attachment. (A) cell viability immediately after thawing assessed by trypan blue exclusion. (B) cell viability post thawing and plating for 24h assessed by MTT assay and, (C) cell attachment after thawed and plated for 24h assessed by SRB assay. Statistical significance as compared to fresh hepatocytes (controls): *$p<0.05$, **$p<0.01$, and ***$p<0.001$.

Fresh hepatocytes

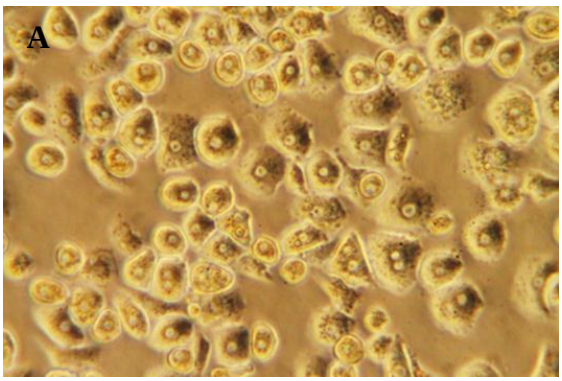

Cryopreserved hepatocytes

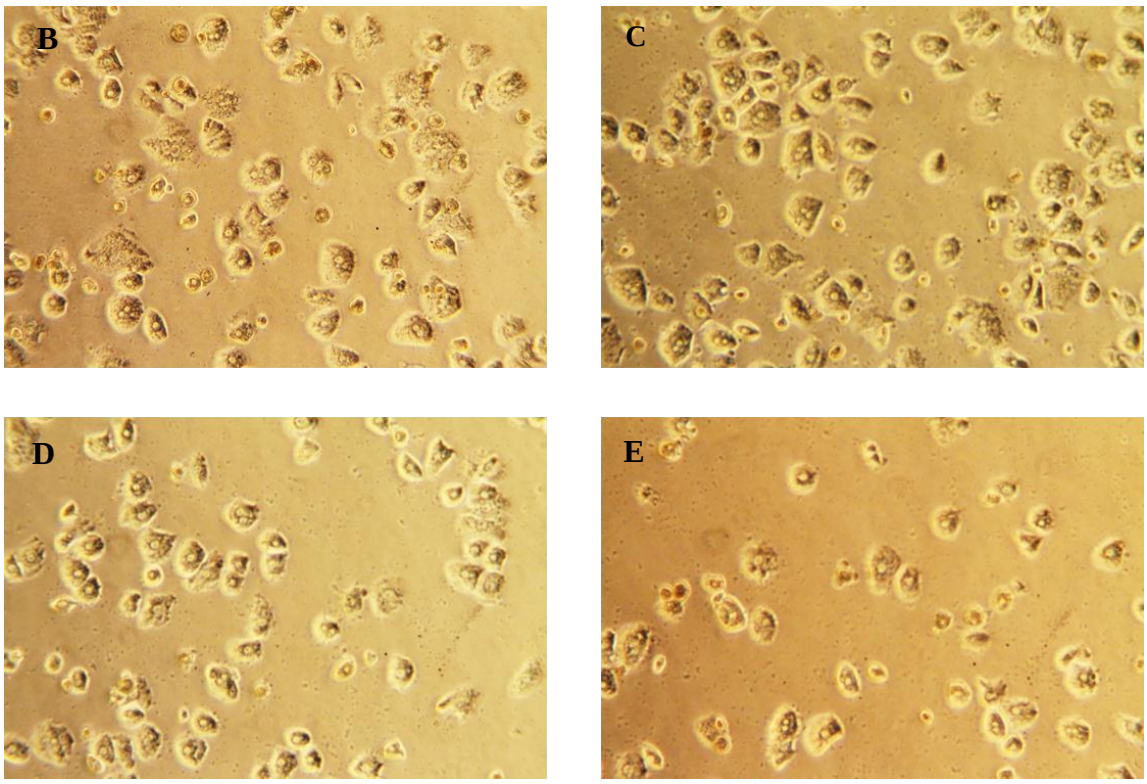

Figure 6.4: Representative images of human hepatocyte morphology after plating and maintained in culture for 24h (under light microscopy); (A) fresh hepatocytes (control). Cryopreserved hepatocytes using (B) UW/DMSO/glucose, (C) HTK/DMSO/glucose, (D) CryoStor CS10, and (E) Bambanker.

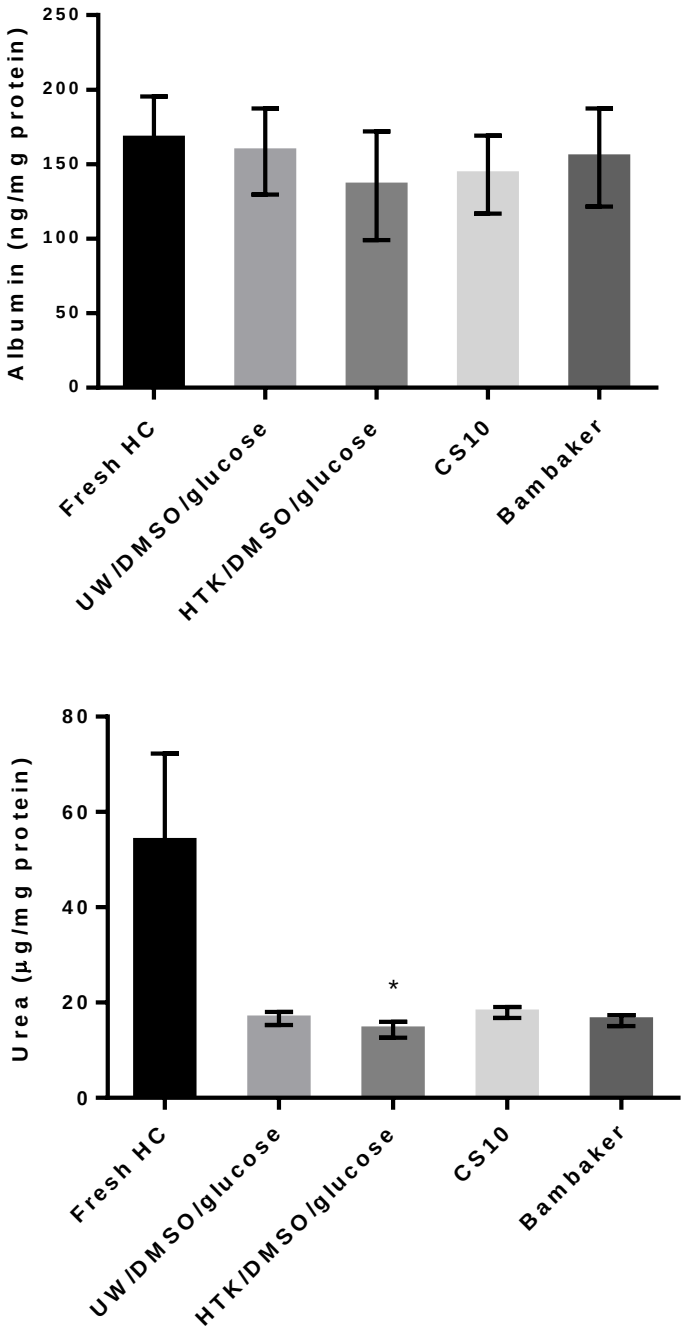

Figure 6.5: Effects of cryopreservation using four different freezing solutions on human hepatocyte-specific functions (albumin and urea production) after plating for 24h. Statistical significance compared to fresh hepatocytes (HC; control): *p<0.05.

The results obtained from experiments using rat hepatocytes showed a similar outcome to human hepatocytes. Cell viability of cryopreserved cells in all groups was significantly lower than the fresh cells (73.1±2.0%, $p<0.01$). Comparing between cryopreserved cells, CryoStor CS10 group (54.0±2.6%) demonstrated significantly higher cell viability than Bambanker (41.0±1.5%, $p=0.003$), HTK/DMSO/glucose (40.0±1.2%, $p=0.002$), and UW/DMSO/glucose (45.3±0.8%, $p=0.04$). Interestingly, cells cryopreserved in UW/DMSO/glucose were able to maintain their overall mitochondrial activity and attachment after plating and culturing for 24h (MTT=0.35±0.07 and SRB=1.50±0.10 OD reading unit) better than the other three groups, and showed no statistical difference compared to fresh cells (MTT=1.52±0.68 and SRB=3.01±0.85), (Figure 6.6). When compared to fresh cells, urea production was significantly decreased in all cryopreserved cells ($p<0.05$), however, albumin production was significantly reduced only in cells cryopreserved in Bambanker ($p=0.02$), (Figure 6.7).

The similar results for the freezing solution on human hepatocytes were detected with UW/DMSO/glucose, CryoStor CS10 and Bambanker. For rat hepatocytes, CryoStor CS10 showed better outcome in cell viability immediately after thawing, while UW/DMSO/glucose demonstrated better cell attachment and viability afterward. In addition, hepatocyte functions of cell cryopreserved with HTK/DMSO/glucose and Bambanker were dramatically dropped than those with UW/DMSO/glucose and CryoStor CS10. Therefore, UW/DMSO/glucose which is freezing solution used for clinical use at King's College Hospital, and CryoStor CS10 were chosen for study of cryopreservation of microbeads.

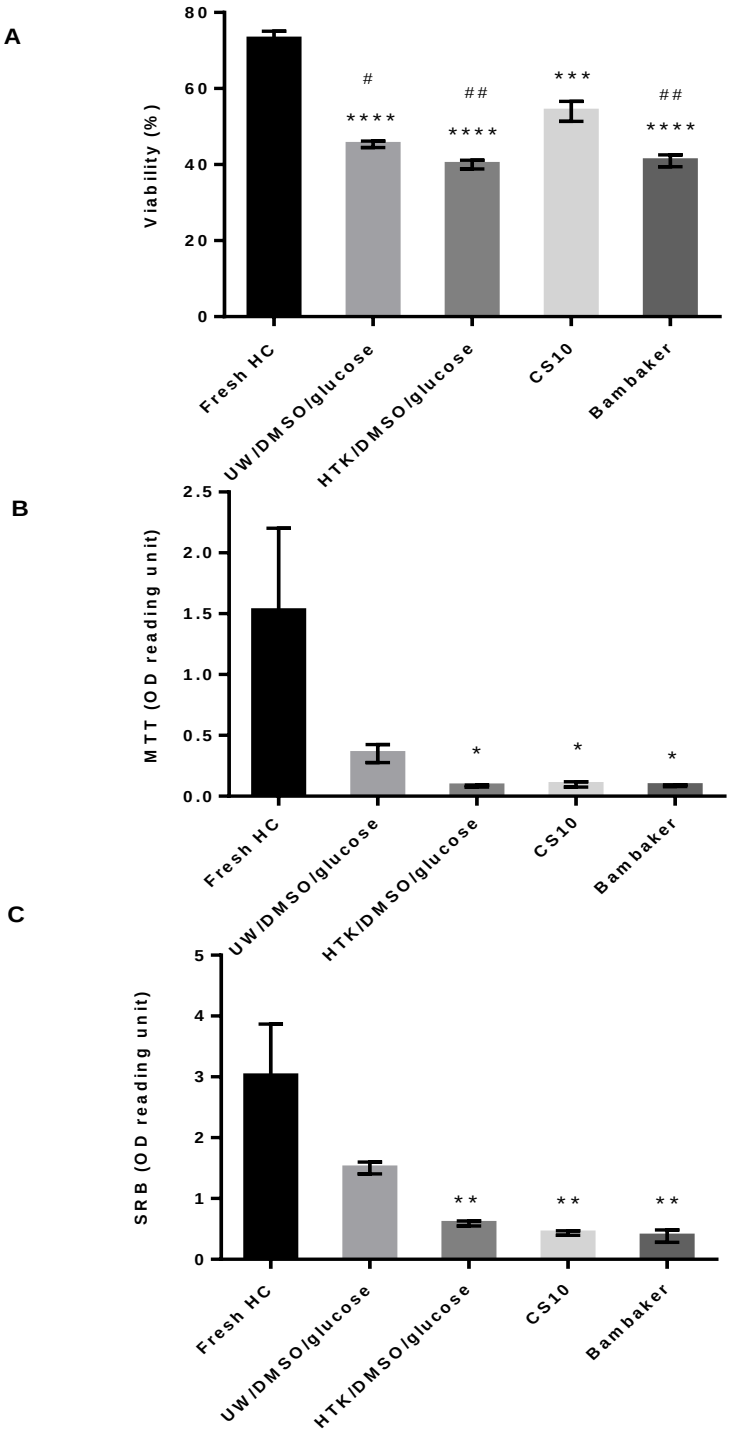

Figure 6.6: Effects of cryopreservation using four different freezing solutions on rat hepatocyte viability and cell attachment. Cell viability assessed (A) immediately after thawing using trypan blue exclusion, and (B) post-thawing and plating for 24h using MTT assay. (C) SRB assay for cell attachment after thawing and plating for 24h. Statistical significance compared to fresh hepatocytes (control): *$p<0.05$, **$p<0.01$, ***$p<0.001$ and ****$p<0.0001$. Statistical significant compared to CryoStor CS10: #$p<0.05$ and $^{\#\#}p<0.01$.

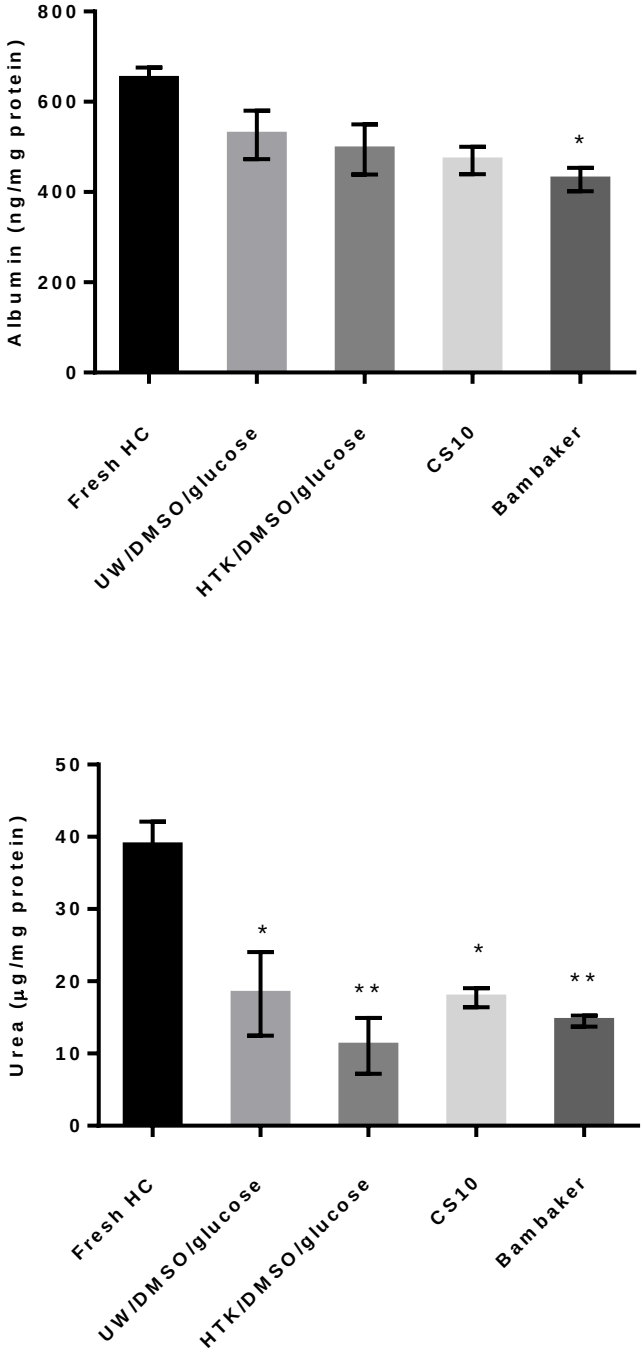

Figure 6.7: Effects of cryopreservation using four different freezing solutions on rat hepatocyte-specific functions (albumin and urea production) after plating for 24h. Statistical significance compared to fresh HC (control): *$p<0.05$ and **$p<0.01$.

6.3.2 Effect of Freezing Solutions on Hepatocyte Microbeads

There was no significant difference between cell viability of cryopreserved HMBs immediately post thawing and after maintenance in culture for 7 days (assessed by FDA/PI and MTT assay). Hepatocyte function of cryopreserved HMBs assessed by albumin production, urea synthesis and cytochrome P450 activity (CYP1A1/2) also demonstrated comparable results between the two freezing solutions (Figure 6.8). Interestingly, there was little difference in cell viability and functionality of cryopreserved HMBs after thawing and then after maintenance in culture throughout the 7 days, while fresh HMBs showed a significant decrease in cell viability and urea production. When comparing between fresh and cryopreserved HMBs, there was a significant decrease in both viability and urea synthesis in cryopreserved HMBs. These reductions were more apparent immediately after thawing and on day1 in culture ($p<0.0001$) than on days 3 and 7. However, albumin production was unexpectedly significantly higher in cryopreserved HMBs in both groups than those of fresh at each time points ($p\leq0.01$), (Figure 6.8B). In contrast, there was no significant difference in CYP1A1/2 activity between fresh and cryopreserved HMBs.

The same effects of freezing solutions on HMBs were observed on rat hepatocyte microbeads (RMBs), (Figure 6.9). However, the difference between fresh and cryopreserved RMBs was more prominent than in HMBs experimental groups. On day 1, albumin production of fresh RMBs (736.9±113.7 ng/mg protein) was significantly higher than RMBs cryopreserved with UW/DMSO/glucose (359.2±43.5 ng/mg protein, $p=0.001$) and CryoStor CS10 (390.0±26.6 ng/mg protein, $p=0.002$) and the level continued to increase up to day 7. Moreover, fresh RMBs showed significantly higher CYP1A1/2 activity than cryopreserved RMBs on day 1 (fresh vs. UW/DMSO/glucose, $p=0.04$, and fresh vs. CryoStor CS10, $p=0.004$) and on day 3 (fresh vs. both groups, $p<0.05$).

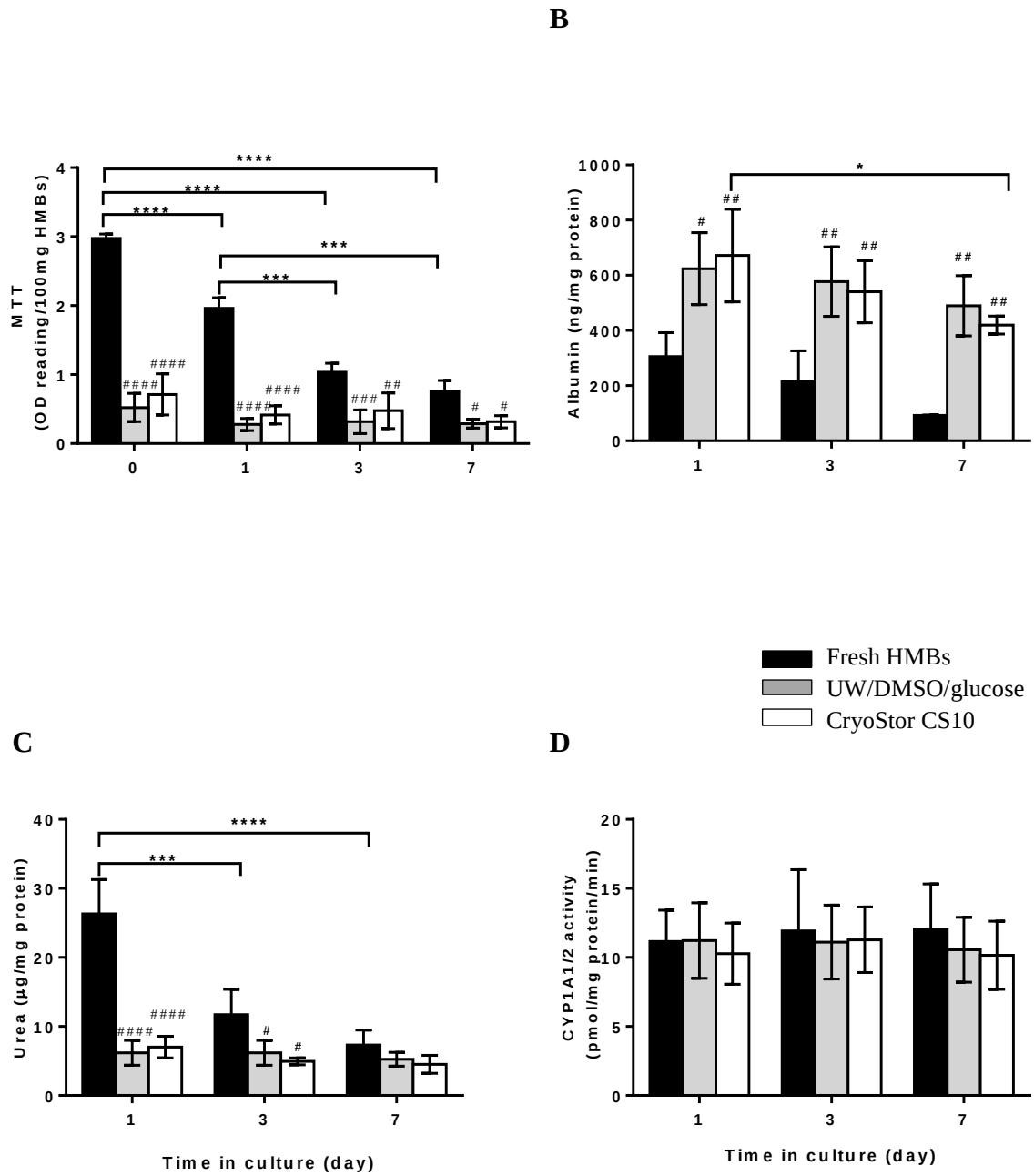

Figure 6.8: Effects of two freezing solutions on cell viability and function of HMBs after thawing and maintenance in culture for 7 days; (A) cell viability, (B) albumin production, (C) urea production and (D) CYP1A1/2 activity. Statistical significance: *p<0.05, **p<0.01, ***p<0.001, and ****p<0.0001. Statistical significance compared to fresh HMBs: #p<0.05, ##p<0.01, ### p<0.001, and #### p<0.0001.

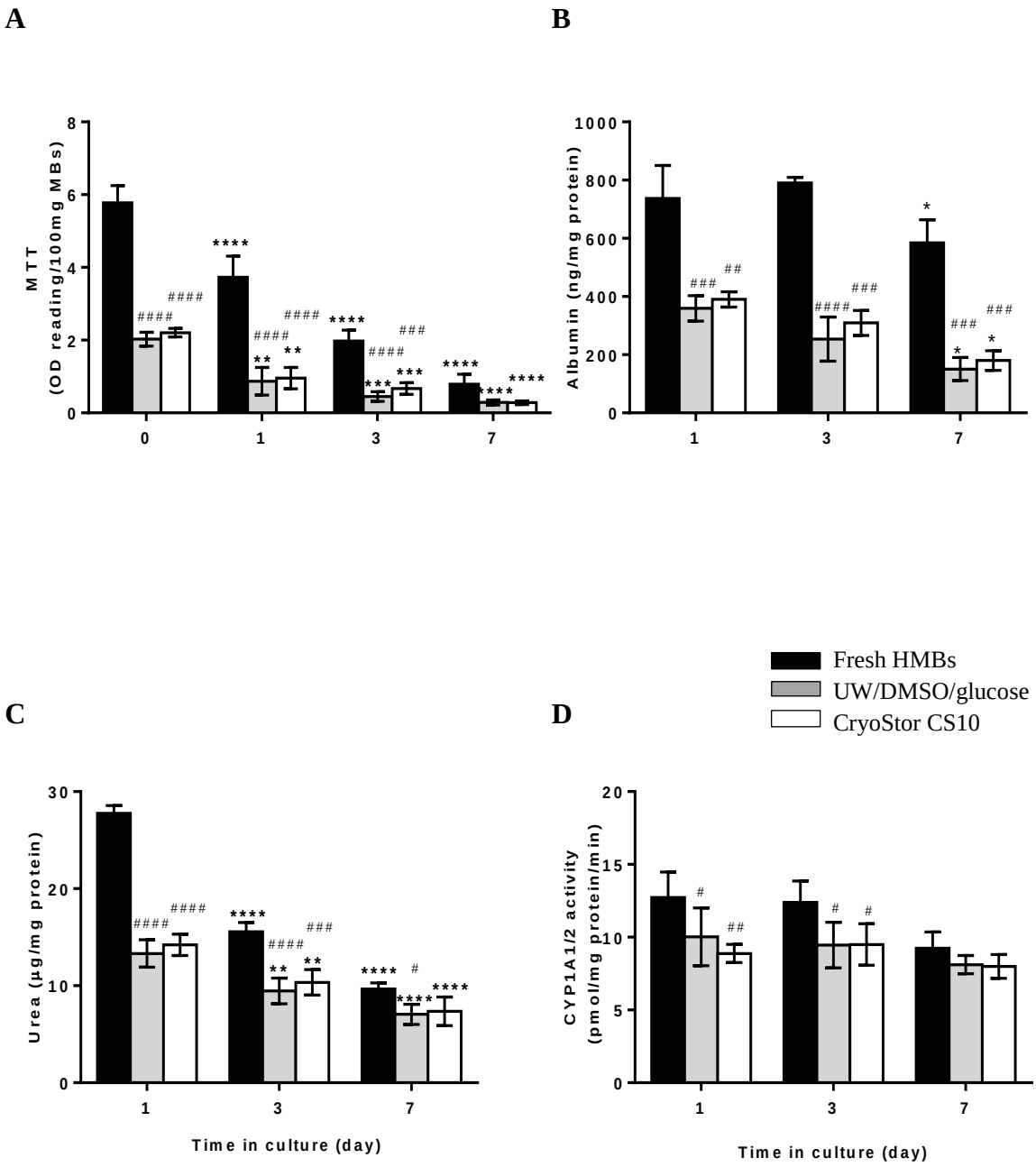

Figure 6.9: Effects of two freezing solutions on cell viability and function of RMBs after thawing and 7 days maintenance in culture. (A) cell viability, (B) albumin production, (C) urea production, and (D) CYP1A1/2 activity. [Statistical significance compared to either immediately post thawing or compared to day 1: *p<0.05, **p<0.01, ***p<0.001 and ****p<0.0001; and compared to fresh HMBs: #p<0.05 and ##p<0.01, ### p<0.001 and #### p<0.0001].

The morphology of cryopreserved microbeads (HMBs and RMBs) examined under light microscopy (LM) and scanning electron microscopy (SEM) was intact and well-preserved when compared to fresh samples (Figure 6.11). However, further investigation of ultrastructure of hepatocytes within microbeads using transmission electron microscopy (TEM) showed that microbeads cryopreserved in CryoStor CS10 provided slightly more cells with preserved ultrastructure than those in UW/DMSO/glucose. Figure 6.11 shows TEM images of examples of healthy hepatocytes versus necrotic and apoptotic hepatocytes within microbeads from fresh microbeads and cryopreserved microbeads. Good healthy hepatocytes exhibited a round nucleus with well-defined nuclear membrane, which was continuous with the rough-surfaced endoplasmic reticulum. They contained abundant smooth membranes and with intact cristae in mitochondria. In contrast, apoptotic hepatocytes showed condensation of nuclear chromatin located near the nuclear membrane. Plasma membrane had lost its fine demarcated continuity. Oedematous mitochondria due to ruptured outer mitochondrial membrane, secondary to necrosis were observed. The number of extensive vacuoles was increased, while intact cytoplasmic organelles were clearly seen.

Overall, UW/DMSO/glucose and CryoStor CS10 had similar effects on cryopreservation of hepatocyte microbeads. Therefore, UW/DMSO/glucose which is the freezing media used for cryopreservation of clinical grade human hepatocytes was chosen as the freezing solution in further cryopreservation experiments.

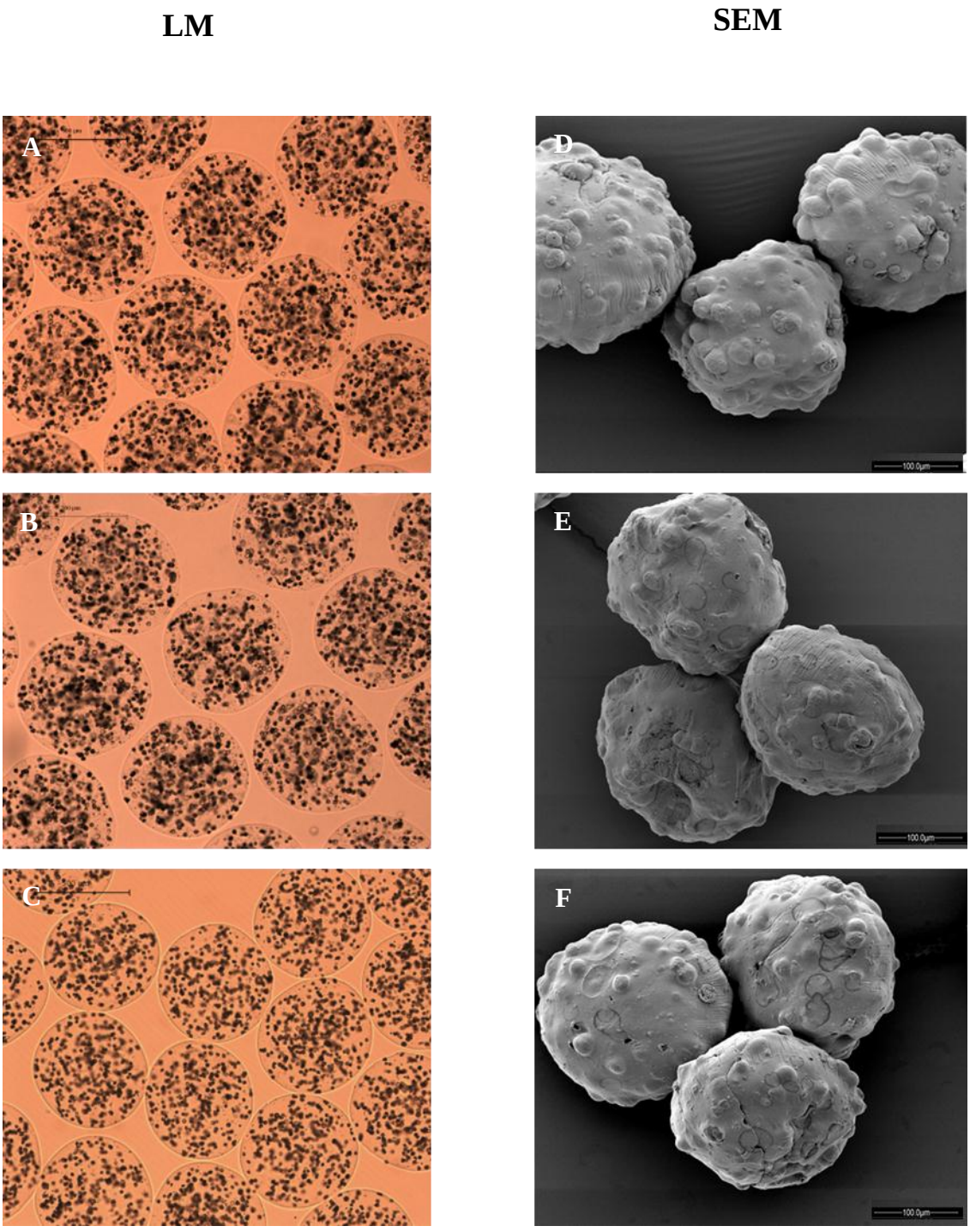

Figure 6.10: Human hepatocyte microbeads morphology under light microscopy (LM; A, B and C) and scanning electron microscopy (SEM; D, E, and F). (A, D) fresh hepatocyte microbeads (control), (B, E) hepatocyte microbeads cryopreserved with UW/DMSO/glucose, and (C, F) hepatocyte microbeads cryopreserved using CryoStor CS10. Scale bar are 500µm (LM) and 100µm (SEM).

Healthy hepatocytes within MBs **Apoptotic hepatocytes within MBs**

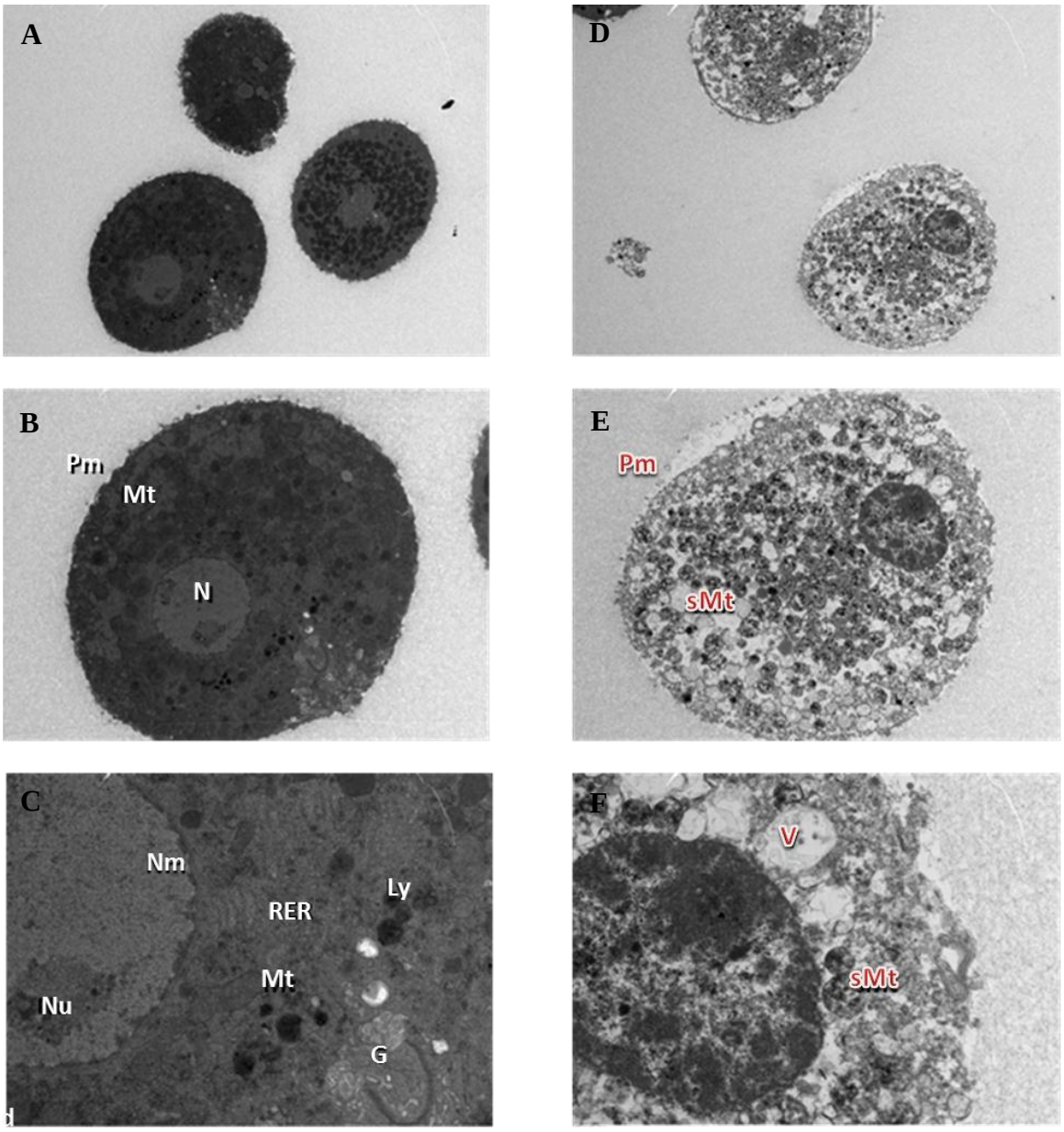

Figure 6.11: Transmission electron microscopy (TEM) of hepatocytes within microbeads after 24h culture. Representative TEM images of normal healthy hepatocytes (left panel) and necrotic/apoptotic hepatocytes (right panel). (A, D) at low magnification; 690x, (B, E) at magnification of 1400x, and (C, F) at high magnification; 4800x. G, Golgi apparatus; Ly, lysosomes, Mt, mitochondria; N, nuclei; Nu, nucleoli; Nm, nuclear membrane; Pm, plasma membrane; RER, rough-surfaced endoplasmic reticulum; sMt, swelling mitochondria; and V, vacuole.

6.3.3 Effects of Cytoprotectants on Hepatocytes Microbeads

RMBs cryopreserved in UW/DMSO/glucose (basal medium) containing 60μM ZVAD resulted in a significantly higher cell viability immediately post thawing (MTT=6.12±1.12 OD reading/100mg RMBs) than those cryopreserved with standard basal freezing medium alone (3.51±0.31, p=0.002). After 1 day in culture, there was a slight decrease in cell viability of ZVAD group (5.79±0.58), however viability remained significantly higher than of basal medium alone (2.42±0.45, p<0.0001), DFO group (3.39±0.49, p=0.006) and fresh RMB (3.41±0.44, p=0.007). Moreover, RMBs in HSA group gave significantly higher viability (4.48±1.11, p=0.006) than those in basal medium group. Furthermore, fresh RMBs gave better viability compared to the other groups (p<0.0001) on the day of production (day 0), but had similar viability at day 3 and day 7 (Figure 6.12). The results of cell viability assessed by fluorescence staining correlated well with the MTT assay data (Figure 6.13).

There were no significant differences between hepatocyte-specific functions in the four RMBs cryopreserved groups. The fresh RMBs gave a significantly higher albumin production at day 1 (p<0.0001) and day 3 (p<0.0001) compared to other four groups. At day 7, albumin synthesis of fresh RMB group (1331±55.8 ng/mg protein) remained higher than both the basal medium (950.3±104.8, p=0.03) and HSA (943.9±48.5, p=0.02) groups, but was not significantly different compared to both the DFO (1017±55.6) and ZVAD (1061±107.6) groups. Similar findings were observed in urea production where the fresh RMB group provided significantly higher production at day 1 than all other groups (p<0.0001), but not on day 3 and day 7. Interestingly, on day 3 there were significantly higher CYP1A1/2 activities in RMBs cryopreserved using HAS (20.7±2.5 pmol/mg protein/min, p=0.001), DFO (20.6±2.0, p=0.001) and ZVAD (20.0±1.9, p=0.003) groups, compared to fresh RMBs (15.1±2.6), (Figure 6.14).

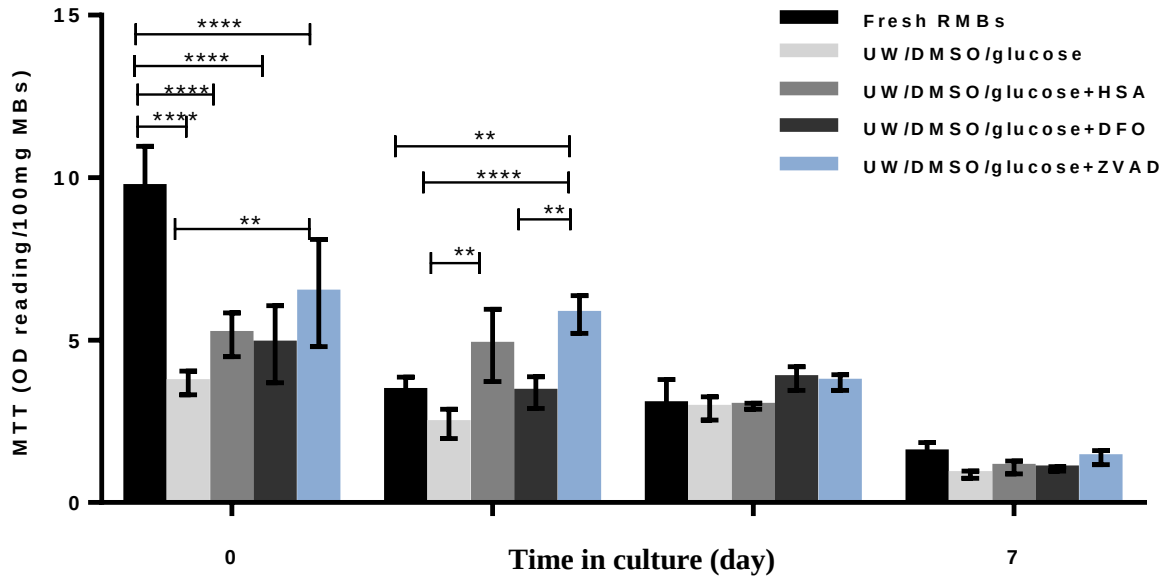

Figure 6.12: Effect of cryopreservation with different cytoprotectants on viability of RMBs after thawing and maintained in cultured for 7 days assessed by MTT assay. [Statistical significance: *p<0.05, **p<0.01, ***p<0.001 and ****p<0.0001].

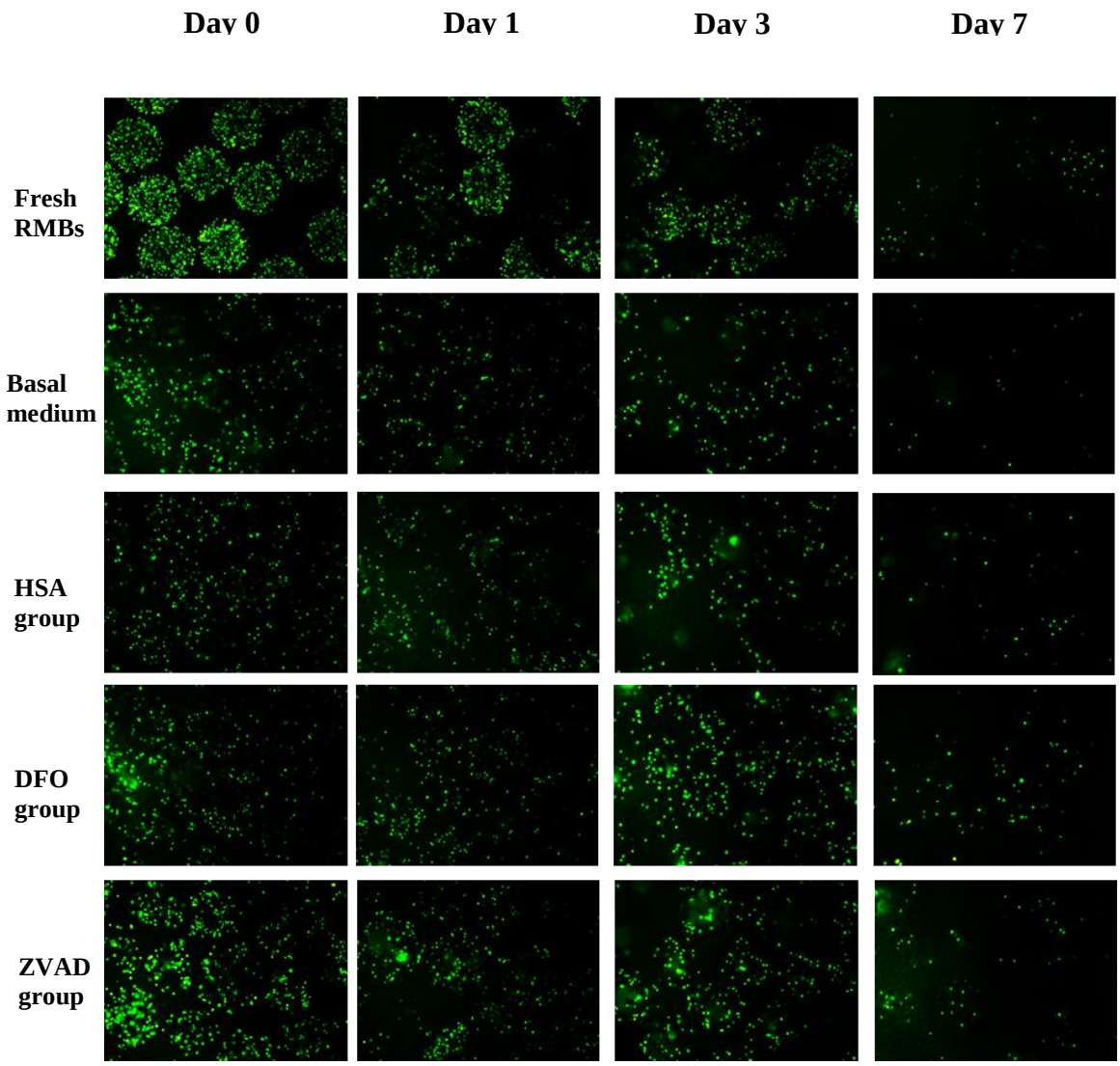

Figure 6.13: Effect of cryopreservation with different cytoprotectants on viability of RMBs after thawing and maintained in cultured for 7 days. Representative images of FDA staining showed viable cell (green) within RMBs.

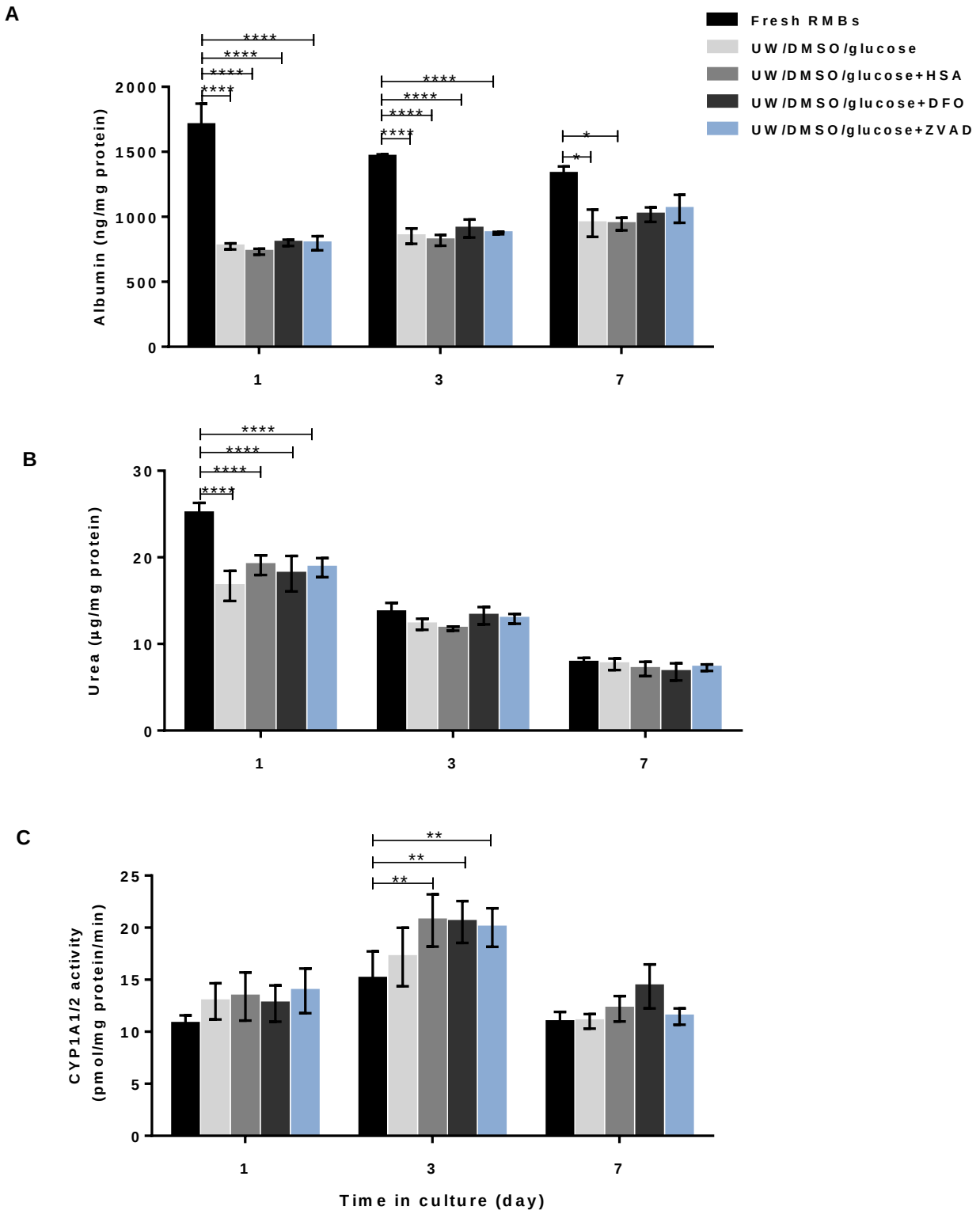

Figure 6.14: Effect of cryopreservation with different cytoprotectants on hepatocyte-specific functions of RMBs after thawing and maintenance in culture for 7 days (A) albumin production, (B) urea production, and (C) CYP1A1/2 activity. [Statistical significance: *p<0.05, **p<0.01, ***p<0.001 and ****p<0.0001].

Among cryopreserved RMBs groups, the ZVAD group had the highest percentage of well-preserved hepatocyte ultrastructure within microbeads (76.9% of the fresh RMBs group), followed by the HSA, the DFO and the basal medium groups, at 67.4%, 44.7% and 34.8% of the fresh RMB group, respectively. Representative TEM images of intact ultrastructure of hepatocytes RMBs obtained from fresh and cryopreserved groups at day 1 in culture are shown in Figure 6.15.

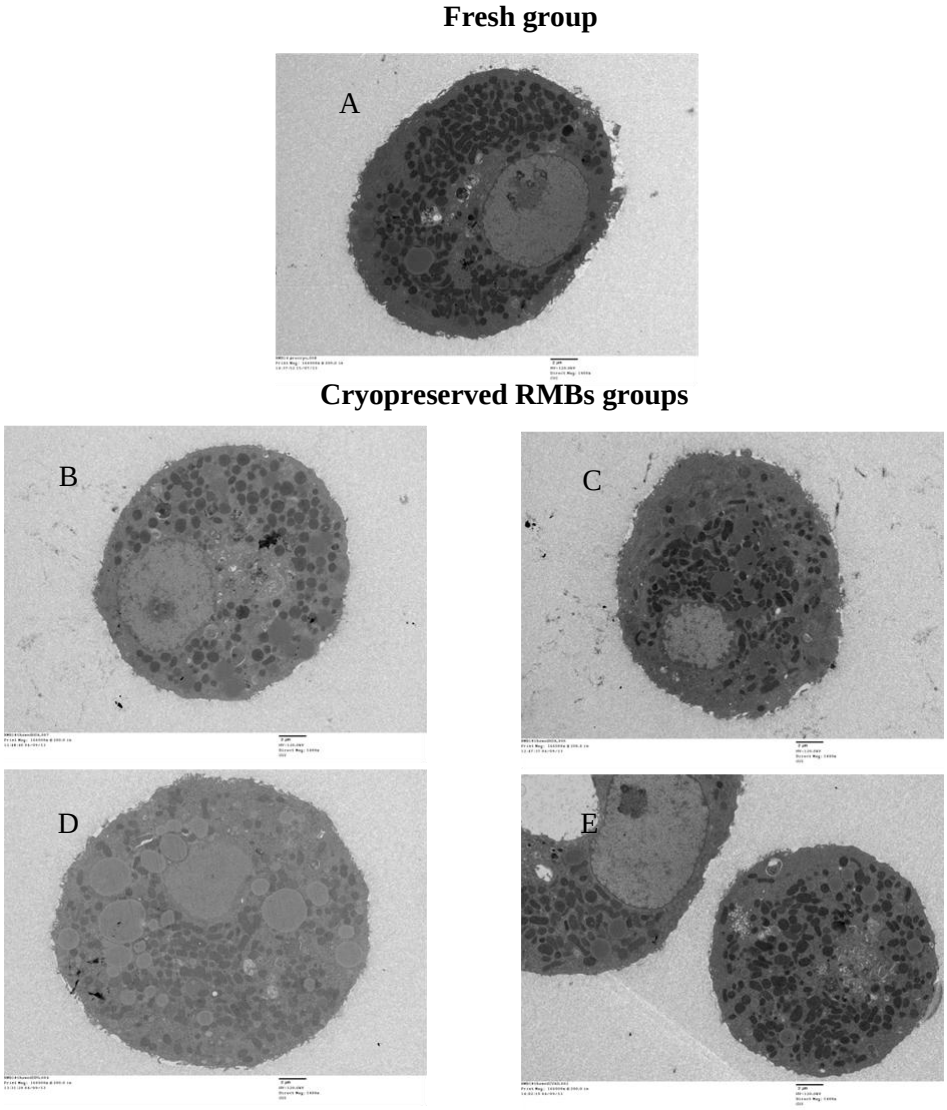

Figure 6.15: Representative TEM images (1400x) of RMBs obtained after 1 day in culture (A) fresh RMB, and cryopreserved RMBs in (B) basal medium alone, (C) HSA, (D) DFO and (E) ZVAD groups. Scale bar 2µm.

6.3.4 Detection of Apoptotic Cells in Cryopreserved Rat Hepatocyte Microbeads

The anti-apoptotic effects of cytoprotectants on RMBs were assessed by detection of sub-G1 phase of the cell cycle using PI staining and FACS analysis. Apoptotic cells (fragmented nuclei) were arrested in Sub-G1 cycle. As summarised in Table 6.4, RMBs in the basal medium alone had the highest percent of cell in sub-G1 stage (40.1%); whereas the lowest was detected in the ZVAD group (12.6%). Noticeably, the sub-G1 arrest of RMBs in the basal medium alone was decreased to 19.3% when incubated with ZVAD (60µM) for 30min immediately after thawing before maintenance in culture. Figure 6.16 shows representative FACS histograms of cell population after thawing and maintenance in culture for 24h.

Table 6.4: Percentage of nuclei in sub-G1 phase detected by FACS

Sample	Apoptotic nuclei in sub-G1 (%)
UW/DMSO/glucose (basal medium)	40.13
Basal medium+HSA	16.15
Basal medium +DFO	15.08
Basal medium +ZVAD	12.63
UW/DMSO/glucose thawed then incubated with ZVAD for 30min	19.27

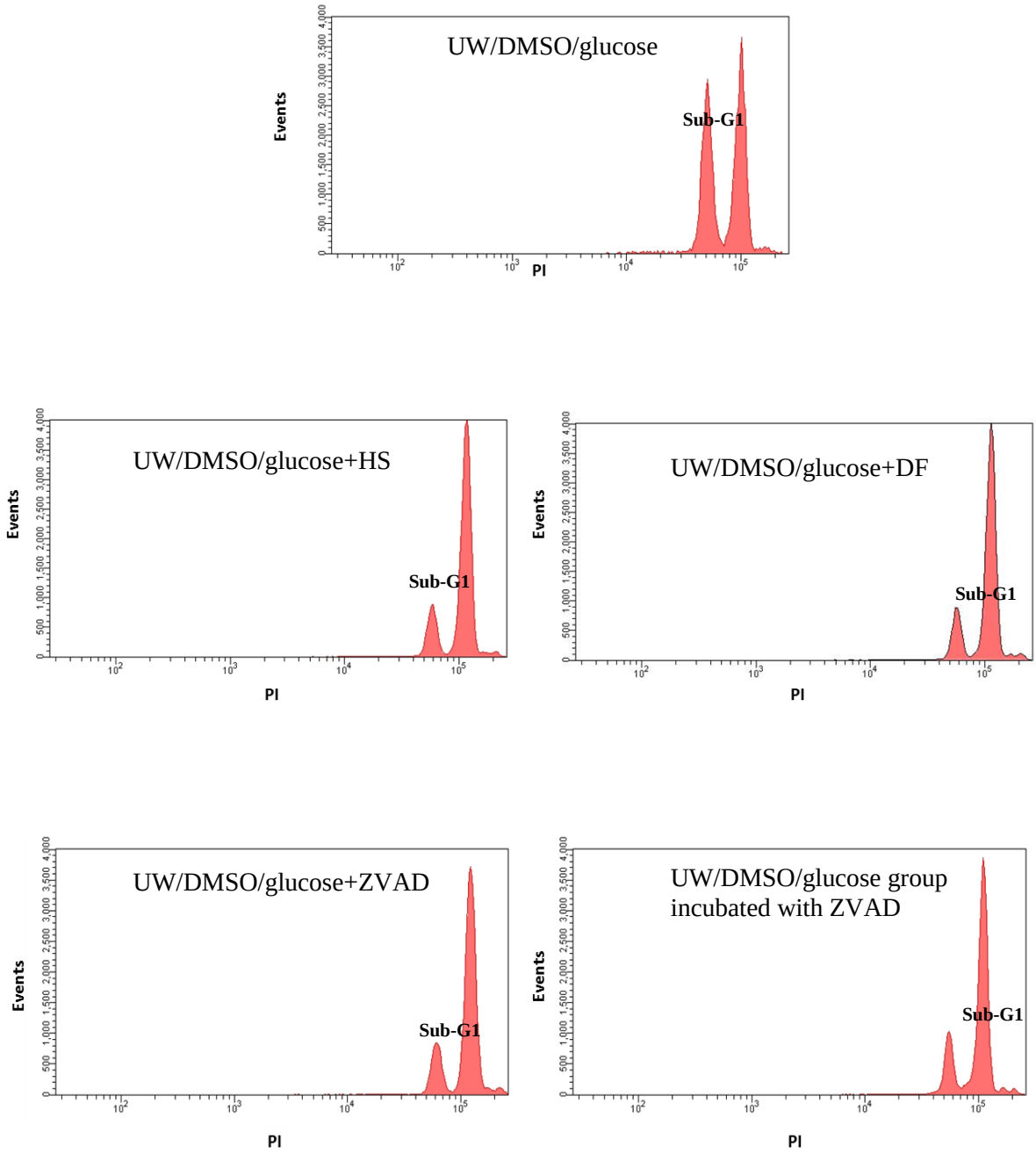

Figure 6.16: Representative histograms of cell cycle analysis using FACS. Cryopreserved RMBs were thawed, and then cultured for 24h. Hepatocytes were released from microbeads and analysed using PI staining and FACs.

6.4 Discussion

Research into cryopreservation of encapsulated hepatocytes has recently started. However, there are no published studies on optimised protocols for cryopreservation of human hepatocyte microbeads especially for clinical use. There are many steps involved in cryopreservation and storage of microbeads. This current study was focused on optimising cryopreservation solutions that potentially can be used for cryopreservation of clinical grade microbeads. This study has investigated the effect of cryopreservation solutions on cell viability and functionality of cryopreserved hepatocyte microbeads.

6.4.1 Basal freezing solution

In the initial experiments basal freezing solutions were studied [UW/DMSO/glucose and HTK/DMSO/glucose and 2 commercially available solutions, CryoStor CS10 and Bambanker]. UW and HTK are organ preservation solutions which are not suitable to protect cells during cryopreservation. Therefore, 10% DMSO and 5% glucose were added based on the optimised protocol for cryopreservation of clinical grade human hepatocytes (Terry et al. 2010). The results showed that this basal freezing media did not have sufficient effects on the outcome of cryopreservation in this study. This could be due to the effects of cryoprotectant added namely DMSO and glucose. CryoStor CS10 and UW/DMSO/glucose were superior to both HTK/DMSO/glucose and Bambanker for cryopreservation of hepatocyte suspensions. In addition, hepatocyte cryopreservation in UW/DMSO/glucose showed higher cell attachment and overall mitochondrial activity after 24h in culture, while in CryoStor CS10 cells had a higher viability immediate post thawing. This may be due to the effect of glucose concentration in UW/DMSO/glucose (300mM) compared to that in CryoStor CS10 (5mM). The benefit of using a high concentration of glucose (300mM) is that it leads to an increase in ATP cell content resulting in better of hepatocyte mitochondrial function (Stéphenne et al. 2007; Terry et al. 2010). It also protects cells against osmotic pressure which helps in the protection of cell membranes. Membrane protection contributes to preservation of cell attachment molecules on the plasma membrane leading to improvement of cell attachment. Furthermore, Janssen et al. (2003) also found that UW maintains a high intracellular ATP levels in human liver endothelial cells after ischemia and reperfusion demonstrated by MTT assay. However, UW/DMSO/glucose and CryoStor CS10 showed similar outcome in terms of cell functionality in present study. This could be explained by solutions containing similar compounds that are beneficial for protection of the cells during cryopreservation.

UW solution is an intracellular-based solution which is known as a gold standard medium for organ preservation (Southard and Belzer 1995). Several studies have shown the beneficial effects of UW for cryopreservation of hepatocytes (Terry et al. 2005; Dandri et al. 2001; Kunieda et al. 2003; Arikura et al. 2002). It is composed of important components which are 1) Non-permeating cryoprotectants; potassium lactobionate, raffinose and hydroxyethyl starch to prevent cells from swelling and to stabilise the cell membranes 2) adenosine, glutathione and allopurinol to promote ATP production and reduce oxidant damage to cells 3) K_2HPO_4 for buffering designed to work at low temperature leading to prevention of intracellular acidosis and 4) dexamethasone which help in membrane stabilization and 5) insulin which is growth and trophic factor (Southard et al. 1990). Additionally, Carini et al. (1999) found that UW solution effectively prevented sodium influx into the hypoxic hepatocyte due to its low sodium content.

CryoStor CS10 is a recently developed freezing solution which has been clinically used for stem cell banking (Woods et al. 2009). It was developed from HypoThermosol (HTS), an organ preservation solution. HTS is "intracellular-like" solution consists of multiple components which are important to maintain ionic and osmotic balance under hypothermic conditions (Table 6.1). Key components to protect cells from osmotic swelling are lactobionate, sucrose and mannitol. Dextran-40, acts as a colloid, and elevates the intracellular pressure to stabilise cell membranes. Similar to UW solution, it also contains adenosine and glutathione. However, it contains a low level of glucose (5mM) to provide energy for the cells. HTS use HEPES as a buffer which is effective in stabilising pH at low temperature. HTS serve as a platform for CryoStor family; CS 2, CS 5 and CS 10; the number after "CS" indicates the percentage of DMSO. Baust et al. (2001) have shown the beneficial effects of the HTS-base cryopreservation solution through reduction of cryopreservation-induced delayed-onset cell death, which is the cell death associated with cryopreservation developing over time post thawing. They demonstrated that improvement in cell survival was associated with a reduction in overall level of both apoptosis and necrosis after thawing. Subsequently, Sosef et al. showed that rat hepatocytes cryopreserved in CryoStor CS10 gave high viability and long-term hepatocyte-specific functions for up to 14 days (Sosef et al. 2005) .

The HTK-base freezing solution used in this study was the least effective for cryopreservation of both human and rat hepatocytes. This finding supports previously published studies, Staatsburg et al. (2002) demonstrated superiority of UW solution over Celsior and HTK solutions for cold storage of rat liver in limiting liver cell damage. Janssen et al. (2003) found that the level of cell necrosis and mitochondrial dysfunction in human hepatocytes after preservation at 4°C for 48h followed by reperfusion for 6h was significantly lower in UW solution compared to HTK. In addition, Rauen and Groot found that organ preservation

solutions with the exception of UW solution, increased cell injury during cold storage (LDH release after 18h at 4°C: HTK 76 ± 2%, Euro-Collins 78±17%, histidine-lactobionate 81±15%; control: Krebs–Henseleit buffer 20±6%). They studied the individual components of the preservation solutions, and suggested that histidine and phosphate which functions as the buffering system caused the toxicity (Rauen and de 2008). Furthermore, Baicu and Taylor (2002) recommended using HEPES instead of histidine and phosphate to avoid cytoxicity.

Bambanker demonstrated lower efficacy compared to both UW-based freezing solution and CryoStor CS10 in the present study. In addition, abnormal cell shape and disintegrated hepatocytes were most frequently observed when cells were cryopreserved in Bambanker. Bambanker can be used for the freezing and preservation of wide variety of cells including human gastric epithelial cells, human T-cell, and stem cells (Hikichi et al. 2007; Tamai et al. 2013; Naito et al. 2013). However, there was no study using Bambanker for cryopreservation of hepatocytes. The current results showed that Bambanker is not suitable for hepatocyte cryopreservation.

UW/DMSO/glucose and CryoStor CS10 were further studied in order to compare the efficacy on cryopreservation of hepatocyte microbeads. The results showed that there were no significant differences between CryoStor CS10 and UW/DMSO/glucose with both cryopreserved HMBs and RMBs. In addition, both freezing solutions which contained DMSO (10%) in addition to other cryoprotectants and metabolites as describe above were able to maintain microbeads integrity after thawing. Morphology under LM and SEM indicated that appearance of cryopreserved microbeads was comparable to fresh microbeads. This suggested that alginate microbeads could be cryopreserved with 10% DMSO using a slow freezing step protocol without damaging microbeads integrity. This finding is supported by other studies, where Pravdyuk et al. (2013) found that using DMSO at a concentration of lower than 10% or cryopreservation using rapid 1-step freezing resulted in critical damage of encapsulated mesenchymal stem cells. Another study showed that an encapsulated kidney cell line cryopreserved in 25% DMSO with a rapid cooling protocol resulted in low post thawing viability with 20-40% damage to microbeads (Chin et al. 2004).

The viability and functionality of microbeads after thawing were dramatically decreased compared to fresh microbeads in this study. This indicates that using these two freezing media as protocol for cryopreservation of hepatocyte microbeads were not sufficient to protect cells against both apoptosis cell death related to cryopreservation. However, cytochrome P450 (CYP1A1/2) activities were well preserved and showed minimal reduced compared to fresh microbeads. Similarly, Aoki et al. (2005) also demonstrated that cryopreserved

microencapsulated hepatocytes retain gene expression of OAT22 and CYP3A2/9 up to 50 days. Moreover, the results showed that cryopreserved HMBs gave higher albumin production than fresh HMBs at all-times, which is unexplained. It was noticeable that cryopreserved HMBs maintained their viability and functionality over 7 days, while the fresh HMBs continued to decrease. The reason for this is unknown, however, Dixit et al. (1993) postulated that cryopreservation "selects" only good hepatocytes to be preserved a viable on thawing.

UW/DMSO/glucose and CryoStor CS10 provided a similar outcome on cryopreservation of hepatocyte microbeads. UW/DMSO/glucose was chosen as a basal freezing medium used in further experiments. UW-based freezing solution was selected because UW has been widely used in clinical transplantation and less expensive than CryoStor CS10.

6.4.2 Cytoprotectants

Recent studies demonstrated that apoptosis plays an important role in cryopreservation failure (Baust et al. 2000; Baust et al. 2001; Yagi et al. 2001). The understanding of pathways involved with cryopreservation-induced molecular cell death could lead to improvement in the cryopreservation outcome as cytoprotectants can be added to specifically target or control the apoptosis pathway. Apoptosis signal transduction can be initiated at different levels (cell membrane or mitochondria) but is then followed by common proteolytic caspase cascade pathways (caspase-8,-9 and -3), (Baust et al. 2002). The known initiators of apoptosis associated with cryopreservation are membrane alteration, ionic imbalance and biochemical changes (Baust et al. 2009). Three cytoprotectants including the pan-caspase inhibitor; ZVAD, the iron chelator; DFO, and human serum albumin (HSA) were investigated. These cytoprotectants target different sites of cryopreservation induced cell death to enhance efficacy of cryopreserved hepatocyte microbeads (Table 6.3). The results demonstrated that ZVAD gave positive effects on cell viability and functionality of RMBs when this cytoprotectant was added to basal freezing media. The beneficial effects on cell viability were greater than with either DFO and HAS. This was shown by both overall mitochondrial activity and fluorescent staining for viable cells. RMBs cryopreserved with ZVAD had a reduction in cell apoptosis following cryopreservation when compared to basal freezing media alone or other cytoprotectant groups, observed on TEM. This was also supported by the PI staining (DNA defragmentation)/FACS which showed that sub-G1 population was lowest in the ZVAD group. In addition, adding ZVAD after thawing lowered the degree of apoptosis (Table 6.4) but was not as effective as adding it in the freezing medium. The possible explanation is that the process of apoptosis has already started at the time of hepatocyte isolation and continues throughout cryopreservation

and after thawing. Therefore the earlier the addition of the anti-apoptosis agent, the more beneficial effects are observed. The current data is consistent with previously published studies showing the beneficial effects of ZVAD used in cryopreservation and cold storage (Yagi et al. 2001; Mahler et al. 2003). It is worth mentioning that the cytoprotective effects of ZVAD are dose-dependent, and related to the cell type to be preserved. Nyberg et al. (2001) investigated the anti-apoptotic effects of a range of ZVAD concentrations (0-120µM) on gel-entrapped rat hepatocytes in a bioartificial liver device and found that at the concentration of 60µM was the optimal dose as was used in the current study.

The addition of human HSA showed some beneficial effects on cell viability and function. In fact, HSA seemed to be a good additive as it has a mechanical protection and buffering capacity which may have protected cells from apoptosis. Addition of HSA to the freezing medium is believed to be beneficial not only for the cells, but also for the microbeads physical integrity too (Schneider et al. 2003). Importantly, it is widely used and clinically approved. However, the results obtained showed that HSA was not as effective as ZVAD. This could be due to the concentration used being too low (2% v/v) to overcome the stress during cryopreservation and post-thaw. There have been no previously reported studies using HSA for cryopreservation of microbeads. De Castro et al. (2006) evaluated the efficacy of HSA as a substitute of fetal bovine serum during culturing of microencapsulated cell line (C2C12) and found that 1% HSA could be used instead of FBS. Whereas, Bao et al. (2013) showed that a custom made serum-free medium containing 3% HSA was suitable for culturing rat hepatocyte spheroid.

Similar to HSA, DFO also had positive effects on cryopreserved RMBs (the reason could be that of inadequate concentration of DFO used in this study). DFO was one of the choices as a cytoprotectant compound due to its properties and being approved for clinical use. DFO has been reported to be effective in reduction of necrosis and apoptosis of hepatocytes during cold storage. Cold-induce injury caused by reactive oxygen species is associated with an increased intracellular chelatable iron (Vairetti et al. 2001; Kerkweg et al. 2002). Niu et al. (2010) showed cell death was significantly reduced when 5mM DFO was added before and after cold incubation. Terry et al. (unpublished data) found similar benefits on cell attachment when adding 1-10mM DFO in the freezing solution. In addition, Liu et al. (2013) also showed that serum-free media supplemented with 1mM DFO provided beneficial effects in reducing cellular damage of rat hepatocytes spheroids.

It must be noted, these set of experiments were done using only RMBs due to the lack of good quality fresh human hepatocytes. Therefore, further experiments are needed to examine the effects of these cytoprotectants on HMBs. In addition, more experiments including the testing of

vary concentrations of HSA and DFO and the possible synergistic effects when added to the freezing media at the same time should be carried out.

In conclusion, cryopreservation of hepatocyte microbeads using UW solution containing 10%DMSO, 5%glucose and a cytoprotectant such as ZVAD were shown to have beneficial effects on the reduction of cellular and physical damage leading to maintenance of cell viability and function post thawing. This initial optimisation protocol for cryopreservation of hepatocyte microbeads supports the hypothesis that the development of freezing solution containing of cryoprotective agents together with compounds targeting apoptosis during the cryopreservation process could improve the outcome of cryopreservation. Finally, the efficacy of cryopreserved microbeads must be tested in vivo before clinical implication.

CHAPTER 7

7. Hepatocyte Microbead Transplantation in a Rat Model of Acute Liver Failure

7.1 Introduction

ALF is a severe condition associated with high mortality. Intrahepatic hepatocyte transplantation has shown benefit as a bridge to transplantation (Habibullah et al. 1994; Fisher and Strom 2006). However, invasive catheter placement in the liver in a coagulopathic patient and use of immunosuppression are perceived as high risk factors. The concepts of hepatocyte microbeads transplantation into the peritoneal cavity has become an attractive option (Umehara et al. 2001; Mai et al. 2005). This approach allows cell transplantation without using immunosuppression and also avoids the risk of bleeding. Moreover, cryopreservation of microencapsulated hepatocytes may protect cells from cryoinjury leading to improved cell viability and function on thawing (Aoki et al. 2005; Kusano et al. 2008) allowing banked microbeads to be available for emergency transplantation in ALF patients.

Success of microencapsulated hepatocytes for treatment of ALF in rats was first reported in 1986 by Wong and Chang, since then there have been a number of studies which showed the promising outcome of both fresh and cryopreserved microencapsulated hepatocytes in ALF animal models (Sun et al. 1987; Rivas-Vetencourt et al. 1997; Umehara et al. 2001; Aoki et al. 2005; Mai et al. 2005; Mei et al. 2009; Sgroi et al. 2011). However, the translation to clinical use for treatment of ALF has not been established so far. The well-known challenge is the clinical grade biomaterials and chemicals needed to produce GMP grade microencapsulated cells. In addition, hepatocyte microencapsulation used in previous studies were of alginate-poly-L-lysine-sodium alginate (APA) which can elicit a host immune reaction (Orive et al. 2006; Tam et al. 2011).

Based on the work described in previous chapters, the optimised HMBs produced with GMP/sterile grade materials demonstrated good viability, functionality, mechanical stability, as well as biocompatibility and permeability *in vitro*. Moreover, cryopreservation of hepatocyte microbeads using an optimised protocol established in Chapter 6 provided an acceptable post-thaw outcome including cell function and physical integrity of microbead *in vitro.*

The aims of this study were: to investigate the suitability of the optimised HMBs for transplantation in normal rats; to evaluate the safety and efficacy of transplantation of freshly prepared RMBs and cryopreserved RMBs in a rat model of ALF using by D-galactosamine administration.

7.2 Material and Methods

7.2.1 Materials

D-galactosamine hydrochloride (D-GalN; Sigma-Aldrich, Gillingham, UK), microtainer® tube, CoaguCheck® XS system (Roche Diagnostics, Mannheim, Germany), and PocketChem BA (Manarini Diagnostics, Wokingham, UK).

7.2.2 Methods

7.2.2.1 Experimental Design

7.2.2.1.1 Intraperitoneal Transplantation of HMBs in Normal Rats

The initial phase of this study was to investigate the function and immune response of the optimised HMBs (Chapter 4) *in vivo* by transplantation into normal Sprague Dawley rats to assess their suitability for future clinical application. Animals were divided into two groups (n=3 each). Group 1, transplanted with EMBs, and group 2 transplanted with HMBs. The microbeads were produced using cryopreserved human hepatocytes and immediately transplanted intraperitoneally after production. Blood samples were collected on day 1, 3, and 7 post-transplantation to evaluate the function of HMBs. Blood samples pre-transplantation (day 0) and EMBs groups were used as controls. Transplanted rats were followed for 1 week. At day 7, microbeads were retrieved from the abdomen by laparotomy under anaesthesia. The retrieved microbeads were collected for further analysis. The diagram in Figure 7.1 summarises the experiment.

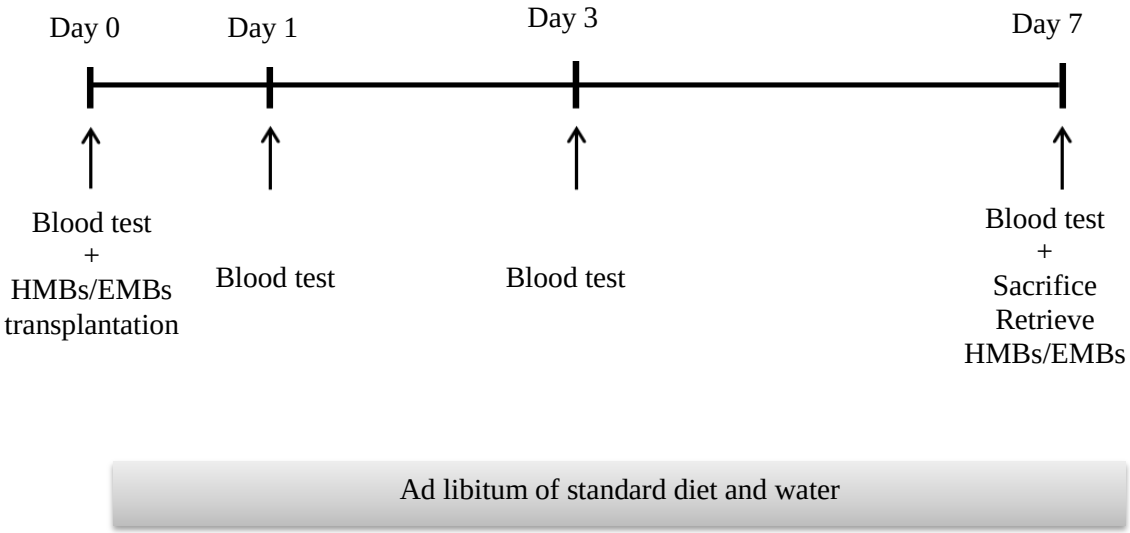

Figure 7.1: Schematic diagram of intraperitoneal transplantation of HMBs into rats.

7.2.2.1.2 Intraperitoneal Transplantation of Fresh and Cryopreserved RMBs in Rats with ALF

The second phase of the study was to investigate the safety and efficacy of fresh RMBs and cryopreserved RMBs in rats with ALF. Animals were injected with D-galactosamine (D-GalN) to induce ALF. RMBs were transplanted into the peritoneal cavity of ALF animals 24-28h after D-GalN injection. The ALF animals were divided into four experimental groups: group 1 (n=6), received vehicle injection of medium (Sham); group 2 (n=4), transplanted with EMBs; group 3 (n=5), transplanted with fresh RMBs; and group 4 (n=6), transplanted with cryopreserved RMBs. Animals were followed up for 7 days after transplantation. Survival rate and biochemical assays were evaluated at different time points. Euthanasia was performed on surviving animals at day 7 post-transplantation or at any time if they were distressed. At that time, microbeads and liver tissue were collected for analysis. The diagram in Figure 7.2 summarises the experiment.

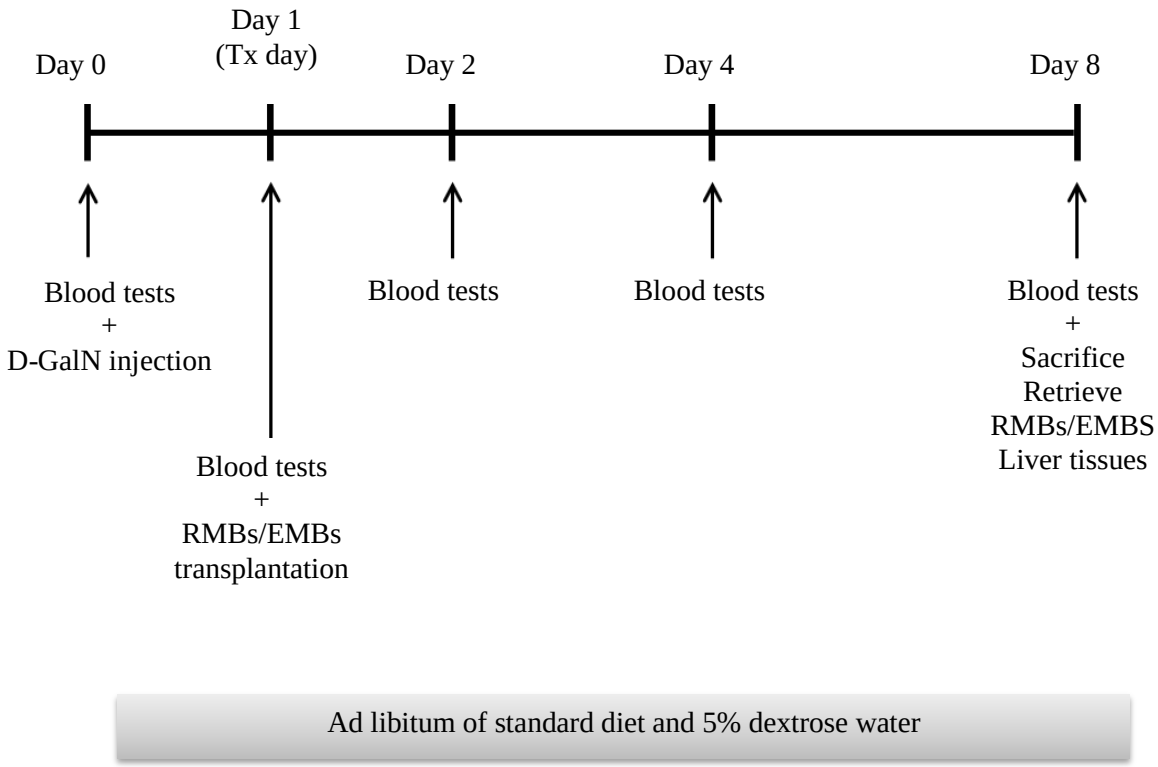

Figure 7.2: Schematic diagram of intraperitoneal transplantation of RMBs in ALF rats.

7.2.2.2 Animals

Sprague Dawley (Harlan Olec, UK), male rats 8-12 weeks old and weight between 200 to 400g were used as hepatocyte donors and the recipients of hepatocyte microbeads. Animals were maintained in conventional housing facilities and received standard care. They were housed in a room kept at a temperature of 21±2°C, humidity of 55±10% and 12-hour light-dark cycle with ad libitum food and water. After acclimatisation, all experimental procedures were performed following protocols approved by the ethical committee of King's College London in accordance with the UK Animals (Scientific) Procedures Act of 1986.

7.2.2.3 Human Hepatocytes

Human hepatocytes used in these experiments were cryopreserved cells from King's College Hospital hepatocyte research bank stored at -140°C. Hepatocytes were thawed using the quick thawing technique (Section 2.2.8.3). Cell viability and number were checked with trypan blue (Section 2.2.3) after thawing. Cells with viability ≥60% were used for encapsulation.

7.2.2.4 Rat Hepatocytes

Isolation of rat hepatocytes were performed according to the procedures described in Section 2.2.2. Cell number and viability were accessed using trypan blue (Section 2.2.3). Cells with viability ≥60% were used for encapsulation.

7.2.2.5 Encapsulation of Hepatocytes

Human and rat hepatocyte microbeads were prepared using the optimised technique established in Chapter 4. Hepatocytes used for encapsulation in each set of experiments were obtained from identical donors and also the same batch. After production, microbeads were divided into three aliquots for transplantation, cryopreservation and culture. Microbeads were maintained in CMRL prior to transplantation (according to results in Chapter 4 that showed viability and function of hepatocytes microbeads were well maintained in CMRL at least for 3h at RT). Microbeads were kept in culture for *in vitro* study for 7 days. EMBs were produced using the same technique but without cells (Section 2.2.6). Microbeads were examined under the light microscopy immediately after production before transplantation. Microbeads were transplanted when most of them (>95%) were intact and of uniform size.

7.2.2.6 Cryopreservation and Thawing of RMBs

The RMBs were cryopreserved using optimised freezing media and protocol according to the studies in Chapter 6. Briefly, RMBs were slowly mixed with freezing media, containing UW/10%DMSO/5%glucose/ZVAD (60µM), at the ratio of 1ml RMB to 4ml freezing media. RMBs suspension was then transferred into 5ml cryovials and kept on ice for 30min before being placed in the CRF. The freezing protocol used was based on the one used by Massie et al (2011). Cryopreserved RMBs were stored at 140 °C for 2 days. The RMBs thawed using the quick thawing method (Section 2.2.8.3). Post-thaw RMBs were resuspended in CMRL for transplantation and some were placed in culture for *in vitro* studies.

7.2.2.7 Evaluation of Viability and Hepatocyte Metabolic Function of HMBs and RMBs

Fresh HMBs, fresh RMBs and cryopreserved RMBs were cultured in supplemented medium and incubated at 37°C in 5% CO_2 for 7 days (Section 2.2.7).

Cell viability of hepatocyte microbeads was evaluated using MTT assay together with FDA/PI staining at day 0 (immediately after production, after thawing or after retrieval from animals), day 1, day 3 and day 7 (Section 2.2.11).

The amount of albumin production (Section 2.2.12.1), urea synthesis (Section 2.2.12.2) and CYP1 A1/2 activity (Section 2.2.12.3) of hepatocyte microbeads *in vitro* were analysed in culture medium collected at day 1, day 3 and day 7.

7.2.2.8 Induction of Acute Liver Failure

A model of acute liver failure using D-GalN was performed in Sprague Dawley rats. D-GalN was freshly prepared at the time of use by dissolving in dH_2O to a final concentration of 240mg/ml and the pH was adjusted to 7.4 using 5M NaOH. Each rat was received a single intraperitoneal injection of D-GalN at a dose of 1.2 g/kg. After injection, all animals were allowed a standard diet and 5% dextrose water ad libitum to prevent hypoglycemia.

7.2.2.9 Intraperitoneal Transplantation of Microbeads

The microbeads were suspended in transplant medium (CMRL) and were transplanted intraperitoneally via 18-guage intravascular catheter into rats under sterile technique. Each animal received microbeads suspension at dose of 10ml/kg, hence approximately $8.75x10^6$ to $10.5x10^6$ cells per rat. The plain transplant medium was injected into peritoneum using 25-gauge needle in sham group (group 1). Animals were anesthetised with isoflurane throughout the procedure.

7.2.2.10 Blood Tests

Animals were placed in a warming cabinet (39^oC) for 15-20 minutes before blood sampling. The rats were restrained using a restraint tube and their tails were cleaned in order to see the blood vessel. Immersion of the tails in warm water was also applied to enhance visibility of the tail vessels in some animals. Blood samples (0.5ml) were taken from lateral tail veins via 23G butterfly needle collected in microtainer® tube (serum separator tube). Gentle pressure was applied on the bleeding site to ensure haemostasis before the animals returned to a cage. The blood samples were then allowed to clot for ≥30min followed by centrifugation at 10,000xg for 5min to separate serum. The serums were kept at -80°C for further analysis.

7.2.2.10.1 Measurement of Human Albumin

Assessment of HMBs function was performed on peripheral blood of rats collected from tail vein on day 1, 3, and 7 post-transplantation. Human serum albumin in rat serum samples was detected using ELISA quantitation kits (Section 2.2.10.1).

7.2.2.10.2 Measurement of Prothrombin Time, Ammonia, Liver Enzymes and Creatinine

Assessment of the severity of hepatic damage after D-GalN-induced ALF was performed on blood samples collected on day 1, 2, 4 and 8 post-ALF induction compared to day 0 (baseline control). Prothrombin time (PT), ammonia, alanine aminotransferase (ALT), aspartate aminotransferase (AST), bilirubin and creatinine were analysed at the same time point. PT and ammonia were determined using fresh whole blood without anticoagulants (8µl and 20µl, respectively). PT was measured using an automated coagulation monitor device (CoaguCheck® XS system, Roche Diagnostic, Mannheim, Germany) with the maximum recorded value of >96 seconds. Ammonia was determined using a blood ammonia analyser (PocketChem BA, Manarini Diagnostics, Wokingham, UK). The measurement range of this test is 7-286µmol/L. ALT, AST, bilirubin and creatinine were measured in serum samples (150µl) using a routine biochemical AutoAnalyser (Advia 2400; Siemen Healthcare Diagnostics, Camberley, UK).

7.2.2.11 Animals Follow-up and Microbeads Retrieval

General appearance, body weight and neurological status of all animals were recorded before ALF induction as a baseline condition, and then were recorded on day 1, day 3 and day7 post transplantation. The neurological status was classified into four stages of hepatic coma which were grade 1 (lethargy), grade 2 (confusion and stupor but awake), grade 3 (sleeping most of the time, but arousable, with occasional convulsions), and grade 4 unarousable and unresponsive to pain, occasional convulsions) according to Ryan et al. (2001). Survival rate was followed for 7 days post-transplantation. Animals were euthanised at day 7 or when distress was observed, and microbeads and liver tissue were harvested from the abdomen by laparotomy. To retrieve microbeads, the peritoneal cavity was flushed several times with CMRL (50ml) followed by thorough inspection of the abdominal cavity for signs of inflammation or adhesion.

7.2.2.12 Evaluation of Retrieved Microbeads and Liver Histology

The retrieved microbeads were examined for morphology, including host cell adhesion to their surface to determine the extent of host immune responses (Figure 7.3). Cell viability and function of retrieved microbeads were evaluated after maintained in culture for 24h after retrieval. Histopathology analysis was performed on liver tissue.

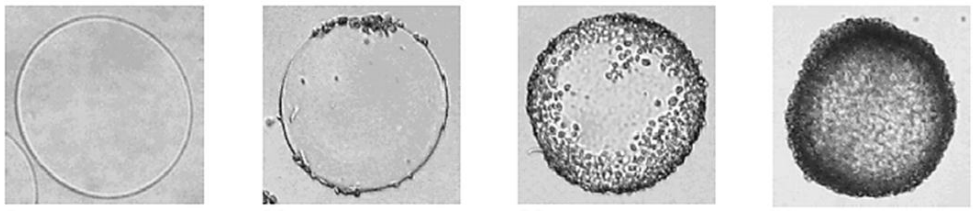

Figure 7.3: Classification of host immune reaction by the degree of host cells covering on the surface of retrieved microbeads [adapted from Tam et al (2011)].

7.2.2.13 Statistic Analysis

Survival curves were calculated using the Kaplan-Meier method and compared with a log-rank test. A value of $p<0.05$ was considered statistically significant. Other statistical analysis methods used are as described in Section 2.2.13.

7.3 Results

7.3.1 Intraperitoneal Transplantation of HMBs into Rats

7.3.1.1 In Vitro Studies of HMBs and Morphology

The viability of (cryopreserved) hepatocytes before encapsulation assessed by trypan blue was 70%. Viability immediately after encapsulation was evaluated by FDA/PI (Figure 7.4A) and MTT assay (2.59 OD reading/100mg HMBs). The viability decreased after maintenance in culture for 7 days at which time MTT was about only 10% of the initial value. The albumin and urea production gradually decreased according to the time in culture. However, CYP1A1/2 activity was increased at day 3 and then diminished slightly at day 7. The viability and function of HMBs over one week in culture was summarised in Table 7.1. 98% of HMBs and EMBs obtained were uniform in shape and size with (Figure 7.4B).

Table 7.1: The HMBs viability and hepatocyte-specific function at different time points in culture.

Time in culture	**Viability and function of HMBs**			
	MTT (OD reading/ 100mgHMBs)	**Albumin production (ng/mg protein)**	**Urea production (µg/mg protein)**	**CYP1A1/2 activity (pmol/mg protein)**
Day 1	1.10	699.5	16.60	5.36
Day 3	0.60	398.4	6.55	10.24
Day 7	0.29	192.2	2.20	8.41

A

Viability

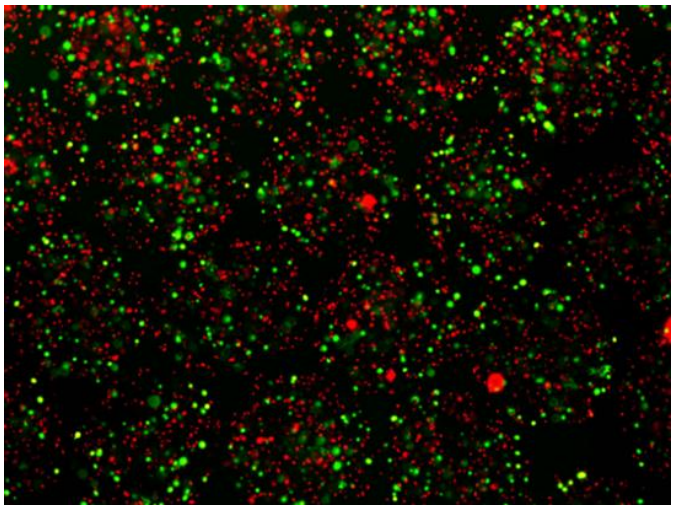

B

Morphology

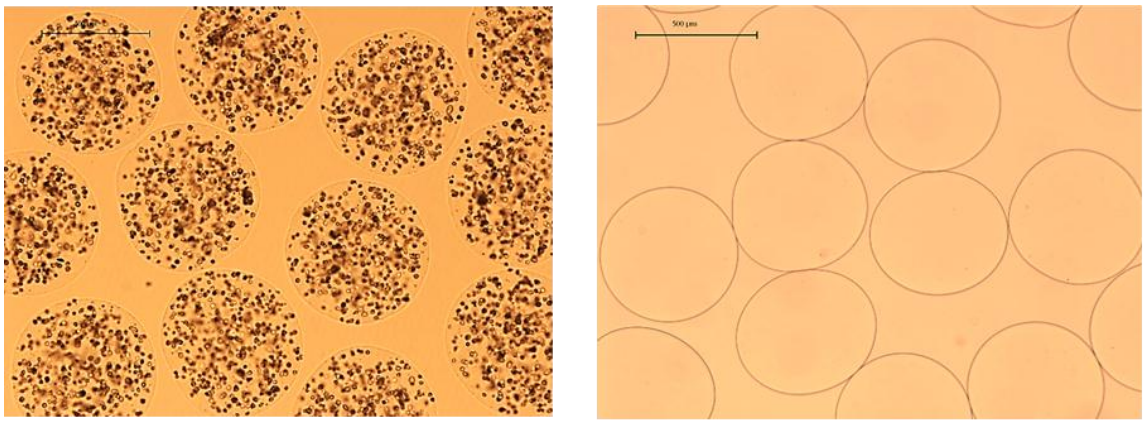

Figure 7.4: Microbeads morphology and cell viability immediately after production and prior to transplantation. (A) Cell viability of HMBs demonstrated by FDA (green)/PI (red) staining and (B) HMBs (left) and EMBs (right) under light microscopy, scale bar = 500µm.

7.3.1.2 In Vivo Study of HMBs in Normal Rats

Seven days post-transplantation, microbeads in both EMBs and HMBs groups were freely dispersed throughout the peritoneal cavity. There were no signs of inflammation or adhesion of microbeads to any structure within peritoneal cavity (Figure 7.5A). A large proportion of microbeads were retrieved from rats transplanted with EMBs (73.3±6.7%), and HMBs (62.2±2.2%). Some microbeads were loosely attached to the omentum and mesentery which came off easily after flushing with transplant medium. The retrieved microbeads were intact without any deformities. There was a small number of EMBs (≤ 1%) minimally covered with adherent host cells, while with HMBs the surface was totally clear (Figure 7.5B).

The function of transplanted HMBs was evaluated by detection of human serum albumin in peripheral blood of rats. Human serum albumin was detected in rats transplanted with HMBs on day 1 (32.6±5.8 ng/ml), day 3 (10.3±2.9) and was just detectable on day 7 (1.7±0.1) post-transplantation (Figure 7.6). The level of human albumin production from HMBs on day 3 and day 7 was statistically lower than first day after transplantation ($p<0.01$). The viability and hepatocyte function of transplanted HMBs was also examined on recovered (retrieved) samples. There were viable cells in retrieved HMBs as demonstrated by fluorescence staining, and MTT activity both immediately after recovery (0.5±0.1 OD reading/100mg HMBs) and after culturing for 24h (0.6±0.3). Moreover, albumin (10.2±0.6 ng/mg protein) and urea (1.19 ± 0.02 µg/mg protein) were detected in the culture medium. CYP1A1/2 activity was detected at level of 7.9±1.1 pmol/mg protein/min. These results indicated that the retrieved encapsulated hepatocytes continued to function *in vitro*.

A

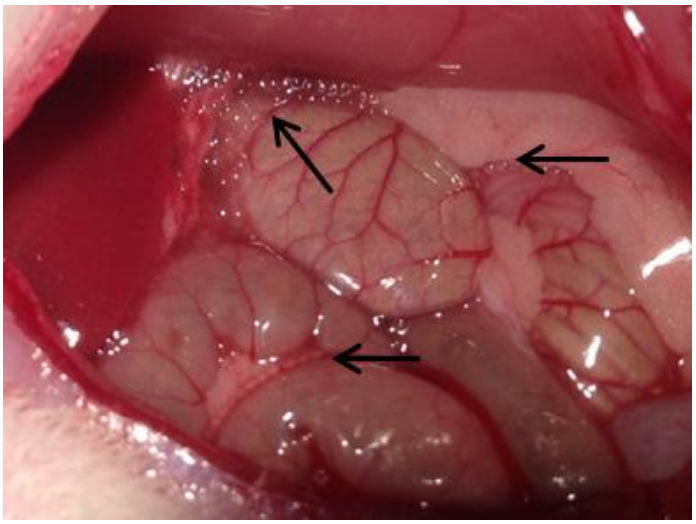

B

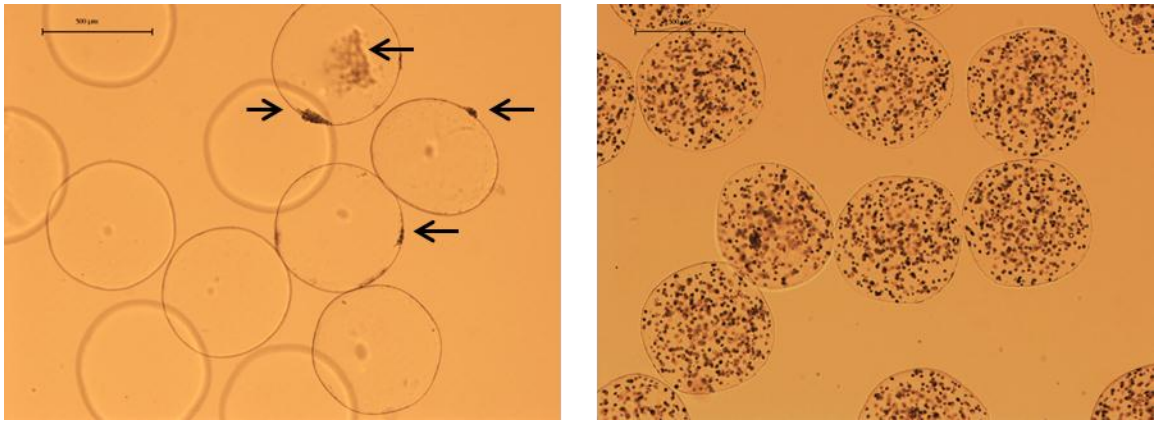

Figure 7.5: Microbeads 7 days post-transplantation. (A) Microbeads were freely distributed in the peritoneal cavity. Many were seen attached along the omentum (black arrow) and no inflammation or fibrosis was observed. (B) Recovered EMBs (left) partly covered with (<50%) host cells (black arrows), and HMBs (right) no evidence of cell adhesion.

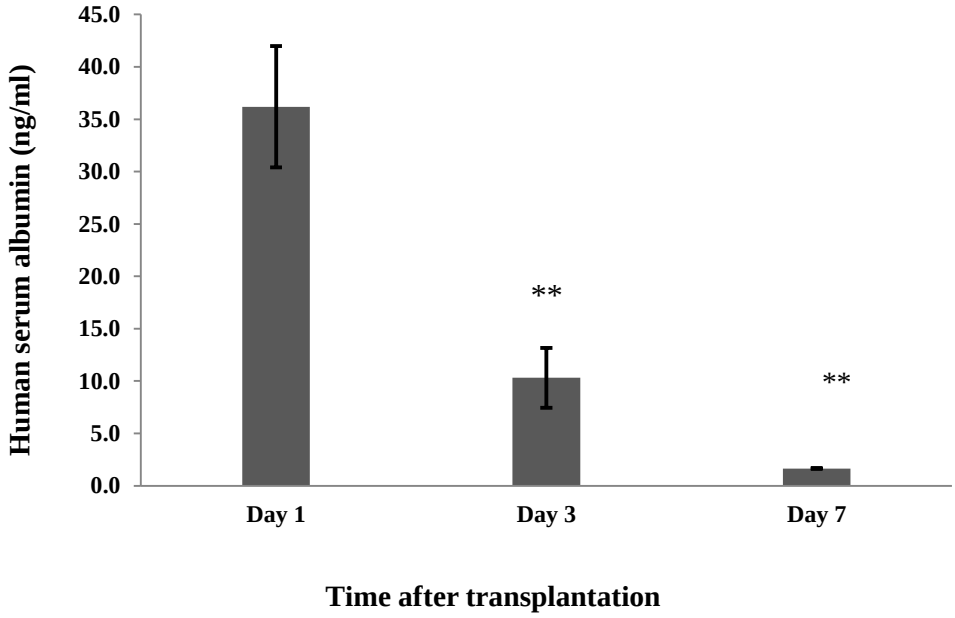

Figure 7.6: Human serum albumin levels in serum samples of rats transplanted with HMBs. [**p<0.01]

7.3.2 *In Vitro* Study of Fresh and Cryopreserved RMBs

After microencapsulation, RMBs obtained were uniform in shape and the viability of RMBs was 7.65±1.26 OD reading/100mg microbeads. Cryopreserved RMBs maintained their cell viability and morphology after thawing. Figure 7.7 shows the viability of fresh RMBs immediately after production and cryopreserved RMBs post-thawing, respectively. Over the period of one week in culture, cell viability and hepatocyte-specific functions of both fresh and cryopreserved RMBs were comparable. Cryopreserved RMBs tended to have a lower initial cell viability and urea production compared to fresh microbeads, however the levels were maintained for a later period, while with fresh RMBs they continued to drop (Figure 7.8). Cell viability of fresh and cryopreserved RMBs progressively decreased, and the significant reduction in viability was observed in fresh RMBs between days 1 and 7 (6.30±0.30 vs 1.45±0.15; $p<0.05$), but this was not observed in cryopreserved RMBs (Figure 7.8A). Urea production also continuously decreased in both fresh and cryopreserved RMBs (Figure 7.8C). Albumin production remained stable during the study. CYP1A1/2 activity of RMBs in both groups showed similar pattern but slightly increased by day 3, then decreased by day 7 to the same level as day 1 (Figure 7.8B and D).

Fresh RMBs

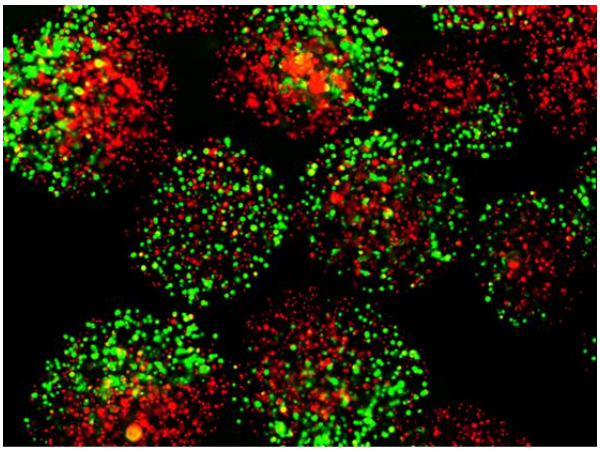

Cryopreserved RMBs

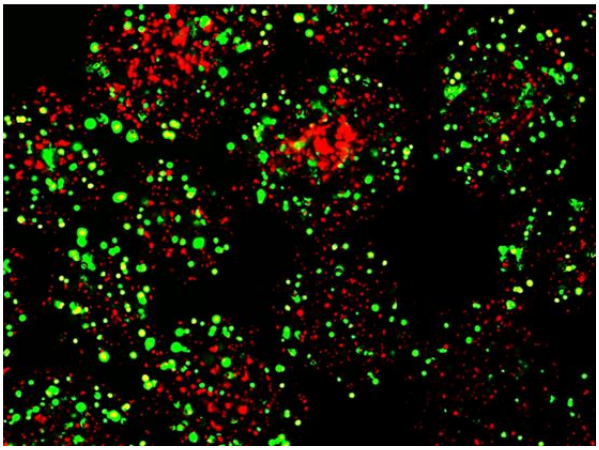

Figure 7.7: Cell viability of fresh and cryopreserved RMBs prior to transplantation. Representative images of FDA (green)/PI (red) staining demonstrating cell viability of fresh RMBs immediately after production (top panel) and cryopreserved microbeads immediately after thawing (bottom panel).

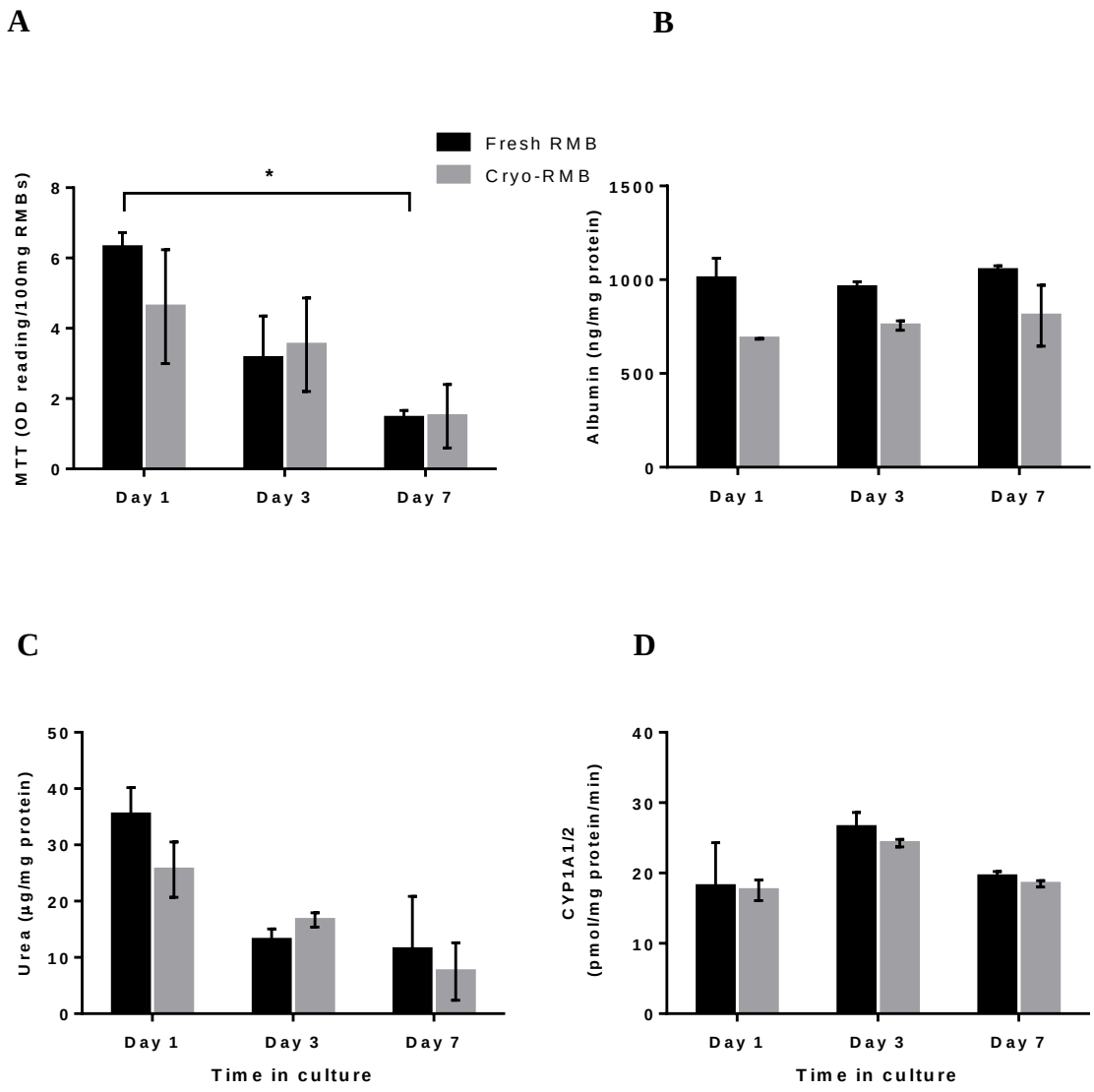

Figure 7.8: *In vitro* data of fresh and cryopreserved RMBs. (A) cell viability; MTT assay, (B) albumin production, (C) urea production, and (D) CYP1A1/2 activity; *p<0.05.

7.3.3 Acute liver Failure Induction

Out of 44 rats, 21 showed ALF determined by PT >36sec (INR≥3) at 24h after ALF induction. When comparing ALF-rats (n=21) to the ones without ALF (n=23), there was no statistical differences in baseline parameters including body weight, PT or ammonia levels. A statistical significant increase in liver function tests was observed in ALF-rat at 24h after ALF induction compared to normal baseline ($p<0.0001$). These included ammonia, median 25 (range 7-67 µmol/l) vs 6 (6-26 µmol/l); PT, 63.6 (37.4-96.0 sec) vs 12.1 (9.6-12.4 sec); AST, 2549 (1017-6255 IU/l) vs 105 (78-163 IU/l); ALT, 2263 (803-5584 IU/l) vs 69 (39-93 IU/l); and bilirubin, 3 (1-13 µmol/l) vs 1 (1-1 µmol/l), at 24h versus baseline control, respectively (Figure 7.9).

7.3.4 Transplantation of RMBs in ALF-rats

Intraperitoneal transplantation of EMBs (group 2), fresh RMBs (group 3), cryopreserved RMBs (group 4) and transplant medium injection (group 1; sham) was performed on day 1 (24-28h) after ALF induction under general anesthesia. All of animals fully recovered after the procedure without any post-operative complications and became ambulatory. Encephalopathy was limited in the animals throughout the follow up period. Only two animals had hepatic coma grade 2-3. One was observed on day 2 and the other on day 3 after ALF induction.

7.3.4.1 Animal Survival

All animals survived immediately after post transplantation. In group 1, one animal developed hepatic coma and suffered from respiratory distress and eventually died on day 3. Two animals in group 2, transplanted with EMBs, died on day 2 and day 3 after ALF induction. On day 4, three animals in group 4 transplanted with cryopreserved RMBs found dead. All animal in group 3 transplanted with fresh RMBs were survived up to one week post-transplantation. The 72-hour survival rates were 83.3%, 50%, 100% and 100% in group 1, 2, 3 and 4, respectively. The 96-hour survival rate decreased to 50% in group 4, while other groups remained stable. Subsequently, the survival rate did not change in all experimental groups. The rats in group 3 were survived better than the other three groups; however there was no statistical significance between the groups (Figure 7.10).

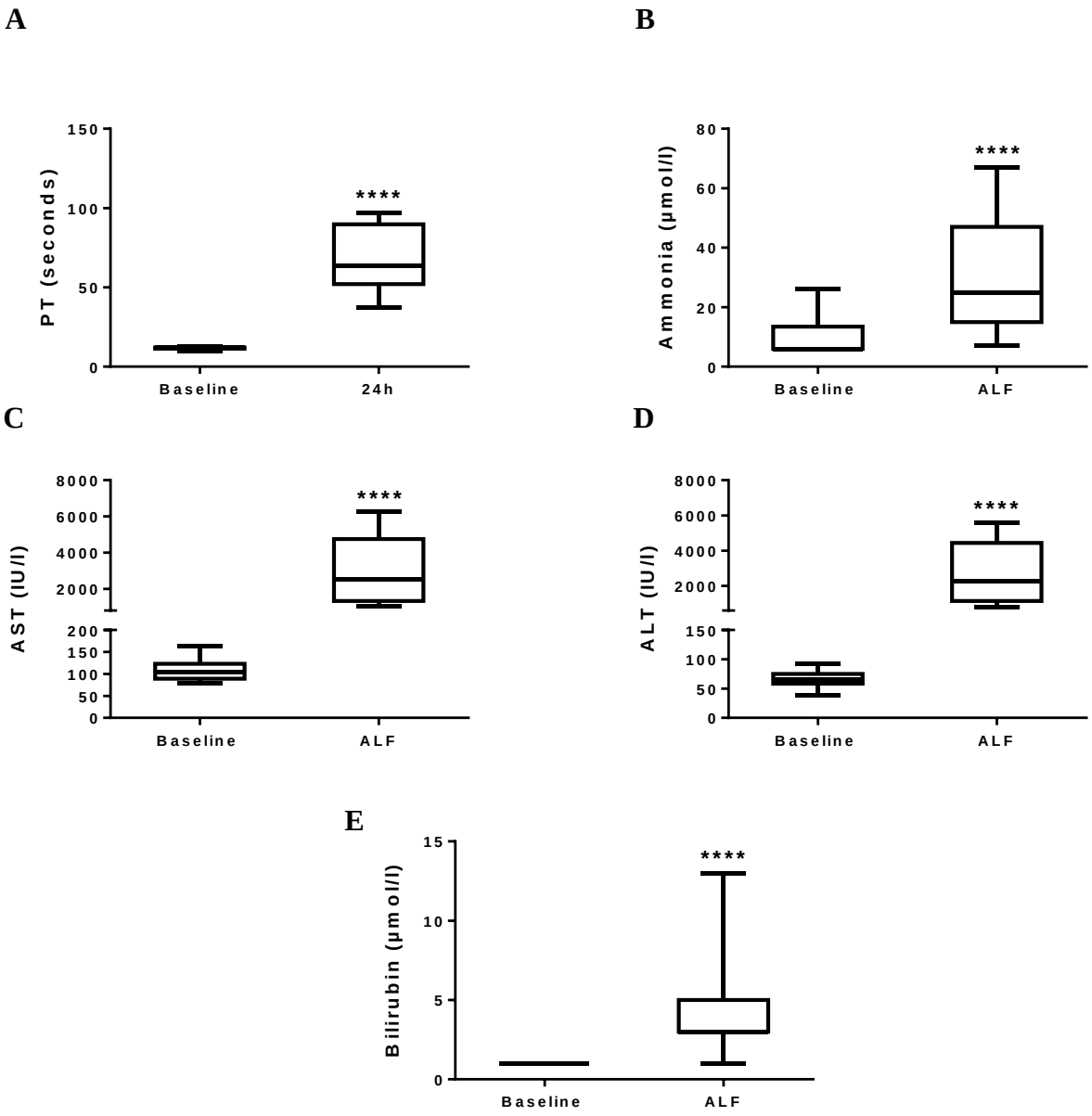

Figure 7.9: Biochemical profiles of acute liver injury. Liver functions test assessed 24h after D-galactosamine (D-GalN) administration compared to baseline controls; (A) blood ammonia level, (B) prothrombin time (PT), (C) serum aspartate aminotransferase (AST) level, (D) serum alanine aminotransferase (ALT) level, and (E) serum bilirubin level. Data are expressed as median and range. [Statistical significance*p<0.05, **p<0.01, ***p<0.001 and ****p<0.0001].

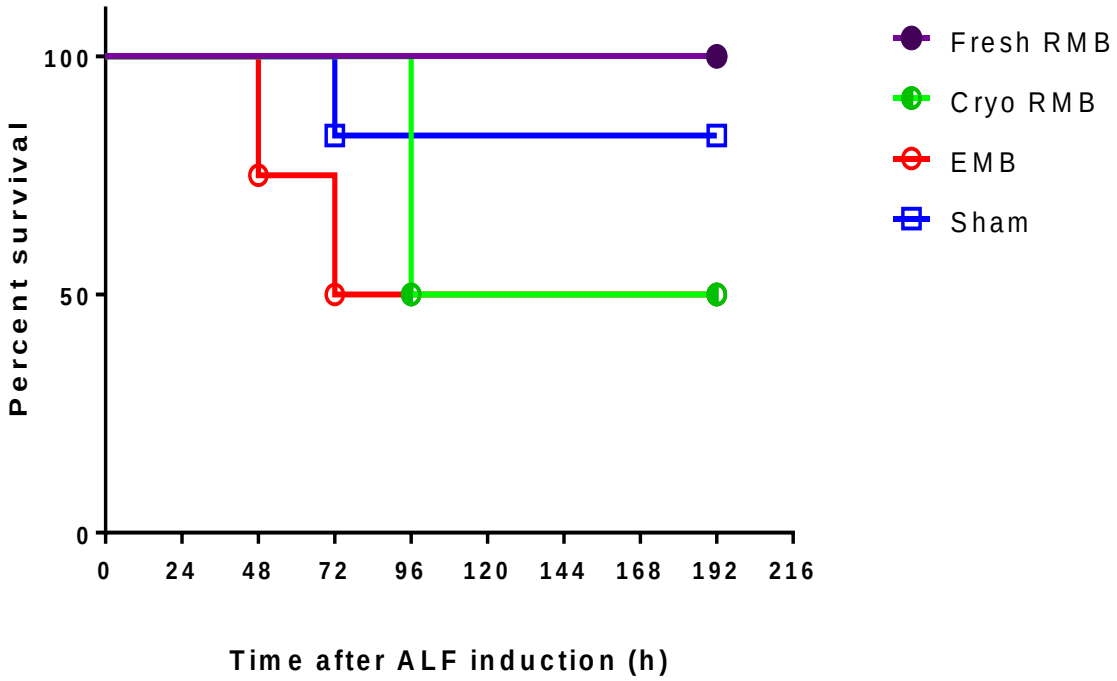

Figure 7.10: Effect of intraperitoneal transplantation of RMBs on survival rate of rats with ALF.

7.3.4.2 Liver Function Tests and Creatinine Level

The overall blood tests of liver function results showed an increase from baseline to significant levels by 24h, which then progressively rose up to reach a peak at 48h after ALF induction, indicating maximum liver injury. A general improvement in liver function was observed in surviving animals on day 4 post-ALF induction. Noticeably, all parameters almost completely returned to normal levels (baseline) on day 8 post-ALF induction (Figure 7.11). There was no significant difference in biochemical profiles including PT, ammonia, ALT, bilirubin and creatinine levels at 24h after ALF induction. However, the AST level was significantly higher in group 4 (median 4594, range 1372-5795 IU/l) compared to group 3 (1244, range 1017-2672 IU/l; $p<0.05$). This degree of liver injury was similar in all groups before receiving any treatment. The differences between groups were clearly seen on the following day after transplantation of microbeads (day 2 post-ALF induction). Transplantation of fresh RMBs in group 3 decreased the severity of ALF showing statistically significant lower levels of liver enzymes including ALT (1937, range 1407-2461 IU/l; $p<0.01$), AST (1997, range 1565-2613 IU/l; $p<0.001$) and bilirubin (41.5, range 37-61 µmol/l; $p<0.01$) than those of the other three groups. In addition, the creatinine levels in rats transplanted with fresh RMBs (24.5, range 22-31 umol/l) and cryopreserved RMBs (29.5, range 25-36) were significantly lower than in those transplanted with EMBs (48, range 45-51; $p<0.01$). PT and ammonia levels were not significantly different between the four groups, however, one animal in group 2, transplanted with EMBs had an extremely high ammonia level (>286µmol/l). There was no significant difference between groups in any of the blood tests performed on days 4 and 8 post-ALF induction.

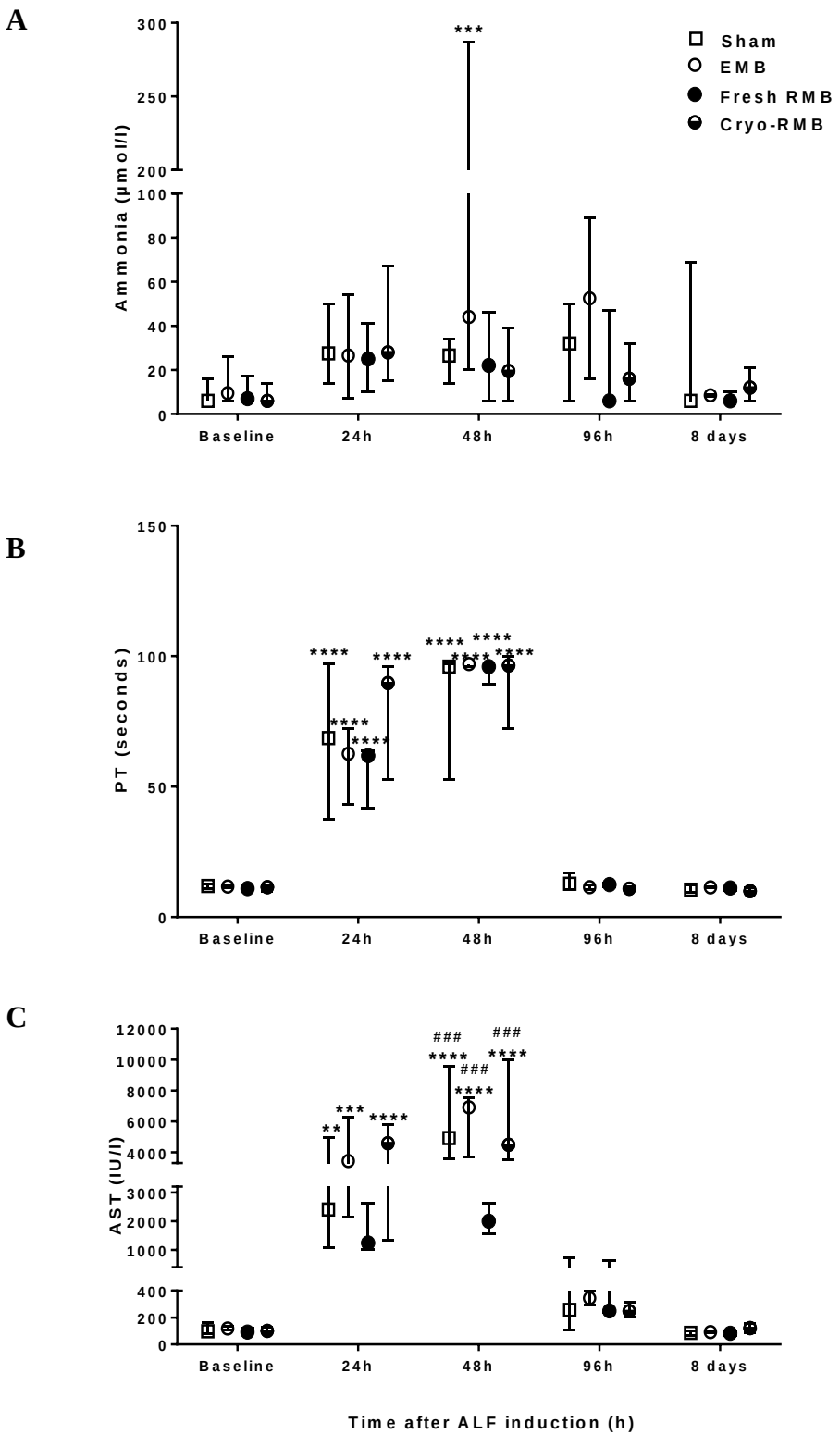

Figure 7.11 (Continued).

(Continued)

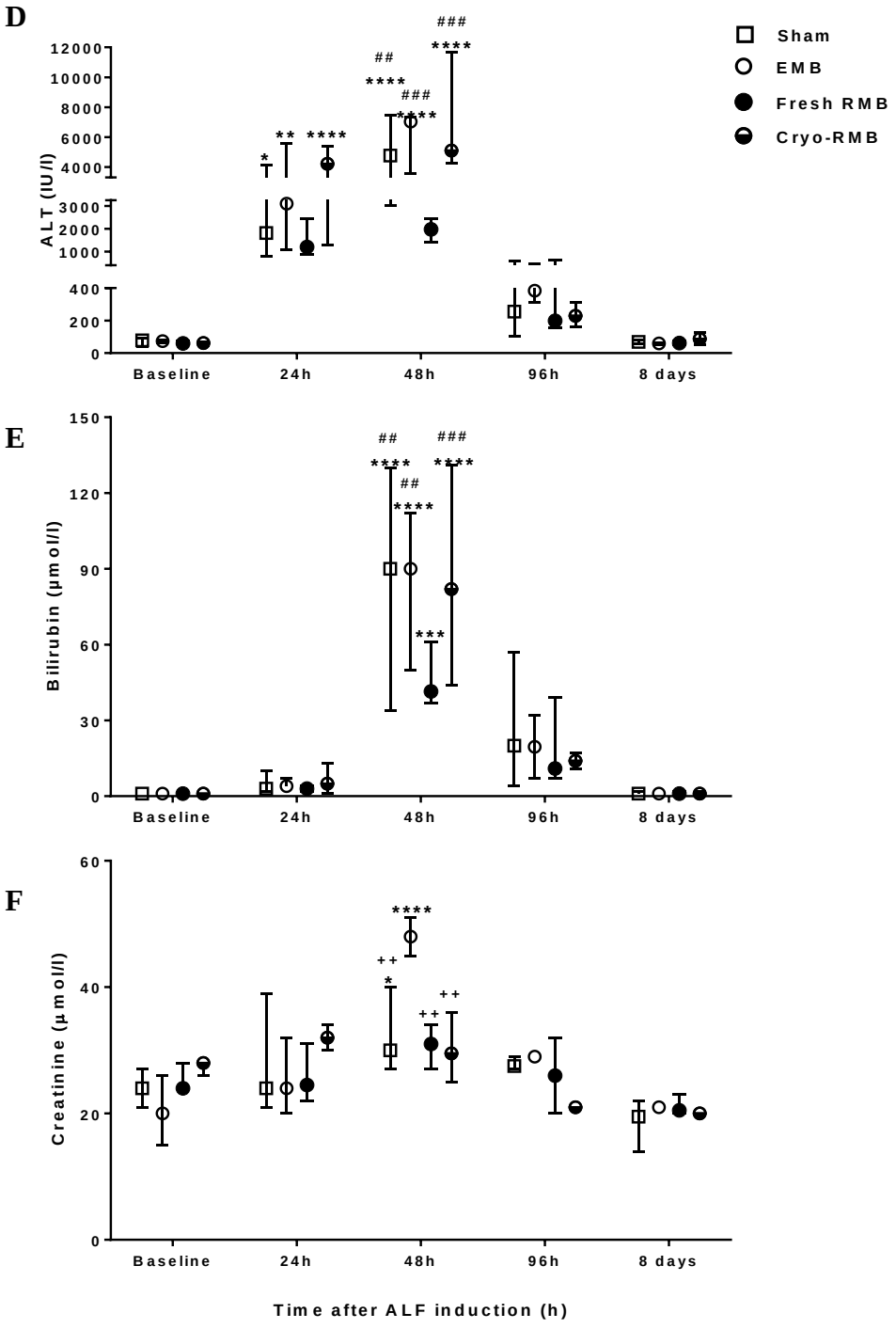

Figure 7.11: Biochemical parameters of rats with D-GalN induced ALF. (A) blood ammonia level, (B) PT, (C) serum AST level, (D) serum ALT level, (E) serum bilirubin level, and (F) serum creatinine level. Significance*p<0.05, **p<0.01, ***p<0.001 and ****p<0.0001 compared to baseline level. Significance: $^{\#}$p<0.05 and $^{\#\#}$p<0.01, and $^{\#\#\#}$ p<0.001 compared to group 3 (transplanted with fresh RMBs at 48h after ALF induction. Significance $^{++}$p<0.01 compared to group 2 (transplanted with EMBs) at 48h after ALF induction.

7.3.4.3 Body Weight of ALF-rats

The animal weight loss showed similar trend as the liver function tests, when animals had lost weight starting from 24h after ALF induction. The overall maximum weight loss was observed on day 2 post-ALF induction except in the sham group that continuously lost weight (peaked on day 4). Animals in group 2, 3 and 4 started to gain weight on day 4. Noticeably, animals in group 3 and 4, transplanted with fresh and cryopreserved RMBs had significantly recovered from the weight loss better those in the sham group ($p<0.01$). On day 8, animals in all groups had returned to their baseline weight (Figure 7.12).

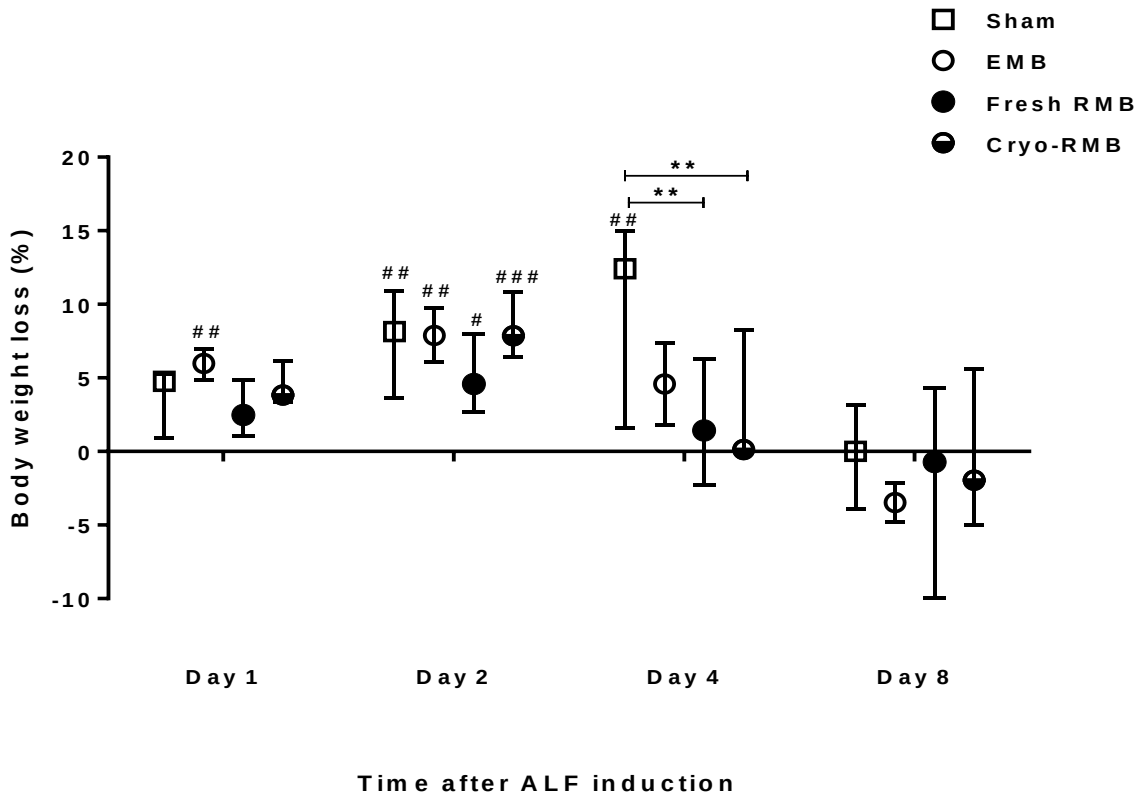

Figure 7.12: Assessment of body weight of ALF-rats. Data are expressed as percentage of weight loss compared to individual baseline, and represented as median (range); **p<0.01. Statistical significance compared to values on day 8: #p<0.05 and ##p<0.01.

7.3.4.4 Metabolic Morphology and Function of Retrieved Microbeads

Microbeads were recovered from surviving animals after 7 days of transplantation (n=10) and at the other time points when the animals died or were euthanised (n=5). Microbeads were found scattered throughout the peritoneal cavity, and loosely attached to the omentum and mesentery in the three groups (group 2, 3 and 4). No signs of inflammation or adhesion were observed. The total volume of microbeads retrieved was found to be 70±2.4% of transplanted microbeads. The morphology and integrity of microbeads in all groups were well maintained. The retrieved RMBs from 2 animals in group 4 (cryopreserved RMBs) had some host cells adherent to the microbeads surface (2-5%), whereas retrieved RMBs from the other 4 animals were clean. There was hardly any host cells adherent to the surface of retrieved microbeads in groups 2 (EMBs) and 3 (fresh RMBs). The retrieved RMBs in group 3 and group 4 showed viable cells and hepatocyte-specific functions in culture (Figure 7.13 and 7.14). Retrieved RMBs from group 4 had a significantly higher cell viability (MTT=0.61±0.10 OD reading/100mgRMBs; $p<0.05$) and albumin production (1161±11.2 ng/mg protein; $p<0.01$) than those retrieved from group 3 (0.39±0.04 and 1033±22.5, respectively).

Fresh RMBs

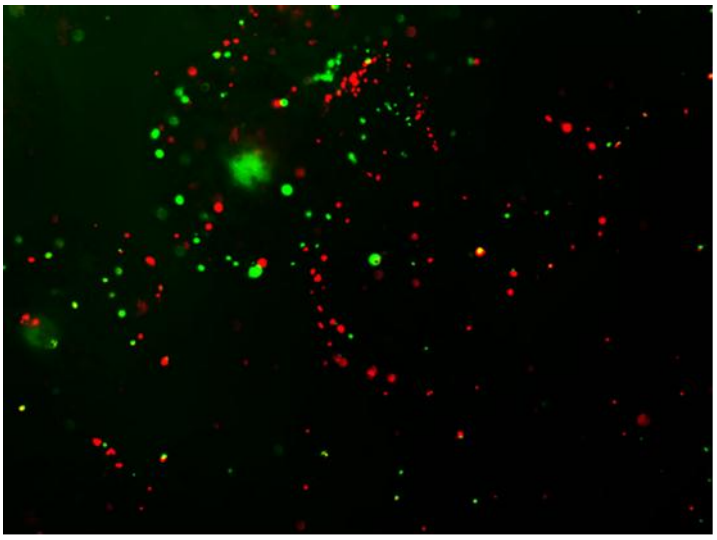

Cryopreserved RMBs

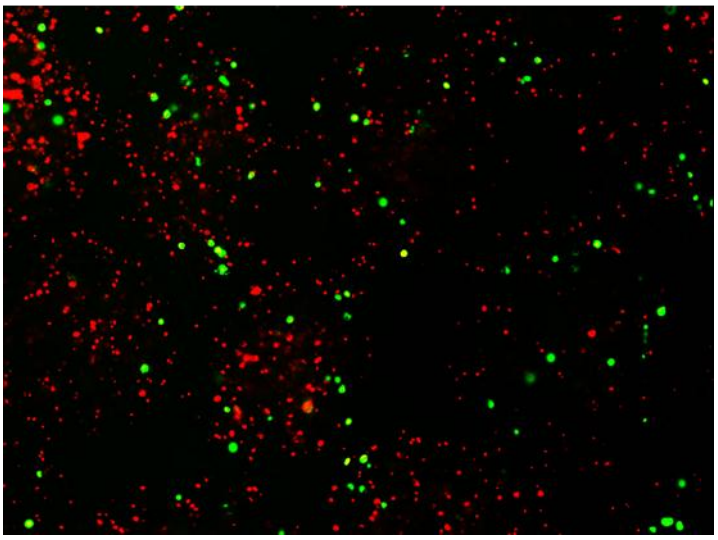

Figure 7.13: Retrieved microbeads after transplantation for 1 week. FDA (green)/PI (red) staining demonstrated cell viability in retrieved fresh (top panel) and cryopreserved microbeads RMBs (bottom panel)

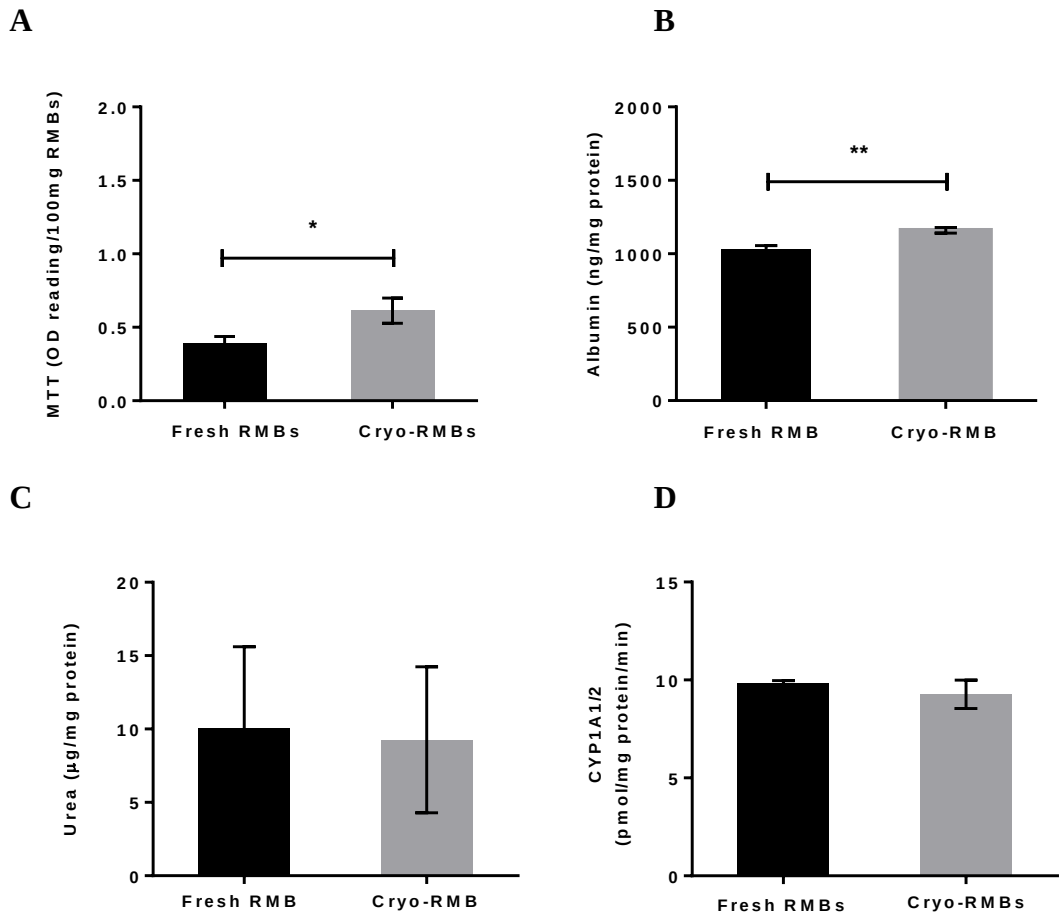

Figure 7.14: Viability and metabolic function of retrieved RMBs after transplantation for 7 days. (A) MTT assay, (B) albumin production, (C) urea production and (D) CYP1A1/2 activity. [*p<0.05 and **p<0.01].

7.3.4.5 Liver Histopathology

Gross appearance of liver in surviving rats looked similar to normal controls. On the other hand, livers of severe ALF rats (died) were pale yellowish in color, hemorrhagic and with atrophy leading to a liver weight loss three times greater than that of surviving rats (5.9±0.7g and 14.8±0.2g, respectively), (Figure 7.15A and B). Histopathology of surviving rats showed completely normal intact lobular architecture without signs of hepatocellular injury one week post RMBs transplantation (Figure 7.15C). Livers from dead ALF-rats showed evidence of hepatocellular necrosis affecting periportal and centrilobular regions (Figure 7.15D-F).

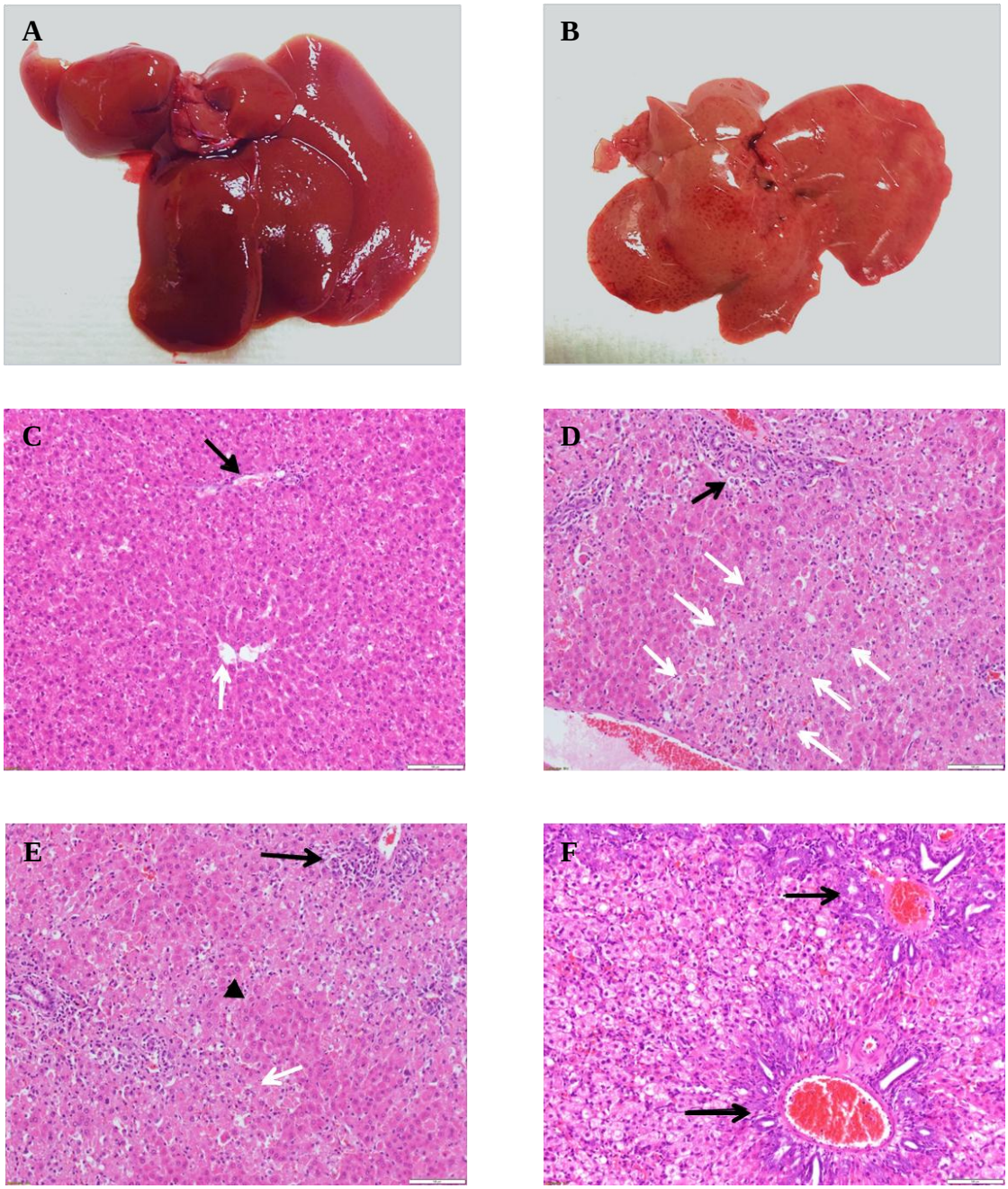

Figure 7.15: Liver gross anatomy and histopathology of rats with ALF. (A) Surviving rats at day 7 post transplantation and (B) dead rats at day 2 after D-GalN injection. Representative of histopathology of liver tissue from rat with D-GalN induced ALF; H&E staining (200x), [scale bars= 100µm]. (C) surviving rat at 7 days post transplantation showed normal lobular architecture; portal tract [black arrow] and central lobular region [white arrow], (D)-(E) dead rat at 48h after ALF induction showed confluent hepatocellular necrosis affecting centrilobular and periportal region with mild inflammatory cell infiltration [black arrow head], and (F) dead rat at 72hr post-ALF induction showed ductular reaction in keeping with an attempt to regeneration nearby hepatocytes shows cytoplasmic vacuolation.

7.4 Discussion

7.4.1 Intraperitoneal Transplantation of HMBs in Rats

This study demonstrated encouraging results in terms of the physical integrity, biocompatibility, viability, and functionality of optimised HMBs during and after xenotransplantation into wild type rats without the need for immunosuppression. Transplantation of the optimised microbeads *in vivo* showed EMBs and HMBs retrieved were intact and maintained their shape and size after 1 week in the peritoneum. Most microbeads were free from host cell adhesion. Previous studies reported transplanted microcapsules (sodium alginate-poly-L-lysine-sodium alginate copolymer; APA) surrounded with fibrous tissue within 4 days to 4 weeks (Umehara et al. 2001; Mei et al. 2009; Zhang et al. 2011). However, in this study there was no evidence of fibrosis or tissue adhesion surrounding the microbeads. The possible explanations could be that the ultra-pure alginate used did not provoke the host immune response which is supported by the *in vitro* data previously described in Chapter 5. Previous studies used poly-L-lysine in microbeads which could have induced immune reaction against the microbeads. Interestingly, there were no host cells adherent to HMBs despite human hepatocytes being administered to rats (xenotransplantation). The detection of human albumin in the serum of rats transplanted with HMBs, and the *in vitro* demonstration of viability, albumin and urea production by the retrieved HMBs proves that the microbeads remained functional. The low level of human albumin in rat serum on day 7 could be possibly explained by the use of cryopreserved cells to prepare microbeads in this experiment, and also the total number of cells transplanted was low. In addition, as the albumin produced was human, the rat immune system might have reacted against the foreign protein and started to eliminate it from the blood. Overall, these findings show that the optimised microencapsulation protocol protects cells from host immune response, while allowing cell survival and function.

7.4.2 Viability and Function of Fresh RMBs and Cryopreserved RMBs

It is well known that isolated primary hepatocytes are difficult to maintain in culture, and that cryopreservation also has substantial detrimental effects on their function and viability. Interestingly, the results from this current study showed that there was no significant difference in function of encapsulated cells between fresh and cryopreserved RMBs over the period of one week in culture. Although, the cryopreserved RMBs showed slightly lower viability, urea and albumin production level at day 1, this remained stable afterwards. Albumin synthesis and cytochrome P450 activity were well preserved in both groups. These findings suggest that an

optimised protocol for production of hepatocyte microbeads has been established in this present study. Moreover, the microbeads cryopreservation protocol tested gave encouraging results too (Chapter 4 and Chapter 6).

7.4.3 D-galactosamine and Acute Liver Failure

The ALF rat model using D-GalN intraperitoneal injection was used because the liver injury caused by this compound closely resembles that of human ALF in terms of histology and biochemical parameters. The severity of liver damage was dose-dependent and is more predictable (Keppler et al. 1968; Diaz-Buxo et al. 1997; Kalpana et al. 1999) than the acetaminophen model, plus the extrahepatic toxicity of D-GalN is not significant. The main concern of chemical model is that variable factors such as species, strain, sex, weight and time of administration could play an important role in the severity of the response (Terblanche and Hickman 1991). The dosage used was based on previous studies, as a dose of 850mg/kg to 1g/kg was too low and allowed for a spontaneous recovery of liver injury. Keppler et al (1968) showed that D-GalN injected intraperitoneally at dose of 1.5g/kg produced ALF features within 24-48 in Wistar rat equally in both sex. Rivas-Vetencourt et al. (1997) using 3g/kg (intraperitoneally) to induce Sprague Dawley rats and found that mortality rate>85%. They suggested that at this high dose the persistence of D-GalN in the circulation may be toxic to the encapsulated cells when transplanted at 24h after administration. However, Jauregui et al demonstrated that D-GalN (1g/kg; intravenously) was completely cleared from rabbits' blood after 3-6h after administration (Jauregui et al. 1995).

In the current study, the induction of ALF was carefully conducted in consideration the animals and the variable factors involved to minimise the variation of response. However, variable effects of D-GalN at the dose of 1.2g/kg were observed in the study. The PT ≥36 sec (INR≥3) was the main criterion of ALF in this study, since the impaired synthetic function of coagulation factors (I, II, V, VII and X) is a highly sensitive indicator of liver injury owing to the relatively short half-life. In humans, a diagnosis of ALF is made in patients who develop coagulopathy with encephalopathy in adults. In children, the signs of hepatic encephalopathy may be subtle and difficult to identify hence the diagnosis is based on INR ≥2 alone or INR ≥1.5 plus hepatic encephalopathy (Squires et al. 2006; Bernal et al. 2010). Four animals had a PT range from 18 to 32 sec. All of them spontaneously recovered within 72h after ALF induction. The mortality rate at this dose was about 20% in untreated animals similar to that in the previous study in our department by Puppi et al. (2014). The animals transplanted with empty microbeads and

cryopreserved microbeads showed 50% mortality rate. However, it is difficult to interpret the result based on the small subgroups of animals and increased potential for type 2 error.

7.4.4 Intraperitoneal Transplantation of RMBs

To determine the efficacy and safety of optimised microbeads, we transplanted RMBs in rats with ALF as this approach would better mimic the transplantation of HMBs in patients. This current study showed promising outcome of intraperitoneal transplantation of optimised microbeads in ALF-rats. The technique was safe without any immediate or late complications. The hepatocytes inside the microbeads survived and were able to function without using immunosuppression. Rats with transplantation of RMBs all survived, which tended to be better than with cryopreserved RMBs, EMBs and untreated animals, however, this did not reached statistical significance as the number of animals was small. The low mortality of ALF with D-GalN at this dose (Puppi et al. 2014) made it difficult to assess survival. Interestingly, transplantation with cryopreserved RMBs prolonged survival rate at 72h similar to transplantation with fresh RMBs. Nevertheless, the mortality rate in the cryopreserved group increased to 50% at 96h. There was a significant improvement in biochemical parameters of liver injury including ALT, AST, and bilirubin of the fresh RMBs group compared to the other three groups. We also evaluated serum creatinine to determine the severity of ALF and multiorgan failure and found that both fresh and cryopreserved RMBs groups had significantly lower creatinine levels than the EMB group. Additionally, the body weight, one of the indicators of animal well-being was also significantly better in both fresh and cryopreserved RMBs groups compared to control groups (EMBs and sham). The liver histology of surviving rats showed complete recovery 7 days after transplantation. These data suggest that intraperitoneal transplantation of fresh hepatocyte microbeads containing only a small part of the total liver mass could support the failing liver and improve outcome. The possible reason why transplantation with cryopreserved RMBs did not show significant improvement of liver injury as effectively as fresh RMBs is the small number of cells transplanted. It could be hypothesised that transplantation of cryopreserved hepatocyte microbeads required a greater cell number to provide sufficient metabolism in order to support and improve survival rate compared to freshly prepared microbeads. However, a larger volume transplanted into peritoneal cavity might lead to intra-abdominal hypertension and abdominal compartment syndrome with compromised blood flow to abdominal organs and multiple organ dysfunction syndrome and death. This perhaps could be avoided by repeating transplantation in the next following day.

Other investigators showed that transplantation of cryopreserved encapsulated cells improve survival rate in ALF mice. However, the total cell number transplanted in those studies was high up to 30% of liver mass (Mai et al. 2005; Mei et al. 2009). Umehara et al. proposed that transplanting encapsulated cells at 4% of total liver volume improved metabolism and survival rate of ALF-rats (Umehara et al. 2001). The optimal cell number required to provide efficient function in the clinical setting of ALF remains controversial and further studies are needed.

Transplantation of the optimised fresh or cryopreserved microbeads in this rat model of ALF also showed encouraging results in terms of the physical integrity and biocompatibility of hepatocyte microbeads and their survival and function. The retrieved microbeads were intact and maintained their shape and size in the peritoneal cavity. Minimal percentage of host cell adherence was observed. Nevertheless, cryopreserved RMBs seemed to have higher number of host cell adherent on the surface than non-cryopreserved microbeads. This could be due to the uneven damage to the microbead surface and/or the permeability change that may have occurred during cryopreservation and thawing. The reaction of the individual animal may be important as data showed that the host cell adherence on microbeads was found in 2 out of 6 animals only. The cell viability and the detection of albumin and urea production, and cytochrome activity produced by the retrieved RMBs confirmed the microbeads were functioning after transplantation. A significantly higher cell viability and albumin synthesis were observed in the cryopreserved RMBs compared to fresh RMBs after retrieval. This result was again in agreement with the *in vitro* study which showed that cryopreserved microbeads maintained their metabolic functions well over a week.

In conclusion, the current study shows that the optimised protocol using production of GMP grade materials provided high quality and biocompatible hepatocyte microbeads. The alginate encapsulated cells maintained their hepatocyte-specific functions both *in vitro* and *in vivo*. Intraperitoneal transplantation of optimised microbeads provided metabolic support in ALF without immunosuppression. This along with the safety of this approach allows repeated transplantation if required. Transplantation of cryopreserved microbeads is an attractive option and comprehensive investigations are required. Therefore, these high quality alginate human hepatocyte microbeads are potentially suitable for clinical transplantation.

CHAPTER 8

8. General Discussion and Conclusions

The concept of hepatocyte microencapsulation for treatment of liver disease was developed over two decades ago. Transplantation of microencapsulated hepatocytes has been studied in animal models of acute liver failure with promising outcomes. Hepatocyte microbeads (HMBs) can replace the missing metabolic and synthetic functions of damaged hepatocytes either for a short period bridging the patient to liver transplantation or allowing time for the liver to regenerate and recovery. Importantly, encapsulation avoids the need for immunosuppression. The progress in this field has been slow mainly due to the poor biocompatibility of the biomaterials used and reproducibility of the technique. In order to implement HMBs as a therapeutic option in clinical practice, some important parameters needed to be optimised. These parameters include (i) mechanical and chemical stability, (ii) morphology and permeability, (ii) inflammatory potential of microbeads containing hepatocytes, (iv) the cell viability and function performance of microbeads, and (v) biosafety (Santos et al. 2013; Rokstad et al. 2014). Another important issue that must be considered is long-term storage of HMBs, such as cryopreservation of these microbeads to make them readily available for emergency use. There are no published protocols for production of microbeads for the clinical treatment of acute liver disease. The main purpose of the current study was aimed at clinical translation, therefore a stepwise comprehensive investigation and optimisation of the important parameters involved were conducted.

This study has used a highly purified (ultra-pure) type of alginate to produce GMP grade alginate microencapsulated human hepatocytes. Optimisation of polymerisation time required a careful balance between the mechanical stability and its effects on cell viability and function, and permeability of HMBs. It was observed that polymerisation for 15min provided good mechanical stability without any detrimental effects on cell viability and function of HMBs compared to a shorter (10min) and a longer duration (20min) polymerisation time. Investigation of the effects of cell density on the physical integrity, cell viability and function of the encapsulated hepatocytes was required, since overcrowding within a microbead may result in competition for nutrients and increased cell death. Microbeads produced with cell density up to of $3.5x10^6$cell/ml alginate were found to be uniform in shape and intact. The even distribution of cells and cell viability across the microbeads were demonstrated using confocal microscopy imaging and 3D reconstruction. A cell density of $3.5x10^6$cell/ml alginate showed a good cell viability and function. After establishing the protocol for production of HMBs, permeability of

these optimised microbeads was evaluated. It was found that the maximum molecular weight of protein that can diffuse through microbeads was 164kDa.

It is well established that APA has strong immunogenicity due to the positive charge of PLL, therefore uncoated alginate microbeads were used in the current study to minimise the host immune reaction. The potential immunogenicity of these optimised microbeads was investigated with human polymorphonuclear cells (PBMCs). Initially freshly prepared empty microbeads (EMBs) and HMBs were co-cultured with PBMCs. No evidence of cellular immune activation was found. Unexpectedly, EMBs and particularly HMBs had a significant inhibitory effect on monocyte activation marker expression. The later study better mimicked the real transplantation setting by incubating microbeads with ascitic fluid followed by co-culturing with PBMCs. Microbeads showed excellent biocompatibility by demonstrating no immune cell adherence onto their surface, and no differences in immune activation and cytokine production levels. Nevertheless, it would be ideal to directly measure the amount of protein adsorbed on the surface of microbeads. These proteins would include immunoglobulins and complement particularly C3 that can activate classical and alternative complement pathways. In the i*n vivo* study, the evaluation of immunogenicity was performed in both xenogenic and syngeneic transplantation in immunocompetent animals. The degree of immune response was evaluated by the assessment of host cell adhesion on microbead's surface, percentage of microbeads recovery and cell viability of recovered microbeads. The results were encouraging and demonstrated that both freshly prepared and cryopreserved HMBs hardly stimulated host immune reaction. These *in vitro* and *in vivo* results also suggest that the optimised HMBs has the potential for clinical application.

The cryopreservation of microbeads part of this study focused on developing a modified cryopreservation solution by adding cytoprotectants to reduce some of the detrimental effects of stress related to apoptotic cell death during freezing and post-thawing. The cryopreservation protocol was based on a previously published study (Massie et al. 2011). Improvements of the ultrastructure of encapsulated hepatocytes, viability and some functions were observed in HMBs cryopreserved with UW solution containing of 10% DMSO, 5% glucose and 60µM ZVAD. Human serum albumin and desferoxamine also showed positive effects on cryopreserved HMBs. These findings have resulted in improvement of the cryopreservation outcome that could be implemented in the cryopreservation protocols for future clinical use. However, optimisation of cryopreservation of microbeads remains complex and involves many steps. Hepatocyte microbeads consist of two elements to freeze which are mainly the water in the alginate structure and the entrapped cells which makes it more difficult for cryopreservation especially controlling the intracellular ice formation. Therefore, further studies are needed to

develop an optimised protocol that systematically evaluates the freezing solutions, freezing and thawing stages. In addition, using advanced techniques such as cryomicroscopy for evaluation the degree of cryodamage would be of interest.

Ttransplantation of optimised HMBs in immunocompetent rats, the function of these microbeads was evaluated for 7 days and host immune response after transplantation was assessed on day 7 post-transplantation. Human serum albumin was detected throughout the 7 days and no inflammatory reaction was observed in the peritoneal cavity or on the microbeads. The therapeutic effect and the safety/acceptability of rat hepatocyte microbeads produced were confirmed in rats with acute liver failure. The results suggested that freshly prepared hepatocyte microbeads containing hepatocytes equivalent to a small part of total liver mass could provide effective metabolic function to support the failing liver, but not when cryopreserved hepatocytes microbeads were used, as a greater number of cells is required due to loss of hepatocyte function. It would be interesting to investigate the optimum dose of encapsulated hepatocytes that efficiently provides metabolic function to support damaging liver and lead to an improved survival rate. Although in this model recovery of animals and restoration of liver function were achieved in less than 7 day, long-term effect and biocompatibility of microbeads after transplantation is another issue needs to be evaluate.

8.1 Limitations of the Study

Optimisation of Microbeads

Ideally, freshly isolated hepatocytes should be used in all experiments. However, the scarcity of good quality donor liver for hepatocyte isolation for every set of experiments remained an important issue. Also the quality of cells obtained from liver resections of patients with malignancy was relatively low, viability 40-50%, due to the steatotic liver tissue which might have resulted from the underlying disease and chemotherapy effects consistent with the findings of Bhogal and colleagues (2011).

The common techniques used to determine permeability are inverse-size exclusion chromatography (Brissová et al. 1998), more recently, radiolabeled IgG (Mørch et al. 2007), and confocal laser scanning microscopy to detect fluorescently labeled IgG (Qi et al. 2012). In present study, permeability was evaluated with proteomic analysis as it provides information including identification and quantity of proteins that diffuse out of microbeads in the supernatants. However, smaller proteins such as factor VII may have been masked by abundant and larger proteins such as albumin.

Cryopreservation of Microbeads

The use of rat hepatocytes instead of human hepatocytes to optimise microbead cryopreservation protocol was useful due to the insufficient supply of high quality human hepatocytes. Although, the initial results showed similar outcomes using both human and rat hepatocytes, it would have been better to conduct all experiments using human hepatocytes.

Animal Experiments

The achieved rate of ALF after D-GalN induction was unexpectedly low in this study. Also there was a considerable variation in the severity of ALF between animals given the same dose of D-GalN. Therefore, establishing an ALF animal model that is highly reproducible and close to clinical features in humans is important. As the sample size of the current study was small, it is difficult to draw definite conclusions about some data such as survival rate which may have been affected by type 2 error. It must be noted that due to time constraint it was difficult to study a larger number of animals. Further work should be carried out in large scale experiments and also in larger animal models of ALF to help confirm the efficacy of microbead transplantation with both fresh and cryopreserved microbeads.

8.2 Conclusion and Future Work

8.2.1 Conclusion

In conclusion, the work described fulfilled the central hypothesis of this thesis, and the results suggest that the optimised protocol established for production of GMP grade human hepatocyte microbeads could be safely use for transplantation in patients with ALF.

8.2.2 Future Work

It is well known that, human hepatocytes are fragile and vulnerable after isolation. Therefore, co-encapsulation of hepatocytes with other types of cells such as mesenchymal stem cells or non-parenchymal cell could be beneficial, as several studies have shown their beneficial effects in terms of prolonging cell viability and enhancing metabolic function (Table 1.6). The mechanisms of action between these cells and hepatocytes remain unknown whether from direct contact or paracrine effects. It would be interesting to study the effects of co-encapsulation of human hepatocytes with various types of cells and elucidate the mechanisms of action between

them. This might require the use of in alginate microbeads with a depolymerised center as cell-to-cell contact is essential.

There is still potential for improvements in cryopreservation of hepatocyte microbeads. Further experiments are still needed to achieve an optimised protocol to provide improve cell viability and function of hepatocyte microbeads. The stepwise development of cryopreservation protocol by focusing on structural (physical) preservation of microbeads and encapsulated cells together with inhibition of cellular death cascades (biological) will improve the outcome of the protocol. We believe that clinically a large amount of hepatocyte microbeads may be required immediately for emergency cases such as ALF. Therefore, scaling-up production of microbeads and establishing a bank of cryopreserved clinical grade hepatocyte microbeads are both of major importance.

9. REFERENCES

Adams R, Wang M, Crane A, Brown B, Darlington G, Ledley F. Effective cryopreservation and long-term storage of primary human hepatocytes with recovery of viability, differentiation, and replicative potential. Cell Transplant 1995;4(6):579-586.

Alexandre E, Viollon-Abadie C, David P, Gandillet A, Coassolo P, Heyd B, Mantion G, Wolf P, Bachellier P, Jaeck D, Richert L. Cryopreservation of adult human hepatocytes obtained from resected liver biopsies. Cryobiology 2002;44(2):103-113.

Anderson J, Rodriguez A, Chang D. Foreign body reaction to biomaterials. Seminars in immunology 2008;20(2):86-100.

Aoki K, Hakamada K, Umehara Y, Seino K, Itabashi Y, Sasaki M. Intraperitoneal transplantation of microencapsulated xenogeneic hepatocytes in totally hepatectomized rats. Transplant Proc 2000;32(5):1118-1120.

Aoki T, Jin Z, Nishino N, Kato H, Shimizu Y, Niiya T, Murai N, Enami Y, Mitamura K, Koizumi T, Yasuda D, Izumida Y, Avital I, Umehara Y, Demetriou A, Rozga J, Kusano M. Intrasplenic transplantation of encapsulated hepatocytes decreases mortality and improves liver functions in fulminant hepatic failure from 90% partial hepatectomy in rats. Transplantation 2005;79(7):783-790.

Aoki T, Koizumi T, Kobayashi Y, Yasuda D, Izumida Y, Jin Z, Nishino N, Shimizu Y, Kato H, Murai N, Niiya T, Enami Y, Mitamura K, Yamamoto T, Kusano M. A novel method of cryopreservation of rat and human hepatocytes by using encapsulation technique and possible use for cell transplantation. Cell Transplant 2005;14(9):609-620.

Arikura J, Kobayashi N, Okitsu T, Noguchi H, Totsugawa T, Watanabe T, Matsumura T, Maruyama M, Kosaka Y, Tanaka N, Onodera K, Kasai S. UW solution: a promising tool for cryopreservation of primarily isolated rat hepatocytes. J Hepatobiliary Pancreat Surg 2002;9(6):742-749.

Baicu S, Taylor M. Acid-base buffering in organ preservation solutions as a function of temperature: new parameters for comparing buffer capacity and efficiency. Cryobiology 2002;45(1):33-48.

Bao J, Fisher J, Lillegard J, Wang W, Amiot B, Yu Y, Dietz A, Nahmias Y, Nyberg S. Serum-free medium and mesenchymal stromal cells enhance functionality and stabilize integrity of rat hepatocyte spheroids. Cell Transplant 2013;22(2):299-308.

Bao J, Shi Y, Sun H, Yin X, Yang R, Li L, Chen X, Bu H. Construction of a portal implantable functional tissue-engineered liver using perfusion-decellularized matrix and hepatocytes in rats. Cell Transplant 2011;20(5):753-766.

Basta G, Montanucci P, Luca G, Boselli C, Noya G, Barbaro B, Qi M, Kinzer K, Oberholzer J, Calafiore R. Long-term metabolic and immunological follow-up of nonimmunosuppressed patients with type 1 diabetes treated with microencapsulated islet allografts: four cases. Diabetes Care 2011;34(11):2406-2409.

Baust J, Gao D, Baust J. Cryopreservation: An emerging paradigm change. Organogenesis. 2009;5(3):90-96.

Baust J, Buskirk R, Baust J. Gene Activation of the Apoptotic Caspase Cascade Following Cryogenic Storage | Abstract. Cell Preservation Technology 2002;1(1):63-80.

Baust J, Van B, Baust J. Cell viability improves following inhibition of cryopreservation-induced apoptosis. In Vitro Cell Dev Biol Anim 2000;36(4):262-270.

Baust J, Van B, Baust J. Modulation of the cryopreservation cap: elevated survival with reduced dimethyl sulfoxide concentration. Cryobiology 2002;45(2):97-108.

Baust J, Vogel M, Van B, Baust J. A molecular basis of cryopreservation failure and its modulation to improve cell survival. Cell Transplant 2001;10(7):561-571.

Bernal W, Auzinger G, Dhawan A, Wendon J. Acute liver failure. Lancet 2010;376(9736):190-201.

Bernal W, Wendon J. Acute liver failure. N Engl J Med 2013;369(26):2525-2534.

Bernuau J, Rueff B, Benhamou JP. Fulminant and sub fulminant liver failure definitions and causes. Seminars in liver disease 1986;6(2):97-106.

Bhogal R, Hodson J, Bartlett D, Weston C, Curbishley S, Haughton E, Williams K, Reynolds G, Newsome P, Adams D, Afford S. Isolation of primary human hepatocytes from normal and diseased liver tissue: a one hundred liver experience. PLoS One 2011;6(3):10.

Bilir B, Guinette D, Karrer F, Kumpe D, Krysl J, Stephens J, McGavran L, Ostrowska A, Durham J. Hepatocyte transplantation in acute liver failure. Liver Transpl 2000;6(1):32-40.

Brissová M, Lacík I, Powers A, Anilkumar A, Wang T. Control and measurement of permeability for design of microcapsule cell delivery system. J Biomed Mater Res 1998;39(1):61-70.

Bruni S, Chang T. Encapsulated hepatocytes for controlling hyperbilirubinemia in Gunn rats. Int J Artif Organs 1991;14(4):239-241.

Cai Z, Shi Z, O'Shea G, Sun A. Microencapsulated hepatocytes for bioartificial liver support. Artif Organs 1988;12(5):388-393.

Calafiore R, Basta G, Luca G, Lemmi A, Montanucci M, Calabrese G, Racanicchi L, Mancuso F, Brunetti P. Microencapsulated pancreatic islet allografts into nonimmunosuppressed patients with type 1 diabetes: first two cases. Diabetes Care 2006;29(1):137-138.

Canaple L, Rehor A, Hunkeler D. Improving cell encapsulation through size control. J Biomater Sci Polym Ed 2002;13(7):783-796.

Cardone M, Salvesen G, Widmann C, Johnson G, Frisch S. The regulation of anoikis: MEKK-1 activation requires cleavage by caspases. Cell 1997;90(2):315-323.

Carini R, De C, Bellomo G, Albano E. Intracellular Na+ accumulation and hepatocyte injury during cold storage. Transplantation 1999;68(2):294-297.

Chan C, Berthiaume F, Nath B, Tilles A, Toner M, Yarmush M. Hepatic tissue engineering for adjunct and temporary liver support: critical technologies. Liver Transpl 2004;10(11):1331-1342.

Chang TM, Prakash S. Therapeutic uses of microencapsulated genetically engineered cells. Mol Med Today 1998;4(5):221-227.

Chang TMS. Therapeutic applications of polymeric artificial cells. Nat Rev Drug Discov 2005;4(3):221-235.

Chang T. Semipermeable Microcapsules, Science 1964;146:524-525.

Chen Z, Ding Y, Xu Q, Yu D. Bioartificial liver inoculated with porcine hepatocyte spheroids for treatment of canine acute liver failure model. Artif Organs 2003;27(7):613-622.

Chesné C, Guillouzo A. Cryopreservation of isolated rat hepatocytes: a critical evaluation of freezing and thawing conditions. Cryobiology 1988;25(4):323-330.

Chesné C, Guyomard C, Fautrel A, Poullain M, Frémond B, De J, Guillouzo A. Viability and function in primary culture of adult hepatocytes from various animal species and human beings after cryopreservation. Hepatology 1993;18(2):406-414.

Chin H, Yu H, Chye N. Strategies for the cryopreservation of microencapsulated cells. Biotechnol Bioeng 2004;85(2):202-213.

Cirone P, Bourgeois JM, Austin RC, Chang PL. A novel approach to tumor suppression with microencapsulated recombinant cells. Hum Gene Ther 2002;13(10):1157-1166.

Clayton HA, London NJ, Colloby PS, Bell PR, James RF. The effect of capsule composition on the biocompatibility of alginate-poly-l-lysine capsules. J Microencapsul 1991;8(2):221-233.

Coward S, Legallais C, David B, Thomas M, Foo Y, Mavri-Damelin D, Hodgson H, Selden C. Alginate-encapsulated HepG2 cells in a fluidized bed bioreactor maintain function in human liver failure plasma. Artif Organs 2009;33(12):1117-1126.

Dandri M, Burda M, Gocht A, Török E, Pollok J, Rogler C, Will H, Petersen J. Woodchuck hepatocytes remain permissive for hepadnavirus infection and mouse liver repopulation after cryopreservation. Hepatology 2001;34(4 Pt 1):824-833.

De Vos P, De Haan BJ, Wolters GH, Strubbe JH, Van Schilfgaarde R. Improved biocompatibility but limited graft survival after purification of alginate for microencapsulation of pancreatic islets. Diabetologia 1997;40(3):262-270.

De Vos P, De Haan B, Pater J, Van Schilfgaarde R. Association between capsule diameter, adequacy of encapsulation, and survival of microencapsulated rat islet allografts. Transplantation 1996;62(7):893-899.

De Vos P, De Haan B, Van Schilfgaarde R. Effect of the alginate composition on the biocompatibility of alginate-polylysine microcapsules. Biomaterials 1997;18(3):273-278.

De Vos P, Bucko M, Gemeiner P, Navrátil M, Svitel J, Faas M, Strand BL, Skjak-Braek G, Morch YA, Vikartovská A, Lacík I, Kolláriková G, Orive G, Poncelet D, Pedraz JL, Ansorge-Schumacher MB. Multiscale requirements for bioencapsulation in medicine and biotechnology. Biomaterials 2009;30(13):2559-2570.

De Vos P, Faas M, Strand B, Calafiore R. Alginate-based microcapsules for immunoisolation of pancreatic islets. Biomaterials 2006;27(32):5603-5617.

De Vos P, van H, de H, Busscher H. Tissue responses against immunoisolating alginate-PLL capsules in the immediate posttransplant period. J Biomed Mater Res 2002;62(3):430-437.

De Castro M, Orive G, Gascón A, Hernandez R, Pedraz J. Evaluation of human serum albumin as a substitute of foetal bovine serum for cell culture. Int J Pharm 2006;310(1-2):8-14.

De Groot M, Schuurs T, van S. Causes of limited survival of microencapsulated pancreatic islet grafts. J Surg Res 2004;121(1):141-150.

Demetriou A, Brown R, Busuttil R, Fair J, McGuire B, Rosenthal P, Am E, Lerut J, Nyberg S, Salizzoni M, Fagan E, de H, Broelsch C, Muraca M, Salmeron J, Rabkin J, Metselaar H, Pratt D, De L, McChesney L, Everson G, Lavin P, Stevens A, Pitkin Z, Solomon B. Prospective, randomized, multicenter, controlled trial of a bioartificial liver in treating acute liver failure. Ann Surg 2004;239(5):660-667.

Demetriou A, Reisner A, Sanchez J, Levenson S, Moscioni A, Chowdhury J. Transplantation of microcarrier-attached hepatocytes into 90% partially hepatectomized rats. Hepatology 1988;8(5):1006-1009.

Desille M, Mahler S, Seguin P, Mallédant Y, Frémond B, Sébille V, Bouix A, Desjardins J, Joly A, Desbois J, Lebreton Y, Campion J, Clément B. Reduced encephalopathy in pigs with ischemia-induced acute hepatic failure treated with a bioartificial liver containing alginate-entrapped hepatocytes. Crit Care Med 2002;30(3):658-663.

Dhawan A. Acute liver failure in children and adolescents. Clin Res Hepatol Gastroenterol 2012;36(3):278-283.

Dhawan A, Puppi J, Hughes R, Mitry R. Human hepatocyte transplantation: current experience and future challenges. Nat Rev Gastroenterol Hepatol 2010;7(5):288-298.

Diaz-Buxo J, Blumenthal S, Hayes D, Gores P, Gordon B. Galactosamine-induced fulminant hepatic necrosis in unanesthetized canines. Hepatology 1997;25(4):950-957.

Diener B, Utesch D, Beer N, Dürk H, Oesch F. A method for the cryopreservation of liver parenchymal cells for studies of xenobiotics. Cryobiology 1993;30(2):116-127.

Dixit V, Darvasi R, Arthur M, Brezina M, Lewin K, Gitnick G. Restoration of liver function in Gunn rats without immunosuppression using transplanted microencapsulated hepatocytes. Hepatology 1990;12(6):1342-1349.

Dixit V, Arthur M, Gitnick G. Repeated transplantation of microencapsulated hepatocytes for sustained correction of hyperbilirubinemia in Gunn rats. Cell Transplant 1992;1(4):275-279.

Dixit V, Arthur M, Gitnick G. A morphological and functional evaluation of transplanted isolated encapsulated hepatocytes following long-term transplantation in Gunn rats. Biomater Artif Cells Immobilization Biotechnol 1993;21(2):119-133.

Dixit V, Darvasi R, Arthur M, Brezina M, Lewin K, Gitnick G. Restoration of liver function in Gunn rats without immunosuppression using transplanted microencapsulated hepatocytes. Hepatology 1990;12(6):1342-1349.

Dixit V, Darvasi R, Arthur M, Lewin K, Gitnick G. Cryopreserved microencapsulated hepatocytes--transplantation studies in Gunn rats. Transplantation 1993;55(3):616-622.

Donato M, Gómez-Lechón M, Castell J. A microassay for measuring cytochrome P450IA1 and P450IIB1 activities in intact human and rat hepatocytes cultured on 96-well plates. Anal Biochem 1993;213(1):29-33.

Durkut S, Elçin A, Elçin Y. In vitro evaluation of encapsulated primary rat hepatocytes pre- and post-cryopreservation at -80°C and in liquid nitrogen. Artif Cells Nanomed Biotechnol 2013; in print.

Duvivier-Kali V, Omer A, Lopez-Avalos M, O'Neil J, Weir G. Survival of microencapsulated adult pig islets in mice in spite of an antibody response. Am J Transplant 2004;4(12):1991-2000.

Duvivier-Kali V, Omer A, Parent R, O'Neil J, Weir G. Complete protection of islets against allorejection and autoimmunity by a simple barium-alginate membrane. Diabetes 2001;50(8):1698-1705.

Emerich DF, Thanos CG, Goddard M, Skinner SJM, Geany MS, Bell WJ, Bintz B, Schneider P, Chu Y, Babu RS, Borlongan CV, Boekelheide K, Hall S, Bryant B, Kordower JH. Extensive neuroprotection by choroid plexus transplants in excitotoxin lesioned monkeys. Neurobiol Dis 2006;23(2):471-480.

Engberg A, Rosengren-Holmberg J, Chen H, Nilsson B, Lambris J, Nicholls I, Ekdahl K. Blood protein-polymer adsorption: Implications for understanding complement-mediated hemoincompatibility. J Biomed Mater Res A. 2011; doi: 10.1002/jbm.a.33030.

Espevik T, Otterlei M, Skjåk-Braek G, Ryan L, Wright SD, Sundan A. The involvement of CD14 in stimulation of cytokine production by uronic acid polymers. Eur J Immunol 1993;23(1):255-261.

Faraj W, Dar F, Bartlett A, Melendez H, Marangoni G, Mukherji D, Vergani G, Dhawan A, Heaton N, Rela M. Auxiliary liver transplantation for acute liver failure in children. Ann Surg 2010;251(2):351-356.

Fisher R, Bu D, Thompson M, Tisnado J, Prasad U, Sterling R, Posner M, Strom S. Defining hepatocellular chimerism in a liver failure patient bridged with hepatocyte infusion. Transplantation 2000;69(2):303-307.

Fisher R, Strom S. Human hepatocyte transplantation: worldwide results. Transplantation 2006;82(4):441-449.

Frisch S, Francis H. Disruption of epithelial cell-matrix interactions induces apoptosis. J Cell Biol 1994;124(4):619-626.

Fujita R, Hui T, Chelly M, Demetriou A. The effect of antioxidants and a caspase inhibitor on cryopreserved rat hepatocytes. Cell Transplant.2005;14(6):391-396.

Fuller B. Cryoprotectants: the essential antifreezes to protect life in the frozen state. Cryo Letters 2004;25(6):375-388.

Fuller B, Morris G, Nutt L. Functional recovery of isolated rat hepatocytes upon thawing from-196C. Cryo Lett 1980;:139-146.

Gattás-Asfura K, Stabler C. Chemoselective cross-linking and functionalization of alginate via Staudinger ligation. Biomacromolecules 2009;10(11):3122-3129.

Glicklis R, Shapiro L, Agbaria R, Merchuk J, Cohen S. Hepatocyte behavior within three-dimensional porous alginate scaffolds. Biotechnol Bioeng 2000;67(3):344-353.

Haan B, Rossi A, Faas M, Smelt M, Sonvico F, Colombo P, Vos P. Structural surface changes and inflammatory responses against alginate-based microcapsules after exposure to human peritoneal fluid. J Biomed Mater Res A 2011;98(3):394-403.

Habibullah CM, Syed IH, Qamar A, Taher-Uz Z. Human fetal hepatocyte transplantation in patients with fulminant hepatic failure. Transplantation 1994;58(8):951-952.

Hang H, Shi X, Gu G, Wu Y, Gu J, Ding Y. In vitro analysis of cryopreserved alginate-poly-L-lysine-alginate-microencapsulated human hepatocytes. Liver Int 2010;30(4):611-622.

Haque T, Chen H, Ouyang W, Martoni C, Lawuyi B, Urbanska A, Prakash S. In vitro study of alginate-chitosan microcapsules: an alternative to liver cell transplants for the treatment of liver failure. Biotechnol Lett 2005;27(5):317-322.

Heng B, Yu Y, Ng S. Slow-cooling protocols for microcapsule cryopreservation. J Microencapsul 2004;21(4):455-467.

Hengstler J, Utesch D, Steinberg P, Platt K, Diener B, Ringel M, Swales N, Fischer T, Biefang K, Gerl M, Böttger T, Oesch F. Cryopreserved primary hepatocytes as a constantly available in vitro model for the evaluation of human and animal drug metabolism and enzyme induction. Drug Metab Rev 2000;32(1):81-118.

Hernandez R, Orive G, Murua A, Pedraz J. Microcapsules and microcarriers for in situ cell delivery, Adv Drug Deliv Rev 2010;62:711-730.

Herrera M, Fonsato V, Bruno S, Grange C, Gilbo N, Romagnoli R, Tetta C, Camussi G. Human liver stem cells improve liver injury in a model of fulminant liver failure. Hepatology 2013;57(1):311-319.

Hikichi T, Wakayama S, Mizutani E, Takashima Y, Kishigami S, Van T, Ohta H, Bui H, Nishikawa S, Wakayama T. Differentiation potential of parthenogenetic embryonic stem cells is improved by nuclear transfer. Stem Cells 2007;25(1):46-53.

Hoofnagle J, Carithers R, Shapiro C, Ascher N. Fulminant hepatic failure: summary of a workshop. Hepatology 1995;21(1):240-252.

Hortelano G, Al-Hendy A, Ofosu FA, Chang PL. Delivery of human factor IX in mice by encapsulated recombinant myoblasts: a novel approach towards allogeneic gene therapy of hemophilia B. Blood 1996;87(12):5095-5103.

Hughes R, Mitry R, Dhawan A. Current status of hepatocyte transplantation. Transplantation 2012;93(4):342-347.

Janssen H, Janssen P, Broelsch C. Celsior solution compared with University of Wisconsin solution (UW) and histidine-tryptophan-ketoglutarate solution (HTK) in the protection of human hepatocytes against ischemia-reperfusion injury. Transpl Int 2003;16(7):515-522.

Jauregui H, Mullon C, Trenkler D, Naik S, Santangini H, Press P, Muller T, Solomon B. In vivo evaluation of a hollow fiber liver assist device. Hepatology 1995;21(2):460-469.

Joly A, Desjardins J, Fremond B, Desille M, Campion J, Malledant Y, Lebreton Y, Semana G, Edwards-Levy F, Levy M, Clement B. Survival, proliferation, and functions of porcine hepatocytes encapsulated in coated alginate beads: a step toward a reliable bioartificial liver. Transplantation 1997;63(6):795-803.

Kalpana K, Ong H, Soo K, Tan S, Prema R. An improved model of galactosamine-induced fulminant hepatic failure in the pig. J Surg Res 1999;82(2):121-130.

Karlsson J, Toner M. Long-term storage of tissues by cryopreservation: critical issues. Biomaterials 1996;17(3):243-256.

Katenz E, Vondran F, Schwartlander R, Pless G, Gong X, Cheng X, Neuhaus P, Sauer I. Cryopreservation of primary human hepatocytes: the benefit of trehalose as an additional cryoprotective agent. Liver Transpl 2007;13(1):38-45.

Keppler D, Lesch R, Reutter W, Decker K. Experimental hepatitis induced by D-galactosamine. Exp Mol Pathol 1968;9(2):279-290.

Kerkweg U, Li T, de G, Rauen U. Cold-induced apoptosis of rat liver cells in University of Wisconsin solution: the central role of chelatable iron. Hepatology 2002;35(3):560-567.

Khalil M, Shariat-Panahi A, Tootle R, Ryder T, McCloskey P, Roberts E, Hodgson H, Selden C. Human hepatocyte cell lines proliferating as cohesive spheroid colonies in alginate markedly upregulate both synthetic and detoxificatory liver function. J Hepatol 2001;34(1):68-77.

Khan A, Habeeb A, Parveen N, Naseem B, Babu R, Capoor A, Habibullah C. Peritoneal transplantation of human fetal hepatocytes for the treatment of acute fatty liver of pregnancy: a case report. Trop Gastroenterol 2004;25(3):141-143.

Khuroo M, Khuroo M, Farahat K. Molecular adsorbent recirculating system for acute and acute-on-chronic liver failure: a meta-analysis. Liver Transpl 2004;10(9):1099-1106.

Kim A, Hwang J, Kim H, Kim H, Song J, Yang Y, Yoon K, Lee D, Khang G. Reduction of inflammatory reaction in the use of purified alginate microcapsules. J Biomater Sci Polym Ed 2013;24(9):1084-1098.

Kinasiewicz A, Gautier A, Lewiska D, Smietanka A, Legallais C, Weryński A. Three-dimensional growth of human hepatoma C3A cells within alginate beads for fluidized bioartificial liver. Int J Artif Organs 2008;31(4):340-347.

Kobayashi T, Aomatsu Y, Iwata H, Kin T, Kanehiro H, Hisanaga M, Ko S, Nagao M, Nakajima Y. Indefinite islet protection from autoimmune destruction in nonobese diabetic mice by agarose microencapsulation without immunosuppression. Transplantation 2003;75(5):619-625.

Koebe H, Mühling B, Deglmann C, Schildberg F. Cryopreserved porcine hepatocyte cultures. Chem Biol Interact 1999;121(1):99-115.

Kunieda T, Maruyama M, Okitsu T, Shibata N, Takesue M, Totsugawa T, Kosaka Y, Arata T, Kobayashi K, Ikeda H, Oshita M, Nakaji S, Ohmoto K, Yamamoto S, Kurabayashi Y, Kodama M, Tanaka N, Kobayashi N. Cryopreservation of primarily isolated porcine hepatocytes with UW solution. Cell Transplant 2003;12(6):607-616.

Kusano T, Aoki T, Yasuda D, Matsumoto S, Jin Z, Nishino N, Hayashi K, Odaira M, Yamada K, Koizumi T, Izumida Y, Mitamura K, Enami Y, Niiya T, Murai N, Kato H, Shimizu Y, Kou K, Furukawa Y, Matsusita M, Todo S, Shioda S, Kusano M. Microencapsule technique protects hepatocytes from cryoinjury. Hepatol Res 2008;38(6):593-600.

Lanza RP, Kühtreiber WM, Ecker D, Staruk JE, Chick WL. Xenotransplantation of porcine and bovine islets without immunosuppression using uncoated alginate microspheres. Transplantation 1995;59(10):1377-1384.

Lanza R, Ecker D, Kühtreiber W, Marsh J, Chick W. A simple and inexpensive method for transplanting xenogeneic cells and tissues into rats using alginate gel spheres. Transplant Proc 1995;27(6):3322.

Lanza R, Hayes J, Chick W. Encapsulated cell technology. Nat Biotechnol 1996;14(9):1107-1111.

Lawson A, Ahmad H, Sambanis A. Cytotoxicity effects of cryoprotectants as single-component and cocktail vitrification solutions. Cryobiology 2011;62(2):115-122.

Lazar A, Peshwa M, Wu F, Chi C, Cerra F, Hu W. Formation of porcine hepatocyte spheroids for use in a bioartificial liver. Cell Transplant 1995;4(3):259-268.

Leal-Egaña A, Díaz-Cuenca A, Bader A. Determination of the decay rate constant for hepatocytes immobilized in alginate microcapsules. J Microencapsul 2010;27(1):86-93.

Lee K, Park J, Yoon J, Lee J, Kim S, Jung H, Lee S, Kim S, Lee H, Lee D, Joh J. The viability and function of cryopreserved hepatocyte spheroids with different cryopreservation solutions. Transplant Proc 2004;36(8):2462-2463.

Lee W, Squires R, Nyberg S, Doo E, Hoofnagle J. Acute liver failure: Summary of a workshop. Hepatology 2008;47(4):1401-1415.

Lewińska D, Rosiński S, Weryński A. Influence of process conditions during impulsed electrostatic droplet formation on size distribution of hydrogel beads. Artif Cells Blood Substit Immobil Biotechnol 2004;32(1):41-53.

Li HB, Jiang H, Wang CY, Duan CM, Ye Y, Su XP, Kong QX, Wu JF, Guo XM. Comparison of two types of alginate microcapsules on stability and biocompatibility in vitro and in vivo. Biomedical materials (Bristol, England) 2006;1(1):42-47.

Lim F, Sun AM. Microencapsulated islets as bioartificial endocrine pancreas. Science 1980;210(4472):908-910.

Liu H, Yu Y, Glorioso J, Mao S, Rodysil B, Amiot B, Rinaldo P, Nyberg S. Cold Storage of Rat Hepatocyte Spheroids. Cell Transplant 2013;:10.

Liu J, Gluud L, Als-Nielsen B, Gluud C. Artificial and bioartificial support systems for liver failure. Cochrane Database Syst Rev 2004; (1):CD003628.

Liu Z, Chang T. Effects of bone marrow cells on hepatocytes: when co-cultured or co-encapsulated together. Artif Cells Blood Substit Immobil Biotechnol 2000;28(4):365-374.

Liu Z, Chang T. Increased viability of transplanted hepatocytes when hepatocytes are co-encapsulated with bone marrow stem cells using a novel method. Artif Cells Blood Substit Immobil Biotechnol 2002;30(2):99-112.

Lohr M, Hoffmeyer A, Kroger J, Freund M, Hain J, Holle A, Karle P, Knofel W, Liebe S, Muller P, Nizze H, Renner M, Saller R, Wagner T, Hauenstein K, Gunzburg W, Salmons B.

Microencapsulated cell-mediated treatment of inoperable pancreatic carcinoma, Lancet 2001;357:1591-1592.

Longhi M, Ma Y, Mitry R, Bogdanos D, Heneghan M, Cheeseman P, Mieli-Vergani G, Vergani D. Effect of CD4+ CD25+ regulatory T-cells on CD8 T-cell function in patients with autoimmune hepatitis. J Autoimmun 2005;25(1):63-71.

Loretz L, Li A, Flye M, Wilson A. Optimization of cryopreservation procedures for rat and human hepatocytes. Xenobiotica 1989;19(5):489-498.

Loven A, Olsen A, Friis C, Andersen B. Phase I and II metabolism and carbohydrate metabolism in cultured cryopreserved porcine hepatocytes. Chem Biol Interact 2005;155(1-2):21-30.

Lowry O, Rosenbrough N, Farr A, Randall R. Protein measurement with the Folin phenol reagent. J Biol Chem 1951;193(1):265-275.

Lv G, Zhao L, Zhang A, Du W, Chen Y, Yu C, Pan X, Zhang Y, Song T, Xu J, Li L. Bioartificial liver system based on choanoid fluidized bed bioreactor improve the survival time of fulminant hepatic failure pigs. Biotechnol Bioeng 2011;108(9):2229-2236.

Mahler S, Desille M, Frémond B, Chesné C, Guillouzo A, Campion J, Clément B. Hypothermic storage and cryopreservation of hepatocytes: the protective effect of alginate gel against cell damages. Cell Transplant. 2003;12(6):579-592.

Mai G, Nguyen T, Morel P, Mei J, Andres A, Bosco D, Baertschiger R, Toso C, Berney T, Majno P, Mentha G, Trono D, Buhler L. Treatment of fulminant liver failure by transplantation of microencapsulated primary or immortalized xenogeneic hepatocytes. Xenotransplantation 2005;12(6):457-464.

Malpique R, Osório L, Ferreira D, Ehrhart F, Brito C, Zimmermann H, Alves P. Alginate encapsulation as a novel strategy for the cryopreservation of neurospheres. Tissue Eng Part C Methods 2010;16(5):965-977.

Manwaring V, Heywood W, Clayton R, Lachmann R, Keutzer J, Hindmarsh P, Winchester B, Heales S, Mills K. The identification of new biomarkers for identifying and monitoring kidney disease and their translation into a rapid mass spectrometry-based test: evidence of presymptomatic kidney disease in pediatric Fabry and type-I diabetic patients. J Proteome Res 2013;12(5):2013-2021.

Massie I, Selden C, Hodgson H, Fuller B. Cryopreservation of encapsulated liver spheroids for a bioartificial liver: reducing latent cryoinjury using an ice nucleating agent. Tissue Eng Part C Methods 2011;17(7):765-774.

Massie I, Selden C, Morris J, Hodgson H, Fuller B. Cryopreservation of encapsulated liver spheroids using a cryogen-free cooler: high functional recovery using a multi-step cooling profile. Cryo Letters 2011;32(2):158-165.

Mazur P. Cryobiology: the freezing of biological systems. Science 1970;168(3934):939-949.

Mazur P. Freezing of living cells: mechanisms and implications. Am J Physiol 1984;247(31):C125-C142.

Mei J, Sgroi A, Mai G, Baertschiger R, Gonelle-Gispert C, Serre-Beinier V, Morel P, Bühler L. Improved survival of fulminant liver failure by transplantation of microencapsulated cryopreserved porcine hepatocytes in mice. Cell Transplant 2009;18(1):101-110.

Meyburg J, Schmidt J, Hoffmann G. Liver cell transplantation in children. Clin Transplant 2009;21:75-82.

Millis J, Cronin D, Johnson R, Conjeevaram H, Conlin C, Trevino S, Maguire P. Initial experience with the modified extracorporeal liver-assist device for patients with fulminant hepatic failure: system modifications and clinical impact. Transplantation 2002;74(12):1735-1746.

Mitry R. Isolation of human hepatocytes. Methods Mol Biol 2009;481:17-23.

Mitry R, Bansal S, Hughes R, Mieli-Vergani G, Dhawan A. In vitro effects of sera from children with acute liver failure on metabolic and synthetic activity of cryopreserved human hepatocytes. J Pediatr Gastroenterol Nutr 2009;48(5):604-607.

Mitry R, Sarraf C, Havlík R, Habib N. Detection of adenovirus and initiation of apoptosis in hepatocellular carcinoma cells after Ad-p53 treatment. Hepatology.2000;31(4):885-889.

Mitry R, Sarraf C, Wu C, Pignatelli M, Habib N. Wild-type p53 induces apoptosis in Hep3B through up-regulation of bax expression. Lab Invest 1997;77(4):369-378.

Mitry R, Lehec S, Hughes R. Cryopreservation of human hepatocytes for clinical use. Methods Mol Biol 2010;640:107-113.

Mochida S, Nakayama N, Matsui A, Nagoshi S, Fujiwara K. Re-evaluation of the Guideline published by the Acute Liver Failure Study Group of Japan in 1996 to determine the indications of liver transplantation in patients with fulminant hepatitis. Hepatol Res. 2008;38(10):970-979.

Mørch Y, Donati I, Strand B, Skjåk-Braek G. Effect of Ca2+, Ba2+, and Sr2+ on alginate microbeads. Biomacromolecules 2006;7(5):1471-1480.

Mørch Y, Donati I, Strand B, Skjåk-Braek G. Molecular engineering as an approach to design new functional properties of alginate. Biomacromolecules 2007;8(9):2809-2814.

Murua A, Orive G, Hernández R, Pedraz J. Cryopreservation based on freezing protocols for the long-term storage of microencapsulated myoblasts. Biomaterials 2009;30(20):3495-3501.

Murua A, Portero A, Orive G, Hernández RM, de Castro M, Pedraz JL. Cell microencapsulation technology: towards clinical application. J Control Release 2008;132(2):76-83.

Nagaki M, Naito T, Ohnishi H, Akaike T, Muto Y, Moriwaki H. Effects of plasma from patients with fulminant hepatic failure on function of primary rat hepatocytes in three-dimensional culture. Liver Int. 2005;25(5):1010-1017.

Naito H, Yoshimura M, Mizuno T, Takasawa S, Tojo T, Taniguchi S. The advantages of three-dimensional culture in a collagen hydrogel for stem cell differentiation. J Biomed Mater Res A 2013;101(10):2838-2845.

Najimi M, Khuu D, Lysy P, Jazouli N, Abarca J, Sempoux C, Sokal E. Adult-derived human liver mesenchymal-like cells as a potential progenitor reservoir of hepatocytes? Cell Transplant 2007;16(7):717-728.

Neufeld D. Isolation of rat liver hepatocytes. Methods Mol Biol 1997;75:145-151.

Newsome P, Plevris J, Nelson L, Hayes P. Animal models of fulminant hepatic failure: a critical evaluation. Liver Transpl 2000;6(1):21-31.

Niu X, Arthur P, Jeffrey G. Iron and oxidative stress in cold-initiated necrotic death of rat hepatocyte. Transplant Proc 2010;42(5):1563-1568.

Nyberg S, Hardin J, Matos L, Rivera D, Misra S, Gores G. Cytoprotective influence of ZVAD-fmk and glycine on gel-entrapped rat hepatocytes in a bioartificial liver. Surgery 2000;127(4):447-455.

Nyberg S, Shirabe K, Peshwa M, Sielaff T, Crotty P, Mann H, Remmel R, Payne W, Hu W, Cerra F. Extracorporeal application of a gel-entrapment, bioartificial liver: demonstration of drug metabolism and other biochemical functions. Cell Transplant 1993;2(6):441-452.

O'Grady J. Acute liver failure. Postgrad Med J 2005;81(953):148-154.

O'Grady J, Schalm S, Williams R. Acute liver failure: redefining the syndromes. Lancet 1993;342(8866):273-275.

Oppert M, Rademacher S, Petrasch K, Jörres A. Extracorporeal liver support therapy with Prometheus in patients with liver failure in the intensive care unit. Ther Apher Dial 2009;13(5):426-430.

Orive G, Ponce S, Hernández RM, Gascón AR, Igartua M, Pedraz JL. Biocompatibility of microcapsules for cell immobilization elaborated with different type of alginates. Biomaterials 2002;23(18):3825-3831.

Orive G, Hernández RM, Gascón AR, Calafiore R, Chang TMS, De Vos P, Hortelano G, Hunkeler D, Lacík I, Shapiro AMJ, Pedraz JL. Cell encapsulation: promise and progress. Nat Med 2003;9(1):104-107.

Orive G, Hernández RM, Rodríguez Gascón A, Calafiore R, Chang TMS, de Vos P, Hortelano G, Hunkeler D, Lacík I, Pedraz JL. History, challenges and perspectives of cell microencapsulation. Trends Biotechnol 2004;22(2):87-92.

Orive G, Tam SK, Pedraz JL, Hallé JP. Biocompatibility of alginate-poly-L-lysine microcapsules for cell therapy. Biomaterials 2006;27(20):3691-3700.

Ostrowska A, Bode D, Pruss J, Bilir B, Smith G, Zeisloft S. Investigation of functional and morphological integrity of freshly isolated and cryopreserved human hepatocytes. Cell Tissue Bank 2000;1(1):55-68.

Otterlei M, Ostgaard K, Skjåk-Braek G, Smidsrød O, Soon-Shiong P, Espevik T. Induction of cytokine production from human monocytes stimulated with alginate. J Immunother 1991;10(4):286-291.

Parry S, Sebbag M, Feldmann M, Brennan F. Contact with T cells modulates monocyte IL-10 production: role of T cell membrane TNF-alpha. J Immunol 1997;158(8):3673-3681.

Pegg D. The history and principles of cryopreservation. Semin Reprod Med 2002;20(1):5-13.

Prakash S, Chang TM. Microencapsulated genetically engineered live E. coli DH5 cells administered orally to maintain normal plasma urea level in uremic rats. Nat Med 1996;2(8):883-887.

Pravdyuk A, Petrenko Y, Fuller B, Petrenko A. Cryopreservation of alginate encapsulated mesenchymal stromal cells. Cryobiology 2013;66(3):215-222.

Prüsse U, Bilancetti L, Bučko M, Bugarski B, Bukowski J, Gemeiner P, Lewińska D, Manojlovic V, Massart B, Nastruzzi C, Nedovic V, Poncelet D, Siebenhaar S, Tobler L, Tosi A, Vikartovská A, Vorlop KD. Comparison of different technologies for alginate beads production. Chemical Papers 2008;62(4):364-374.

Puppi J, Modo M, Dhawan A, Lehec S, Mitry R, Hughes R. Ex vivo magnetic resonance imaging of transplanted hepatocytes in a rat model of acute liver failure. Cell Transplant 2014;23(3):329-343.

Qi M, Mørch Y, Lacík I, Formo K, Marchese E, Wang Y, Danielson K, Kinzer K, Wang S, Barbaro B, Kolláriková G, Chorvát D, Hunkeler D, Skjåk-Braek G, Oberholzer J, Strand B. Survival of human islets in microbeads containing high guluronic acid alginate crosslinked with Ca2+ and Ba2+. Xenotransplantation 2012;19(6):355-364.

Qiu L, Wang J, Wen X, Wang H, Wang Y, Lin Q, Du Z, Duan C, Wang C. Transplantation of co-microencapsulated hepatocytes and HUVECs for treatment of fulminant hepatic failure. Int J Artif Organs 2012;35(6):458-465.

Quong D, Neufeld R, Skjåk-Braek G, Poncelet D. External versus internal source of calcium during the gelation of alginate beads for DNA encapsulation. Biotechnol Bioeng 1998;57(4):438-446.

Rahman T, Selden C, Khalil M, Diakanov I, Hodgson H. Alginate-encapsulated human hepatoblastoma cells in an extracorporeal perfusion system improves some systemic parameters of liver failure in a xenogeneic model. Artif Organs 2004;28(5):476-482.

Rauen U, de G. Inherent toxicity of organ preservation solutions to cultured hepatocytes. Cryobiology 2008;56(1):88-92.

Ringel M, von M, Santos R, Feilen P, Brulport M, Hermes M, Bauer A, Schormann W, Tanner B, Schön M, Oesch F, Hengstler J. Hepatocytes cultured in alginate microspheres: an optimized technique to study enzyme induction. Toxicology 2005;206(1):153-167.

Rivas-Vetencourt P, Aranda E, Sorio L, Quero Z, Martinez A, Vegas A, Zerpa M. Xenotransplantation of isolated encapsulated porcine hepatocytes in the treatment of a highly fulminant hepatic failure model. Transplant Proc 1997;29(1-2):920-922.

Robitaille R, Dusseault J, Henley N, Desbiens K, Labrecque N, Hallé J. Inflammatory response to peritoneal implantation of alginate-poly-L-lysine microcapsules. Biomaterials 2005;26(19):4119-4127.

Rokstad A, Brekke O, Steinkjer B, Ryan L, Kolláriková G, Strand B, Skjåk-Bræk G, Lacík I, Espevik T, Mollnes T. Alginate microbeads are complement compatible, in contrast to polycation containing microcapsules, as revealed in a human whole blood model. Acta Biomater 2011;7(6):2566-2578.

Rokstad A, Lacík I, de V, Strand B. Advances in biocompatibility and physico-chemical characterization of microspheres for cell encapsulation. Adv Drug Deliv Rev 2014;68:111-130.

Rozga J, Williams F, Ro M, Neuzil D, Giorgio T, Backfisch G, Moscioni A, Hakim R, Demetriou A. Development of a bioartificial liver: properties and function of a hollow-fiber module inoculated with liver cells. Hepatology 1993;17(2):258-265.

Ryan C, Anilkumar T, Ben-Hamida A, Khorsandi S, Aslam M, Pusey C, Gaylor J, Courtney J. Multisorbent plasma perfusion in fulminant hepatic failure: effects of duration and frequency of treatment in rats with grade III hepatic coma. Artif Organs 2001;25(2):109-118.

Sakai S, Kawakami K. Both ionically and enzymatically crosslinkable alginate-tyramine conjugate as materials for cell encapsulation. J Biomed Mater Res A 2008;85(2):345-351.

Sana G, Lombard C, Vosters O, Jazouli N, Andre F, Stephenne X, Smets F, Najimi M, Sokal E. Adult human hepatocytes promote CD4+ T cell hyporesponsiveness via interleukin-10 producing allogeneic dendritic cells. Cell Transplant 2013; in print.

Santos E, Pedraz J, Hernández R, Orive G. Therapeutic cell encapsulation: ten steps towards clinical translation. J Control Release 2013;170(1):1-14.

Sarkis R, Benoist S, Honiger J, Baudrimont M, Delelo R, Balladur P, Capeau J, Nordlinger B. Transplanted cryopreserved encapsulated porcine hepatocytes are as effective as fresh hepatocytes in preventing death from acute liver failure in rats. Transplantation 2000;70(1):58-64.

Schacterle G, Pollack R. A simplified method for the quantitative assay of small amounts of protein in biologic material. Anal Biochem 1973;51(2):654-655.

Schaefer B, Schmitt C. The role of molecular adsorbent recirculating system dialysis for extracorporeal liver support in children. Pediatr Nephrol 2013;28(9):1763-1769.

Schmidt J, Rowley J, Kong H. Hydrogels used for cell-based drug delivery. J Biomed Mater Res A 2008;87(4):1113-1122.

Schneider A, Attaran M, Meier P, Strassburg C, Manns M, Ott M, Barthold M, Arseniev L, Becker T, Panning B. Hepatocyte transplantation in an acute liver failure due to mushroom poisoning. Transplantation 2006;82(8):1115-1116.

Schneider S, Feilen P, Cramer H, Hillgärtner M, Brunnenmeier F, Zimmermann H, Weber M, Zimmermann U. Beneficial effects of human serum albumin on stability and functionality of alginate microcapsules fabricated in different ways. J Microencapsul 2003;20(5):627-636.

Schneider S, Feilen P, Brunnenmeier F, Minnemann T, Zimmermann H, Zimmermann U, Weber M. Long-term graft function of adult rat and human islets encapsulated in novel alginate-based microcapsules after transplantation in immunocompetent diabetic mice. Diabetes 2005;54(3):687-693.

Schwinger C, Koch S, Jahnz U, Wittlich P, Rainov N, Kressler J. High throughput encapsulation of murine fibroblasts in alginate using the JetCutter technology. J Microencapsul 2002;19(3):273-280.

Selden C, Shariat A, McCloskey P, Ryder T, Roberts E, Hodgson H. Three-dimensional in vitro cell culture leads to a marked upregulation of cell function in human hepatocyte cell lines--an important tool for the development of a bioartificial liver machine. Ann N Y Acad Sci 1999;875:353-363.

Selden C, Spearman C, Kahn D, Miller M, Figaji A, Erro E, Bundy J, Massie I, Chalmers S, Arendse H, Gautier A, Sharratt P, Fuller B, Hodgson H. Evaluation of encapsulated liver cell spheroids in a fluidised-bed bioartificial liver for treatment of ischaemic acute liver failure in pigs in a translational setting. PLoS One 2013;8(12):10.

Senuma Y, Lowe C, Zweifel Y, Hilborn J, Marison I. Alginate hydrogel microspheres and microcapsules prepared by spinning disk atomization. Biotechnol Bioeng 2000;67(5):616-622.

Serp D, Cantana E, Heinzen C, Von S, Marison I. Characterization of an encapsulation device for the production of monodisperse alginate beads for cell immobilization. Biotechnol Bioen 2000;70(1):41-53.

Serra M, Correia C, Malpique R, Brito C, Jensen J, Bjorquist P, Carrondo M, Alves P. Microencapsulation technology: a powerful tool for integrating expansion and cryopreservation of human embryonic stem cells. PLoS One 2011;6(8):10.

Sgroi A, Mai G, Morel P, Baertschiger R, Gonelle-Gispert C, Serre-Beinier V, Buhler L. Transplantation of encapsulated hepatocytes during acute liver failure improves survival without stimulating native liver regeneration. Cell Transplant 2011;20(11-12):1791-1803.

Shi X, Zhang Y, Gu J, Ding Y. Coencapsulation of hepatocytes with bone marrow mesenchymal stem cells improves hepatocyte-specific functions. Transplantation 2009;88(10):1178-1185.

Silva J, Day S, Nicoll-Griffith D. Induction of cytochrome-P450 in cryopreserved rat and human hepatocytes. Chem Biol Interact 1999;121(1):49-63.

Soltys K, Soto-Gutiérrez A, Nagaya M, Baskin K, Deutsch M, Ito R, Shneider B, Squires R, Vockley J, Guha C, Roy-Chowdhury J, Strom S, Platt J, Fox I. Barriers to the successful treatment of liver disease by hepatocyte transplantation. J Hepatol 2010;53(4):769-774.

Sommer B, Sutherland D, Matas A, Simmons R, Najarian J. Hepatocellular transplantation for treatment of D-galactosamine-induced acute liver failure in rats. Transplant Proc 1979;11(1):578-584.

Soon-Shiong P, Heintz RE, Merideth N, Yao QX, Yao Z, Zheng T, Murphy M, Moloney MK, Schmehl M, Harris M. Insulin independence in a type 1 diabetic patient after encapsulated islet transplantation. Lancet 1994;343(8903):950-951.

Soriano H, Wood R, Kang D, Ozaki C, Finegold M, Bishoff F. Hepatocellular transplantation in children with fulminant liver failure. Hepatology 239A 1997;26

Sosef M, Baust J, Sugimachi K, Fowler A, Tompkins R, Toner M. Cryopreservation of isolated primary rat hepatocytes: enhanced survival and long-term hepatospecific function. Ann Surg 2005;241(1):125-133.

Southard J, Belzer F. Organ preservation. Annu Rev Med 1995;46:235-247.

Southard J, van G, Ametani M, Vreugdenhil P, Lindell S, Pienaar B, Belzer F. Important components of the UW solution. Transplantation 1990;49(2):251-257.

Squires RH, Shneider BL, Bucuvalas J, Alonso E, Sokol RJ, Narkewicz MR, Dhawan A, Rosenthal P, Rodriguez-Baez N, Murray KF, Horslen S, Martin MG, Lopez MJ, Soriano H, McGuire BM, Jonas MM, Yazigi N, Shepherd RW, Schwarz K, Lobritto S, Thomas DW, Lavine JE, Karpen S, Ng V, Kelly D, Simonds N, Hynan LS. Acute liver failure in children: The first 348 patients in the pediatric acute liver failure study group. J Pediatr 2006;148(5):652-658.e2.

Stabler C, Wilks K, Sambanis A, Constantinidis I. The effects of alginate composition on encapsulated betaTC3 cells. Biomaterials 2001;22(11):1301-1310.

Steinberg P, Fischer T, Kiulies S, Biefang K, Platt K, Oesch F, Böttger T, Bulitta C, Kempf P, Hengstler J. Drug metabolizing capacity of cryopreserved human, rat, and mouse liver parenchymal cells in suspension. Drug Metab Dispos 1999;27(12):1415-1422.

Stéphenne X, Najimi M, Sokal E. Hepatocyte cryopreservation: is it time to change the strategy? World J Gastroenterol 2010;16(1):1-14.

Stéphenne X, Najimi M, Ngoc D, Smets F, Hue L, Guigas B, Sokal E. Cryopreservation of human hepatocytes alters the mitochondrial respiratory chain complex 1. Cell Transplant 2007;16(4):409-419.

Straatsburg I, Abrahamse S, Song S, Hartman R, Van G. Evaluation of rat liver apoptotic and necrotic cell death after cold storage using UW, HTK, and Celsior. Transplantation 2002;74(4):458-464.

Strom S, Chowdhury J, Fox I. Hepatocyte transplantation for the treatment of human disease. Semin Liver Dis 1999;19(1):39-48.

Struecker B, Raschzok N, Sauer I. Liver support strategies: cutting-edge technologies. Nat Rev Gastroenterol Hepatol 2013;10.

Stutchfield B, Simpson K, Wigmore S. Systematic review and meta-analysis of survival following extracorporeal liver support. Br J Surg 2011;98(5):623-631.

Stylianou J, Vowels M, Hadfield K. Novel cryoprotectant significantly improves the post-thaw recovery and quality of HSC from CB. Cytotherapy 2006;8(1):57-61.

Sun A, Cai Z, Shi Z, Ma F, O'Shea G. Microencapsulated hepatocytes: an in vitro and in vivo study. Biomater Artif Cells Artif Organs 1987;15(2):483-496.

Sutherland D, Numata M, Matas A, Simmons R, Najarian J. Hepatocellular transplantation in acute liver failure. Surgery 1977;82(1):124-132.

Swales N, Luong C, Caldwell J. Cryopreservation of rat and mouse hepatocytes. I. Comparative viability studies. Drug Metab Dispos 1996;24(11):1218-1223.

Tam SK, Bilodeau S, Dusseault J, Langlois G, Hallé JP, Yahia LH. Biocompatibility and physicochemical characteristics of alginate-polycation microcapsules. Acta Biomater 2011;7(4):1683-1692.

Tam SK, de H, Faas M, Hallé J, Yahia L, de V. Adsorption of human immunoglobulin to implantable alginate-poly-L-lysine microcapsules: effect of microcapsule composition. J Biomed Mater Res A 2009;89(3):609-615.

Tam SK, Dusseault J, Bilodeau S, Langlois G, Hallé J, Yahia L. Factors influencing alginate gel biocompatibility. J Biomed Mater Res A 2011;98(1):40-52.

Tamai Y, Hasegawa A, Takamori A, Sasada A, Tanosaki R, Choi I, Utsunomiya A, Maeda Y, Yamano Y, Eto T, Koh K, Nakamae H, Suehiro Y, Kato K, Takemoto S, Okamura J, Uike N, Kannagi M. Potential contribution of a novel Tax epitope-specific CD4+ T cells to graft-versus-Tax effect in adult T cell leukemia patients after allogeneic hematopoietic stem cell transplantation. J Immunol 2013;190(8):4382-4392.

Tang L, Eaton J. Fibrin(ogen) mediates acute inflammatory responses to biomaterials. J Exp Med 1993;178(6):2147-2156.

Teng Y, Wang Y, Li S, Wang W, Gu R, Guo X, Nan X, Ma X, Pei X. Treatment of acute hepatic failure in mice by transplantation of mixed microencapsulation of rat hepatocytes and transgenic human fetal liver stromal cells. Tissue Eng Part C Methods 2010;16(5):1125-1134.

Terblanche J, Hickman R. Animal models of fulminant hepatic failure. Dig Dis Sci 1991;36(6):770-774.

Terry C, Dhawan A, Mitry R, Lehec S, Hughes R. Optimization of the cryopreservation and thawing protocol for human hepatocytes for use in cell transplantation. Liver Transpl 2010;16(2):229-237.

Terry C, Dhawan A, Mitry R, Hughes R. Cryopreservation of isolated human hepatocytes for transplantation: State of the art. Cryobiology 2006;53(2):149-159.

Terry C, Dhawan A, Mitry R, Lehec S, Hughes R. Preincubation of rat and human hepatocytes with cytoprotectants prior to cryopreservation can improve viability and function upon thawing. Liver Transpl 2005;11(12):1533-1540.

Terry C, Mitry R, Lehec S, Muiesan P, Rela M, Heaton N, Hughes R, Dhawan A. The effects of cryopreservation on human hepatocytes obtained from different sources of liver tissue. Cell Transplant 2005;14(8):585-594.

Thanos CG, Calafiore R, Basta G, Bintz BE, Bell WJ, Hudak J, Vasconcellos A, Schneider P, Skinner SJM, Geaney M, Tan P, Elliot RB, Tatnell M, Escobar L, Qian H, Mathiowitz E, Emerich DF. Formulating the alginate-polyornithine biocapsule for prolonged stability: evaluation of composition and manufacturing technique. J Biomed Mater Res A 2007;83(1):216-224.

Thanos C, Bintz B, Emerich D. Stability of alginate-polyornithine microcapsules is profoundly dependent on the site of transplantation. J Biomed Mater Res A 2007;81(1):1-11.

Thu B, Gåserød O, Paus D, Mikkelsen A, Skjåk-Braek G, Toffanin R, Vittur F, Rizzo R. Inhomogeneous alginate gel spheres: an assessment of the polymer gradients by synchrotron radiation-induced X-ray emission, magnetic resonance microimaging, and mathematical modeling. Biopolymers 2000;53(1):60-71.

Tuñón M, Alvarez M, Culebras J, González-Gallego J. An overview of animal models for investigating the pathogenesis and therapeutic strategies in acute hepatic failure. World J Gastroenterol 2009;15(25):3086-3098.

Uludag H, De Vos P, Tresco PA. Technology of mammalian cell encapsulation. Adv Drug Deliv Rev 2000;42(1-2):29-64.

Umehara Y, Hakamada K, Seino K, Aoki K, Toyoki Y, Sasaki M. Improved survival and ammonia metabolism by intraperitoneal transplantation of microencapsulated hepatocytes in totally hepatectomized rats. Surgery 2001;130(3):513-520.

Uygun B, Soto-Gutierrez A, Yagi H, Izamis M, Guzzardi M, Shulman C, Milwid J, Kobayashi N, Tilles A, Berthiaume F, Hertl M, Nahmias Y, Yarmush M, Uygun K. Organ reengineering

through development of a transplantable recellularized liver graft using decellularized liver matrix. Nat Med 2010;16(7):814-820.

Vairetti M, Griffini P, Pietrocola G, Richelmi P, Freitas I. Cold-induced apoptosis in isolated rat hepatocytes: protective role of glutathione. Free Radic Biol Med 2001;31(8):954-961.

Vaithilingam V, Kollarikova G, Qi M, Lacik I, Oberholzer J, Guillemin GJ, Tuch BE. Effect of prolonged gelling time on the intrinsic properties of barium alginate microcapsules and its biocompatibility. J Microencapsul 2011;28(6):499-507.

Van Raamsdonk JM, Chang PL. Osmotic pressure test: a simple, quantitative method to assess the mechanical stability of alginate microcapsules. J Biomed Mater Res 2001;54(2):264-271.

Vogler E. Protein adsorption in three dimensions. Biomaterials 2012;33(5):1201-1237.

Vrana N, Matsumura K, Hyon S, Geever L, Kennedy J, Lyons J, Higginbotham C, Cahill P, McGuinness G. Cell encapsulation and cryostorage in PVA-gelatin cryogels: incorporation of carboxylated ε-poly-L-lysine as cryoprotectant. J Tissue Eng Regen Med 2012;6(4):280-290.

Wang L, Sun J, Li L, Harbour C, Mears D, Koutalistras N, Sheil A. Factors affecting hepatocyte viability and CYPIA1 activity during encapsulation. Artif Cells Blood Substit Immobil Biotechnol 2000;28(3):215-227.

Whelehan M, Marison I. Microencapsulation using vibrating technology. J Microencapsul 2011;28(8):669-688.

Williams C, Malik A, Kim T, Manson P, Elisseeff J. Variable cytocompatibility of six cell lines with photoinitiators used for polymerizing hydrogels and cell encapsulation. Biomaterials 2005;26(11):1211-1218.

Wong H, Chang T. Bioartificial liver: implanted artificial cells microencapsulated living hepatocytes increases survival of liver failure rats. Int J Artif Organs 1986;9(5):335-336.

Wong H, Chang T. The viability and regeneration of artificial cell microencapsulated rat hepatocyte xenograft transplants in mice. Biomater Artif Organs 1988;16(4):731-739.

Woods E, Perry B, Hockema J, Larson L, Zhou D, Goebel W. Optimized cryopreservation method for human dental pulp-derived stem cells and their tissues of origin for banking and clinical use. Cryobiology 2009;59(2):150-157

Wu Y, Gupta S. Hepatic preconditioning for transplanted cell engraftment and proliferation. Methods Mol Biol 2009;481:107-116.

Yagi T, Hardin J, Valenzuela Y, Miyoshi H, Gores G, Nyberg S. Caspase inhibition reduces apoptotic death of cryopreserved porcine hepatocytes. Hepatology 2001;33(6):1432-1440.

Yin C, Mien Chia S, Hoon Quek C, Yu H, Zhuo RX, Leong KW, Mao HQ. Microcapsules with improved mechanical stability for hepatocyte culture. Biomaterials 2003;24(10):1771-1780.

Zhang F, Wan H, Li M, Ye J, Yin M, Huang C, Yu J. Transplantation of microencapsulated umbilical-cord-blood-derived hepatic-like cells for treatment of hepatic failure. World J Gastroenterol 2011;17(7):938-945.

Zimmermann H, Zimmermann D, Reuss R, Feilen PJ, Manz B, Katsen A, Weber M, Ihmig FR, Ehrhart F, Gessner P, Behringer M, Steinbach A, Wegner LH, Sukhorukov VL, Vásquez JA, Schneider S, Weber MM, Volke F, Wolf R, Zimmermann U. Towards a medically approved technology for alginate-based microcapsules allowing long-term immunoisolated transplantation J Mater Sci Mater Med 2005;16(6):491-501.

Zimmermann H, Shirley SG, Zimmermann U. Alginate-based encapsulation of cells: past, present, and future. Curr Diab Rep 2007;7(4):314-320.

Zimmermann U, Thürmer F, Jork A, Weber M, Mimietz S, Hillgärtner M, Brunnenmeier F, Zimmermann H, Westphal I, Fuhr G, Nöth U, Haase A, Steinert A, Hendrich C. A novel class of amitogenic alginate microcapsules for long-term immunoisolated transplantation. Ann N Y Acad Sci 2001;944:199-215.

10. APPENDICES

Appendix I: A summary of human liver tissues used for hepatocyte isolation.

No.	Tissue	Type	CIT/WIT	Age/ Sex	Viability	Remark
1	Segment 4	DBD	8h	36/F	63%	Mild-mod fatty
2	Left lobe	DBD	9h	52/M	70%	Mod fatty
3	Segment 4	DBD	10h	34/M	60%	
4	Left lateral segment	DBD	9h 30min	40/F	72%	
5[a]	Left lateral segment	DCD	27min	35/M	53%	Severe fatty
6[a]	Resection	Biliary cyst	NA	62/F	67%	
7[a]	Resection	Colorectal CA	NA	70/M	66%	
8	Segments 1& 4	DBD	11h 30min	26/M	69%	
9	Left lateral segment	DBD	11h 30min	59/F	71%	Mild-mod fatty
10	Segments 1& 4	DBD	9h 30min	13/F	65%	
11	Right lobe	DBD	11h 20min	17/F	72%	
12	Resection	Cholangio-CA	NA	66/F	60%	Mod fatty
13	Left lateral segment	DCD	27min	64/F	60%	
14	Right lobe	DBD	6h	47/M	76%	
15	Left lateral segment	DBD	13h	39/F	80%	Mild-mod fatty
16	Resection	Liver cyst	NA	46/F	78%	
17	Right lobe	DCD	14min	49/M	74%	
18	Right lobe	DCD	22min	29/M	67%	
19	Segment 1&4	DBD	7h	31/F	65%	
20	Segment 1	DBD	7h	18/F	83%	
21	Segment 1	DBD	8h	35/F	77%	
22	Segment 1&4	DBD	22h	37/M	60%	Mild-mod fatty
23	Left lobe	DCD	14min	17/M	78%	Mild-mod fatty
24	Resection	NET	NA	68/F	77%	Mod fatty
25	Segment 1&4	DBD	16h	42/M	68%	
26	Right lobe	DCD	27min	60/M	86%	

Appendix II: Cryopreserved human hepatocytes

No.	Tissue	Type	CIT/WIT	Age/Sex	Viability		
					Fresh	Post-thaw	Percoll®
1	Right lobe	DBD	NA	8/F	85%	60%	-
2	Whole liver	DCD	NA	29/M	79%	49%	63%
3	Left lobe	DCD	13min	67/M	76%	45%	65%
4	Left lateral segment	DBD	5h	52/F	72%	48%	72%
5	Segment 1	DBD	14h 20min	37/F	74%	46%	62%
6	Left lateral segment	DCD	16min	58/M	72%	42%	64%
7	Right lobe	DCD	NA	6/F	78%	45%	63%
8	Segment 4	DBD	7h	12/M	86%	62%	-
9	Left lateral segment	DCD	23min	68/M	84%	48%	60%
10	Right lobe	DBD	6h	47/M	76%	50%	70%

[a] Hepatocytes used in optimisation of Percoll® protocol. CA, cancer/carcinoma; CIT, cold ischemic time; DBD, donor after brain-dead; DCD, donor after cardiac death; NA, not available; NET, neuroendocrine tumor; and WIT, warm ischemia time.

Appendix III: Proteomics analysis in supernatants of HMBs culture medium.

Accession	Entry	Protein description	MW	Amount (fmol)
CH10_HUMAN	P61604	10 kDa heat shock protein mitochondrial	10924	10.2902
FABPL_HUMAN	P07148	Fatty acid binding protein liver	14199	46.8011
UK114_HUMAN	P52758	Ribonuclease UK114	14484	27.3915
PROF1_HUMAN	P07737	Profilin 1	15044	8.5285
SODC_HUMAN	P00441	Superoxide dismutase Cu Zn	15925	13.8232
ISCU_HUMAN	Q9H1K1	Iron sulfur cluster assembly enzyme ISCU	17987	62.957
TWST1_HUMAN	Q15672	Twist related protein 1	20941	17.279
PEBP1_HUMAN	P30086	Phosphatidylethanolamine binding protein 1	21043	32.4102
PRDX6_HUMAN	P30041	Peroxiredoxin 6	25019	15.6806
GPX5_HUMAN	O75715	Epididymal secretory glutathione peroxidase	25186	18.0216
GSTA1_HUMAN	P08263	Glutathione S transferase A1	25614	57.4934
GSTA2_HUMAN	P09210	Glutathione S transferase A2	25647	30.7457
DCXR_HUMAN	Q7Z4W1	L xylulose reductase	25896	19.3082
PA1_HUMAN	Q9BTK6	PAXIP1 associated protein 1	27699	4.7046
CES1P_HUMAN	Q9UKY3	Putative inactive carboxylesterase 4	30659	17.8128
NPM_HUMAN	P06748	Nucleophosmin	32554	5.0989
ARGI1_HUMAN	P05089	Arginase 1	34713	10.5881
ECH1_HUMAN	Q13011	Delta 3 5 Delta 2 4 dienoyl CoA isomerase	35793	9.2902
FETUA_HUMAN	P02765	Alpha 2 HS glycoprotein	39299	184.094
ALDOB_HUMAN	P05062	Fructose bisphosphate aldolase B	39448	56.0584
ADH1B_HUMAN	P00325	Alcohol dehydrogenase 1B	39828	105.182
ADH1A_HUMAN	P07327	Alcohol dehydrogenase 1A	39832	12.718
ADH1G_HUMAN	P00326	Alcohol dehydrogenase 1C	39841	11.2842
OTC_HUMAN	P00480	Ornithine carbamoyltransferase mitochondrial	39909	12.4154
ADH4_HUMAN	P08319	Alcohol dehydrogenase 4	40195	42.0025
ACTG_HUMAN	P63261	Actin cytoplasmic 2	41765	10
THIM_HUMAN	P42765	3 ketoacyl CoA thiolase mitochondrial	41897	28.2113
SPYA_HUMAN	P21549	Serine pyruvate aminotransferase	42982	28.8985
HPPD_HUMAN	P32754	4 hydroxyphenylpyruvate dioxygenase	44905	7.3992
HSDL2_HUMAN	Q6YN16	Hydroxysteroid dehydrogenase like protein	45365	2.7366
ASSY_HUMAN	P00966	Argininosuccinate synthase	46501	26.2836
P00924	ENO1YEAST	Enolase 1 EC 4 2 1 11 2 phosphoglycerate dehydrogenase	46642	100

Accession	Entry	Protein description	MW	Amount (fmol)
ENOA_HUMAN	P06733	Alpha enolase	47139	12.1431
PSG1_HUMAN	P11464	Pregnancy specific beta 1 glycoprotein 1	47193	278.194
SOX4_HUMAN	Q06945	Transcription factor SOX 4	47233	20.2055
AATM_HUMAN	P00505	Aspartate aminotransferase mitochondrial	47487	13.5309
CALR_HUMAN	P27797	Calreticulin	48111	12.1226
GATM_HUMAN	P50440	Glycine amidinotransferase mitochondrial	48424	11.7616
AP1M1_HUMAN	Q9BXS5	AP 1 complex subunit mu 1	48556	7.5842
SBP1_HUMAN	Q13228	Selenium binding protein 1	52357	9.1889
K2C8_HUMAN	P05787	Keratin type II cytoskeletal 8	53671	18.1546
AL1A1_HUMAN	P00352	Retinal dehydrogenase 1	54826	24.7068
ALDH2_HUMAN	P05091	Aldehyde dehydrogenase mitochondrial	56345	6.2671
GABT_HUMAN	P80404	4 aminobutyrate aminotransferase	56402	15.204
ATPB_HUMAN	P06576	ATP synthase subunit beta mitochondrial	56524	9.6364
UGPA_HUMAN	Q16851	UTP glucose 1 phosphate uridylyltransferase	56904	11.7059
CH60_HUMAN	P10809	60 kDa heat shock protein mitochondrial	61016	10.657
DHE3_HUMAN	P00367	Glutamate dehydrogenase 1 mitochondrial	61359	29.2852
DHE4_HUMAN	P49448	Glutamate dehydrogenase 2 mitochondrial	61395	1.9264
EST1_HUMAN	P23141	Liver carboxylesterase 1	62481	35.8419
ALBU_HUMAN	P02768	Serum albumin	69321	450.054
PCKGM_HUMAN	Q16822	Phosphoenolpyruvate carboxykinase GTP	70684	2.7961
TRFL_HUMAN	P02788	Lactotransferrin	78131	91.6639
RHG10_HUMAN	A1A4S6	Rho GTPase activating protein 10	89318	8.1146
ITIH2_HUMAN	P19823	Inter alpha trypsin inhibitor heavy chain H2	106396	14.0697
CPSM_HUMAN	P31327	Carbamoyl phosphate synthase ammonia	164834	44.8113

Proteins having at least two peptides identifications found in supernatants of HMBs culture medium are listed by molecular weight. Green, 100% confident; yellow, 50% confident; and pink, possible hit.

11. LIST OF PUBLICATIONS

11.1 Publication

Jitraruch S, Qin H, Dhawan A, Hughes RD, Lehec SC, and Mitry RR (2012). Hepatocyte Transplantation, 'Omics' and Gene Therapy in the management of Liver Diseases. In: Dhawan A, ed. (Vol. 16). *Concise Pediatric and Adolescent Hepatology*. Karger AG: Basel (Switzerland), 240-256

Jitraruch S, Dhawan A, Hughes RD, Filippi C, Soong D, Philippeos C, Lehec SC, Longhi M.S, Heaton ND and Mitry RR (2014). Alginate Microencapsulated Hepatocytes Optimised for Transplantation in Acute Liver Failure. [submitted to *PLoS ONE*].

11.2 Abstracts

Jitraruch S, Dhawan A, Hughes RD, Filippi C, Soong D, Lehec SC, Longhi MS, Mitry RR (2014). Alginate Microencapsulated Human Hepatocytes Optimised for Clinical Transplantation. *12th Divisions of Immunology, Infection and Inflammatory Disease & Transplantation Immunology and Mucosal Biology Postgraduate Research Symposium, London, UK (June 2014; Poster presentation).*

Jitraruch S, Dhawan A, Hughes RD, Filippi C, Soong D, Lehec SC, Longhi MS, Mitry RR (2014). Alginate Microencapsulated Human Hepatocytes Optimised for Clinical Transplantation. *The 2014 Joint International Congress of ILTS, ELITA & LICAGE, London, UK (June 2014;* ***Rising Star Award****).*

Jitraruch S, Dhawan A, Longhi MS, Hughes RD, Filippi C, Lehec SC, Klem FB, Mitry RR (2013). *In Vitro* Immunogenicity of Alginate Microencapsulated Human Hepatocytes. *12th Congress of the Cell Transplantation Society, Milan, Italy (July 2013; Oral presentation).*

Jitraruch S, Dhawan A, Hughes RD, Soong D, Lehec SC, Mitry RR (2013). Alginate Microencapsulated Human Hepatocytes: Assessment of Physical Integrity and Effect of Cell Density on Hepatocyte Viability and Metabolic Function. *12th Congress of the Cell Transplantation Society, Milan, Italy (July 2013; Poster presentation).*

Jitraruch S, Dhawan A, Hughes RD, Soong D, Lehec SC, Mitry RR (2013). Alginate Microencapsulated Human Hepatocytes: Assessment of Physical Integrity and Effect of Cell Density on Hepatocyte Viability and Metabolic Function. *11th Divisions of Immunology, Infection and Inflammatory Disease & Transplantation Immunology and Mucosal Biology Postgraduate Research Symposium, London, UK (June 2013; Oral presentation).*

Jitraruch S, Dhawan A, Hughes RD, Lehec SC, Mitry RR (2013). Human Hepatocyte Alginate Microbeads: Physical Integrity, and Effect of Cell Density on Hepatocyte Viability and Metabolic Function. *46th Annual Meeting of European Society for Paediatric Hepatology, Gastroenterology and Nutrition, London, UK (May 2013; Oral presentation).*

Jitraruch S, Dhawan A, Hughes RD, Soong D, Lehec SC, Mitry RR (2012). Human Hepatocyte Alginate Microbeads preparation under GMP conditions and assessment of Cell Viability, Metabolic Function and Physical Integrity. *63rd Annual Meeting of the American Association for the Study of Liver Disease, Boston, USA (November 2012; Poster presentation).*

Jitraruch S, Dhawan A, Hughes RD, Soong D, Lehec SC, Heaton ND, Mitry RR (2012). Alginate-encapsulated Hepatocytes – An Optimised Protocol for Depolymerisation and Cell Release. *10th Divisions of Immunology, Infection and Inflammatory Disease & Transplantation Immunology and Mucosal Biology Postgraduate Research Symposium, London, UK (May 2012; Poster presentation).*

Jitraruch S, Dhawan A, Hughes RD, Lehec SC, Mitry RR (2011). Alginate-encapsulated Human Hepatocytes – Assessment of Microbead Integrity. *20th United European Gastroenterology Week, Amsterdam, Netherlands (October 2011; Poster presentation).*